This is to certify that the

thesis entitled

The Cyanohydrin (Kiliani) Reaction: Mechanism Studies by ^{13}C NMR Spectroscopy and Application to the Synthesis of Isotopically-Enriched Carbohydrates

presented by

Anthony Stephen Serianni

has been accepted towards fulfillment
of the requirements for

Ph.D. degree in Biochemistry

Robert Barker

Major professor

Date 12/17/79

THE CYANOHYDRIN (KILIANI) REACTION: MECHANISM STUDIES BY ^{13}C NMR SPECTROSCOPY AND APPLICATION TO THE SYNTHESIS OF ISOTOPICALLY-ENRICHED CARBOHYDRATES

By

Anthony Stephen Serianni

A DISSERTATION

Submitted to
Michigan State University
in partial fulfillment of the requirements
for the degree of

DOCTOR OF PHILOSOPHY

Department of Biochemistry

1979

ABSTRACT

THE CYANOHYDRIN (KILIANI) REACTION: MECHANISM STUDIES BY ^{13}C NMR SPECTROSCOPY AND APPLICATION TO THE SYNTHESIS OF ISOTOPICALLY-ENRICHED CARBOHYDRATES

By

Anthony Stephen Serianni

The classical Kiliani (cyanohydrin) reaction was studied by ^{13}C NMR and GLC. ^{13}C NMR studies were facilitated by the use of [^{13}C]cyanide and/or [^{13}C]-enriched aldoses. The effects of aldose configuration, carbon-chain length and derivatization on the rate and extent of cyanide consumption, and on the overall rate of aldononitrile disappearance, were investigated. Hydrolytic intermediates in the reaction of K^{13}CN with D-erythrose were identified and characterized by ^{13}C NMR and GLC with the use of standard compounds and/or NMR parameters. Reaction sequences, at several pH values, were determined from time-resolved reaction profiles produced from ^{13}C NMR spectral data. At high pH (10.5, 12.7), the reaction sequence appears to be cyanide + D-erythrose → aldononitriles → imido-1,4-lactones → carbinolamines → aldonamides. Aldonamides hydrolyze (via carbinolamines and aldono-lactones) to aldonates. At lower pH (7, 8.5), the direct conversion of imido-1,4-lactone to aldono-1,4-lactone becomes appreciable. Ammonia, which is released in this reaction, can react with imido-1,4-lactones to yield amidines. A by-product reaction between imido-lactones and aldononitriles is proposed. ^{13}C NMR parameters (δ and J)

and GLC retention times for the reactants, intermediates and products are tabulated.

From observations made during the study of the Kiliani synthesis, a new method for the preparation of isotopically-enriched carbohydrates was developed. Cyanohydrins can be formed rapidly and essentially quantitatively at pH 8.0 ± 0.5 with minimal hydrolysis, and they are stable at pH 4.0. The nitriles can be hydrogenolyzed to aldoses with palladium-barium sulfate (5%) at 1 atm to 60 lb in^{-2} and pH 1.7 to 4.2 depending on the structure of the nitrile. The mixed aldononitrile epimers are reduced without purification and the product aldoses purified by chromatography. Aldononitrile phosphate epimers are separated, prior to reduction, by chromatography at pH 3.9. Using the above procedure and $K^{13}CN$, C_2-C_6 aldoses and C_2-C_5 aldose phosphates were prepared with [^{13}C]-enrichment at various carbon atoms.

In addition to the introduction of carbon isotopes, catalytic hydrogenolysis of cyanohydrins provided a route to carbohydrates enriched with hydrogen and oxygen isotopes. The technique permitted the simultaneous incorporation of carbon and hydrogen isotopes at C-1 and H-1, respectively, and oxygen isotopes at O-2 for each cycle of cyanide addition and catalytic reduction, as shown in the following scheme.

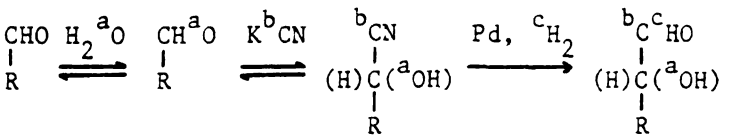

^{13}C NMR and ^{1}H NMR parameters for several [^{13}C]- and [^{2}H]-enriched carbohydrates and their derivatives are tabulated and discussed in terms of configuration and solution conformation.

To my parents, Elizabeth and Anthony,

For the love and patience they showed,
For the home they created,
For the values in life they gave, and
The sacrifices they made.

For ears that heard,
And for their smiles.
For many an unselfish deed;
For carrying the load when their backs were tired.

For giving me life.

ACKNOWLEDGEMENTS

I am deeply grateful to Dr. Robert Barker for the guidance, friendship and encouragement he provided during the course of this study.

I thank my colleagues in the laboratory for the countless discussions, where constructive criticism and encouragement were ideally interwoven.

I am indebted to Ms. Terry Auld, who risked her sanity and sacrificed her social life by patiently and meticulously typing this thesis.

I would also like to thank the Biochemistry Department at Cornell University for permitting me to complete this thesis during the first few months of my appointment.

I acknowledge financial support by a grant from the National Institute of General Medical Sciences, and thank the Stable Isotopes Resource of the Los Alamos National Laboratory for the supply of potassium [^{13}C]cyanide.

TABLE OF CONTENTS

LIST OF TABLES

LIST OF FIGURES

LIST OF ABBREVIATIONS

ADP	adenosine 5'-diphosphate
AMP	adenosine 5'-monophosphate
ATP	adenosine 5'-triphosphate
BSTFA	N,O-bis(trimethylsilyl)trifluoroacetamide
^{13}C NMR	^{13}C nuclear magnetic resonance spectroscopy
FDP	D-fructose 1,6-bisphosphate
GLC	gas-liquid chromatography
^{1}H NMR	^{1}H nuclear magnetic resonance spectroscopy
Me_3Si	trimethylsilyl
Me_4Si	tetramethylsilane
NOE	nuclear Overhauser enhancement
P	phosphate
P_2	bisphosphate
$Pd/BaSO_4$	palladium-barium sulfate
POPOP	1,4-bis[2-(5-phenyloxazolyl)]benzene
PPO	2,5-diphenyloxazole
TMCS	chlorotrimethylsilane
TMSCN	trimethylsilylcyanide
UMP	uridine 5'-monophosphate

I. INTRODUCTION

The development of Fourier-transform ^{13}C NMR spectroscopy in the late 1960's provided a powerful and practical new tool to aid in the elucidation of chemical structure and in the quantitation of the dynamics of chemical and biochemical reactions and interactions. The problem of low ^{13}C resonance sensitivity, caused by the low natural abundance of 1.1% (1) and a magnetic moment one-quarter that of ^{1}H, prompted the use of Fourier-transform methods of detection and broad-band ^{1}H decoupling. The latter technique not only resulted in the elimination of ^{13}C-^{1}H spin multiplets but also produced a threefold enhancement of ^{13}C resonances derived from a change in the Boltzmann distribution of ^{1}H energy level populations during ^{1}H excitation. This enhancement is known as nuclear Overhauser enhancement (NOE). For studies that require the determination of ^{13}C-^{1}H coupling constants, gated ^{1}H-decoupling techniques are employed which permit ^{1}H-coupled spectra with NOE.

Other alternatives to improve sensitivity include increasing the field strength of the spectrometer, lowering the temperature of the sample, increasing sample size and/or increasing the isotopic abundance of the ^{13}C isotope. The last alternative, [^{13}C]-enrichment, is generally time-consuming and expensive, and high-yield chemical and/or biochemical synthetic routes must be available. In addition, selective [^{13}C]-enrichment is preferred, since ^{13}C NMR spectra of uniformly enriched compounds (>70 atom % isotopic enrichment) are complicated by extensive homonuclear ^{13}C coupling with a concomitant loss in sensitivity. However, [^{13}C]-enrichment provides the only means of

evaluating spin-spin coupling between carbon, $J_{^{13}C,^{13}C}$, since ^{13}C-^{13}C coupling cannot be measured at natural abundance levels. Selective enrichment also allows easier evaluation of the fate of the enriched nucleus in chemical and biochemical conversions.

Carbohydrates occupy a unique role in the study of organic chemistry and a central role in the chemistry of biological systems. In the first sense, they are a class of poly-hydroxylic compounds especially suited for systematic study of configuration-conformation and structure-reactivity relationships since complete groups are available composed of compounds with similar empirical formula and carbon skeletons but different carbon stereochemistry. In the second sense, these compounds are involved in energy-producing catabolic reactions in biological systems, in cell-cell interactions in the form of oligosaccharides on glycoproteins and glycolipids, in the immune response as components of glycosylated antibodies, in biological structures in the form of polysaccharides like cellulose, and in energy storage in polysaccharides like starch and glycogen.

^{13}C NMR is particularly suited for the study of carbohydrates. ^{1}H-Decoupled ^{13}C NMR spectra are not complicated by multiplets and are characteristically measured over 200 ppm of the applied field, which significantly decreases resonance overlap and facilitates the observation of the various tautomeric forms. By comparison, ^{1}H NMR spectra are measured over 10 ppm of the field, and are further complicated by ^{1}H-^{1}H coupling and non-first-order behavior. ^{1}H NMR spectra of carbohydrates can be interpreted, however, with the aid of selective ^{1}H-decoupling, selective deuteration, computer simulation and/or high-field spectrometers. In cases where both ^{13}C NMR and ^{1}H NMR spectra

are interpretable for [^{13}C]-enriched compounds, chemical shifts of the protons and carbons, and homonuclear (^{1}H-^{1}H, ^{13}C-^{13}C) and heteronuclear (^{1}H-^{13}C) coupling constants can be compared and evaluated in terms of structure and conformation.

[^{13}C]-Enrichment lowers the concentration of sample required for convenient detection into the range of most biological applications (μM) by significantly decreasing the acquisition time to obtain ^{13}C NMR spectra of the enriched carbon.

A. Statement of the Problem

^{13}C NMR spectroscopy offers several advantages over traditional methods in the study of reaction mechanisms and intermediates. Spectra are frequently less complex than ^{1}H spectra, while the tedium often associated with radioactive tracer work is eliminated in many instances. Specific [^{13}C]-enrichment permits easy observation of a single nucleus during the course of a reaction by ^{13}C NMR, and the simultaneous use of [^{13}C]- and [^{2}H]-enriched reactants in tracer studies has been well established. Rates of chemical exchange (10^{1}-10^{6} sec^{-1}) can be calculated from the line-widths of the participating nuclei (2). Several studies of reaction mechanisms and reactive intermediates have been reviewed by Stothers (3).

During this study, ^{13}C NMR was employed to elucidate the mechanism of the classical Kiliani reaction. [^{13}C]-Enriched reactants were employed to facilitate the detection of intermediates. The Kiliani reaction, which involves the addition of cyanide to an aldose, with subsequent alkaline hydrolysis of the intermediates, was examined using [^{13}C]cyanide and several aldoses. Identification and characterization

of all intermediates and elucidation of the overall mechanism was accomplished for the reaction as applied to D-erythrose.

A new method for the incorporation of carbon, hydrogen and oxygen isotopes into carbohydrates was developed from observations made during the study of the Kiliani reaction. Aldoses, aldose phosphates and their derivatives were enriched with ^{13}C, ^{14}C and/or ^{2}H, and several ^{13}C and ^{1}H NMR parameters were measured and related to chemical structure, configuration and conformation. Several [^{13}C]-enriched carbohydrates were converted enzymatically to biologically-important compounds to demonstrate their chemical integrity as enzyme substrates and the versatility of combining chemical and biochemical methods in the preparation of [^{13}C]-enriched carbohydrate derivatives.

B. Survey of the Literature

1. Cyanide in chemistry and biochemistry

The chemistry of the cyano group is extensive and has been thoroughly examined by several authors (4). It is the intent of this brief review to discuss the salient features of chemical and biochemical reactions involving cyanide in particular.

Hydrogen cyanide, or hydrocyanic acid (HCN), is a weak acid (pK_a = 9.21) (5). Cyanide ion is an ambident nucleophile, that is, it can react with electrophilic centers from the more electronegative nitrogen or from the more nucleophilic carbon. Silver cyanide, AgCN, generally reacts at the nitrogen to produce isocyanides. Boullanger, Marmet and Descotes (6) have recently reported the preparation of glycosyl isocyanides from the glycosyl halides by Walden-inversion at C-1. Glycosyl isocyanides, as well as other isocyanides, thermally rearrange

to cyanides at elevated temperatures (>140°C).

Alkali salts of hydrogen cyanide (KCN, NaCN) generally react as $N \equiv C^-$ with carbonyls in 1,2-addition to form cyanohydrins, or with conjugated carbonyl compounds in 1,4-addition to produce β-cyanoketones or β-cyanoaldehydes. The latter reaction, known as hydrocyanation, has been recently reviewed by Nagata and Yoshioka (5).

Cyanide adds readily to aldehydes in 1,2-addition, and racemic mixtures result. Prelog and Wilhelm (7) have shown that stereoselectivity (~10% optical purity) can be achieved in the reaction of HCN with benzaldehyde in chloroform by adding an optically-active alkaloid to the reaction mixture. Ketones are generally less reactive than aldehydes toward 1,2-addition. However, silyl derivatives of cyanide [trimethylsilylcyanide (TMSCN) (8) and t-butyldimethylsilylcyanide (9)] react rapidly and completely with ketones to yield 2-O-trimethylsilyl cyanohydrins.

Other reactions include Strecker synthesis of α-amino acids (10, 11), and the asymmetric synthesis of amino acids by addition of cyanide to Schiff bases (12). The former reaction, shown in Scheme I, is termolecular

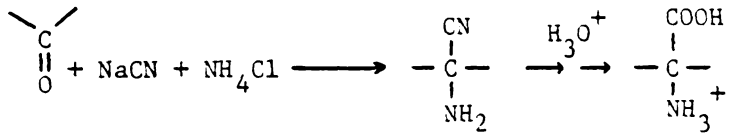

Scheme I

and involves reaction between a carbonyl compound, NH_4Cl and NaCN. Ammonia addition occurs either by displacement of OH-2 of the initially-formed cyanohydrin with inversion, or by formation of a Schiff base with the carbonyl prior to cyanide addition. The resulting α-amino

nitrile is hydrolyzed in acid to the α-amino acid. The asymmetric preparation of α-amino acids involves the formation of a Schiff base with an aliphatic aldehyde and an optically-active benzylamine. After addition of cyanide and hydrolysis of the α-aminonitrile to the carboxylic acid, the 2°-benzylamine is reduced catalytically with Pd/C to the primary amine.

Cyanide ion will displace halides in S_N2 reactions. For example, Bayly and Turner (13) prepared 2-deoxy-3,5-O-ethylidene-D-[1-^{14}C] ribononitrile from 1-deoxy-2,4-O-ethylidene-1-iodo-D-erythritol and $K^{14}CN$ in dimethylformamide at 45°C in 68 percent yield.

Cyanide ion acts catalytically in benzoin condensation (14, 15) and in chemical decarboxylation of α-keto acids (16), as shown in Figure 1. This catalysis is dependent on the reversibility of cyanide addition and the ability of the -C ≡ N moiety to stabilize a negative charge on the α-carbon through resonance.

In biological systems, the thiazolium ring of thiamine acts as a -C ≡ N equivalent (17-19), catalyzing biological benzoin condensation and decarboxylation reactions (Figure 2). The cyanogenic plant glycoside, amygdalin (*1*), is composed of cellobiose

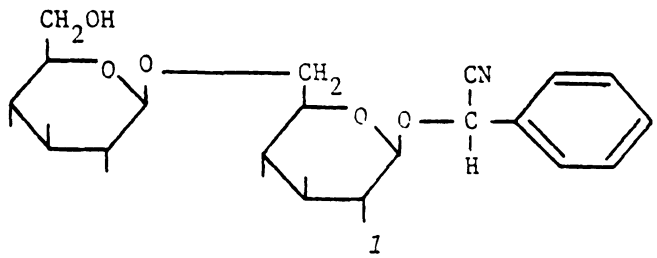

1

glycosidically-linked to OH-2 of mandelonitrile. Two β-glucosidases (20) have been identified that cleave *1* to two molecules of glucose and mandelonitrile. A nitrilase or hydroxynitrile lyase (21) catalyzes the

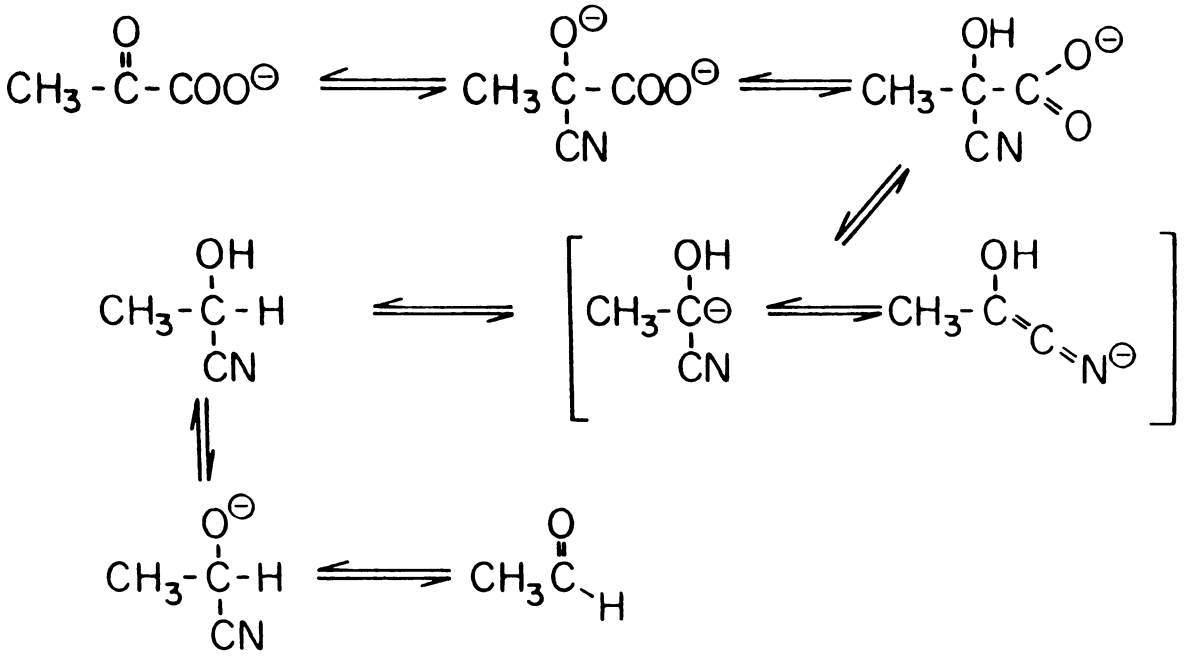

Figure 1. Cyanide-catalyzed decarboxylation of α-keto acids.

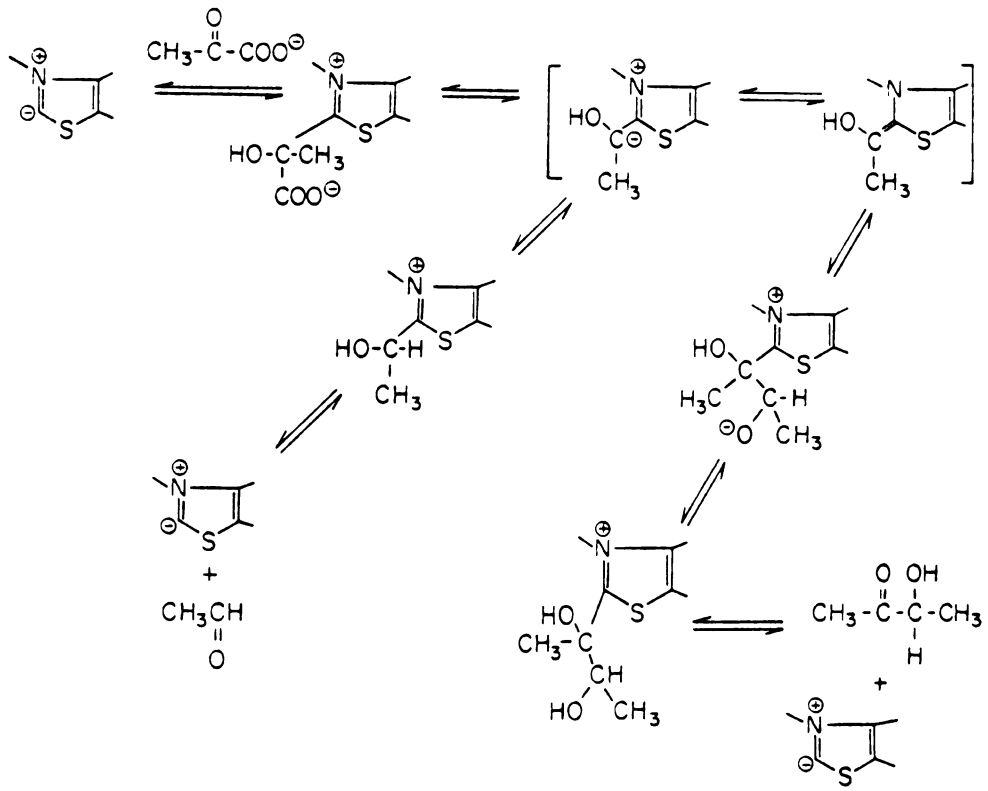

Figure 2. Thiamine-catalyzed benzoin condensation and decarboxylation of pyruvic acid (18).

conversion of mandelonitrile to HCN and benzaldehyde as shown in Scheme II.

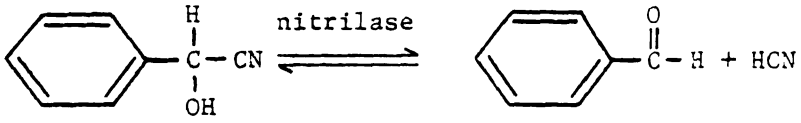

Scheme II

The biological functions and formation of the cyano group have been reviewed by Ferris (22).

Hydrogen cyanide assumes a central role in primitive or pre-biotic chemistry, as discussed by Calvin (23). It has been detected as a first-transformation product in Miller electric-discharge experiments using methane-ammonia-water-hydrogen mixtures. HCN, its oligomers and polymers have been implicated in the pre-biotic formation of α-amino acids (Strecker synthesis), purines like adenine [$(HCN)_5$], pyrimidines and porphyrins.

2. The Kiliani (cyanohydrin) reaction

The preparation of 2-hydroxyacids from carbonyl compounds through cyanohydrins was an early discovery in organic chemistry. Simpson and Gautier (24) prepared DL-lactic acid from acetaldehyde and HCN in 1867. Staedeler (25) prepared α-hydroxyisobutyric acid by condensing HCN with acetone and hydrolyzing acetone cyanohydrin with HCl.

In a series of papers, Kiliani (26) first applied the cyanohydrin reaction to the reducing sugars (Scheme III). C-2 Fpimeric aldonic acids are formed from

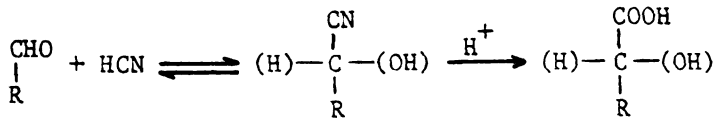

$R = (CHOH)_n\ CH_2OH$

Scheme III

the addition of cyanide to both faces of the planar carbonyl carbon. Kiliani (27-35) prepared epimeric aldonic acids from the following monosaccharides: L-arabinose, D-glucose, D-galactose and D-fructose. He also demonstrated that aldonic acids could be lactonized.

Rupp (36) and Hudson (37) later modified the Kiliani reaction by using aqueous solutions of alkali cyanide and aldose in the presence of $CaCl_2$ or $BaCl_2$ instead of slightly basic liquid HCN. The cyanohydrins (aldononitriles) were hydrolyzed *in situ* in the alkaline solution.

The Kiliani reaction has been applied analytically by Militzer (38) as a direct measure of reducing groups. In addition, Mednieks and Winzler (39) reacted the following carbohydrate derivatives and complex carbohydrates with $K^{14}CN$ during [^{14}C]-labeling studies on mucopolysaccharides and related substances: N-acetylglucosamine, fucose, glucuronate, hyaluronate hexasaccharide, chondroitin sulfate and hyaluronate.

Militzer (40) completed the first systematic study of the effects of aldose structure, temperature and pH on the rate of cyanide consumption. Arabinose, galactose, glucose and 2-ketogluconate reacted quantitatively at 50 mM with a twofold excess of cyanide at pH 9.1, but at different rates. Reaction times for complete addition at 25°C varied from 3 h for arabinose to 72 h for 2-ketogluconate. Glucose reacted with cyanide completely after 18 h at 25°C. Militzer (40) noted that reducing disaccharides gave rates similar to glucose, but that disaccharides with β-linkages (cellobiose, lactose) gave noticeably slower rates than those with α-linkages (maltose, melibiose). Differences in the rates of reaction were explained in terms of the amount of aldehydo form in solution.

Militzer (40) observed that increasing temperature from 25°C to 40°C caused a significant increase in the rate of cyanide consumption while lowering the pH of the reaction from pH 9.2 to pH 6.5 caused a significant decrease in the rate. At acid pH (<pH 6.5), rates of cyanide addition to common sugars were almost zero.

During their studies on the preparation of [^{14}C]-labeled carbohydrates with [^{14}C]cyanide (41-45), Isbell and his colleagues observed that the ratio of epimeric aldonates formed in the cyanohydrin reaction was dependent on reaction conditions. For example, the addition of NaCN to D-arabinose in basic solution produced 73% D-gluconate, while the same reaction, carried out in moderately acidic solution, produced 70% D-mannonate (41).

Varma and French (46) have conducted the only investigation on the mechanism of the Kiliani reaction, as applied to α-D-arabinose. Using paper and gas-liquid chromatography (GLC) to examine reaction mixtures, they concluded that the initially-formed cyanohydrins cyclize to pyranoid imidolactones (imido-1,5-lactones), which subsequently hydrolyze and/or aminolyze (via carbinolamines) to aldonamides and/or lactones, respectively. Aldonamides hydrolyze, via carbinolamines and aldonolactones, to aldonates. Ring-form of the lactones was not established. The mechanism is shown in Figure 3. The Varma-French study, however, did not clearly (a) demonstrate that the manipulations of paper and gas-liquid chromatography do not alter components and/or ratio of components in the original reaction mixture, (b) identify the imidolactone intermediate by either preparation of a standard or determination of a reliable physical constant, (c) determine the ring-forms (furanoid or pyranoid) of the imidolactones and aldonolactones, (d) establish the

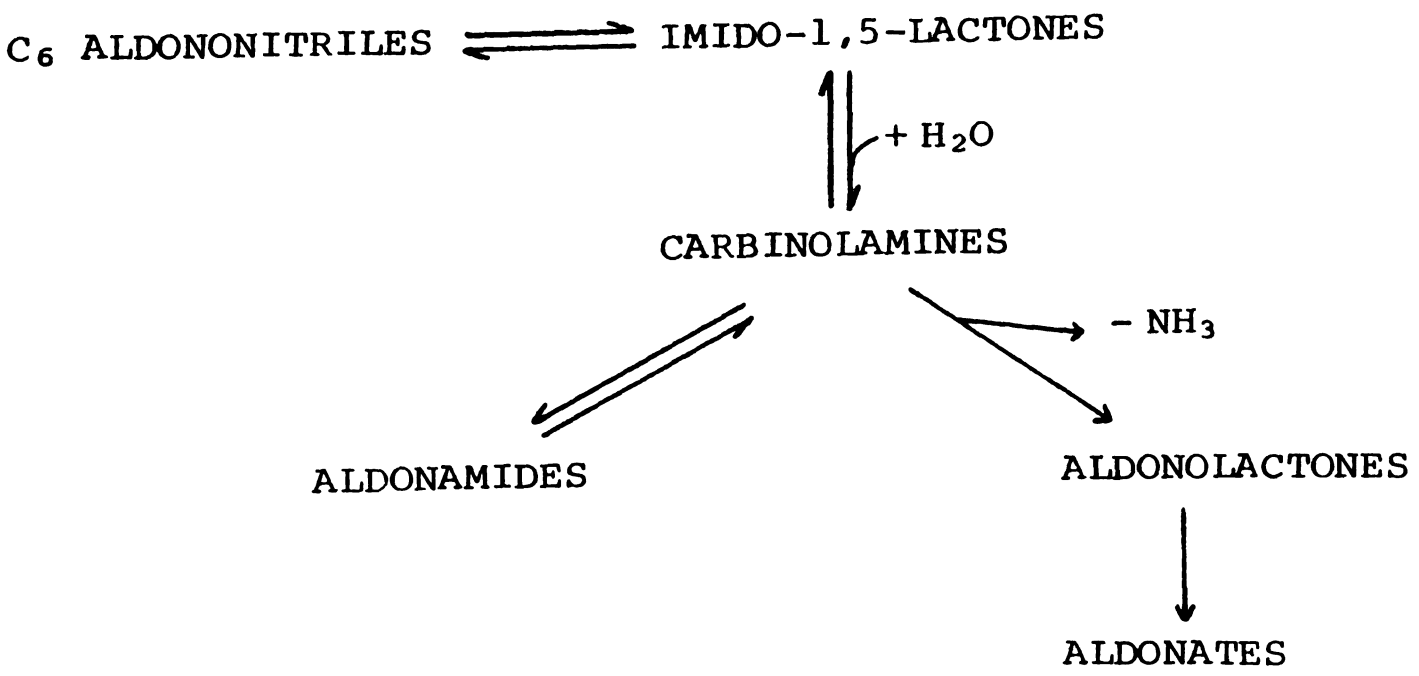

Figure 3. Varma and French (46) mechanism of the Kiliani synthesis applied to α-D-arabinose.

order of appearance and disappearance of the proposed intermediates and the effect of pH on these events, (e) explain the observed effect of pH on the ratio of epimeric products (41), and (f) provide evidence for the existence of tetrahedral (carbinolamine) intermediates.

The present study of the Kiliani reaction resulted from the desire to prepare [^{13}C]-enriched aldoses and their derivatives in high yield based on [^{13}C]cyanide. The reaction of several carbohydrates and their derivatives with cyanide was examined under a variety of conditions of pH, temperature and concentration of reactants using ^{13}C NMR and gas-liquid chromatography (GLC). The effects of aldose configuration, carbon-chain length and derivatization on the rate and extent of cyanide condensation, and on the rate of aldononitrile disappearance were investigated.

To study the intermediates in the hydrolysis reaction, the condensation of K^{13}CN with D-erythrose at 18°C and 0.3 M was examined. The appearance of hydrolytic intermediates was recorded as a function of time by ^{13}C NMR analysis of reaction mixtures. Reaction intermediates, when feasible, were prepared by standard routes with [^{13}C]-enrichment at specific sites to provide standard ^{13}C chemical shifts and ^{13}C-^{13}C coupling constants, to provide standard GLC retention times, and to permit examination of their hydrolysis individually. D-[1-^{13}C], [2-^{13}C] and [3-^{13}C]Erythrose were used as parent aldoses to assist in the characterization of the intermediates. Data are interpreted in terms of formation and stability of intermediates, and their routes of hydrolysis under various reaction conditions.

3. Synthesis of monosaccharides

a. Aldoses and amino-aldoses

Classical routes for the preparation of monosaccharides include Wohl degradation (47), Ruff degradation (48), controlled oxidation of polyols with lead tetraacetate [$Pb(OAc)_4$] and sodium periodate ($NaIO_4$), Kiliani-Fischer synthesis (49, 50), nitromethane synthesis (51, 52), diazomethane synthesis (53), enzymatic syntheses, and epimerizations.

The Kiliani-Fischer synthesis of aldoses is perhaps the most widely recognized method. The Kiliani reaction, discussed in the previous section, was extended by Fischer (49), who discovered that aldonolactones could be reduced with sodium amalgam (Na/Hg) to aldoses. The Kiliani-Fischer reaction has been used extensively for the preparation of [^{14}C]-labeled aldoses from [^{14}C]cyanide by Isbell and his colleagues (41-45). This application and others that employ isotopically-enriched cyanide have been reviewed by Pichat (54). The method has been applied to the preparation of the higher-carbon aldoses, that is, aldoses having more than a six-carbon linear skeleton. The utility of the method is demonstrated by the work of Philippe (55), who lengthened D-glucose up to D-glucodecose (C_{10}) by serial application of the synthesis. The preparation of higher carbon aldoses and alditols has been reviewed by Hudson (50).

In recent years, aldonolactones, or their acylated derivatives, have been reduced with a variety of reagents, including diborane in THF (56) and disiamylborane in THF (57). In this regard, Guidici and Fluharty (58) reduced D-erythrono-1,4-lactone with disiamylborane in THF to produce D-erythrose in 60% yield. Although acylated aldoses are obtained in high yield (>90%) by reduction of protected aldonolactones

with disiamylborane, removal of the acyl groups is often accompanied by degradation of the product aldose.

It is apparent that [^{13}C]-enriched pentoses and hexoses can be prepared in good yield by the Kiliani-Fischer synthesis, and D-[1-^{13}C]glucose, D-[1-^{13}C]mannose and D-[1-^{13}C]galactose have been prepared in this fashion (59). However, only [1-^{13}C]- and [2-^{13}C]-enriched hexoses are accessible, since the C_2-C_4 [1-^{13}C]aldoses cannot be prepared by the Kiliani-Fischer reaction.

The amino-sugar, glucosamine, was originally prepared (60) by the addition of HCN to D-arabinosylamine, hydrolysis of the 2-aminonitrile with concentrated HCl to the corresponding acid, dehydration to the 2-aminolactone, and reduction to the 2-amino-2-deoxyaldose with Na/Hg. The reaction scheme is shown in Figure 4. The overall yield is about 1 percent. The reaction was modified by preparing the 2-aminonitriles from the starting aldose with HCN in the presence of ammonia or other amines (Strecker addition). Kuhn and his associates (61-64) later demonstrated that 2-aminonitriles, which are isolable, could be reduced with palladium directly to 2-amino-2-deoxyaldoses, as shown in Figure 4, in yields based on the aldose of more than 70 percent.

Kuhn and Klesse (65) demonstrated that D-glucono- and D-mannononitriles could be prepared in pyridine and reduced catalytically in dilute acid with palladium-barium sulfate ($Pd/BaSO_4$) to D-glucose and D-mannose, respectively. Bayly and Turner (13) have used platinum oxide to prepare 2-deoxy-D-erythro-[1-^{14}C]pentose from the corresponding nitrile.

During the investigation of the mechanism of the Kiliani reaction, we observed that aldononitriles form rapidly and essentially

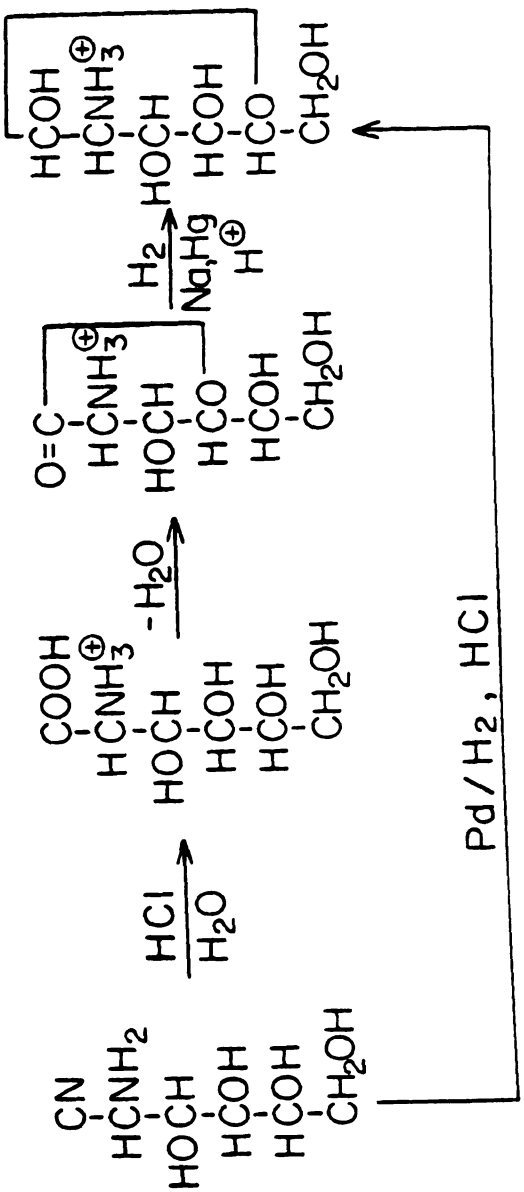

Figure 4. Preparation of D-glucosamine (61).

quantitatively at pH 8.0 ± 0.5 with minimal hydrolysis, and that they are stable at pH 4.0. Aldononitriles were hydrogenolyzed to aldoses in 70 to 80 percent yield with palladium-barium sulfate at pH 1.7 to 4.2 and 1 atm to 60 lb. in^{-2} H_2, depending on the structure of the cyanohydrin. The reaction was used to prepare [^{13}C]-enriched C_2 to C_6 aldoses. The reaction scheme is shown in Figure 5 and is compared with the traditional Kiliani-Fischer reaction.

b. Aldose phosphates

The formation of phosphoric esters of carbohydrates is an essential stage in biological synthesis, interconversion and degradation of pentoses and hexoses. For example, D-glucose is phosphorylated by hexokinase and Mg^{2+}-ATP to form D-glucose 6-P during glycolysis. D-Glucose 6-P is isomerized by phosphoglucoisomerase to D-fructose 6-P or is converted to D-glucose 1-P by phosphoglucomutase. D-Glucose 1-P is a precursor in the enzymatic synthesis of the polysaccharides amylase, amylopectin and glycogen. Studies on these and other metabolic events require the appropriate phosphate esters to measure enzyme activity and inhibition, to investigate enzyme-substrate interactions, and to examine the solution structures of the phosphate esters.

Chemical syntheses of aldose phosphates commonly involve the phosphorylation of protected carbohydrate derivatives. For example, 1,2-epoxides have been used in the preparation of glucose 3-P (66) and glucose 6-P (67). 1,2-O-Isopropylidene-D-xylose has been treated with diphenyl phosphochloridate to yield the 5-phenyl phosphate, which is hydrolyzed in alkali and acid to produce a mixture of D-xylose 3-P and D-xylose 5-P (68). Stverteczky et al. (69) prepared D-arabinose 3-P from 5,6-anhydro-3-O-benzyl-1,2-O-isopropylidene-D-glucofuranose (2) by

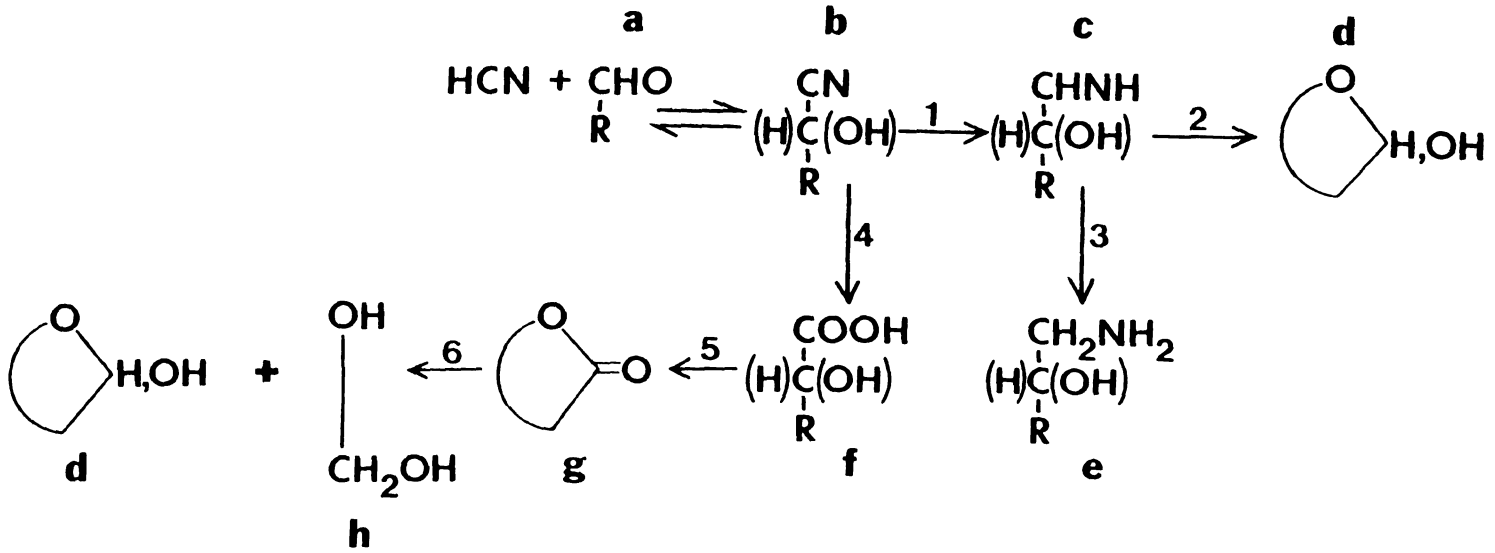

Figure 5. Comparison between the traditional Kiliani-Fischer pathway (reactions 4, 5, 6) and the new pathway (reactions 1, 2). a = starting aldose, b = aldononitrile, c = aldimine, d = product aldose, e = 1-amino-1-deoxyalditol, f = aldonic acid, g = aldonolactone, h = alditol. Compounds e and h are reaction by-products.

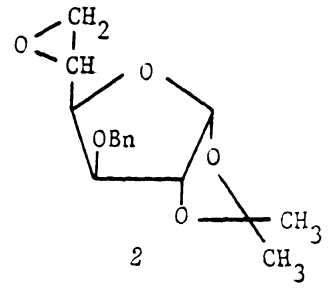

Bn = benzyl

2

phosphorylation of the latter compound with K_2HPO_4 to produce the 6-phosphate. Acid hydrolysis, periodate cleavage and hydrogenolysis yields D-arabinose 5-P. Michelson and Todd (70) prepared D-ribose 5-P by phosphorylating 2,3-O-isopropylidene-D-methyl ribofuranoside. 1,3,4-Tri-O-acetyl-N-acetyl-β-D-glucosamine yields, after treatment with diphenyl phosphochloridate, hydrogenolysis with PtO_2 and acid hydrolysis, D-glucosamine 6-P (71).

Maehr and Smallheer (72) have recently prepared D-arabinose 5-P and D-xylose 5-P from methyl α-D-arabinofuranoside and 1,2-O-isopropylidene-D-xylofuranose, respectively, by treatment with dibenzyl or diphenylphosphochloridate. The resulting 5-esters were hydrogenolyzed and hydrolyzed in acid to afford the product aldose phosphates.

Ballou and Fischer (73) and Ballou et al. (74) prepared D-glyceraldehyde 3-P from mannitol in nine steps and D-erythrose 4-P from D-erythrose in eight steps, respectively. These syntheses yield the C_3 and C_4 aldose phosphate as the dimethyl acetal derivative which, unlike the free aldose phosphate, can be stored without decomposition. Treatment with Dowex 50 X8 (H^+) affords the free aldose phosphate. Klybas et al. (75) prepared D-erythrose 4-P directly by lead tetraacetate oxidation of D-glucose 6-P.

Aldose phosphates can be prepared enzymatically in many instances through the use of isomerases and kinases, as discussed by Leloir and

Cardini (76).

The preparation of [^{13}C]-enriched aldose phosphates, therefore, could be accomplished by these methods, but often from [^{13}C]-enriched precursors frequently more complex than the aldose phosphate. However, addition of [^{13}C]cyanide to C_2, C_3 and C_4 aldose phosphates at pH 8.0 yields C_3, C_4 and C_5 aldononitrile phosphates almost quantitatively. Hydrogenolysis of the aldononitrile phosphates with Pd/$BaSO_4$ at pH 1.7 ± 0.1 and atmospheric pressure afford [1-^{13}C]aldoses with terminal phosphate esters in 75-85% yield. The method was applied serially to produce aldose phosphates enriched with ^{13}C at positions other than C-1. For millimolar preparations of aldose phosphates, procedures are described to prepare glycolaldehyde-P and D-glyceraldehyde 3-P in 80-90% yield from economical starting materials for use as parent aldose phosphates in cyanide condensation.

c. Deuterated carbohydrates

The preparation of deuterated carbohydrates is frequently accomplished by reduction of carbonyl derivatives with NaB^2H_4. Lemieux and Stevens (77) prepared 1,2:5,6-di-O-isopropylidene-α-D-glucofuranose-6, 6'-d_2 by reduction of 1,2-O-isopropylidene-α-D-glucofuranurono-6,3-lactone with $LiAl^2H_4$. Gray and Barker (78) prepared D-glyceraldehyde-3, 3'-d_2 3-phosphate by reduction of 2-O-benzyl-D-arabinono-1,4-lactone with NaB^2H_4 to produce the intermediate 2-O-benzyl-D-arabinitol-1,1'-d_2. α-D-Galactose-6,6'-d_2 was prepared by reduction of methyl D-galacturonisides with NaB^2H_4 (79). Other methods of deuteration include base-catalyzed ^1H-^2H exchange in ^2H_2O using 2-O-benzyl derivatives (77), reduction of aldonolactones with sodium amalgam in ^2H_2O (80), and enzyme-catalyzed solvent exchange (81-84). These methods have been

discussed by Barnett and Corina (85).

Koch and Stuart (86) and Balza et al. (87) have recently prepared deuterated carbohydrates (methylglycopyranosides, oligosaccharides, nucleosides) by ^{1}H-^{2}H exchange in $^{2}H_2O$ in the presence of Raney nickel. Nucleosides are fully deuterated in the base portion, with no incorporation of ^{2}H detected in the glycosyl moiety. Position(s) of deuteration in the carbohydrate derivatives were determined by ^{13}C or ^{1}H NMR since incorporation was not always predictable or specific.

The traditional methods of deuteration, therefore, are limited by the availability of the appropriate carbonyl compound or by the non-specificity of incorporation. In addition, reduction of *keto* derivatives is complicated by the formation of two diastereomeric products, which must be separated.

Hydrogenolysis of aldononitriles provides a convenient and simple method for the incorporation of ^{2}H into the simple aldoses and aldose phosphates in 70 to 80 percent yield. An aldose is condensed with cyanide at pH 8.0 ± 0.5 to produce the 2-epimeric cyanohydrins, which are stabilized by lowering the pH to 4.0. The cyanohydrins are hydrogenolyzed in $^{2}H_2O$ solution with $^{2}H_2$ over palladium to yield the [1-^{2}H]-enriched 2-epimeric aldoses having one more carbon than the parent compound. The aldoses can be separated as described previously (88, 89). [^{2}H]-Enriched aldose phosphates can be prepared from aldononitrile phosphates in a similar fashion.

Isotopes of oxygen (^{17}O, ^{18}O) are commonly introduced into carbohydrates by oxygen exchange between a carbonyl derivative and isotopically-labeled water (90) and are trapped by reduction of the carbonyl with $NaBH_4$. A complementary method involves oxygen-exchange between

O-1 of an aldose and isotopically-labeled water followed by trapping with cyanide. Hydrogenolysis of the [2-^{17}O,^{18}O] cyanohydrins affords the corresponding aldoses enriched with the oxygen isotope at OH-2.

The method of preparing aldononitriles and reducing them with palladium-barium sulfate provides a means for the independent or simultaneous incorporation of carbon, hydrogen and oxygen (91) isotopes into the carbohydrate molecule, as shown in Scheme IV.

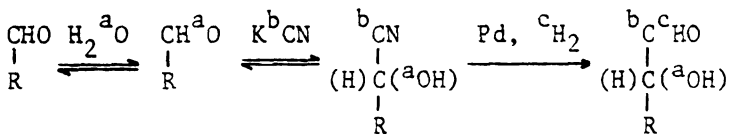

Scheme IV

Starting materials are readily available and the reaction can be applied serially, permitting the preparation of a wide variety of isotopically-enriched carbohydrates and their derivatives.

4. NMR spectroscopy of carbohydrates

a. ^{1}H NMR spectroscopy

A major interest in the study of carbohydrates lies in the determination of the various forms present in solution and in the solid state. The advent of ^{1}H NMR spectroscopy was of utmost importance for the determination of anomeric configuration and conformation of carbohydrates and their derivatives in solution. ^{1}H NMR provides a means to distinguish α- and β-forms of the pyranosyl ring based primarily on H-1 chemical shifts and H-1 — H-2 coupling constants. The predominant conformers (chair) of the pyranose ring ($^{1}C_{4}$ and $^{4}C_{1}$) are separated by large energy barriers, and, therefore, can usually be distinguished from the magnitudes of the coupling constants between H-1 and H-2

(Scheme V).

Conformational analysis of the furanose ring is complicated by a dynamic equilibrium between the various forms (pseudorotation) with small energy barriers between individual conformers (~12-20 KJ mole $^{-1}$). The two major forms are the envelope (E) and twist (T) forms, where one or two atoms are outside the plane of the ring, respectively. If the rate of interconversion between conformers is sufficiently rapid, the observed chemical shifts and couplings represent weighted averages of chemical shifts and couplings of the individual conformers.

Studies on the configuration and conformation of carbohydrates in solution using ^{1}H NMR are based on the dihedral-angle dependence of vicinal (three-bond) proton coupling constants discovered by Karplus (92). This relationship states that dihedral angles of 0° and 180° produce maximal ^{1}H-^{1}H coupling (8-10 Hz) while a dihedral angle of 90° produces a minimum value (0-1 Hz). The equation had the following form,

$$^{3}J_{H,H'} = A + B\cos\ \Theta + C\cos\ 2\Theta$$

where Θ = dihedral angle, A = 4.42 Hz, B = -0.5 Hz and C = 4.5 Hz. The equation was calculated based on a carbon-carbon bond length of 1.543 Å with both carbons sp^{3}-hybridized. Karplus (93) has emphasized, however, that the relationship between coupling constant and dihedral angle is subject to parameters other than dihedral angle, namely, the electronegativity of substituents and carbon-carbon and carbon-hydrogen bond lengths. Estimations of dihedral angles to an accuracy of one or two degrees is tenuous at best.

The use of ^{1}H NMR to determine anomeric configuration and

conformation of carbohydrates and other cyclic compounds has been discussed by several investigators (94-98). The composition and conformation of carbohydrates in solution has been reviewed by Angyal (99). Conformations of deoxyribose and ribose moieties in nucleosides, nucleotides, and oligonucleotides were recently discussed by Davies(100).

In brief review, Hall (101) examined the conformations of several benzoylated ribofuranosides by ^{1}H NMR using a modified Karplus equation for application to the carbohydrate molecule,

$$J = J_o \cos^2 \theta - 0.28$$

where J_o = 9.26 Hz for $0 \leq \theta \leq 90°$ and J_o = 10.36 Hz for $90° \leq \theta \leq 180°$. Results from this study showed that 1,3,5-tri-O-benzoyl-α-D-ribofuranose has the E^1 conformation, that is, C-2, C-3, C-4 and O-4 are essentially co-planar with C-1 above the plane defined by these nuclei.

In 1966, Lemieux and Stevens (77) examined the 100 MHz ^{1}H NMR spectra of D-xylose, D-lyxose, D-arabinose, D-ribose, D-glucose, D-mannose and D-galactose. Anomeric protons were observed at 4.6-5.3 ppm relative to tetramethylsilane (Me_4Si), and the remaining protons were observed upfield (3.3-4.2 ppm). Generally, axial protons on the pyranosyl ring were found to produce signals at higher field than equatorial protons when the compounds considered were epimeric and both in the same chair conformation. This correlation facilitated the determination of the proportions of anomeric forms in solution. Vicinal coupling between H-1 and H-2 was used to establish preferred conformations, since this parameter is often sensitive to conformational change, as shown in Scheme V. Conformational preferences based on ^{1}H NMR data

are in close agreement with those determined from free energy calculations (99).

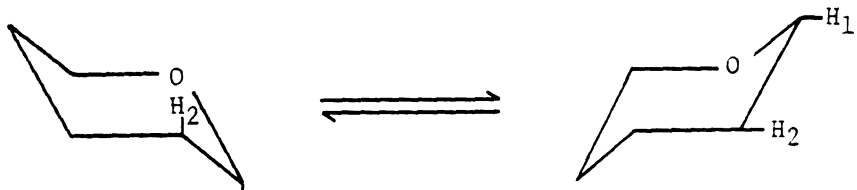

$^4C_1$ = aa — dihedral angle = 180° — predicted $^3J_{H1,H2}$ = 8.6-11.5 Hz

$^1C_4$ = ee — dihedral angle = 60° — predicted $^3J_{H1,H2}$ = 0.6-3.5 Hz

Scheme V

In 1967, Stevens and Fletcher (102) examined the 60 MHz ^{1}H NMR spectra of several furanoid derivatives of D-arabinose, D-lyxose, D-ribose and D-xylose. As discussed above, conformational analysis of the furanoid ring is complicated by pseudorotation, resulting in uncertainties in the dihedral angles between vicinal hydrogen nuclei. Despite these difficulties, preferred conformations were assigned to the various pentofuranosides, although conclusions were highly speculative. The study was also complicated by near magnetic-equivalence of coupled nuclei causing second or greater order behavior in the spectra. Equations were required to determine intrinsic ^{1}H-^{1}H coupling constants from the experimental (apparent) values. In addition, compounds were studied in deuterated chloroform and extrapolation to conformation in aqueous media, where water may play a role in ring stabilization through hydrogen bonding, cannot easily be made. Stevens and Fletcher (102) also observed that, generally, furanoid rings with OH-1 and OH-2 trans have H-1 at higher fields than those with OH-1 and OH-2 cis.

In 1971, Alfoldi et al. (103) studied the conformations of several methyl O-methyl-D-xylofuranosides in pyridine by ^{1}H NMR and concluded

that the α-anomers prefer $^{2}T_{1}$, ^{2}E and $^{2}T_{3}$ conformations, while the β-anomers prefer $^{2}T_{3}$, ^{3}E and $^{3}T_{4}$ conformations. Angyal and Pickles studied the equilibria between the pyranoses and furanoses for the aldoses (104) and deoxyaldoses (105) by ^{1}H NMR, and, recently, De Bruyn and Anteunis (106) established the conformation of β-L-arabinopyranose ($^{4}C_{1}$) in aqueous solution by ^{1}H NMR at 300 MHz . Horton and his colleagues (107) have used ^{1}H NMR to determine the conformation of linear carbohydrates and their derivatives in solution.

In general, ^{1}H NMR spectra of the free aldoses are complicated by the presence of two or more forms in solution. Line-multiplicity and resonance overlap hinder full interpretation, especially for the pentoses and hexoses, which have six and seven non-exchangeable protons for each form, respectively. Selective ^{1}H-decoupling, selective deuteration and analysis at high magnetic fields have been utilized to facilitate the analysis of complex ^{1}H NMR spectra. It is noted that anomeric configuration and conformation cannot be easily determined by ^{1}H NMR of the cyclic ketoses, since these compounds do not possess an anomeric proton.

b. ^{13}C NMR spectroscopy

^{13}C NMR spectroscopy offers an alternative to ^{1}H NMR spectroscopy for configurational and conformational analysis of carbohydrates, but more often complements ^{1}H NMR. In contrast to protons which typically resonate over 10 ppm of the applied magnetic field, carbons typically resonate over 200 ppm, which minimizes apparent magnetic-equivalence between dissimilar carbons. ^{13}C NMR spectra are normally obtained with broad-band ^{1}H-decoupling (108) which effectively removes line-multiplicity due to ^{13}C-^{1}H coupling. Although information from ^{13}C-^{1}H

coupling is lost, ^{1}H-decoupled ^{13}C NMR spectra are simple and usually more easily interpreted than ^{1}H NMR spectra. ^{1}H-Coupled spectra can be obtained, however, when ^{13}C-^{1}H coupling constants need to be evaluated. Moreover, ^{13}C NMR spectra of un-enriched compounds are not complicated by ^{13}C-^{13}C coupling, since ^{13}C has a low natural abundance (1.1 percent). Carbon spectra can also be obtained in water, a convenient and common solvent for carbohydrates, without solvent-line interference.

^{13}C NMR has been used to determine the various forms of carbohydrates present in solution. For example, D-erythrose can potentially exist as five or more forms in solution, as shown in Figure 6: α-furanose, β-furanose, aldehydo, hydrate and dimers and/or oligomers. The 15.08 MHz ^{13}C NMR and 180.04 MHz ^{1}H NMR spectra of D-erythrose are shown in Figure 7. The carbon spectrum is noticeably simpler. The anomeric regions for C-1 (89-105 ppm) and H-1 (5.00-5.30 ppm) are easily identified as downfield from the remaining nuclei. Three major tautomeric forms are observed in both spectra: α-furanose, β-furanose and hydrate (h). Resonance assignments were made as described in later sections. The ^{1}H-decoupled ^{13}C NMR spectrum shows one resonance for each carbon, whereas the ^{1}H spectrum shows multiplets for each proton that arise from ^{1}H-^{1}H coupling. The proton spectrum of D-erythrose is relatively simple compared with those of other aldoses.

^{13}C NMR offers a means to determine the tautomeric equilibria of the ketoses, since anomeric carbons are observed in the spectra. Que and Gray (109), Angyal et al. (110) and Angyal and Bethell (111) have studied equilibrated mixtures of the ketohexoses, 1-deoxyhexuloses, and 3-hexuloses, respectively, by ^{13}C NMR. Furanose, pyranose and keto forms were detected, but keto hydrate forms were not observed in the

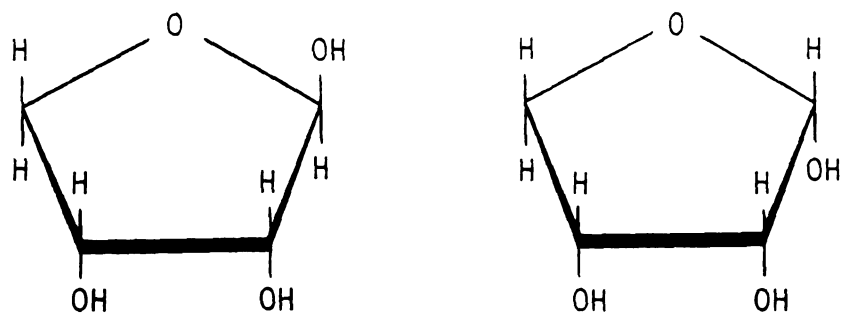

β - furanose

α - furanose

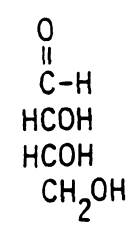

aldehydo

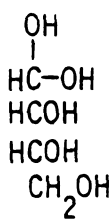

hydrate

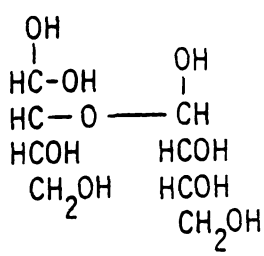

dimers and oligomers

Figure 6. Possible forms of D-erythrose in solution.

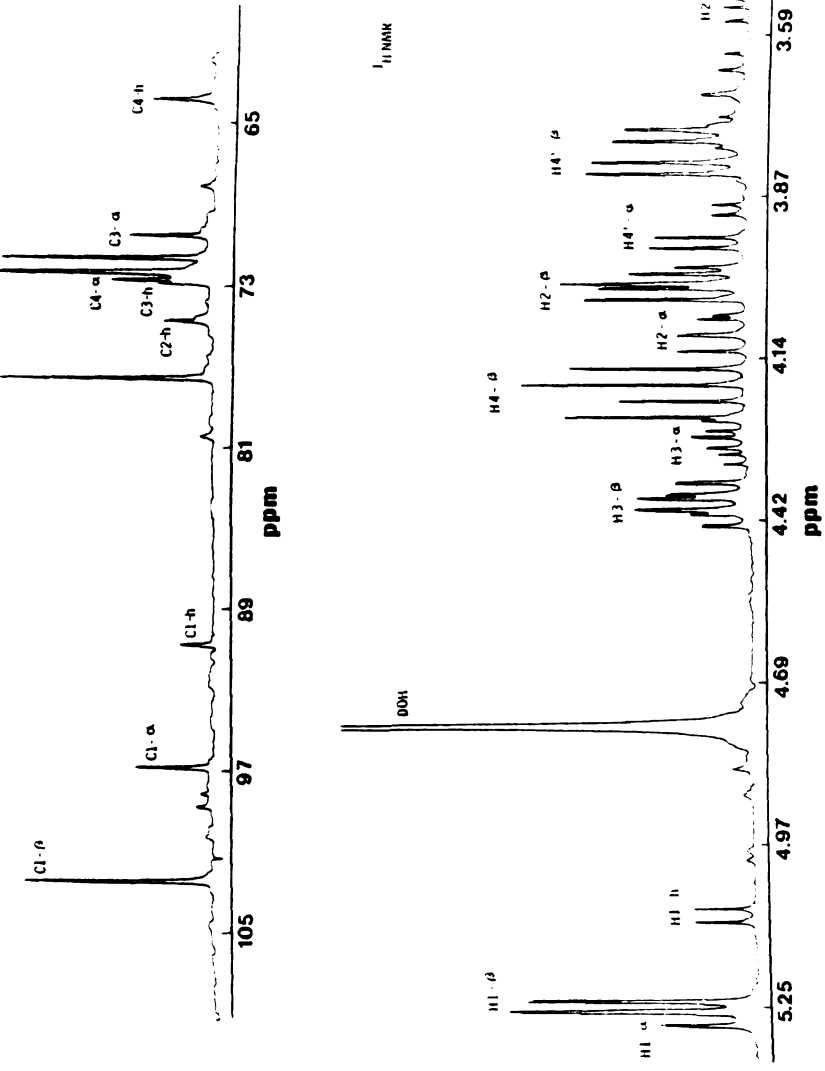

Figure 7. 15.08 MHz ^{13}C NMR and 180.04 MHz ^{1}H NMR spectra of D-erythrose in H_2O and $^{2}H_2O$, respectively.

compounds studied.

Assignments of ^{13}C chemical shifts are established by several methods: (a) the effect of substitution (derivatization) on chemical shift, (b) the magnitudes of scalar or one-bond ^{13}C-^{1}H coupling constants, (c) deuterium isotope shifts, and (d) selective [^{13}C]-enrichment. Rules derived from the effects of substitution on ^{13}C chemical shifts are not always reliable, as discussed by Walker et al. (59), and incorrect assignments have been made based on these rules (112, 113). Ritchie et al. (114) examined the carbon spectra of the methyl glycofuranosides and cyclopentanols and assigned ^{13}C chemical shifts based on substituent effects and shielding factors. For the furanoid ring, however, changes in shielding cannot be totally attributed to configurational factors since conformational components, presently unknown, probably make a major contribution to shielding.

Bock et al. (115), Bock and Pedersen (116) and Bock and Pedersen (117) have measured direct ^{13}C-^{1}H coupling constants ($^{1}J_{C,H}$) in the hexopyranoses, pentopyranoses and their derivatives and have specifically related $^{1}J_{C1,H1}$ to anomeric configuration and conformation. $^{1}J_{C1,H1}$ is approximately 10 Hz smaller ($\sim$160 Hz) when H-1 is axial than when H-1 is equatorial. One-bond ^{13}C-^{1}H coupling constants for other methine carbons of carbohydrates (e.g., $^{1}J_{C2,H2}$) are approximately 20-25 Hz smaller than $^{1}J_{C1,H1}$.

Gorin (79) and Gorin and Mazurek (118, 119) have exploited the effects of deuterium substitution on ^{13}C and ^{1}H NMR spectra to assign ^{13}C chemical shifts. A signal from a ^{13}C nucleus directly bound to a deuteron either disappears or is converted to a triplet at 0.1-0.5 ppm higher field. Progressively smaller upfield shifts are observed for

signals of the β-carbon(s) (∿0.1 ppm) and γ-carbon(s) (∿0.01 ppm). From isotope shifts, carbon nuclei that are one-, two-and three-bonds from the deuteron can be assigned.

Carbon-13 chemical shifts are easily assigned by specific [^{13}C]-enrichment. The [^{13}C]-enriched nucleus is assigned based on its enhanced detection. An α-carbon will be coupled to the [^{13}C]-enriched nucleus, causing splitting of its resonance into a doublet. The enriched nucleus and carbon(s) α to it are, thereby, unequivocally assigned. Walker et al. (59) prepared [1-^{13}C]hexoses and hexopyranosides and assigned the ^{13}C chemical shifts of C-1 and C-2 based on these effects.

Two-bond ($^{2}J_{C,H}$) and three-bond ($^{3}J_{C,H}$) ^{13}C-^{1}H coupling constants have been measured and related to configuration and conformation. Schwarcz and Perlin (120), Schwarcz et al. (121) and Cyr et al. (122) demonstrated with several carbohydrates and their derivatives that the magnitude and sign of two-bond coupling between ^{13}C and ^{1}H depends on the orientation and electronegativity of the substituents appended to the ^{13}C nucleus relative to the proton. Generally, $^{2}J_{C1,H2}$ is large (∿5 Hz) when H-2 is gauche to both oxygen atoms on C-1. Perlin and his colleagues (121, 122) have observed that the sign of $^{2}J_{C,H}$ depends on configuration, with an oxygen anti to the coupled proton making a positive contribution to coupling and a gauche oxygen making a negative contribution. Walker et al. (59) measured $^{2}J_{C1,H2}$ coupling constants in [1-^{13}C]hexoses and hexopyranosides and in [1-^{13}C]2-amino-2-deoxyaldoses (123) and found them to be consistent with these rules.

Bock and Pedersen (124) have recently related $^{2}J_{C,H}$ to configuration and conformation by considering all the oxygen substituents on

both carbons. For example, consider the Newman projection of methyl β-D-mannopyranoside (Figure 8A) viewed from C-2 to C-1. If the projection of the C-2—OH-2 bond on an axis trans to the C-1—H-1 bond is given the value +1.0 (cos 0°), then the projections of C-1—OH-1 and C-1—O-5 will each be +0.5 (cos 60°) and the projection-sum will equal +2.0. Similar projections obtained from the Newman projection of methyl α-D-galactopyranoside (Figure 8B) give a sum of +0.5 (+0.5 from C-1—O-5 and C-1—OMe and -0.5 from C-2—OH-2). Projection-sums were related to coupling constants as follows: +0.5 = +0 Hz; +1.0 = 0-1 Hz; +1.5 = +5.5 Hz; +2.0 = +9.0 Hz. The projection-sum rule (124) was determined from the study of several pyranosyl carbohydrate derivatives and the furanose rings of 3-O-acetyl-1,2:5,6-di-O-isopropylidene-α-D-allofuranose and 3-O-acetyl-1,2:5,6-di-O-isopropylidene-α-D-glucofuranose.

Schwarcz and Perlin (120) have established a Karplus relationship between $^{3}J_{C,H}$ and dihedral angles for the carbohydrates: 60° ≈ 2 Hz, 100° ≈ 0 Hz, 180° ≈ 6 Hz.

Walker et al. (59) measured $^{2}J_{C1,C3}$ and $^{2}J_{C1,C5}$ in the [1-^{13}C]-hexoses and hexopyranosides and discussed these parameters in terms of a dihedral angle dependence, where the angle is defined by the relative orientations of C-3 and C-5 and the electronegative oxygen substituents. $^{3}J_{COCC}$ coupling between C-1 and C-6 was also observed.

Marshall and Müller (125) and Barfield et al. (126) have discussed the angular dependence and substituent dependence of $^{3}J_{C,C}$ for aliphatic carboxylic acids and alcohols, and alicyclic alcohols, respectively. Dihedral angles of 0°, 80° and 180° produce $^{3}J_{C,C}$ values of 2 Hz, 0 Hz and 4 Hz, respectively. $^{3}J_{C,C}$ in the carbohydrates has not

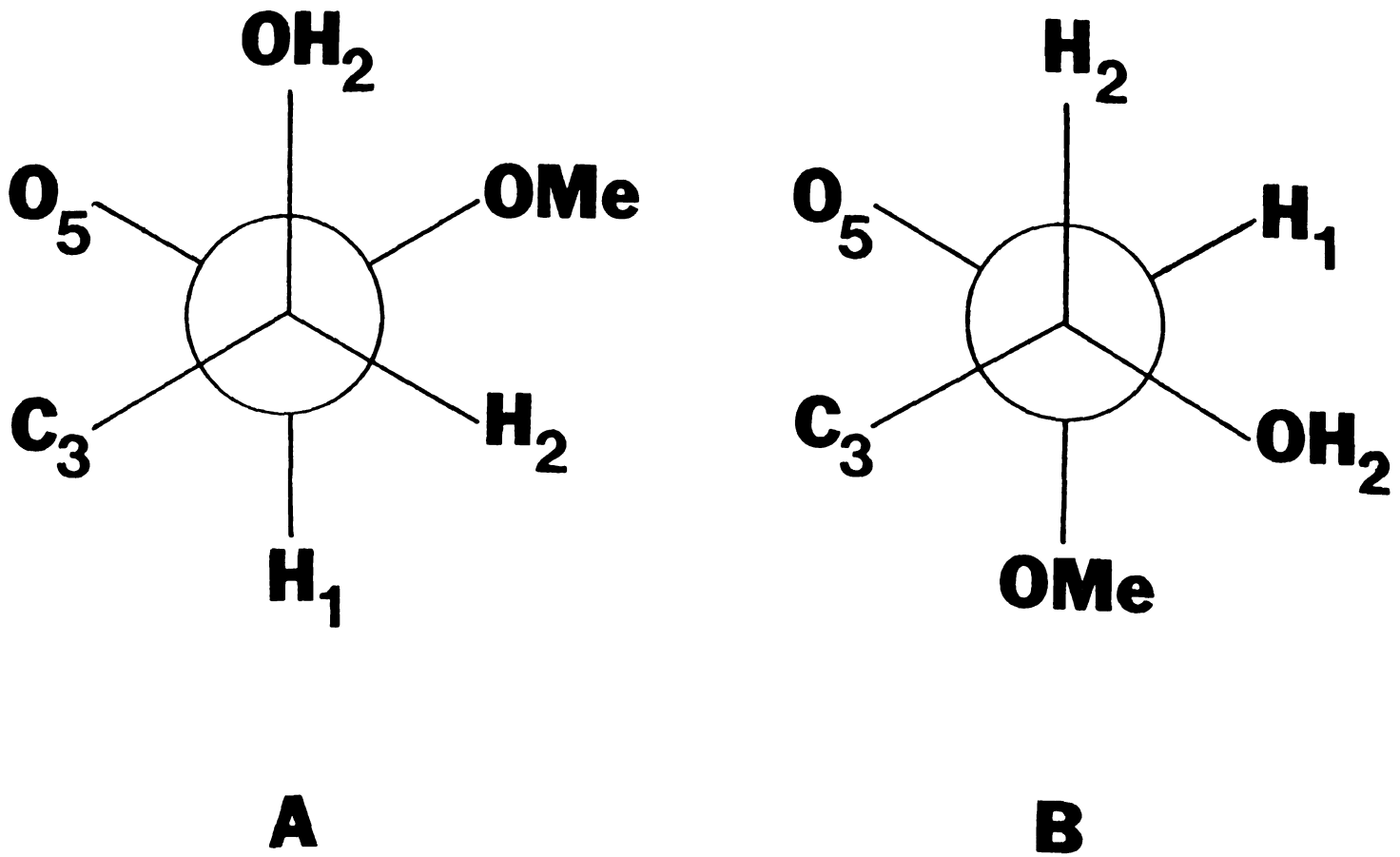

Figure 8. Newman projections of methyl β-D-mannopyranoside (A) and methyl α-D-galactopyranoside (B).

been systematically examined.

In summary, the analysis of carbohydrates by ^{1}H and ^{13}C NMR has been limited to a large extent by the availability of [^{13}C]- and [^{2}H]-enriched derivatives. ^{13}C Chemical shifts can be unequivocally established with [^{13}C]-enriched compounds. Tautomeric forms in solution can be determined with carbohydrates enriched with ^{13}C at the anomeric carbon. Orientational and substituent dependencies of $J_{C,H}$ and $J_{C,C}$, which are useful probes of configuration and conformation in solution, can be ascertained only with model compounds enriched at specific sites with ^{13}C and/or ^{2}H. The full interpretation of complex ^{1}H NMR spectra of carbohydrates is greatly facilitated by [^{2}H]-enriched derivatives. With this need in mind, a method was developed to incorporate isotopes of carbon, hydrogen and/or oxygen at almost any site into carbohydrates and their derivatives. A vast array of isotopically-enriched compounds can be prepared for chemical, biochemical, physical and biomedical uses.

II. EXPERIMENTAL

A. Carbon-13 (^{13}C) NMR Spectroscopy

^{13}C NMR spectra were obtained using a Bruker WP-60 Fourier-transform spectrometer equipped with quadrature detection and operating at 15.08 MHz for carbon. Spectra were obtained with 4 K real spectral points and spectral widths of 2400 Hz or 3000 Hz. Filter widths of 2400 Hz or 6000 Hz were employed. The spectrometer was locked externally to the resonance of $^{2}H_2O$ in a capillary. Chemical shifts are reported relative to external tetramethylsilane (Me_4Si) and are accurate to ±0.1 ppm.

B. Proton (^{1}H) NMR Spectroscopy

^{1}H NMR spectra were obtained at 30°C in $^{2}H_2O$ using a Bruker WH-180 Fourier-transform spectrometer operating at 180.04 MHz for ^{1}H. Spectra were obtained with 8 K real spectral points and a spectral width of 400 Hz. Chemical shifts are reported in ppm downfield from internal sodium 3-(trimethylsilyl)-1-propanesulfonate and are accurate to ±0.01 ppm. $^{2}H_2O$ Solutions were treated with $^{2}H_2O$-washed Chelex resin to remove paramagnetic species (127) prior to ^{1}H NMR analysis.

C. Computer Simulation of Complex ^{13}C and ^{1}H NMR Spectra

^{13}C and ^{1}H chemical shifts and coupling constants in complex ^{13}C and ^{1}H NMR spectra were obtained by comparison of the experimental data with the theoretical spectra generated by the ITRCAL program available from the Nicolet Computer Company, Madison, WI. This program permits the calculation of ^{13}C and ^{1}H NMR spectra by first entering reasonable

estimates of the chemical shifts and coupling constants for the nuclei in question and entering the actual frequency of the lines in the experimental spectrum. By changing the chemical shifts, coupling constants, or both, iteration to a best fit of the theoretical with the real spectrum is obtained. The rms error between a simulated and experimental spectrum was typically 0.15 Hz.

D. Gas-Liquid Chromatography (GLC)

Gas-chromatographic analysis was performed on a Varian Aerograph 1200 equipped with flame-ionization detection. A 1.8 m x 2 mm column of OV-17 (3%) on High Performance Chromosorb W-AW (100-200) from Applied Science was used with a temperature program of 100-230°C at 4°/min. For derivatization, aqueous samples (6 µL) were added rapidly to a mixture of 150 µL of N,O-bis(trimethylsilyl)trifluoroacetamide (BSTFA) containing 1% of chlorotrimethylsilane (TMCS) and 150 µL of dry pyridine, and the mixtures were analyzed after 25 min at 60°C. Retention data are reported relative to the pertrimethylsilylated (Me_3Si) derivative of D-gluconate, and GLC peak-areas were calculated from the product of peak-height and peak-width at one-half height.

E. Phosphate and Radioactivity Assays

Quantitative inorganic and organic phosphate assays were performed according to the procedure described by Leloir and Cardini (128). Radioactivity was assayed on a Beckman LS-100 scintillation counter by using a Triton X-100 (1000 mL)-PPO(8 g)-POPOP(0.2 g)-toluene(2000 mL) cocktail. Aqueous sample (0.2 mL) was dissolved in 2.3 mL of the cocktail for analysis.

F. pH Measurements

pH Measurements were performed with a Corning Digital 110 pH meter equipped with a Corning semi-micro combination electrode. pH Adjustments on solutions of aldose phosphates were made at 25°C prior to NMR analysis at the reported temperatures. pH Measurements in ^2H_2O solutions were corrected using the equation, pH = pD - 0.4 (129).

G. Assays for Reducing Sugars, Aldonic Acids, Glycollic Acid, Formaldehyde and Cyanide

Tetrose solutions were standardized as follows: aliquots (1-4 mL containing 0.1-1.0 mmol of aldose) taken from a stock tetrose solution were added at 4°C to 5 mL solutions containing 1 mmole KCN. Reaction mixtures were adjusted to 10 mL volumes with H_2O. After 1 h at 4°C, the reaction mixtures were incubated at 25°C for 50 h, and excess cyanide was determined in each reaction mixture by the Liebig-Dénigès method (40, 130,131). Stock solutions of the tetroses standardized in this fashion were subsequently used to prepare standard curves for the Nelson reducing sugar assay (132). All other quantitative reducing sugar assays were conducted with standard, crystalline compounds using Nelson's assay (132) or Park and Johnson's reducing sugar determination (133).

Formaldehyde was assayed according to the method of Walker (134). Aldonic acids were assayed essentially according to the method of Frisell and MacKensie (135). Neutral samples (1 mL) were treated with 0.1 mL of 0.1 M sodium periodate and incubated at room temperature for 10 minutes at which time 0.1 mL of a 10% solution of $NaHSO_4$ was added followed by 5.0 mL of chromotropic acid (0.2% in 10 M H_2SO_4). The

samples were placed in a boiling water bath for 20 minutes, cooled, and treated with 1.0 mL of 5% thiourea. Samples were read against a reagent blank at 570 nm.

Glycollic acid was assayed by the method of Lewis and Weinhouse (136). Glycosides were assayed with phenol-sulfuric acid (137).

H. Catalytic Hydrogenolysis

Catalytic hydrogenolysis at >1 atm was carried out with a Parr pressure-apparatus and 250-mL reduction flasks.

Reductions at atmospheric pressure were conducted in an apparatus described by Vogel (138). The reaction vessel consisted of a side-arm flask equipped with an addition funnel tightly secured with a rubber stopper, and stirring was provided magnetically.

All catalytic hydrogenolysis reactions were performed at room temperature.

I. Chemicals

Glycolaldehyde, DL-glyceraldehyde, D-arabinose, D-lyxose, D-ribose, D-xylose, D-glucose, D-mannose, D-galactose, D-ribose 5-P, D-arabinose 5-P, D- and DL-glyceraldehyde 3-P dimethyl acetal, 1,3-dihydroxy-2-propanone-P dimethyl ketal, D-fructose 1,6-P_2, DL-glycerol 1-P, disodium adenosine 5'-triphosphate, DL-calcium glycerate, D-ribono-1,4-lactone, DL-sodium 2-hydroxybutyrate, D-gulono-1,4-lactone, palladium-barium sulfate (5%), and deuterium oxide (^2H_2O) (99.8 atom percent) were obtained from Sigma Chemical Company and used without further purification. Formaldehyde (37 percent aqueous solution) was purchased from Mallinckrodt. L-Threonine (allo-free) was obtained from the United

States Biochemical Corporation. D-Calcium galactonate and D-calcium gluconate were purchased from Pfanstiehl Laboratories, Inc.

Potassium [^{13}C] cyanide ($K^{13}CN$) was supplied by the Los Alamos Scientific Laboratory, University of California, Los Alamos, New Mexico with 99.64 percent purity and 90.7 atom percent [^{13}C]-enrichment. Potassium [^{14}C] cyanide ($K^{14}CN$) was obtained from New England Nuclear and had a specific activity of 45-55 mCi/mmol. Lead tetraacetate, deuterium chloride (^{2}HCl) (20%, 99 atom percent) and sodium deuteroxide ($NaO^{2}H$) (30%, 99 atom percent) were obtained from Aldrich Chemical Company. Acetic acid-$^{2}H_4$ (99.5 atom percent) and deuterium gas ($^{2}H_2$) (99.5 atom percent) were obtained from Merck Sharpe and Dohme Canada Limited.

Ion-exchange resins were purchased from Sigma Chemical Company and converted to the appropriate forms. N,O-Bis(trimethylsilyl) trifluoroacetamide (BSTFA) containing 1% chlorotrimethylsilane (TMCS) was obtained from Pierce Chemical Company. Pyridine for gas chromatographic analyses was distilled from barium oxide and stored over 4 Å molecular sieves.

Glycerol kinase (EC 2.7.1.30) from *E. coli*, D-fructose-1,6-P_2 aldolase (EC 4.1.2.13) from rabbit muscle, alkaline phosphatase (EC 3.1.3.1), acid phosphatase (EC 3.1.3.2) from potato, triose-phosphate isomerase (EC 5.3.1.1) from yeast, D-ribose 5-P isomerase (EC 5.3.1.6) from yeast, D-ribulose 5-P kinase (EC 2.7.1.19) from spinach, hexokinase (EC 2.7.1.1) from yeast, phosphoglucose isomerase (EC 5.3.1.9) from yeast, phosphofructokinase (EC 2.7.1.11) from rabbit muscle and myokinase (EC 2.7.4.3) from rabbit muscle were purchased from Sigma Chemical Company.

J. General Syntheses and Purifications

D-Glyceraldehyde was prepared from D-fructose by oxidation with lead tetraacetate (139). D-Lactaldehyde was prepared from L-threonine by the method of Zagalak et al. (140). 2,4-O-Ethylidene-D-erythrose was prepared according to Perlin (141). Aqueous solutions adjusted to pH ∿8 with dilute NaOH contained approximately 95 percent monomer as determined by ^{13}C NMR. Hydrolysis of this compound with 0.12 M sulfuric acid at 90°C for 35 min yielded D-erythrose (87%). The acidic solution was neutralized with barium carbonate, the mixture filtered through Celite, and the filtrate decolorized with charcoal and deionized with Dowex 1 X8 (OAc^-) and Dowex 50 X8 (H^+). Aqueous solutions of D-erythrose at 0.5 M contain approximately 5 percent dimers and/or higher-order structures. 2,4-O-Ethylidene-D-threose was prepared according to Ball (142). D-Threose was prepared from the acetal as described for the preparation of D-erythrose and was estimated to be greater than 95 percent by ^{13}C NMR.

D-Sodium xylonate and DL-[1-^{13}C]glyceric acid were prepared by hypoiodite oxidation of D-xylose and DL-[1-^{13}C]glyceraldehyde, respectively (143). D-[1-^{13}C]Arabinonamide and D-[1-^{13}C]ribonamide were prepared from the corresponding lactones by the method of Hudson and Komatsu (144).

D-Arabinono-, D-ribono-, D-lyxono- and D-xylononitriles were prepared from the corresponding aldononitrile phosphates (preparation described in Section II, L3a). The aldononitrile 5-phosphates were dephosphorylated by incubating the phosphate overnight at 34°C with potato acid phosphatase (5-10 mg) at pH 4.0. When inorganic P was greater than 90% of the total P present, the reaction mixture was treated with

an equal volume of hot ethanol, incubated for 15 min at 34°C, and centrifuged at 12,000 rpm to remove protein. The supernatant was treated consecutively with Dowex 1 X8 (OAc^-) and Dowex 50 X8 (H^+) to remove organic and inorganic P. The pH of the nitrile solution was maintained below 5 to prevent epimerization. The final solution was concentrated *in vacuo* at 30°C prior to assay by GLC and ^{13}C NMR. Epimeric purity was greater than 95 percent by ^{13}C NMR.

Mixtures of D-[1-^{13}C]sodium ribonate and arabinonate (5 mmol) were purified by chromatography at 25°C on a 2.2 x 51 cm column packed with Dowex 1 X8 (200-400 mesh) resin in the acetate form. Aldonates were applied at pH 9-10 and the column was developed with 0.5 M acetic acid. Fractions (5 mL) were collected at a flow rate of 0.5 mL per min and D-[1-^{13}C]ribonic acid eluted between fractions 200-215. D-[1-^{13}C]Arabinonic acid eluted between fractions 80-120 after changing the eluent to 1 M acetic acid. Aldonic acids were detected by radioactivity or by chromotropic acid assay. Fractions containing the aldonic acids were pooled and evaporated at 35°C *in vacuo* to remove acetic acid. Gas-liquid chromotography and ^{13}C NMR of the corresponding C-2 epimeric sodium salts and standard sodium D-ribonate established configuration and purity (>95%).

Mixtures of D-[1-^{13}C]sodium xylonate and lyxonate (2 mmol) were purified on a similar column at 4°C. The column was developed with a linear gradient of acetic acid (0.3 M - 0.5 M, 4000 mL) at 7.5 mL per 15 min fraction, followed by 0.5 M acetic acid. D-[1-^{13}C]Xylonic acid eluted first (fractions 475-520), followed by D-[1-^{13}C]lyxonic acid (fractions 545-620). Fractions containing the aldonic acids were pooled and evaporated at 35°C *in vacuo* to remove acetic acid. ^{13}C NMR

of the corresponding C-2 epimeric sodium salts and standard sodium D-xylonate established configuration and purity (>95%).

Mixtures of D-sodium erythronate and threonate (2.5 mmol) were purified by chromatography at 4°C on a 2.2 x 60 cm column packed with Dowex 1 X8 (200-400 mesh) resin in the acetate form. The column was developed with a linear gradient acid (3 L, 0.1-0.6 M) followed by 0.6 M acetic acid until the acids eluted as two peaks. Fractions (4 mL) were collected at 0.4 mL per min. Fractions containing the aldonic acids were pooled, and evaporated at 35°C *in vacuo* to remove acetic acid. Gas-liquid chromatography and ^{13}C NMR of the corresponding C-2 epimeric sodium salts and standard sodium threonate established configuration and purity (peak 1, >95% *erythro*; peak 2, >95% *threo*).

D-[1-^{13}C]Ribono-1,4-lactone, D-[1-^{13}C]arabinono-1,4-lactone and D-[1-^{13}C]lyxono-1,4-lactone were prepared by passage of the corresponding purified [1-^{13}C]aldonates through columns containing a tenfold excess of Dowex 50 X8 (200-400 mesh) in the H^+ form and eluting with deionized H_2O. Solutions of the free acids were concentrated to gums at 30°C *in vacuo* and the residues were stored *in vacuo* at 25°C over $MgClO_4$. Lactonization was determined by ^{13}C NMR analysis and, in most cases, was complete in 2-5 days.

Preparation of D-[1-^{13}C]xylono-1,4-lactone by the above method resulted in a mixture containing lactone and other intermolecular esterification products. The 1,4-lactone was prepared by incubating D-[1-^{13}C]xylonic acid at 50°C and pH <1 (HCl) for 30 h. The resulting mixture contained 35% aldono-1,4-lactone and 65% free acid. This mixture was analyzed by ^{13}C to determine ^{13}C chemical shifts and $J_{C,C}$ for the 1,4-lactone.

D-[1-^{13}C]Arabinono-1,5-lactone and D-[1-^{13}C]ribono-1,5-lactone were prepared by catalytic oxidation of D-[1-^{13}C]arabinose and D-[1-^{13}C]ribose, respectively, with Pt/O_2 as described by Conchie et al. (145).

D- and DL-Glyceraldehyde 3-P were prepared from the acetals as described by Ballou and MacDonald (146). 1,3-Dihydroxy-2-propanone phosphate was prepared from the ketal as described by Ballou (147). Silver carbonate (Ag_2CO_3) was prepared from silver nitrate and sodium carbonate as described by McCloskey and Coleman (148).

Glycolaldehyde Phosphate. Disodium DL-glycerol 1-P hexahydrate (8.6 g, 27 mmol) was moistened with 5 mL of H_2O and dissolved in 400 mL of glacial acetic acid with efficient stirring. Upon dissolution of the salt, 1.7 mL of 18 M sulfuric acid was added (149), and addition of lead tetraacetate (24 g, 54 mmol) was made during 15 min. After 2 h, oxalic acid (4.5 g, 50 mmol) was added and stirring was continued for an additional 30 min. The suspension was filtered through Celite and the filtrate was concentrated at 30°C *in vacuo* to approximately 30 mL. The filter cake was washed with 200 mL of H_2O, the concentrate and washings were combined, and barium acetate (13 g, 50 mmol) was added with efficient stirring at 4°C for 15 min. The white suspension was filtered through Celite, the filter was washed with H_2O, and the filtrate and washings were treated with excess Dowex 50 (H^+). The suspension was filtered, the solution concentrated as before to about 200 mL, and the concentrate extracted overnight at 4°C with diethyl ether in a continuous liquid-liquid extraction apparatus. The aqueous solution was recovered, concentrated as before to about 30 mL, and stored at -20°C. Yield: 25 mmol (93%) by total P with a trace of inorganic P. Purity: at least 95% by

^{13}C NMR.

D-Glyceraldehyde 3-P. Disodium D-fructose 6-P dihydrate (3.4 g, 10 mmol) was treated with lead tetraacetate (18 g, 40.5 mmol) in the manner described for the preparation of glycolaldehyde-P, except that 1.1 mL of 18 M sulfuric acid (20 mmol) was added prior to the addition of the oxidant. After Dowex 50 (H^+) treatment, the acidic solution of 2-O-glycoloyl-D-glyceraldehyde 3-P was concentrated to 10 mL and stored at 25°C for 18 h to yield D-glyceraldehyde 3-P and glycollic acid. Alternatively, hydrolysis can be carried out by incubating the acidic solution at 40°C for 6 h. The resulting solution was adjusted to pH 5.5 with 2 M NaOH and applied to a DEAE-Sephadex A-25 (40-120 mesh) column at 4°C in the acetate form, washed with a small amount of H_2O and eluted with a linear gradient of sodium acetate (1500 mL, 0.05-0.6 M, pH 5.5 ± 0.1). Glyceraldehyde 3-P eluted at 0.15 M sodium acetate and was preceded by glycollic acid. Fractions were assayed for D-glyceraldehyde 3-P by organic P analysis and for glycollic acid by the method of Lewis and Weinhouse (136). Fractions containing D-glyceraldehyde 3-P were pooled, treated with excess Dowex 50 (H^+), and concentrated twice *in vacuo* at 30°C to approximately 5 mL to remove acetic acid. Yield: 8.1 mmol (81%) by organic P analysis with a trace of inorganic P. Purity: at least 95% by ^{13}C NMR.

K. Analysis of Cyanohydrin Reaction Mixtures

1. Gas-liquid chromatography (GLC)

Reactions were carried out in 15-mL centrifuge tubes, reaction mixtures were incubated at 18° ± 1°C (water bath) and stirring was provided magnetically. For reactions without pH control, the tube was

charged with KCN (0.6 mmol in 1.2 mL H_2O), followed by the aldose solution (0.6 mmol in 0.8 mL H_2O).

For reactions at controlled pH, the vessel containing the cyanide solution (1.1 mL) was sealed with a stopper fitted with a pH electrode and three polyethylene tubing inlets for adding 4 M HCl, 1 M NaOH and the aldose solution. The pH of the solution (~11) was adjusted to the desired value with 4 M HCl. The aldose solution (0.8 mL) was then added over a period of 0.5 min with efficient stirring. The pH was controlled to ±0.2 units by the addition of 4 M HCl and/or 1 M NaOH. Aliquots were withdrawn at various time intervals , derivatized with BSTFA, and analyzed by GLC.

2. ^{13}C NMR spectroscopy

Reaction mixtures were prepared as described above except that $K^{13}CN$ was used. Reactions without pH control were studied by mixing equal volumes (1 mL) of equimolar solutions of $K^{13}CN$ and aldose in a 10 mm NMR tube. Reaction mixtures at controlled pH were assayed at various times by transferring a 0.5-mL aliquot from the reaction vessel to a 0.5-mL coaxial NMR insert tube. The probe was maintained at 18°C ± 1°C during data acquisition.

To improve detection and quantitation, 55° pulses and 5 sec delay times were employed. Computer integrated peak areas were used to provide quantitation. The areas of all peaks were summed and the proportion of each peak taken in relation to the total.

L. Preparation of Carbon-13 Enriched Aldoses

1. Pentoses and hexoses

a. General method for the preparation of aldononitriles

A three-neck, 25-mL round-bottom flask was constructed as shown in Figure 9. In a typical preparation, the flask is immersed in a water bath at 18°C and charged with an aqueous solution of sodium cyanide (13 mL) prior to sealing the center neck. Port A is clamped and a 10 mL volume of air withdrawn from port B with a syringe. Port B is sealed. Acetic acid (3 M) is added from syringe C until the desired initial pH of the cyanide solution is reached. Port A is opened and the solution of aldose (6 mL) is added slowly from a syringe with efficient stirring. The pH is adjusted during the reaction by addition of 3 M acetic acid or 1 M sodium hydroxide from syringes C and D as required. Samples are withdrawn from port A at 10 min time intervals and the extent of reaction determined by GLC. After the reaction is complete, the pH is lowered to 4.2 ± 0.1 and the contents of the flask are reduced over palladium-barium sulfate.

Concentrations of sodium cyanide and starting aldose, pH requirements, yields and ratios of the epimeric aldononitriles are listed for specific aldoses in Table VI of Results and Discussion. GLC retention times for the Me_3Si derivatives of aldononitriles relative to that of the D-gluconate derivative are given in Table II of Results and Discussion.

b. Catalytic reduction of aldononitriles

Palladium-barium sulfate (5%, 62 mg per mmol of nitrile) was weighed into a 250-mL flask, 10 mL of water was added, and the suspension was reduced with hydrogen at 4.2 kg/cm^2 (60 lb in^{-2}) for 10 min

Figure 9. Reaction vessel for the preparation of aldononitriles.

The necks were sealed with rubber stoppers. Inlets for ports A and B were constructed from 18-gauge needles and PE-60 polyethylene tubing. Inlets for syringes C and D were constructed from 25-gauge needles and PE-20 tubing for finer regulation during additions. Port A contained the reactant aldose solution. Port B was used to withdraw air from the sealed flask. Syringes C and D contained acetic acid (3 M) and sodium hydroxide (M) solutions. The entire assembly was immersed in a water bath at 18° ± 1°C, and stirring was provided magnetically. A, port A; B, port B; C, syringe C; D, syringe D; E, pH electrode; F, 25-mL flask; G, stirring bar; and H, pinch clamps.

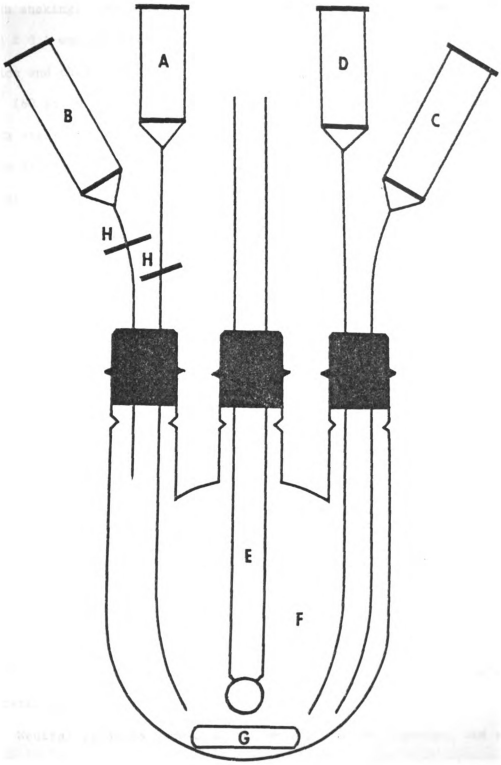

Figure 9.

with shaking. The solution of the C-2 epimeric aldononitriles at pH 4.2 ± 0.1 was transferred to the reduction vessel, which was evacuated twice and then filled with hydrogen to an initial pressure of 4.2 kg/cm^2 (60 lb in^{-2}). The reduction was allowed to proceed for 2 h at 25°C with vigorous agitation, after which time a decrease in hydrogen pressure of 0.14 kg/cm^2 (2 lb in^{-2}) per mmol of nitrile was observed. After completion of the reaction, the solution was filtered through Celite to remove the catalyst. The pH of the filtrate was 4.8 ± 0.2.

c. Purification of the reduction mixture

The filtrate containing the reduction products was acidified to pH 2.8 ± 0.2 with batchwise addition of Dowex 50 X8 (H^+) to remove amine byproducts. The resin was recovered by filtration and washed with dilute acetic acid, and the filtrate and washings were concentrated to a syrup. Hydrolysis products formed during the preparation of the nitriles were removed by dissolving this syrup in water and adjusting the solution to pH 9.5 with dilute sodium hydroxide. After 30 min at room temperature, the alkaline solution was applied to a column of Dowex 1 X8 (OAc^-) that was eluted with water. The effluent was collected in a flask containing an excess of Dowex 50 X8 (H^+). This solution contained the product aldoses and unreacted starting aldose, which are separable by chromatography on ion-exchange resins (88, 89). Aldonic acid byproducts were recovered from the resin by elution with 1 M acetic acid.

Neutral products were analyzed by ^{13}C NMR spectroscopy, and reduced with sodium borohydride for GLC analysis of the alditols.

2. Formaldehyde, glycolaldehyde, glyceraldehyde, and the tetroses

a. Preparation of aldononitriles

Two-, three- and four-carbon aldononitriles were prepared by using the apparatus described in Figure 9. The flask is charged with 0.15 M $K^{13}CN$, sealed, and the pH adjusted to 8.5 ± 0.1 with 2.0 M acetic acid. The starting aldose is added so that the final concentration of both $K^{13}CN$ and aldose is 0.1 M. The pH is maintained at 8.5 ± 0.1 by addition of 2.0 M acetic acid or 1 M sodium hydroxide as required. Samples are taken for analysis of the aldononitriles by GLC or ^{13}C NMR at 10 min intervals. All condensations were complete (>95%) in 20-30 min and virtually no hydrolysis had occurred. The pH was adjusted to 4.0 with 6.0 M acetic acid and then to 1.7 ± 0.1 with 6.0 M hydrochloric acid. At this pH, the aldononitriles are stable for several weeks at 4°C. The preparation and purification of glycolonitrile has been described previously (150). In the present study, this compound and the other aldononitriles were used without purification.

[^{13}C]Formaldehyde was prepared from a solution (0.1 M) of $K^{13}CN$ at 5°C after adjusting the pH as already described, prior to reduction. Caution should be exercised in the preparation of formaldehyde and glycolaldehyde, as hydrogen chloride and formaldehyde on contact can produce the potent carcinogen, bis(chloromethyl)ether (151).

b. Reduction of short-chain aldononitriles

Palladium-barium sulfate (5%, 62 mg per mmol of nitrile) was weighed into a side-arm flask, 5-10 mL of water was added, and the suspension reduced with hydrogen for 15-20 min at atmospheric pressure and 25°C with efficient stirring. During this period, the suspension

changed from brown to a whitish-gray tint. The solution of aldononitriles at pH 1.7 ± 0.1 was added from an addition funnel, and the reduction vessel was evacuated three times prior to a final charging with hydrogen. Reduction times varied with the aldononitrile: hydrogen cyanide, 8 h; glycolonitrile, 18 h; glyceronitrile, 8-10 h; erythrono- and threononitriles, 18 h. Completion of the reaction was determined by ^{13}C NMR and GLC. GLC Retention times for the Me_3Si derivatives of the short-chain aldoses relative to that of the D-gluconate derivative are given in Table II in Results and Discussion. After reduction, the mixture was freed of catalyst by filtration through Celite.

For the preparation of [^{13}C]formaldehyde, the reduction flask was cooled to 5°C prior to the addition of hydrogen cyanide, and the reduction was started immediately after addition, omitting evacuation. The reaction vessel was allowed to warm to room temperature slowly during the reduction.

c. Purification of the reduction mixture

The filtrate containing the reduction products was treated with an excess of Dowex 50 X8 (H^+) resin to remove amine byproducts. This step should be completed immediately after reduction to minimize reaction between byproduct amines and the desired aldose. The resin was removed by filtration and the acidic solution treated with an excess of silver carbonate with stirring until the pH was approximately 6.5. The precipitate (AgCl and Ag_2CO_3) was removed by filtration through Celite and the filtrate treated with an excess of Dowex 50 X8 (H^+) resin with stirring for 60 min at 25°C. After removal of the resin, the clear solution was concentrated at 30°C *in vacuo* to 30 mL and

treated again with Dowex 50 X8 (H^+) for 30 min. The mixture was filtered through Celite, concentrated at 30°C to 30 mL, and treated with an excess of Dowex 1 X8 (200-400 mesh) resin in the acetate form for 10 min. The solution was filtered, concentrated to 3 mL at 30°C, and analyzed by ^{13}C NMR and GLC. Erythrose and threose were separated at 25°C on a column (2.2 x 92 cm) of Dowex 50 X8 (200-400 mesh) resin in the barium form (88); 4 mL fractions were collected at 0.4 mL per min. Threose was eluted between fractions 55 and 65, and erythrose between fractions 105 and 122. Unreacted C_4 nitriles and glyceraldehyde eluted with threose. The column capacity exceeded 4 mmol of tetrose.

Concentration of acidic solutions (pH <2) of erythrose and threose produced oligomeric mixtures of these sugars. Oligomerization may be reversed by heating a 50-70 mM solution of oligomers for 30 min at 90°C with the addition of dilute sulfuric acid to a final concentration of ~0.02 M. The acidic solution, after being neutralized with barium carbonate, and deionized with Dowex 1 (OAc^-) and Dowex 50 (H^+) resins, contains only monomeric tetroses, as evaluated by ^{13}C NMR spectroscopy.

3. Triose, tetrose and pentose phosphates

a. Preparation and purification of aldononitrile phosphates

The $K^{13}CN$ solution (0.15 M) containing 10^7 cpm of $K^{14}CN$ was placed in the sealed flask described in Figure 9 and cooled to 5°C with an ice bath prior to adjustment to pH 8.0 ± 0.1 with 2 M acetic acid. The solution of aldose phosphate at pH 7.5 was added while maintaining the pH of the reaction mixture between 7.5 and 8.0 with additions of 2 M acetic acid and/or 1 M NaOH. Stoichiometric amounts of aldose phosphate and cyanide were used, and the final concentration of

reactants was 0.05-0.1 M. After 15 min at 5°C and pH 7.5-8.0, the ice bath was removed and the reaction mixture allowed to warm to 25°C over a period of 30-40 min. The pH was then adjusted to pH 4.0 ± 0.2 with 2 M acetic acid. Condensation was complete (>95%) when assayed by ^{13}C NMR using a short pulse width (10 μs, 55°) and long delay time (10 s) to facilitate aldononitrile detection.

The racemic mixture of glyceronitrile phosphate was adjusted to pH 1.7 ± 0.1 with Dowex 50 (H^+) and hydrogenolyzed directly to DL-glyceraldehyde 3-P without further purification. Epimeric tetrono- and pentononitrile phosphates were purified by ion-exchange chromatography on a 2.2 x 51 cm Dowex 1 X8 (200-400 mesh) column in the formate form at 4°C. Solutions of aldononitrile phosphates were adjusted to pH 6.5-7.0 prior to application to the column bed. Columns were developed with linear gradients of sodium formate: for 4-carbon aldononitrile phosphates, 3000 mL, 0.2-0.9 M sodium formate, pH 3.9; for 5-carbon aldononitrile phosphates, 3000 mL, 0.05-0.8 M sodium formate, pH 3.9. Fractions (7 mL) were collected at 0.5 mL per min and were assayed by radioactivity or phosphate. The epimeric aldononitrile phosphates typically elute in separate peaks between 1500 mL-2000 mL of the gradient. The nitrile phosphate with cis-2,3-hydroxyl groups is the major product and is eluted last under these conditions. Column capacity exceeds 6 mmol of aldononitrile phosphate.

Fractions containing the aldononitrile phosphates were pooled and adjusted to pH 1.5 with Dowex 50 X8 (H^+). After filtration, the acidic solutions were concentrated to 100 mL *in vacuo* at 30°C and extracted continuously with diethyl ether overnight at 4°C to remove formic acid. The aqueous acidic solutions were recovered, concentrated

in vacuo at 30°C to approximately 10 mL, and adjusted to pH ≤ 2 with Dowex 50 X8 (H^+) for storage prior to hydrogenolysis.

b. Hydrogenolysis of aldononitrile phosphates

Palladium-barium sulfate (5%, 62 mg per mmol of nitrile) was weighed into a side-arm flask, 5-10 mL of H_2O was added, and the suspension was reduced for 15-20 min at atmospheric pressure and 25°C with efficient stirring. During this period, the catalyst changed from a brown to a whitish gray color. The solution of aldononitrile phosphate adjusted to pH 1.7 as described below was added from an addition funnel into the reduction vessel which was filled and evacuated three times prior to a final charging with hydrogen. The concentration of aldononitrile phosphate solution during hydrogenolysis varied between 50 and 100 mM.

Purified four- and five-carbon aldononitrile phosphate solutions were treated with 1 mL of glacial acetic acid per mmol of nitrile phosphate and then with Dowex 50 X8 (H^+) or 2 M NaOH to pH 1.7 ± 0.1. Reductions were carried out as described for the three-carbon homologue.

Aldononitrile phosphates were typically reduced for 6-8 h at 25°C. In a few instances, incomplete reduction was noted. In these cases, the spent catalyst was removed by filtration through Celite and a second reduction was performed to complete the conversion to the aldose phosphate.

Hydrogenolysis products were assayed by ^{13}C NMR to determine the extent of reduction to 1-amino-1-deoxyalditol phosphates and the amount of unreacted aldononitrile phosphates.

After hydrogenolysis, the catalyst was removed by filtration through Celite and the solution treated with excess Dowex 50 X8 (H^+).

After filtration, the solution was concentrated to 10 mL. Typically, the reaction mixture contains product aldose phosphate, 1-amino-1-deoxyalditol phosphate, and a small amount of aldononitrile phosphate. This solution was adjusted to pH 4.5 ± 0.1 with dilute NaOH and applied to a 1.2 x 50 cm DEAE-Sephadex A-25 (OAc^-) column at 4°C which had been equilibrated with 0.05 M sodium acetate at pH 4.5 ± 0.1. The column was developed with a linear acetate gradient (1500 mL, 0.05-0.8 M sodium acetate, pH 4.5 ± 0.1). Fractions (6 mL) were collected with a flow rate of 0.5 mL per min. The 1-amino-1-deoxyalditol phosphate eluted near the void volume, followed in order by aldose phosphate and the aldononitrile phosphate. Fractions containing aldose phosphate were pooled, treated with excess Dowex 50 (H^+), and concentrated *in vacuo* at 30°C to approximately 10 mL. Aldose phosphate solutions were stored at pH 4.0 and -15°C.

c. Characterization of aldose phosphates

Purified [1-^{13}C]-enriched aldose phosphates (100 μmol) in 2 mL of 50 mM Tris-HCl buffer at pH 9.0 were incubated with alkaline phosphatase for 1 h at 36°C. Carbon-13 NMR spectra of the resulting [1-^{13}C]-enriched aldoses were compared with standard spectra.

4. Enzymatic preparation of [^{13}C]-enriched carbohydrates

a. D-[2-^{13}C]Ribulose 1,5-P_2 (D-[2-^{13}C]Erythropentulose 1,5-P_2)

D-[2-^{13}C]Ribose 5-P (0.2 mmol) was incubated with 245 units of D-ribose 5-P isomerase for 30 min at pH 7.5 and 36°C. The resulting mixture containing 28% D-[2-^{13}C]-ribulose 5-P was converted to D-[2-^{13}C]ribulose 1,5-P, by the method of Horecker et al. (152) and purified by the method of Byrne and Lardy (153).

b. L-[3,4-^{13}C]Sorbose 1,6-P_2

DL-[1-^{13}C]Glyceraldehyde 3-P (75 mM) was incubated for 30 min at pH 7.5 and 34°C with triosephosphate isomerase, producing a mixture of L-[1-^{13}C]glyceraldehyde 3-P and [3-^{13}C]dihydroxyacetone phosphate. D-Fructose-1,6-P_2 aldolase was added and the mixture incubated for 4 h at 34°C. The reaction mixture was made 50% in hot ethanol and centrifuged to remove protein. The supernatant was concentrated *in vacuo* at 30°C to 2 mL, adjusted to pH 7.5 ± 0.1, and analyzed by ^{13}C NMR.

c. D-[1-^{14}C,2-^{13}C]Fructose 1,6-P_2 (FDP)

D-[1-^{14}C,2-^{13}C]Glucose (1.4 mmol) was dissolved in 17 mL H_2O, 1.25 g ATP and 0.15 g $MgCl_2$ were added, and the pH was adjusted to 7.4 with 2 M NaOH. Myokinase (500 units), hexokinase (500 units), phosphoglucoisomerase (250 units), and phosphofructokinase (300 units) were added, and the mixture was incubated for 60 min at 34°C while maintaining the pH of the reaction at pH 7.4. Assay by ^{13}C NMR showed complete conversion of glucose to FDP.

The reaction mixture was applied to a 1.7 x 26 cm Dowex 1 X8 (200-400 mesh) column in the chloride form. The column was eluted with 6 L of 0.01 M HCl to remove AMP and ADP. The column was then eluted with 4 L of 0.02 M HCl, 0.02 M LiCl, and 11 mL fractions were collected at 0.5 mL/min. FDP eluted between fractions 130-240 as determined by radioactivity. Fractions containing the phosphate were pooled and concentrated *in vacuo* at 30°C to 200 mL. The solution was neutralized with 0.5 M NaOH to pH 7.0 and $Ba(OAc)_2$ (5.6 mmol) was added with stirring followed by 240 mL of ethanol. The solution was stored at 4°C overnight to facilitate the precipitation of the barium salt of D-[1-^{14}C,2-^{13}C]fructose 1,6-P_2. The precipitate was collected by

centrifugation, suspended in H_2O, and treated with Dowex 50 X8 (H^+). The solution was filtered to remove the resin, concentrated to 3 mL at 30°C *in vacuo*, and adjusted to pH 6.0 with 0.1 M NaOH prior to analysis by ^{13}C NMR. Yield: 1.2 mmol (86%) based on P assay.

d. L-[2-^{13}C]Glyceraldehyde 3-P

DL-[2-^{13}C]Glyceraldehyde (0.1 mmol) in 2 mL H_2O was incubated with 1.5 molar equivalents of Mg^{2+}-ATP and 250 units of glycerol kinase at pH 7.5 and 36°C. After 1.5 h, the pH was adjusted to pH 7.5 and incubated for an additional 60 min. ^{13}C NMR analysis showed the presence of unreacted D-[2-^{13}C]glyceraldehyde and the product, L-[2-^{13}C]glyceraldehyde 3-P. The phosphorylated product can be purified by chromatography on DEAE-Sephadex (OAc^-) as described in Section II, L3b. The unreacted D-[2-^{13}C]glyceraldehyde, which elutes at the void volume of the column, was shown to be 91% D-isomer by reaction with 1,3-dihydroxy-2-propanone phosphate and D-fructose 1,6-bisphosphate aldolase to produce 91% D-[5-^{13}C]fructose 1-phosphate (70.5 and 81.7 ppm) and 9% L-[5-^{13}C]sorbose 1-phosphate (70.9 ppm). Rabbit-muscle aldolase can act on both D- and L-glyceraldehyde, and gives an equimolar mixture of the ketose 1-phosphates when the original mixture of DL-[2-^{13}C]glyceraldehyde is used.

M. Preparation of [^{2}H]-Enriched Aldoses and Derivatives

1. D-[1-^{13}C, ^{14}C, ^{2}H]Erythrose and threose

A solution of K^{13}CN (2 mmol, 13 mL ^2H_2O) at 20°C containing K^{14}CN (10^7 cpm) was added to a 25-mL sealed flask (Figure 9) and adjusted to pH 8.0 ± 0.1 with 0.7 M acetic acid-$^2H_4$. D-Glyceraldehyde (2 mmol) was concentrated from 3 mL of ^2H_2O several times at 30°C *in vacuo*.

The residual gum was dissolved in 4-5 mL $^{2}H_2O$ and added to the solution of $K^{13}CN$. The pH of the reaction mixture was maintained between 8.0 and 8.3 with additions of 0.7 M acetic acid-$^{2}H_4$ and/or 1.0 M $NaO^{2}H$. After 20-25 min, the pH was lowered to 4.0 ± 0.2 with 17 M acetic acid-$^{2}H_4$. A further adjustment of pH to 1.7 ± 0.2 was made with 3 M ^{2}HCl.

Palladium-barium sulfate (5%, 62 mg per mmol of nitrile) was weighed into a 50-mL side-arm flask, 5 mL $^{2}H_2O$ was added, and the system was evacuated and charged three times with N_2. After the last evacuation, the system was charged with $^{2}H_2$ and the catalyst reduced for 15-20 min at atmospheric pressure and 25°C with efficient stirring. The ballast containing $^{2}H_2$ was filled with light mineral oil to prevent entry of H_2O into the reduction apparatus. The [^{13}C]-enriched aldononitriles were then added and the reduction was continued for 10 h, or until the nitriles were completely reduced as determined by GLC. The product epimeric aldoses were deionized and separated as described in Section II, L2c. Products were characterized by ^{1}H and ^{13}C NMR. Yield: 70% based on product weight as gums and on the recovery of radioactivity after separation.

2. D-[2-^{13}C, ^{14}C, ^{2}H]Ribose and arabinose

D-[2-^{13}C,^{14}C,^{2}H]Ribose and arabinose were prepared from D-[1-^{13}C, ^{14}C,^{2}H]erythrose according to a modified procedure described for the preparation of the [1-^{13}C] compounds in Section II, L1. The condensation reaction with KCN in H_2O was carried out at pH 7.8-8.0 for 9 minutes. The solution was adjusted to pH 4.0 with acetic acid and then to pH 3.0 ± 0.1 with HCl. The epimeric nitriles were reduced with Pd/H_2 at 20 psi and 25°C in a Parr apparatus, and the product aldoses were

purified (Section II, L2c) and analyzed by ^{13}C and ^{1}H NMR. Yield as dry gums: 78% after separation.

3. Methyl α-D-[2-^{13}C, ^{14}C, ^{2}H]ribofuranoside and methyl β-D-[2-^{13}C, ^{14}C, ^{2}H]ribofuranoside

D-[2-^{13}C,^{14}C,^{2}H]Ribose was converted to the methyl furanosides by the procedure of Barker and Fletcher (154). The reaction mixture was neutralized by passage through a 1.2 x 5 cm column of Dowex 1 X8 (200-400 mesh) in the acetate form and elution with deionized water. The resulting solution was concentrated at 30°C *in vacuo* and applied to a 1.5 x 23 cm column of Dowex 1 X8 (200-400 mesh) in the hydroxide form (155) and developed with decarbonated distilled H_2O with a flow rate of 0.25 mL/min. Fractions (3 mL) were collected and assayed with phenol-sulfuric acid (137). The α-anomer eluted between fractions 25-35 and the β-anomer eluted between fractions 60-80. Fractions were pooled, concentrated at 30°C *in vacuo* and analyzed by ^{13}C and ^{1}H NMR. Anomers were identified by comparison of ^{13}C chemical shifts for C-2 with those reported previously (114).

Methyl-D-arabinofuranosides were prepared by the procedure of Augestad and Berner (156) and the α- and β-anomers were separated by the method of Austin et al. (155). Anomers were identified by ^{13}C NMR using chemical shifts reported previously (114).

4. Other compounds enriched with ^{13}C, ^{14}C and/or ^{2}H

DL[2-^{14}C,3-^{2}H]Erythrose and threose were prepared from [1-^{2}H] glycolaldehyde by successive condensations of the C_2 and C_3 deuterated aldoses with KCN ($K^{14}CN$) and reduction with Pd/H_2. The two condensations with KCN were modified by using H_2SO_4 rather than HCl to adjust the pH of the reaction mixtures from 4.0 to 1.7 ± 0.1 prior to

reduction. Catalyst was removed by filtration through sintered glass and the reduction products were deionized with $BaCO_3$. The solution was filtered through Celite to remove the $BaSO_4$ precipitate and residual $BaCO_3$, the filter pad was washed well with H_2O, and the filtrate and washings were treated batchwise with Dowex 1 X8 (OAc^-) and Dowex 50 X8 (H^+) successively. The clear, colorless solution was concentrated to 2 mL at 30° *in vacuo* and the mixture separated as described previously (Section II, L2c) on Dowex 50 X8 (200-400) (Ba^{++}).

DL-[1-^{14}C,^{2}H]Glyceraldehyde was prepared from DL-[1-^{14}C]glyceronitrile by reduction with $^2H_2$. Yield after purification, 82%. ^{13}C NMR: 75.5 ppm (C-2, hydrate) and 63.4 ppm (C-3, hydrate).

D-[1-^{14}C]Erythrose 4-phosphate (E4P) was prepared from D-[1-^{14}C]-erythrononitrile 4-P by reduction with H_2. D-[1-^{14}C] E4P was converted to D-[1-^{13}C,^{2}H,2-^{14}C]ribose 5-P by reduction with Pd/$^2H_2$. DL-[1-^{13}C, ^{14}C,^{2}H]Glyceraldehyde 3-P was prepared from DL-[1-^{13}C,^{14}C]glyceronitrile 3-P and purified as described previously (Section II, L3b). Yield based on recovery of phosphate and radioactivity after chromatography, 69% with 5% inorganic P.

N. List of Isotopically-Enriched Compounds

1. [^{13}C]Pentoses and hexoses

D-[1-^{13}C]Glucose, D-[1-^{13}C]mannose, D-[1-^{13}C]galactose, D-[1-^{13}C]-talose, D-[1-^{13}C]allose, D-[1-^{13}C]altrose, D-[1-^{13}C]idose, D-[1-^{13}C]-gulose, D-[1-^{13}C]lyxose, D-[1-^{13}C]xylose, D-[1-^{13}C]ribose, D-[1-^{13}C]-arabinose, D-[2-^{13}C]glucose, D-[2-^{13}C]mannose.

2. [^{13}C]Lower-carbon aldoses (C_1 - C_4) and derivatives

[^{13}C]Formaldehyde, [1-^{13}C]glycolaldehyde, DL-[1-^{13}C]glyceraldehyde, DL-[2-^{13}C]glyceraldehyde, D-[1-^{13}C]erythrose, DL-[2-^{13}C]erythrose, DL-[3-^{13}C]erythrose, D-[1-^{13}C]threose, DL-[2-^{13}C]threose, DL[3-^{13}C]-threose, DL-[1,2-^{13}C]erythrose, DL-[1,2-^{13}C]threose, [1-^{13}C]glycolonitrile, DL-[1-^{13}C]glyceronitrile, DL-[2-^{13}C]glyceronitrile, D-[1-^{13}C]-erythrononitrile, DL-[2-^{13}C]erythrononitrile, DL-[3-^{13}C]erythrononitrile, D-[1-^{13}C]threononitrile, DL-[2-^{13}C]threononitrile, DL-[3-^{13}C]threononitrile, DL-[1,2-^{13}C]erythrononitrile, DL-[1,2-^{13}C]threononitrile, DL-[1-^{13}C]glyceric acid, sodium D-[1-^{13}C]erythronate, sodium D-[1-^{13}C]-threonate.

3. [^{13}C]Aldose phosphates, ketose phosphates and derivatives

DL-[1-^{13}C]glyceraldehyde 3-P, D-[1-^{13}C]threose 4-P, D-[1-^{13}C]-erythrose 4-P, DL-[1-^{13}C]xylose 5-P, DL-[1-^{13}C]lyxose 5-P, DL-[1-^{13}C]-arabinose 5-P, DL-[1-^{13}C]ribose 5-P, D-[2-^{13}C]xylose 5-P, D-[2-^{13}C]-lyxose 5-P, D-[2-^{13}C]arabinose 5-P, D-[2-^{13}C]ribose 5-P, DL-[1,2-^{13}C]-arabinose 5-P, DL-[1,2-^{13}C]ribose 5-P, L-[3,4-^{13}C]sorbose 1,6-P_2, D-[2-^{13}C]ribulose 1,5-P_2, D-[5-^{13}C]fructose 1-P, L-[5-^{13}C]sorbose 1-P, D-[2-^{13}C]fructose 1,6-P_2, DL-[1-^{13}C]glyceronitrile 3-P, D-[1-^{13}C]-threononitrile 4-P, D-[1-^{13}C]erythrononitrile 4-P, DL-[1-^{13}C]xylononitrile 5-P, DL-[1-^{13}C]lyxononitrile 5-P, DL-[1-^{13}C]arabinononitrile 5-P, DL-[1-^{13}C]ribononitrile 5-P, D-[2-^{13}C]xylononitrile 5-P, D-[2-^{13}C]lyxononitrile 5-P, D-[2-^{13}C]arabinononitrile 5-P, D-[2-^{13}C]-ribononitrile 5-P, DL-[1,2^{13}C]arabinononitrile 5-P, and DL-[1,2-^{13}C]-ribononitrile 5-P.

4. Compounds with [^{2}H]-enrichment

DL-[1-^{14}C,^{2}H]glyceraldehyde, D-[1-^{13}C,^{2}H]erythrose, D-[1-^{13}C,^{2}H]-threose, D-[2-^{13}C,^{2}H]ribose, D-[2-^{13}C,^{2}H]arabinose, methyl α-D-[2-^{13}C,^{2}H]ribofuranoside, methyl β-D-[2-^{13}C,^{2}H]ribofuranoside, DL-[3-^{2}H]erythrose, DL-[3-^{2}H]threose, DL-[1-^{13}C,^{2}H]glyceraldehyde 3-P, and D-[1-^{13}C,^{2}H]ribose 5-P.

III. RESULTS AND DISCUSSION

A. The Cyanohydrin Reaction

1. Aldonic acid formation

An aqueous solution containing stoichiometric amounts of cyanide salt and C_4 or C_5 aldose (0.1-0.3 M) at 25°C is sufficiently basic (pH 12-13) to cause rapid hydrolysis of the initially-formed 2-epimeric aldononitriles to the corresponding aldonates. Hydrolysis is complete in 3-4 h except for the aldononitriles derived from D-xylose, which require 11 h for complete hydrolysis. In contrast, the production of aldonates from the nitriles derived from D-glyceraldehyde (0.1-0.3 M) at pH 12-13 is slow, requiring 6-10 days for complete hydrolysis.

At lower pH values (8.5-10.5), hydrolysis of C_5 and C_6 aldononitriles to aldonates is slower, typically requiring several days. Here, the rate of aldonate production is determined by the rate of hydrolysis of aldonamides formed from aldononitriles (see below).

The addition of KCN to glycolaldehyde (0.1-0.3 M) at pH 12-13 yields reaction mixtures of unexpected complexity. No more than 25 percent DL-glycerate is formed along with products from the addition of cyanide to C_4 aldoses produced by aldol condensation of glycolaldehyde. In weakly basic solution (pH 8.0), C_3 and C_4 aldononitriles are stable for extended periods at -15°C.

The ratio of 2-epimeric aldonates produced after the addition of cyanide to an aldose depends on the values of the rate constants indicated in Scheme VI. In this simple scheme, it is assumed that, after aldononitriles are formed,

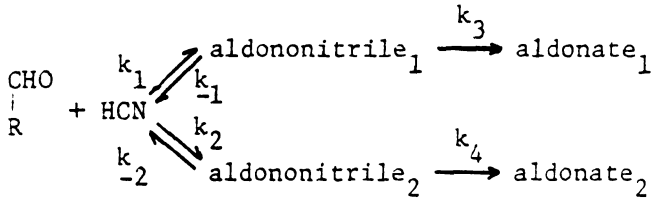

Scheme VI

no intermediate exists that can epimerize at C-2. All of the rate constants are pH-dependent (see below) and product distribution should depend on reaction conditions (Table 1), as observed previously (41-45). Thus, at pH 12-13, the addition of cyanide to D-arabinose (0.1 M) yields 75% D-gluconate, whereas, at pH 9.0, 70% D-mannonate is formed (41) (Table 1). Moderate stereospecificity is also apparent in the case of D-xylose (0.1 M), where 78% of the products have the D-gulo configuration. At pH 9.0 and 0.1 M, 60% D-gulo epimer is formed. It has been proposed that the predominant aldonate has OH-2 trans to OH-4 (157, 158). At pH 12.7, neither D-arabinose nor D-ribose meet this expectation, while at pH 9.0, D-ribose gives the OH-2-OH-4 cis product predominantly (Table 1).

2. Aldononitrile formation

The equilibrium between starting aldose and aldononitrile depends on the concentration of reactants, the structure of parent aldose, and pH.

The condensation of 0.3 M [^{13}C]cyanide and D-erythrose at 18°C can be followed by ^{13}C NMR as a function of pH. Starting at low pH, aldononitrile formation is not observed until the pH of the reaction mixture is raised to 5.1 ± 0.2. At this pH, the ratio of nitriles to unreacted cyanide is approximately 0.7. At pH 6.5 ± 0.2, aldononitrile formation is essentially quantitative (ribo:arabino::54:46). The

Table 1. Aldonate formation: Effect of pH and reactant concentration on the distribution of epimers[a].

Parent Aldose	Concentration (M)	pH[b] (±0.2)	% (GLC) ±3%	% (NMR) ±3%	Predominant Epimer
D-glyceraldehyde	0.1	u	61	60	threo
	0.3[c]	u		59	threo
D-threose	0.1	u	58		lyxo
	0.3[d]	8.5		61	lyxo
D-erythrose	0.1	u	62		arabino
	0.3[c]	u		68	arabino
	0.3[d]	10.5		79	arabino
	0.3[d]	8.5		74	arabino
D-arabinose	0.1	u	75	76	gluco
	0.5	u	69	66	gluco
	0.1	9.0	65	70	manno
D-lyxose	0.1	u		72	galacto
D-ribose	0.1	u	57	56	allo
	0.5	u	53	52	allo
	0.1	9.0	57	61	allo
D-xylose	0.1	u	78	75	gulo
	0.5	u	69		gulo
	0.1	9.0	59	59	gulo

[a] Reactions were carried out at room temperature. NMR Ratios were determined by the examination of the intensities of the hydroxymethyl groups (CH_2OH) in unenriched compounds and/or the carboxylate groups (COO^-) in [1-^{13}C]-enriched compounds. [b] u = uncontrolled pH; for pH-controlled reactions, HOAc and NaOH were employed. [c] Conducted at 18°C. [d] pH Was controlled with HCl instead of HOAc.

absence of unreacted aldose was verified by GLC. As the pH of the reaction mixture is raised above 11, the amount of free aldose in solution and the rate of aldononitrile hydrolysis increase.

Addition of an aldose to a cyanide salt (KCN, NaCN) at 18°C and 0.3 M in the absence of pH control produces an increase in pH from 11.3 to 12.7 during the first 5 min of reaction (Figure 10). This increase results from the condensation of cyanide ion (pK_a = 9.2) (5) with the aldose, with the concomitant formation of an alkoxide intermediate which abstracts a proton from water to produce OH^- (Scheme VII). A gradual rise in pH is noted during the next 50 min as the remaining aldose reacts. The slow decrease in pH after 1 h reflects the rate of hydrolysis of aldononitriles to yield aldonates and ammonium ion.

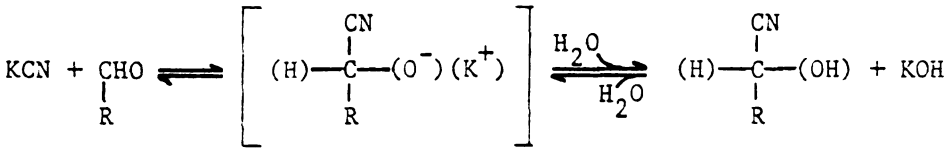

Scheme VII

The extent of aldononitrile formation is reduced when the parent aldose can form a pyranose ring. Aldoses such as the C_2 and C_3 aldoses, which are extensively hydrated in aqueous solution (Section III, B5a), and the C_4 aldoses, which are 88% furanose and 12% hydrate, (Section III, B5a), react with cyanide stoichiometrically and essentially quantitatively at pH 7.5-9.0. On the other hand, pentoses, which are predominantly in the pyranose form in aqueous solution, do not react quantitatively at pH 7.5-9.0, and equilibrated reaction mixtures typically contain ∿15% unreacted aldose. Complete conversion

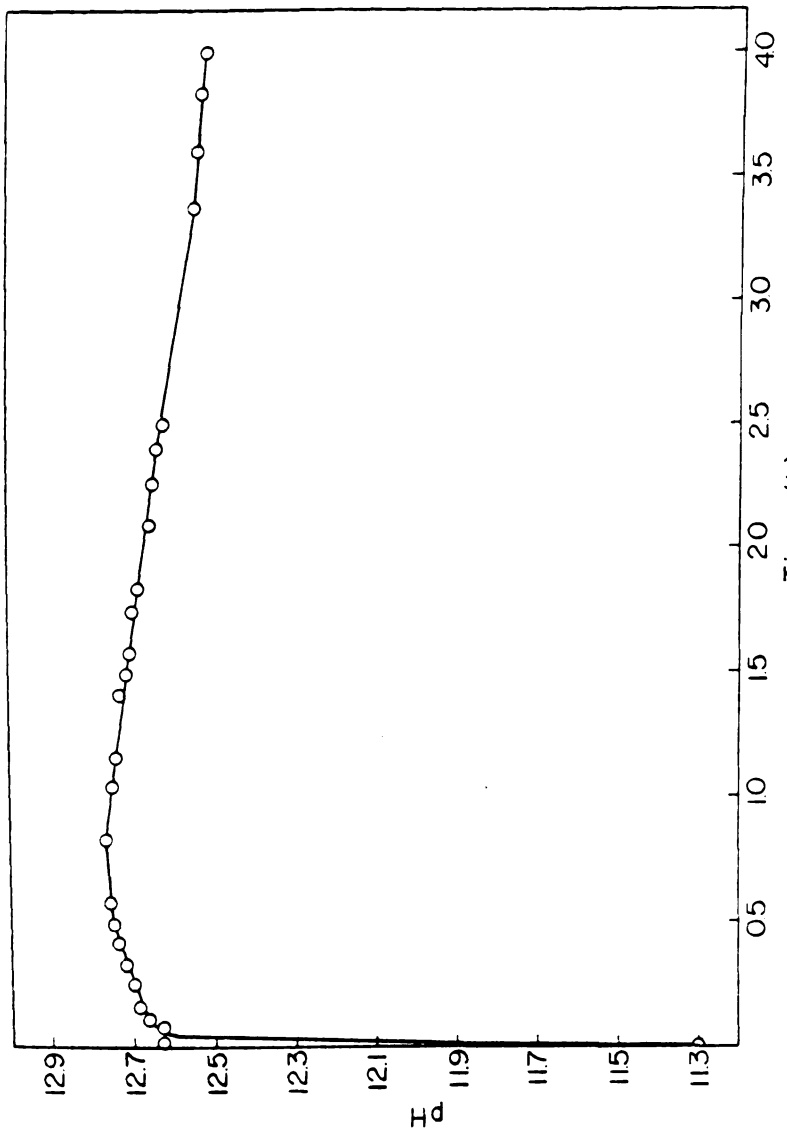

Figure 10. Change in pH during the Kiliani reaction applied to D-erythrose. The reaction mixture was incubated at 18° ± 1°C and was 0.3 M in each reactant. The pH at zero time was taken as the pH of the KCN solution at 0.6 M prior to addition of the aldose.

to the C_6 aldononitriles can be accomplished at pH 8.0 using a three-fold excess of cyanide.

The formation of aldononitriles is reversible at pH 7.0 or above, whereas below pH 4, aldononitriles are stable. This stability permits epimeric mixtures of aldononitrile phosphates to be separated at pH 3.9 by chromatography on ion-exchange resins. Aldononitrile phosphates, separated in this fashion, will revert to epimeric mixtures at pH 7.0 or above.

3. Rates of aldononitrile disappearance

The rate of disappearance of aldononitriles depends on pH and the structure of the aldononitrile. The rate of aldononitrile disappearance at pH >11 is difficult to determine since the change in aldononitrile concentration is determined by two rates, the rate of formation from aldose and the rate of hydrolysis to aldonamides and other products. Both the rate of aldonamide formation and the rate of hydrolysis are high at high pH values. The disappearance of aldononitrile at 18°C was measured by ^{13}C NMR for the [1-^{13}C]aldononitriles *3-8* at several pH values (Chart I, Figure 11). At pH 8.5, the rate of DL-glyceronitrile (*3*) disappearance is negligible (not shown). However, *3* disappears slowly at pH 12.7, with completion in 100 h. The ^{13}C NMR spectrum of the products from the total hydrolysis of DL-[1-^{13}C]glyceronitrile shows a resonance for DL-[1-^{13}C]glycerate and four resonances corresponding to the C-1 carbons of DL-[1-^{13}C]lyxonate, xylonate, arabinonate, and ribonate. GLC confirms the presence of these pentonates and, after removal of excess cyanide as $H^{13}CN$ by aeration, ^{13}C NMR analysis indicates that the pentonates are present in the following proportions: 41% lyxo, 18% xylo, 29% arabino,


Percent in Reaction Mixture

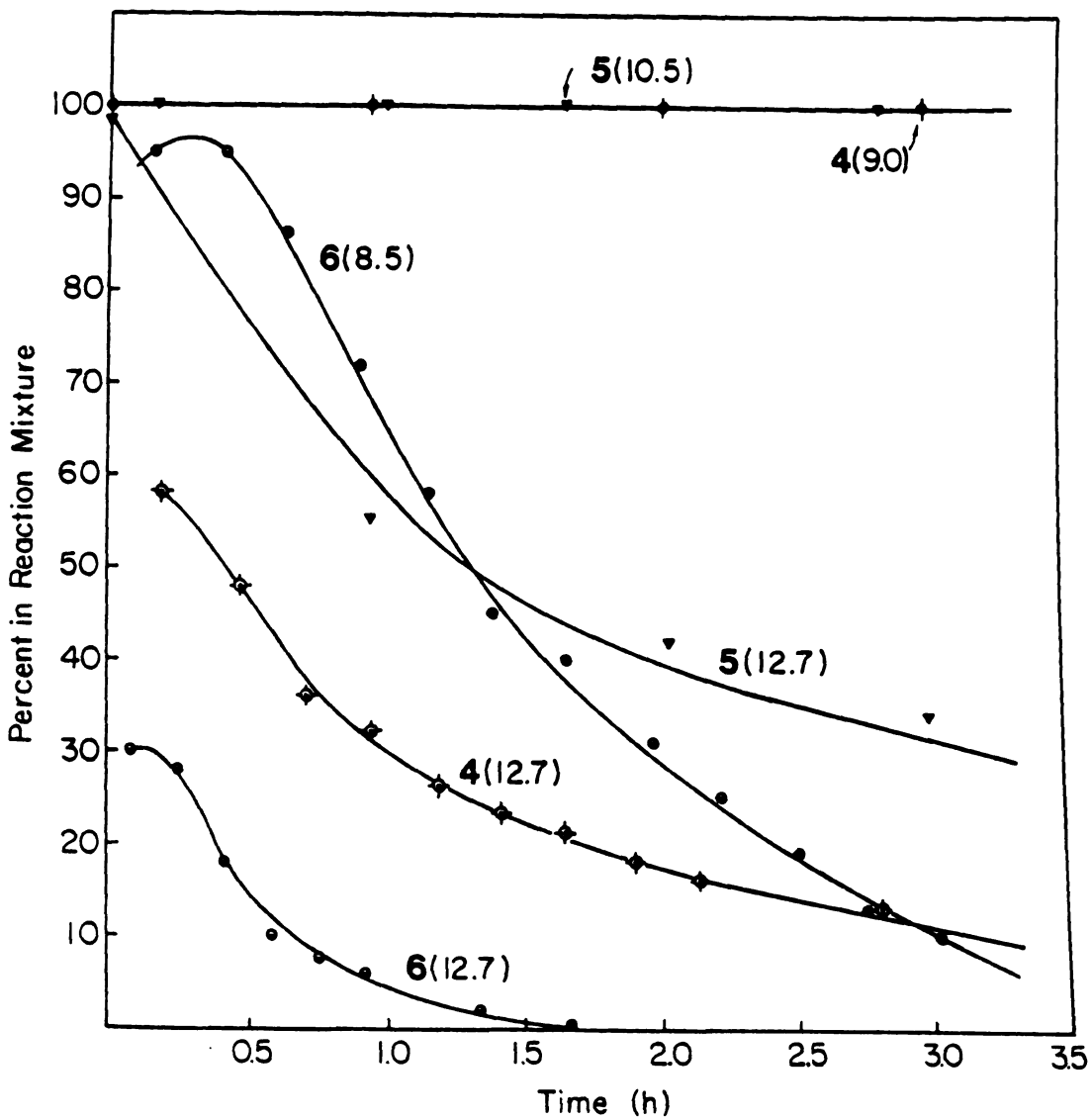

Figure 11. Disappearance of aldononitriles in cyanohydrin reaction mixtures. Reaction mixtures were incubated at 18° ± 1°C and data were obtained from ^{13}C NMR spectra. Concentrations of reactants were 0.3 M except for reactions involving 5, which were conducted at 0.4 M. Experiments were conducted at the pH value in parenthesis. Zero-time points for 4 (pH 9.0) and 5 (pH 10.5 and 12.7) were determined from the amount of aldononitrile in each reaction mixture after 4 h at pH 8.0, pH 8.0 and pH 10.5, respectively. The remaining reactants were conducted with both cyanide addition and hydrolysis at the indicated pH values. 2 = D-[1-^{13}C]erythrono- and threononitrile; 3 = DL-[1-^{13}C]2-hydroxybutyronitrile; 4 = D-[1-^{13}C]arabinono- and ribononitrile.

12% ribo. DL-Glycerate accounts for approximately 5 percent of the total products.

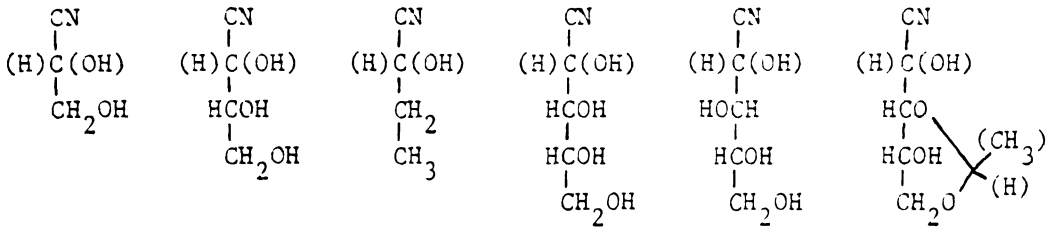

3 4 5 6 7 8

Chart I

Formation of the DL-[1-^{13}C]pentonates is due to reversal of cyanide condensation at alkaline pH to produce free glycolaldehyde, which undergoes aldol condensation to form the DL-tetroses. DL-Pentonates derived from the trans aldol product, DL-threose, compose about 60% of the mixture, and those derived from the cis product, DL-erythrose, compose the remaining 40%. The reaction to be considered in the alkaline hydrolysis of 3 is shown in Scheme VIII.

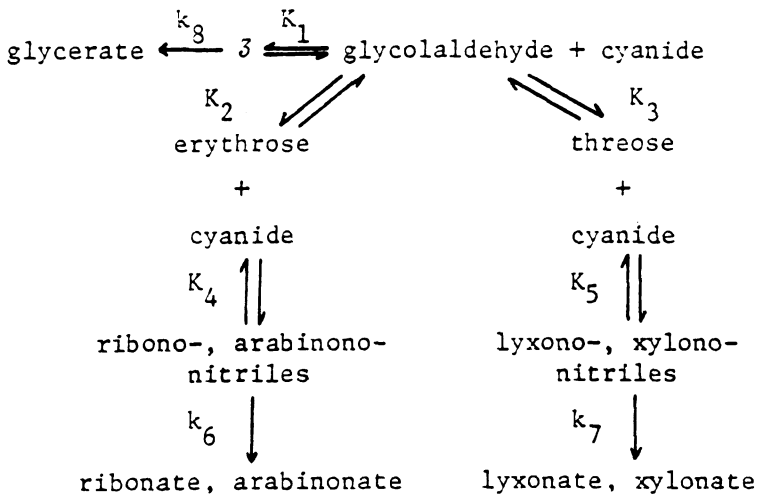

Scheme VIII

The amount of glycerate formed depends on the rate of hydrolysis, k_8, relative to the rates of competing reactions. It is reasonable to assume that $K_1 \simeq K_4 \simeq K_5$ and it is known that k_6 and $k_7 >> k_8$ (Figure 11). The results indicate, therefore, that aldol condensation is favored over hydrolysis of *3* at pH 12.7.

Although trans aldol products predominate in most aldol condensations (159-161), 40 percent of the products in this case are derived from the cis product, DL-erythrose. The amounts of individual pentonates depends on K_2, K_3, K_4, K_5 and the overall rates of aldononitrile hydrolysis, k_6 and k_7. It is reasonable to assume that $K_4 \simeq K_5$ and that $K_3 > K_2$, so that k_6 must be greater than k_7 for the cis products to be found in the high proportion observed. An examination of the rates of disappearance of aldononitriles derived from D-erythrose and from D-threose shows that this is the case (i.e., $k_6 > k_7$) (Figure 12).

Rates of disappearance of C_4 aldononitriles *4* are negligible at pH 9.0 and 18°C (Figure 11). At 18°C, with no pH control, disappearance is more rapid ($t_{1/2} \simeq 1$ h) than for the C_3 homologue *3* ($t_{1/2} \simeq$ 25 h). However, the rate of disappearance of *4* is comparable with that of DL-2-hydroxybutyronitrile *5* ($t_{1/2} \simeq 1$ h). The difference in rates observed between *3* and *4* suggests that cyclization may be an important factor in facilitating hydrolysis. The similarity in the rates of disappearance of *4* and *5*, however, suggests that cyclization is not essential and may be no more facile than the direct, unassisted hydrolysis of the nitrile.

Examination of the products from the hydrolysis of *5* at pH 12.7 and 18°C indicates the presence of 75 percent DL-2-hydroxybutyrate, with the remaining aldonates probably arising from aldol condensation

products of propionaldehyde. The ease of aldolization is a function of the acidity of H-2 of the aldehyde. Removal of the OH group α to the carbonyl would be expected to decrease the acidity of H-2, making carbanion formation more difficult than for glycolaldehyde, thereby favoring hydrolysis over aldolization.

C_5 Cyanohydrins *3* and *7* ($t_{1/2} \approx 1.5$ h) ($t_{1/2} \approx 4.5$ h) disappear more quickly than *3*, *4* and *5*, at pH 8.5 and 18°C. In contrast, compound *8* is stable at pH 8.5 and 18°C. Pentoses produced from *8* are predominantly hydrates in aqueous solution ($\delta_{C-1} = 90.7$ ppm), demonstrating that OH-4 is unavailable for cyclic hemiacetal formation. Thus, *8* probably cannot form cyclic intermediates, which accounts for its slower rate of disappearance relative to the underivatized homologue *6*. Data in Figure 11 suggest that aldononitriles capable of cyclization have significantly greater rates of disappearance and that cyclization to form six-membered rings facilitates hydrolysis better than the cyclization to form five-membered rings. The latter conclusion is not valid, however, and will be discussed later.

Configuration also affects the rate of aldononitrile disappearance (Figure 12). The overall rate of disappearance of the C_5 cyanohydrins derived from D-erythrose (ribo, arabino; *6*) is greater than that of the C_5 aldononitriles derived from D-threose (lyxo, xylo; *7*), with $t_{1/2} \approx 1.5$ h and $t_{1/2} \approx 4.5$ h, respectively, at pH 8.5. Within epimeric pairs, arabinononitrile hydrolyzes more rapidly than ribononitrile, while lyxono- and xylononitriles appear to hydrolyze at approximately the same rate. The ratio of the epimeric C_5 aldononitriles formed initially at pH 8.5 does not always correspond to the ratio of aldonates produced. For example, the ratio of lyxono- to xylononitrile

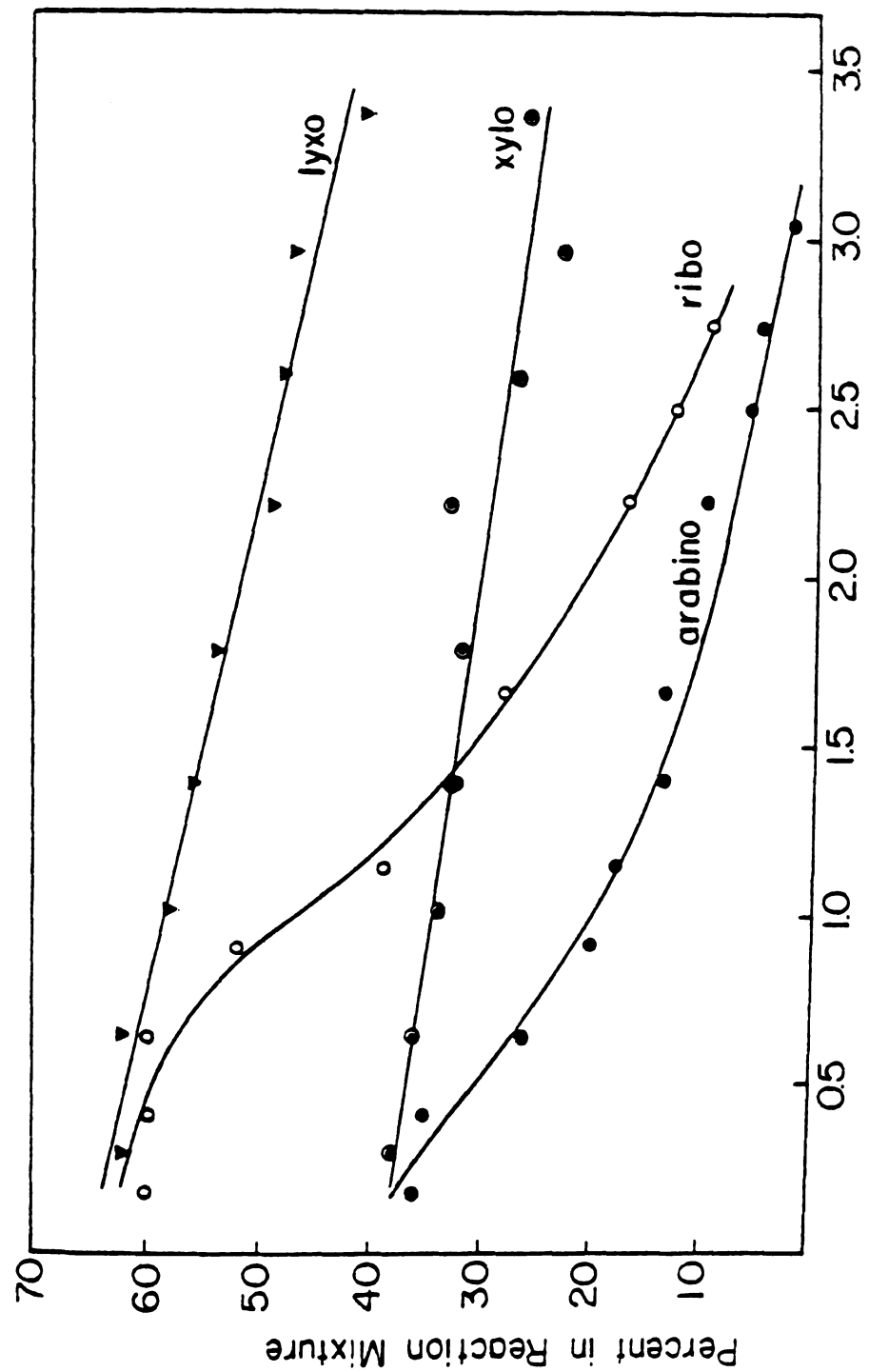

Figure 12. Differences in the rates of aldononitrile disappearance between diastereomers during the cyanohydrin reaction at pH 8.5 ± 0.2. Reaction mixtures were incubated at 18° ± 1°C and were 0.3 M in aldose and [^{13}C]cyanide. Data were determined from ^{13}C NMR spectra.

is 3:2 at pH 8.5. Because their rates of disappearance are similar, the corresponding aldonates are formed in the same ratio (Table 1). On the other hand, arabinono- and ribononitriles are formed in a 2:3 ratio, but hydrolysis yields arabinonate and ribonate in a 7:3 ratio. Clearly, arabinononitrile hydrolyzes more rapidly than the ribo epimer. Data in Figure 12 do not reflect these differences accurately, since rapid equilibration of the epimeric aldononitriles by reversal of cyanide condensation increases the apparent rate of disappearance of ribononitrile and decreases the apparent rate of hydrolysis of the arabino epimer.

4. Characterization of reactants, intermediates and products

Before discussing the sequence of intermediates in the hydrolysis of cyanohydrins, evidence for the identification of the observed intermediates is presented. GLC and ^{13}C NMR parameters of the compounds involved in this study are listed in Tables 2 and 3.

As shown in Figure 13, unreacted aldose and the epimeric aldononitriles, aldonolactones, aldonates and aldonamides are resolvable by GLC. However, derivatization changes the structure and distribution of intermediates so that GLC alone was not a reliable method to examine changes in concentration of intermediates as a function of time.

^{13}C NMR spectroscopy is an ideal tool to assay reaction mixtures, especially when [^{13}C]-enrichment is employed to increase sensitivity and decrease acquisition times. [1-^{13}C]Intermediates observed by ^{13}C NMR in the reaction of K^{13}CN with D-erythrose are shown in Figure 14. The assignments of resonances to aldononitriles, aldonolactones, aldonamides and aldonates were made by comparison with spectra of [1-^{13}C]-enriched standards prepared by alternative routes.

Table 2. GLC retention times of pertrimethylsilylated carbohydrates and derivatives.

Compound	Retention[a]
D-gluconate	1.00
glycolaldehyde	0.25, 0.26, 0.27
D-glyceraldehyde	0.36, 0.83, 0.85, 0.87, 0.90
2,4-O-ethylidene-D-erythrose	0.50, 1.32
D-erythrose	0.37
D-threose	0.33, 0.36
D-arabinose	0.59, 0.64, 0.67
D-lyxose	0.60, 0.65, 0.68
D-ribose	0.60, 0.64
D-xylose	0.57, 0.66, 0.72
D-glycerate	0.41
D-erythronate	0.52
D-threonate	0.56
D-arabinonate	0.77
D-ribonate	0.73
D-lyxonate	0.75
D-xylonate	0.75
D-allonate	0.94
D-altronate	0.99
D-gulonate	0.93
D-idonate	1.02
D-mannonate	0.94
D-galactonate	0.99
D-talonate	0.99
D-glyceronitrile	0.17
D-erythrononitrile	0.41
D-threononitrile	0.41
3,5-O-ethylidene-D-arabinononitrile	0.63
3,5-O-ethylidene-D-ribononitrile	0.63

Table 2 (cont'd).

Compound	Retention[a]
D-arabinononitrile	0.63
D-ribononitrile	0.66
D-lyxononitrile	0.65
D-xylononitrile	0.65
D-gluconononitrile	0.92
D-mannononitrile	0.89
D-galactononitrile, D-talononitrile	0.87, 0.91[b]
D-allononitrile, D-altrononitrile	0.89, 0.90[b]
D-gulononitrile	0.90
D-idononitrile	0.92
D-arabinono-1,4-lactone	0.68
D-ribono-1,4-lactone	0.75
D-arabinonamide	0.85
D-ribonamide	0.80

[a] Retention times are relative to the $(Me)_3Si$ derivative of D-gluconate; column conditions are described in Instrumentation.
[b] Retention times were not assigned.

Table 3. ^{13}C NMR parameters[a] of reactants, intermediates and products of the cyanohydrin reaction.

Compound	pH (±0.2)	^{13}C Chemical Shifts (ppm)					^{13}C-^{13}C Coupling Constants (Hz)			
		C1	C2	C3	C4	C5	$^{1}J_{C1,C2}$	$J_{C1,C3}$	$J_{C1,C4}$	$J_{C1,C5}$
HCN	3.6	113.4								
KCN	11.5	166.4								
D-lactaldehyde, hydrate	6.0	94.3	71.5	18.1						
D-threo, erythro-2,3-dihydroxybutanal	6.0	91.3								
DL-glyceronitrile	12.5	125.7								
	8.5	121.0	63.2	64.6						
DL-2-hydroxy-butyronitrile	3.7	122.2								
	10.5	122.8								
	12.5	126.9								
D-threo-,erythro-2,3-dihydroxybutyronitrile	7.5	120.7, 120.4								
D-threono-,erythrono-nitriles	12.5	125.6, 124.9								
D-lyxononitrile	8.5	121.5								
D-xylononitrile	8.5	120.6								
DL-2-hydroxybutyrate		182.8	74.6	28.3	9.9					
D-lyxono-1,4-lactone		179.6	71.9	71.0	83.0	61.2	56.5	br	1.5	br
D-xylono-1,4-lactone		178.8	73.9		82.1	60.7	56.5			
D-lyxonic acid	1.2	177.6	72.7			64.0	59.4			
D-xylonic acid	1.0	177.4	72.7			63.7	59.4			
D-lyxonate	10.8	180.4	75.2	72.7[b]	73.1[b]	64.3	54.3		c[d]	
D-xylonate	9.8	180.1	74.1	73.9[b]	74.3[b]	63.9	54.3		2.9[d]	
D-threono-,erythrono-amidines	9.5	172.2 171.6								

Table 3 (cont'd.).

Compound	pH (±0.2)	^{13}C Chemical Shifts (ppm)					^{13}C-^{13}C Coupling Constants (Hz)			
		C1	C2	C3	C4	C5	$^{1}J_{C1,C2}$	$J_{C1,C3}$	$J_{C1,C4}$	$J_{C1,C5}$
D-erythrose	6.0									
α		96.8	72.4	70.6	72.9		43.3			
β		102.4	77.7	71.7	72.4		46.9			
hydrate		90.8	74.9	73.0	64.0					
D-arabinononitrile	8.5	121.4	62.8	72.6	71.2		61.6	——	2.9	
	12.5	125.2								
D-arabinono-imido-1,4-lactone	10.5	175.4	75.2	74.3	82.6		51.3	6.6	——	
D-arabinonamide	8.1	180.3	72.2	72.9	72.0	64.4	53.5	——	2.9	——
	13.3	181.8								
D-arabinono-1,4-lactone		177.6	75.2	73.8	82.6	60.7	55.7	7.3	——	br
D-arabinono-1,5-lactone	3.0	176.2								
D-arabinonic acid	2.0	178.4	71.7	73.2	71.9	64.4	60.1	——	2.2	——
D-arabinonate	8.5	180.8	73.0	73.6	72.6	64.6	54.2	——	2.9	——
	13.3	181.0								
D-arabinonoamidine	9.6	173.2					48.4			
D-ribononitrile	8.5	120.1	64.2	73.0	72.9		60.1	——	——	——
	12.5	125.2								
D-ribono-imido-1,4-lactone	10.5	177.3	70.6	71.3	88.2		51.3	2.2	br	
D-ribonamide	8.2	178.7	73.9	74.1	72.3	64.4	52.8	——	——	——
	13.3	181.2								
D-ribono-1,4-lactone		180.0	70.4	71.0	88.2	62.0	55.7	2.2	1.5	——
D-ribono-1,5-lactone	2.6	179.3								
D-ribonic acid	1.7	176.9	73.3	74.2	71.9	64.5	59.4	——	——	——
D-ribonate	8.5	179.7	75.0	74.7	72.9	64.3	53.5	——	——	——
	13.3	179.9								

Table 3 (cont'd.).

Compound	pH (±0.2)	^{13}C Chemical Shifts (ppm)					^{13}C-^{13}C Coupling Constants (Hz)			
		C1	C2	C3	C4	C5	$^{1}J_{C1,C2}$	$J_{C1,C3}$	$J_{C1,C4}$	$J_{C1,C5}$
D-ribonoamidine	9.6	171.6								
U1	9.5	170.0[e]	81.8				41.8			
	3.0	169.5[e]	81.5				45.3			
U2	9.5	122.9[f]	72.3				54.3			
	3.0	115.7[f]	70.6				50.6			
D-5-deoxyarabinono-imido-1,4-lactone	10.5		75.3							
D-5-deoxyribono-imido-1,4-lactone	10.5		70.3							
D-5-deoxylyxono-imido-1,4-lactone	10.5		72.5							
D-5-deoxyxylono-imido-1,4-lactone	10.5		74.7							
D-5-deoxyarabinonamide	10.5		71.8							
D-5-deoxyribonamide	10.5		73.8							

[a] Determined at 18° ± 1°C. Chemical shifts are accurate to ±0.1 ppm and coupling constants to +0.7 Hz. Coupling constants with a —— entry are less than 0.7 Hz and br = broadened resonance. Couplings and chemical shifts with no entry were not determined. [b] Assignment of C-3 and C-4 may be reversed.
[c] Coupling could not be measured at 15.08 MHz due to resonance overlap. [d] May be from $^{2}J_{C1,C3}$.
[e] Split by 4.4 Hz. [f] Split by 3.7 Hz.

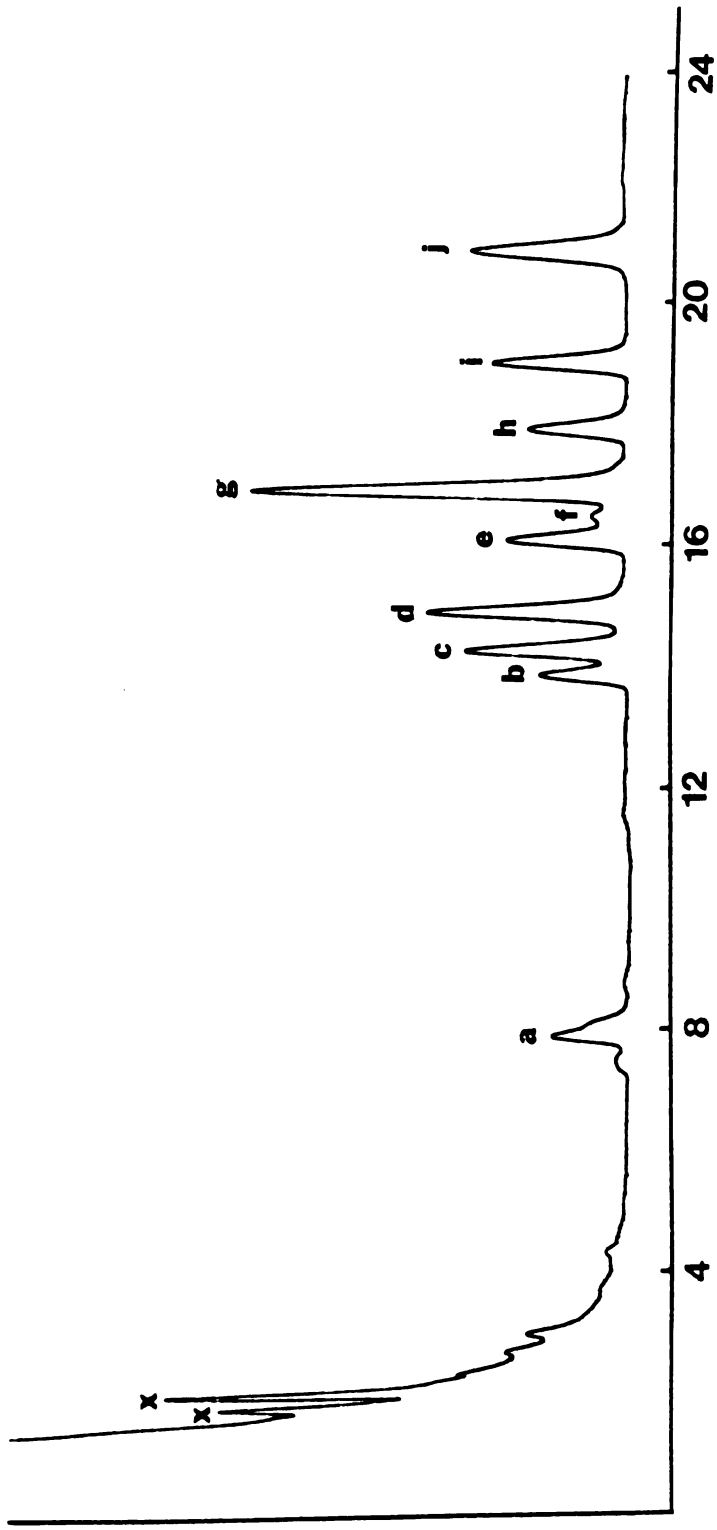

Figure 13. Gas-chromatograph of pertrimethylsilylated parent aldose, intermediates and end-products from the addition of cyanide to D-erythrose. a, D-erythrose; b, D-arabinononitrile; c, D-ribononitrile; d, D-arabinono-1,4-lactone; e, D-ribonate; f, D-ribono-1,4-lactone; g, D-arabinonate; h, D-ribonamide; i, D-arabinonamide. The identity of peak j is unknown but appears to arise from aldonamide derivatization. Peaks x are components of the silylating reagent.

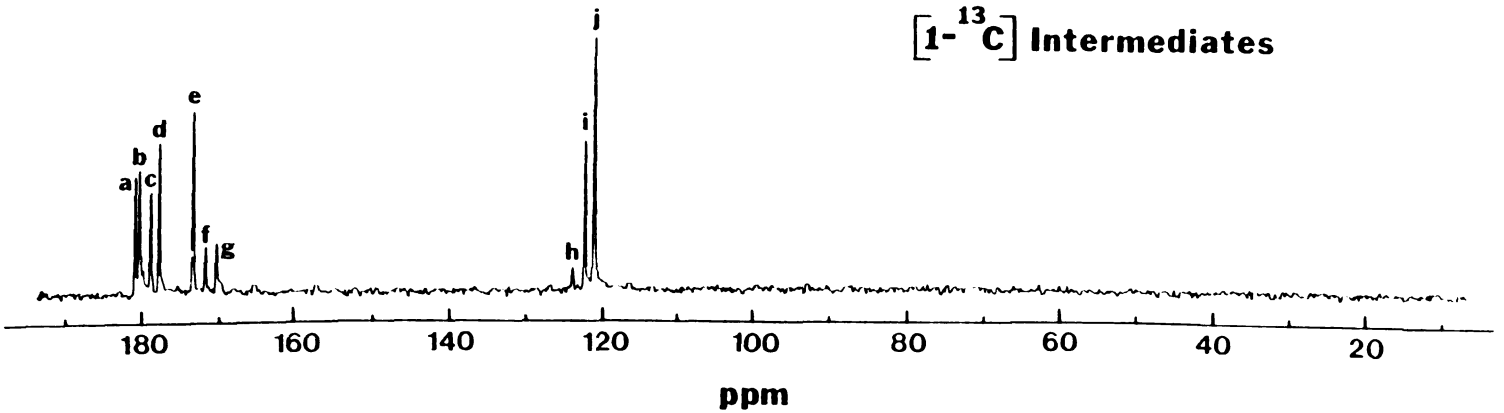

Figure 14. ^{1}H-Decoupled 15.08 MHz ^{13}C NMR spectrum of intermediates with 90.7 atom percent [^{13}C]-enrichment at C-1. The spectrum shows only the enriched carbons (2536 scans). Reaction concentrations: 0.3 M in D-erythrose and [^{13}C]cyanide; pH 7.0 ± 0.4; total reaction time, 11 h; 18° ± 1°C. a, D-[1-^{13}C]arabinonate; b, D-[1-^{13}C]arabinonamide; c, D-[1-^{13}C]ribonamide; d, D-[1-^{13}C]arabinono-1,4-lactone; e, D-[1-^{13}C]arabinono-amidine; f, D-[1-^{13}C]ribono-amidine; g, U1; h, U2; i, D-[1-^{13}C]arabinononitrile; j, D-[1-^{13}C]ribono-nitrile. Shoulder and minor resonance between peaks b and c are D-[1-^{13}C]ribono-1,4-lactone and D-[1-^{13}C]ribonate, respectively.

The ^{13}C NMR parameters of the reaction components are important to establish their presence in the reaction sequence. The chemical shift of cyanide is pH-dependent, with HCN having δ = 113 ppm and CN^- with δ = 166.4 ppm. The short-chain aldoses that exist principally as hydrates have C-1 resonances at 90 ± 2 ppm. Changing OH-3 to H-3' produces a downfield shift in C-1 of 3-4 ppm. Aldononitriles have C-1 resonances at approximately 120 ppm at pH 8.5 that shift downfield ∿5 ppm as the pH is increased to pH 12.7.

C_5 Aldononitrile chemical shifts were assigned by preparing and separating the 2-epimeric [1-^{13}C]aldononitrile phosphates and removing the phosphate group with acid phosphatase. Assignments were also based on observed differences in magnitude of $^3J_{C1,C4}$ for standard linear ribo compound (∿0 Hz) and arabino compounds (∿2.5 Hz) (Table 3). This difference probably reflects the preferred conformations of these compounds in solution (107). Compounds having the arabino configuration are expected to have a planar, extended conformation, where C-1 and C-4 are anti-planar (180°) and maximal coupling occurs based on the Karplus relationship (125). Solution conformation of linear compounds having the ribo configuration are expected to have C-1 to C-4 dihedral angles of approximately 90°, where ^{13}C-^{13}C three-bond coupling is at, or close to, a minimum.

Chemical shifts at 175.4 ppm and 177.3 ppm are assigned to C-1 resonances of imido-1,4-lactones having the arabino and ribo configuration , respectively. These assignments are based on comparison of NMR parameters (δ and J) of these compounds with structurally-related standard 1,4-lactones of known configuration, on their time of appearance during the alkaline hydrolysis of aldononitriles, and on the structure

and proportion of products found after acid hydrolysis (aldono-1,4-lactones). The C-2, C-3 and C-4 chemical shifts of D-ribono- and D-arabinono-1,4-lactones and the respective imido-1,4-lactones are very similar (Table 3), while C-1 of the 1,4-lactones is 2.2-2.7 ppm downfield from the corresponding imido-1,4-lactones. The chemical shift of C-4 is sensitive to ring form, i.e., ring formation involving OH-4 causes downfield shifts (>10 ppm) in C-4 from 71-73 ppm to 83-88 ppm. For example, the C-4 chemical shifts of D-ribono-1,4-lactone and D-ribono-imido-1,4-lactone are found at 88.2 ppm, while those for linear D-ribononitrile, D-ribonamide, D-ribonic acid and D-ribonate are found between 71.9 and 72.9 ppm (Table 3). Although C-4 chemical shifts of the pentose phosphates (Section III, B5b) and tetroses (Section III, B5a) are relatively insensitive to configuration at C-2 and C-3, the C-4 resonances of the 1,4-lactones and imido-1,4-lactones having the ribo configuration (OH-2 and OH-3 cis) are downfield (88.2 ppm) from those having the arabino configuration (OH-2 and OH-3 trans) (82.6 ppm).

$J_{C1,C3}$ and $J_{C1,C4}$ for standard aldono-1,4-lactones and for imido-1,4-lactones having the arabino configuration are about 7 Hz and <0.8 Hz, respectively. $J_{C1,C3}$ and $J_{C1,C4}$ for the ribo isomers are $\sim$2.0 Hz and $\sim$1.5 Hz, respectively. Acid hydrolysis (<pH 4) of an epimeric mixture of [1-^{13}C]imido-1,4-lactones yields an epimeric mixture of [1-^{13}C]aldono-1,4-lactones (162, 163), and the proportion of epimeric 1,4-lactone products corresponds to the proportion of epimers in the imido-1,4-lactone mixture.

Chemical shifts at 171.6 ppm and 173.2 ppm are assigned to C-1 of amidines having the ribo and arabino configuration , respectively.

These assignments of structure and configuration are based on reactions of separated and epimeric mixtures of D-[1-^{13}C]ribo- and arabinononitriles with NH_4Cl at pH 9.5 that yield products with C-1 chemical shifts at 171.6 ppm and 173.2 ppm, respectively. Amidines form readily from imidates under these conditions (164), and cyclic analogues of the latter (imidolactones) form at pH 9.5 during aldononitrile hydrolysis (see below). ^{1}H-Coupled ^{13}C NMR spectra of the [1-^{13}C]amidines show that C-1 does not have directly-bound proton(s).

Chemical shifts at 170 ppm (U1) and 122 ppm (U2) appear in reaction mixtures between pH 7.0 and 10.5. These chemical shifts are pH-dependent (Table 3) with pH <4 causing upfield shifts and splitting ($\sim$4 Hz) of both resonances. Gated ^{1}H-decoupling experiments show that these carbons are not directly bound to proton(s). From reaction of K^{13}CN with D-[1-^{13}C]erythrose, C-2 resonances of U1 and U2 were observed at 81.8 ppm and 72.3 ppm, respectively, and $^{1}J_{C1,C2}$ values of 41.8 and 54.3 Hz, respectively, were calculated. U1 and U2 bind to Dowex 50 (H^+) resin at pH 1-2 and are eluted together with 1 M triethylammonium bicarbonate at pH 7.5, and both hydrolyze in alkali (pH 12.6) and acid (pH 0.6) to aldonates and lactones, respectively. Addition of KCN to [1-^{13}C] U1 and U2 at pH 8.5-9.0 does not cause isotope exchange of the enriched nuclei.

The C-2 chemical shift of U1 suggests a five-membered ring structure and $^{1}J_{C1,C2}$ indicates that both C-1 and C-2 are sp^3-hybridized. The C-1 chemical shift of U2 is found in the aldononitrile region and is nonexchangeable. The resonances of U1 and U2 are split by similar amounts at low pH, indicating that they are in the same molecule. The resonances appear simultaneously in reaction mixtures after

imido-1,4-lactone synthesis. The behavior of U1 and U2 on Dowex 50 (H^+) suggests that they are cationic at low pH. Structure *12* is consistent with these properties. U1 is the C-1 resonance of the furanoid component of dimer *12*, while U2 arises from the acyclic nitrile carbon. Dimer *12* probably forms by the addition of the cyanohydrin alkoxide (Scheme VII) to the protonated imido-1,4-lactone. The amount of *12* formed during the cyanohydrin reaction at pH 8.5 depends on the concentration of the reactants, as expected for a bimolecular reaction (see below). A similar structure (*11*) was proposed by Kuhn and Weiser (165), who treated *9* with CH_3OH-H_2O-HCl and demonstrated the presence of orthoester *10* in the reaction mixture (Chart II). Compound *10* resumably arises from *11*.

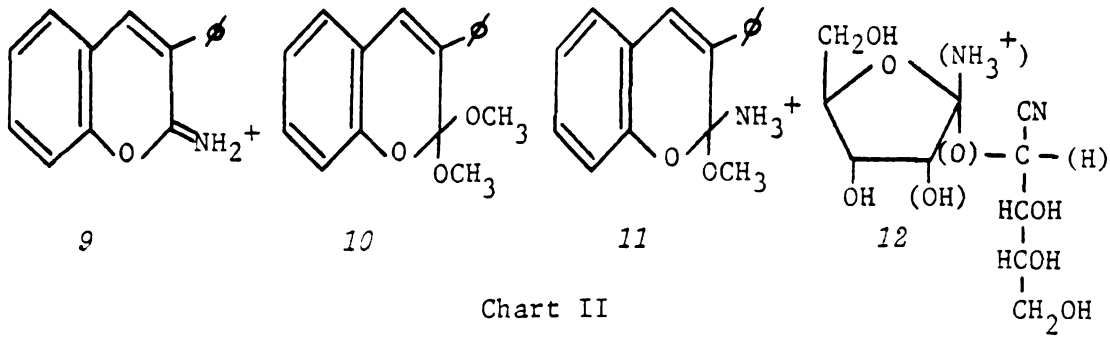

9 *10* *11* *12*

Chart II

Assignments of configurations to the [2-^{13}C]imido-1,4-lactones from the addition of cyanide to D-[1-^{13}C]erythro, threo-2,3-dihydroxybutanal are based on the effect of configuration at C-2 and C-3 on the chemical shift of C-2 (114), on similar ratios of epimeric imido-1,4-lactones found from addition of cyanide to D-erythrose and D-threose under the same conditions, and on similar C-2 chemical shifts of the structurally-related pentono-1,4-lactones (Table 3).

$^1J_{C1,C2}$ was measured for several intermediates simultaneously by

adding $K^{13}CN$ to D-[1-^{13}C]erythrose (Figure 15). $^{1}J_{C1,C2}$ for the intermediates at pH 9.0 increase in the following order: U1 (42 Hz), amidines (48 Hz), imido-1,4-lactones (51 Hz), aldonamides (53 Hz), aldonates (54 Hz), aldono-1,4-lactones (56 Hz), aldonic acids and aldononitriles (60 Hz). A multiply-bonded nitrogen decreases $^{1}J_{C1,C2}$ relative to the oxygen analogue by about 5 Hz.

5. The cyanohydrin reaction applied to D-erythrose: Intermediates in the hydrolysis of D-ribono- and D-arabinononitriles at several pH values

D-Erythrose was selected as the parent aldose for the following reasons: (a) the availability of D-or DL-erythrose enriched with ^{13}C at several positions, (b) ^{13}C resonances of intermediates could be resolved, (c) the role of five- and six- membered ring-formation during hydrolysis of aldononitriles could be examined, (d) differences in the rates of hydrolysis of the epimeric intermediates were observed, and (e) structurally-modified analogs were available. Reactions were carried out at 18° ± 1°C and 0.3 M with stoichiometric amounts of reactants. HCl and/or NaOH were used to control the pH of the reaction mixture to ±0.2 units for experiments conducted at pH 7, 8.5 and 10.5. Reactions at pH 12.7 involved the addition of the aldose to KCN without pH control.

At pH 12.7, several intermediates are observed (Figure 16). Aldononitriles disappear in 1.7 h with the formation and hydrolysis of the aldonamides. Aldonate formation is complete in 3.5 h. The apparent sequence of the reactions appears to be nitrile → amide → aldonate.

Analyses at pH 12.7 are complicated by line-broadening due to chemical exchange and by the pH-dependence of the C-1 chemical shifts in this pH range (Table 3). Consequently, the reaction sequence

Figure 15. ^{1}H-Decoupled 15.08 MHz ^{13}C NMR spectrum of intermediates with 90.7 atom percent [^{13}C]-enrichment at C-1 and C-2.

The spectrum shows only the [^{13}C]-enriched C-1 and C-2 carbon atoms (400 scans). Reaction conditions: 0.3 M in D-[1-^{13}C]erythrose and [^{13}C]cyanide; pH 8.5 ± 0.2; total reaction time, 14 min; 18° ± 1°C. (A) Spectrum showing three regions of [^{13}C]-enrichment: 118-125 ppm and 168-182 ppm for C-1 of the aldononitriles and remaining intermediates, respectively, and 61-83 ppm for C-2 of the intermediates. C-1 Resonances for D-[1-^{13}C]erythrose appear between 90-103 ppm. (B) The expanded C-2 region of A, showing $^{1}J_{C1,C2}$ for U1, D-[1,2-^{13}C]-arabinono-imido-1,4-lactone (AI), D-[1,2-^{13}C]ribono-imido-1,4-lactone (RI), D-[1,2-^{13}C]ribononitrile (RN) and D-[1,2-^{13}C]arabinononitrile (AN). Peaks n are the natural abundance resonances of the aldononitriles.

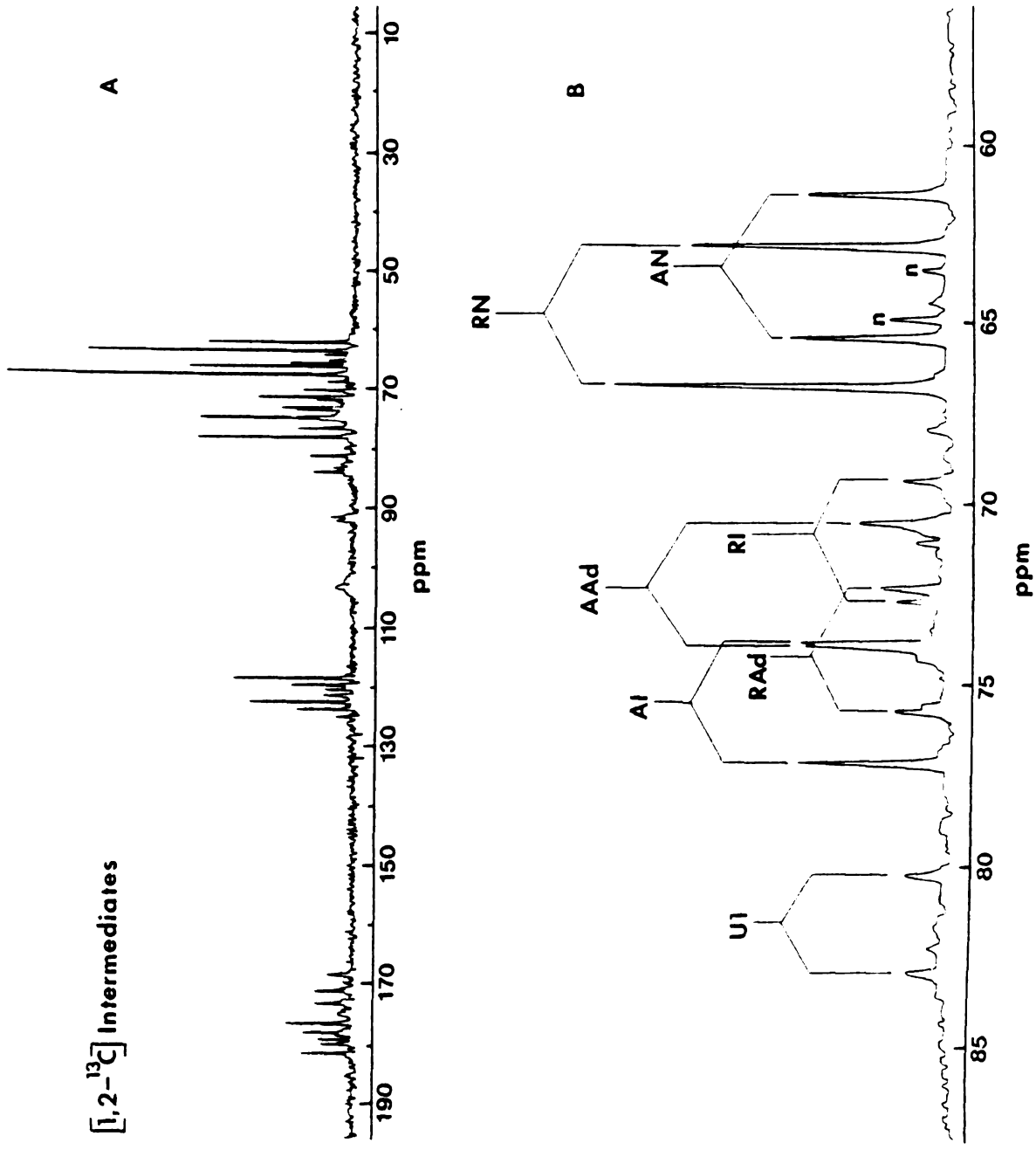
A
[1,2-13C] Intermediates
190
170
150
130
110
90
70
50
30
10
ppm
B
RN
AN
n
n
AAd
RI
AI
RAd
UI
85
80
75
70
65
60
ppm

Figure 15.

Figure 16. Cyanohydrin reaction profile at pH 12.7.

Data were obtained from ^{13}C NMR spectra of [1-^{13}C]-enriched intermediates (100 scans). Reaction conditions: 0.3 M in D-erythrose and [^{13}C]cyanide; 18° ± 1°C. RN, D-[1-^{13}C]ribononitrile; AN, D-[1-^{13}C]arabinononitrile; RAd, D-[1-^{13}C]ribonamide; AAd, D-[1-^{13}C]arabinonamide; RAs, D-[1-^{13}C]ribonate; AAs, D-[1-^{13}C]arabinonate.

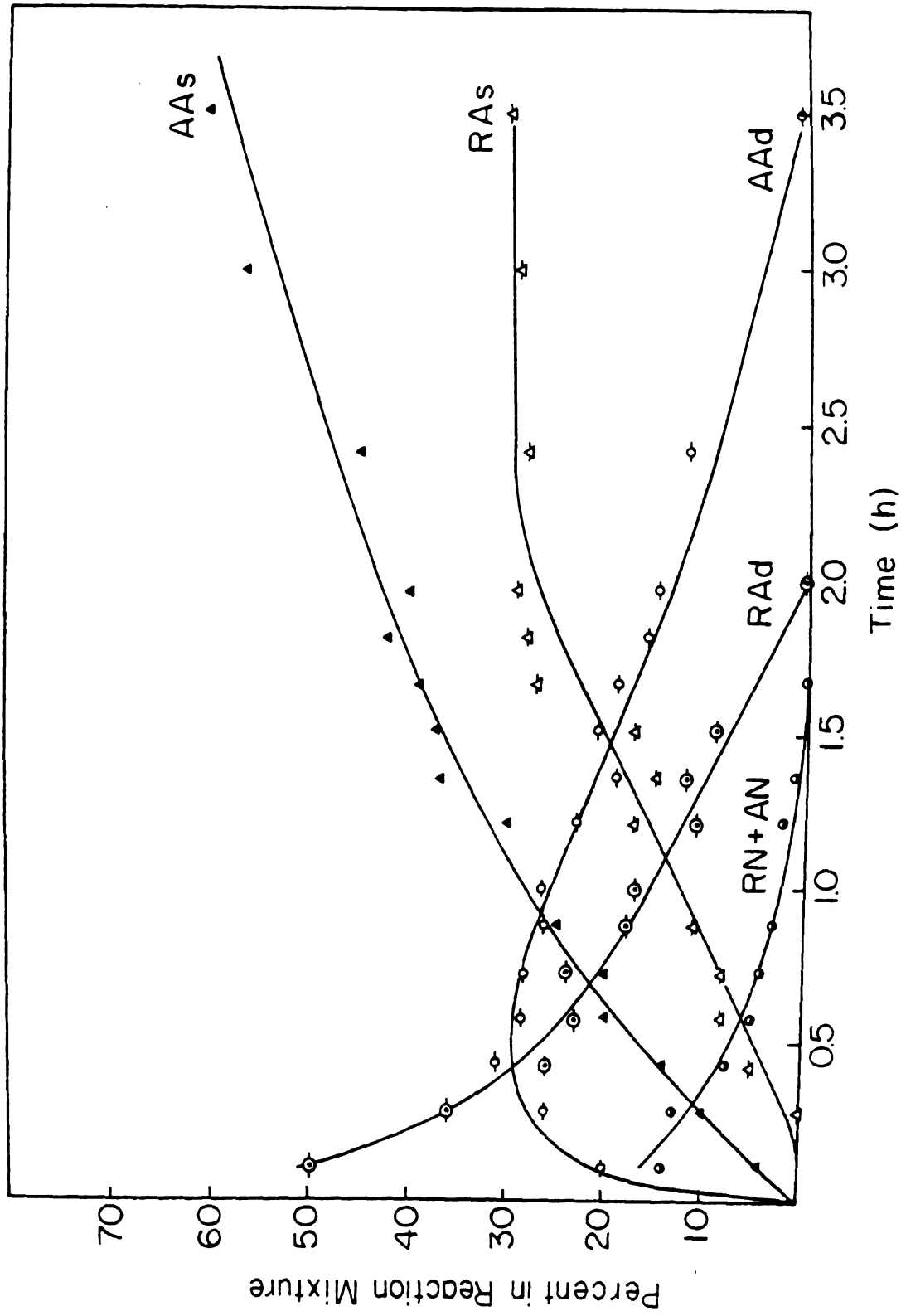
AAs
RAs
AAd
RAd
RN+AN
Time (h)
0.5
1.0
1.5
2.0
2.5
3.0
3.5
Percent in Reaction Mixture
10
20
30
40
50
60
70

Figure 16.

appears deceptively simple. For example, the plot assigned to D-ribonamide contains a component that increases rapidly during the first 10 min which cannot be D-ribonamide itself. As discussed below, the amides, once formed, do not revert to early intermediates nor do they epimerize. On this basis, there cannot be more ribonamide than arabinonamide in the reaction mixture, unless ribonate is the major product; it is not (Table 1).

To examine the reaction at pH 12.7 further, aliquots taken at various times were quenched with HCl to pH 4 (Figure 17). At this pH, resonances are sharp and the intermediates are stable for several hours. In this experiment, the apparent sequence of intermediates is nitrile → aldono-1,4-lactone → amide → aldonate.

The early appearance of large amounts of 1,4-lactones in the quenched reaction mixture does not indicate that they are present as intermediates at pH 12.7. Instead, it reflects the presence of imidolactones. The rate of imidolactone hydrolysis and the products formed (amide and/or lactone) are pH-dependent (162, 163). With decreasing pH, the rate of imidolactone hydrolysis and the percentage of lactone produced increase. We conclude that imidolactones present at pH 12.7 are rapidly hydrolyzed to lactones when the mixture is quenched. The reaction sequence at pH 12.7, therefore, is nitrile → imido-1,4-lactone → amide → aldonate.

Aldononitrile hydrolysis at pH 10.5 (Figures 18A, 18B and 19) differs from hydrolysis at pH 12.7 in several respects. Neither starting aldose nor aldononitriles are detected by ^{13}C NMR or GLC. Instead, imidolactones predominate initially and hydrolyze rapidly to produce amides. The latter hydrolyze slowly to the corresponding aldonates.

Figure 17. Cyanohydrin reaction profile from pH-quenched reactions at pH 12.7.

Data were obtained from ^{13}C NMR spectra of [1-^{13}C]-enriched intermediates (400 scans). Reaction conditions: 0.3 M in D-erythrose and [^{13}C]cyanide; 18° ± 1°C; 0.5 mL aliquots were quenched at various time intervals with 0.7 mL HCl (0.3 M), incubated at 25°C for 20-30 min, and analyzed by ^{13}C NMR after pH adjustment to 5. RN, D-[1-^{13}C]ribononitrile; AN, D-[1-^{13}C]arabinononitrile; AL, D-[1-^{13}C]arabinono-1,4-lactone; RL, D-[1-^{13}C]ribono-1,4-lactone; RAd, D-[1-^{13}C]ribonamide; AAd, D-[1-^{13}C]arabinonamide; AAs, D-[1-^{13}C]arabinonate; RAs, D-[1-^{13}C]ribonate.

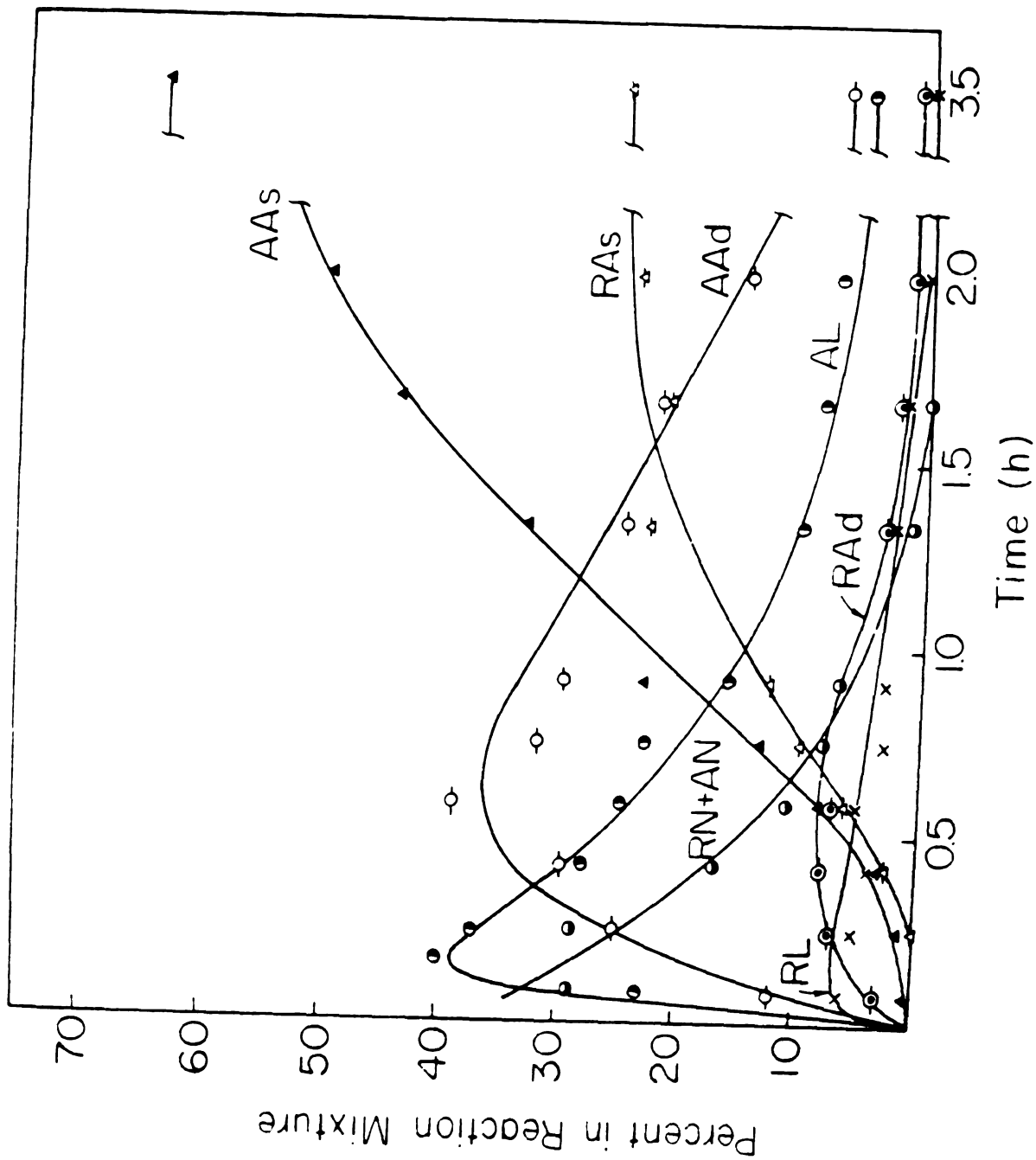
AAs
RAs
AAd
AL
RAd
RN+AN
RL
Percent in Reaction Mixture
Time (h)
70
60
50
40
30
20
10
0.5
1.0
1.5
2.0
3.5

Figure 17.

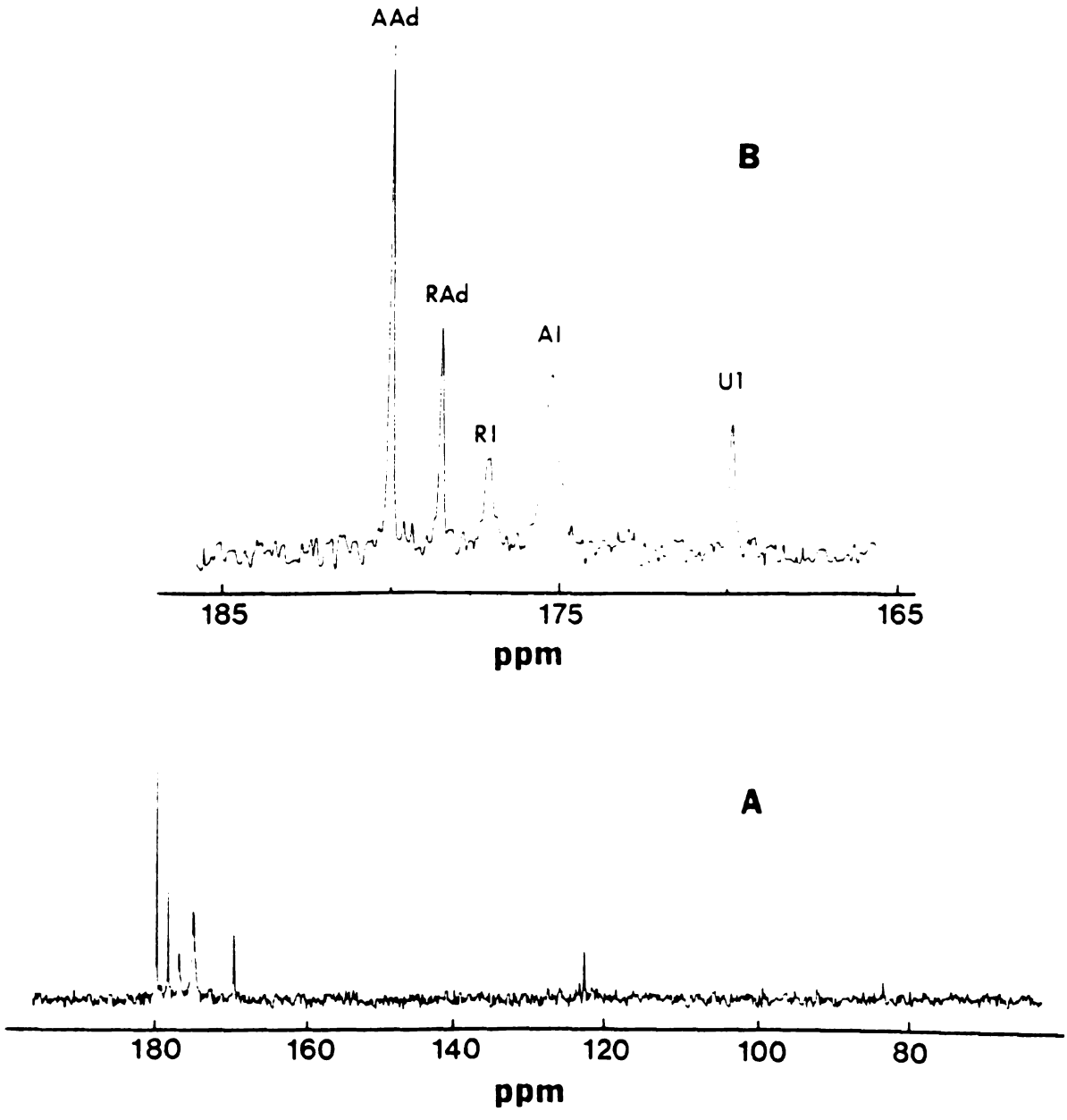

Figure 18. ^{1}H-Decoupled 15.08 MHz ^{13}C NMR spectrum of [1-^{13}C]intermediates after 11 min at pH 10.5, showing imido-1,4-lactone formation. Spectra show only the enriched carbons (128 scans). Reaction conditions: same as described in Figure 16. (A) The ^{13}C NMR spectrum showing the absence of aldononitriles. (B) The expanded 170-180 ppm region of A showing the C-1 resonances of the epimeric imido-1,4-lactones, the epimeric aldonamides, and U1. The resonance of U2 is observable in A at 122.9 ppm. AAd, D-[1-^{13}C]arabinonamide; RAd, D-[1-^{13}C]ribonamide; RI, D-[1-^{13}C]ribono-imido-1,4-lactone; AI, D-[1-^{13}C]arabinono-imido-1,4-lactone.

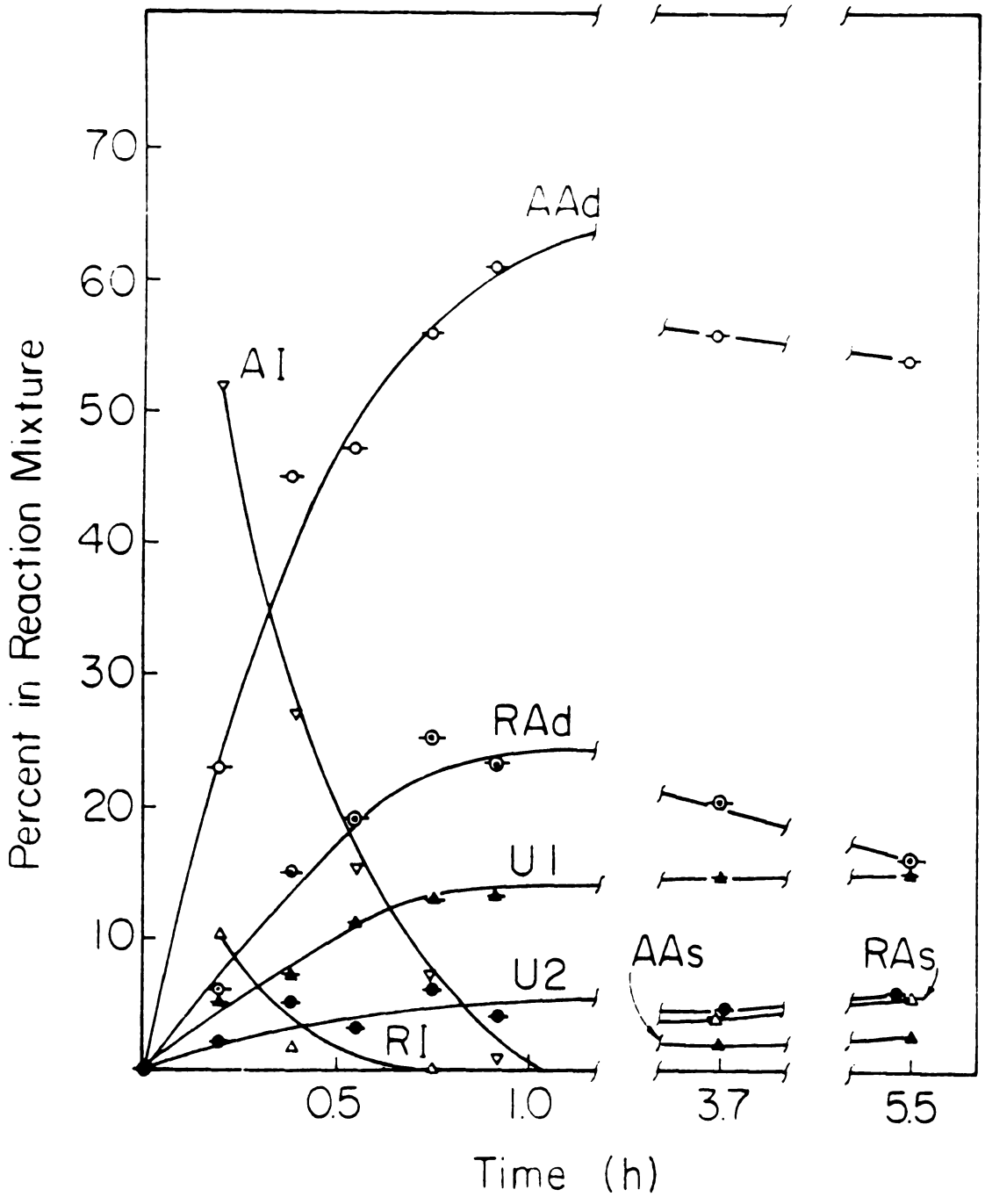

Figure 19. Cyanohydrin reaction profile at pH 10.5. Data were obtained from ^{13}C NMR spectra of [1-^{13}C]-enriched intermediates. Reaction parameters are the same as those described in Figure 18. AI, D-[1-^{13}C]arabinono-imido-1,4-lactone; RI, D-[1-^{13}C]ribono-imido-1,4-lactone; AAd, D-[1-^{13}C]arabinonamide; RAd, D-[1-^{13}C]ribonamide; U1 and U2, dimer *12*.

Dimer *12* is observed (U1, U2) and appears to arise from imidolactone.

Aliquots taken from reaction mixtures at pH 10.5 during the first hour were quenched to pH 4 to determine whether the amount of lactone observed at pH 4 corresponded to the amount of imidolactone present at pH 10.5. As shown in Figure 20, imidolactones present at pH 10.5 are quantitatively converted to aldono-1,4-lactones at pH 4. Assignment of the broad C-1 resonance at 175.3 ppm (Table 2 and Figures 18A, 18B) to D-[1-^{13}C]arabinono-imido-1,4-lactone is based on the observation that D-[1-^{13}C]arabinono-1,4-lactone is the predominant lactone produced in this experiment. The formation of five-membered imidolactones in the cyanohydrin reaction is suggested by the production of aldono-1,4-lactones during acid hydrolysis. At pH 10.5, the reaction sequence appears to be nitrile → imido-1,4-lactone → amide → aldonate.

Aldononitrile hydrolysis at pH 8.5 is slow. During the first 30 min, aldononitriles comprise 95 percent of the reaction mixture (Figure 21). Imidolactone (arabino), observed next, reaches its maximum concentration (5%) after 40 min. Amides are produced slowly and are stable. Dimer *12* is produced concomitantly with amide. D-Arabinono-1,4-lactone forms by hydrolysis of D-arabinono-1,4-imidolactone at pH 8.5. At this intermediate pH value, the products of imidolactone hydrolysis are both lactone and amide, as described by Schmir and Cunningham (162). At pH 8.5, aldonolactones hydrolyze slowly to aldonates. The latter are not formed from amide hydrolysis, which occurs at a negligible rate.

At pH 8.5, ammonia released from the hydrolysis of imidolactones reacts with the protonated imidolactones to produce amidines *13* (~15%).

Figure 20. Conversion of imido-1,4-lactones to aldono-1,4-lactones at pH <4.

The reaction at pH 10.5, 0.3 M and 18° ± 1°C with D-erythrose and [^{13}C]cyanide was examined three times during the first 60 min by ^{13}C NMR to determine the amount of aldonamide (■) and imido-1,4-lactone (O). From the same reaction, three 0.5 mL aliquots were quenched with HCl (0.7 mL, 0.3 M), incubated for 20 min, adjusted to pH 5 and examined by ^{13}C NMR to determine the amount of aldonamide (●) and aldono-1,4-lactone (□). Percentage of intermediates is based on the total peak areas in the spectra arising from the aldonamides, imido-1,4-lactones and 1,4-lactones, and therefore, does not contain a contribution from dimer *12* (U1, U2).

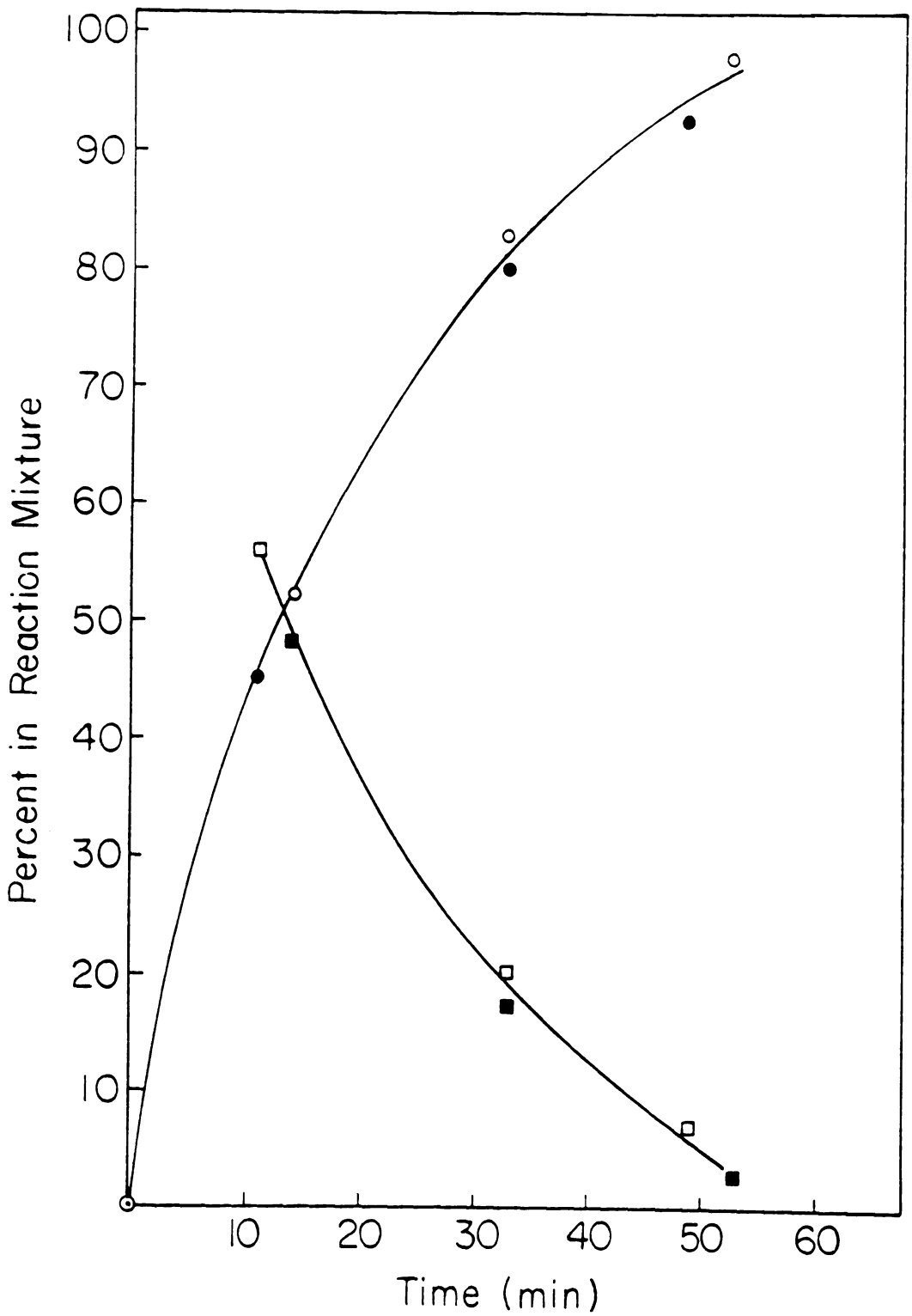
Percent in Reaction Mixture
100
90
80
70
60
50
40
30
20
10
10
20
30
40
50
60
Time (min)

Figure 20.

Figure 21. Cyanohydrin reaction profile at pH 8.5.

Data were obtained from ^{13}C NMR spectra of [1-^{13}C]-enriched intermediates. Reaction conditions are the same as those described in Figure 16. RN, D-[1-^{13}C]ribononitrile; AN, D-[1-^{13}C]arabinononitrile; AI, D-[1-^{13}C]arabinono-imido-1,4-lactone; RAd, D-[1-^{13}C]ribonamide; AAd, D-[1-^{13}C]arabinonamide; AAm, D-[1-^{13}C]arabinono-amidine; AAs, D-[1-^{13}C]arabinonate; RAs, D-[1-^{13}C]ribonate; AL, D-[1-^{13}C]arabinono-1,4-lactone; U1 and U2, dimer *12*.

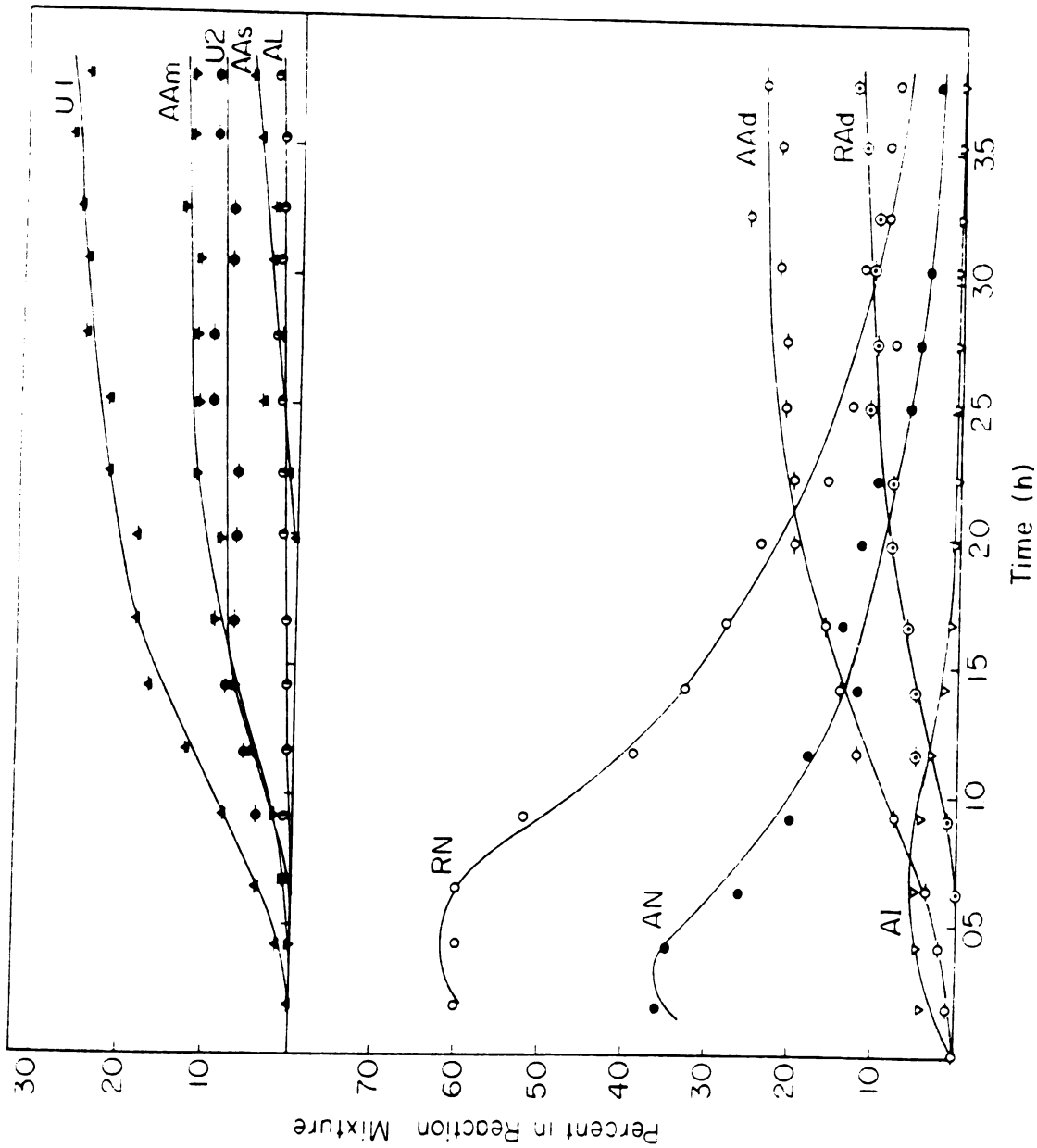
U1
AAm
U2
AAs
AL
AAd
RAd
RN
AN
AI
Percent in Reaction Mixture
Time (h)

Figure 21.

When stoichiometric amounts of NH_4Cl, D-erythrose and [^{13}C]cyanide

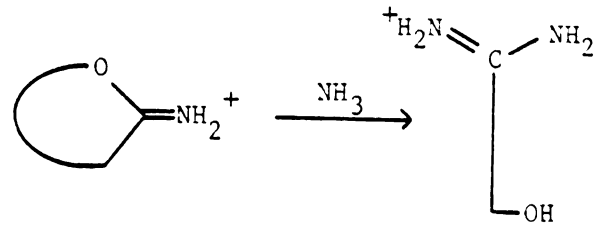

13

are mixed at pH 8.5 or 9.5, amidine formation is stimulated. At pH 8.5, amidine formation is slow (55% in 50 min), whereas,at pH 9.5, it is rapid and almost quantitative. The arabino epimer (δ_{C-1} = 173.2 ppm) and ribo epimer (δ_{C-1} = 171.6 ppm) are produced in both cases in a 3:1 ratio (Figure 22B). At pH 8.5, standard cyanohydrin reaction mixtures contain arabinonoamidine (13%) while the ribo isomer is barely observable (<2%). These observations are consistent with those of Hand and Jencks (164) who observed that the rate of ethyl benzimidate aminolysis is pH-dependent, with the maximum rate occurring at pH 8.9.

Assignment of the arabino configuration to the amidine C-1 resonance at 173.2 ppm is based on the chemical shift of the principal product from aminolysis of authentic D-[1-^{13}C]arabinononitrile at pH 9.5. When D-[1-^{13}C]arabinononitrile is incubated at pH 9.5, a small amount of D-[1-^{13}C]ribononitrile is formed by reversal of the condensation reaction. Thus, when D-[1-^{13}C]arabinononitrile is treated with ammonia at pH 9.5, approximately 10 percent of the amidine formed has the ribo configuration.

Dimer *12* comprises 35 percent of the reaction mixture after 4 h at pH 8.5. It appears to arise from imidolactone, since solutions

Figure 22. Effect of NH_4Cl on the formation of intermediates.

(A) ^{13}C NMR spectrum of the reaction mixture at pH 10.5 after 1 h, showing D-[1-^{13}C]arabinonamide (AAd), D-[1-^{13}C]ribonamide (RAd), and dimer *12* (U1, U2). (B) ^{13}C NMR spectrum of the reaction mixture at pH 9.5 with one equivalent of NH_4Cl after 1 h, showing D-[1-^{13}C]arabinono-amidine (AAm), D-[1-^{13}C]ribono-amidine (RAm), D-[1-^{13}C]arabinonamide (AAd) and D-[1-^{13}C]ribonamide (RAd). Reaction conditions are the same as those described in Figure 16.

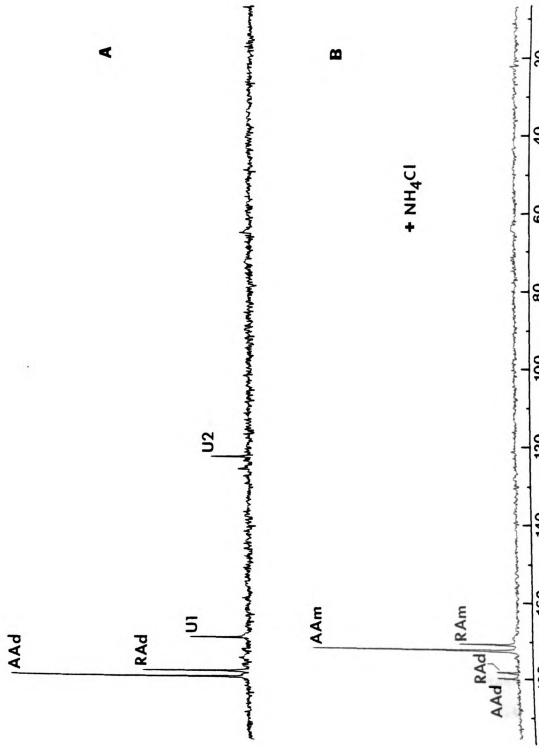
AAd
RAd
U1
U2
A
B
+ NH4Cl
AAm
RAm
RAd
AAd
180
160
140
120
100
80
60
40
20
ppm

Figure 22.

that contain large amounts of imidolactone (Figure 18A, 18B), when adjusted to pH 8.5-9.0 and examined quickly, are found to contain *12* in almost the same proportion as it is found after 4 h at pH 8.5 (Figure 21). At pH 8.5, the apparent sequence of the reaction appears as follows:

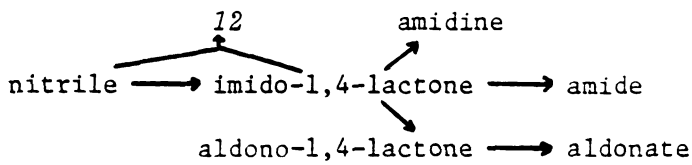

The condensation of HCN with D-erythrose at pH 7 produces aldononitriles in the ratio of 3:2 ribo:arabino, and their hydrolysis is slow. After 11 h, aldononitriles comprise 38 percent of the reaction mixture (Figure 14). Hydrolysis products at this time include aldonates, amides, 1,4-lactones, amidines and dimer *12*. Imidolactones are barely detectable (<2%), and their direct hydrolysis to lactones is faster than at higher pH. The arabino epimers predominate in all of the intermediates except for the aldononitriles. Aldonates are formed by 1,4-lactone hydrolysis since amide hydrolysis is negligible at pH 7. The apparent sequence of the reaction appears similar to that at pH 8.5 with differences occurring only in the relative amounts of intermediates produced.

6. Imidolactone formation

At all pH values, imidolactones appear to play an important role in the hydrolysis of those aldononitriles that can form them. Varma and French (46) have proposed that six-membered imidolactones are intermediates in the reaction of cyanide with D-arabinose. The slow rate of hydrolysis of C_4 aldononitriles (*4*) relative to C_5

aldononitriles (6, 7) suggests that the formation of five-membered imidolactones is not favorable, although there are many examples where ring-closure involving an sp^2-hybridized carbon proceeds to yield the more stable five-membered ring with an exocyclic double bond (166). For these reasons, the ring-forms of the imidolactone and lactone intermediates required further investigation.

The C-1 chemical shifts of 1,4-lactones and 1,5-lactones are not identical, as shown in Table 3. In addition, 1,5-lactones do not revert to 1,4-lactones under conditions where imidolactones hydrolyze to lactones. Therefore, the production of 1,4-lactones probably reflects the presence of imido-1,4-lactones.

Direct evidence for imido-1,4-lactone intermediates was obtained by preparing [1,3-^{13}C]aldononitriles from DL-[2-^{13}C]erythrose and K^{13}CN, and [1,4-^{13}C]aldononitriles from DL-[3-^{13}C]erythrose and K^{13}CN. With these compounds, the chemical shifts of C-3 and C-4 and ^{13}C-^{13}C coupling constants between the enriched nuclei are readily determined (Figures 23A and 24A, Table 3). Following condensation at pH 8.5, the ^{13}C NMR spectra of the aldononitriles were obtained. The reaction mixture was then adjusted to pH 10.5 where rapid conversion of aldononitriles to imidolactones occurs. Results are shown in Figures 23B, 23C and 24B. The ^{13}C chemical shifts and ^{13}C-^{13}C coupling constants of imidolactones obtained from these experiments are similar to those for 1,4-lactones prepared by standard methods. The large downfield shift of C-4 observed in the imidolactones establishes that OH-4, and not OH-5, is involved in imidolactone ring formation.

Further evidence supporting formation of imido-1,4-lactone was

Figure 23. Addition of [^{13}C]cyanide to DL-[2-^{13}C]erythrose.

^{13}C NMR spectra show only [^{13}C]-enriched C-1 and C-3 carbons. (A) ^{13}C NMR spectrum of the reaction mixture after 13.5 min at pH 8.5, showing the formation of DL-[1,3-^{13}C]arabinononitrile (a) and DL-[1,3-^{13}C]ribononitrile (b). $^{2}J_{C1,C3}$ is <0.7 Hz in the aldononitriles. (B) ^{13}C NMR spectrum of the reaction mixture from A after 11 min at pH 10.5. a, DL-[1,3-^{13}C]arabinonamide; b, DL-[1,3-^{13}C]ribonamide; c, DL-[1,3-^{13}C]-ribono-imido-1,4-lactone; d, DL-[1,3-^{13}C]arabinono-imido-1,4-lactone; e, [^{13}C]cyanide. (C) ^{13}C NMR spectrum of the expanded C-3 region of B, showing $J_{C1,C3}$ for the imido-1,4-lactones. Like the linear aldononitriles in A, $J_{C1,C3}$ is <0.7 Hz in the aldonamides.

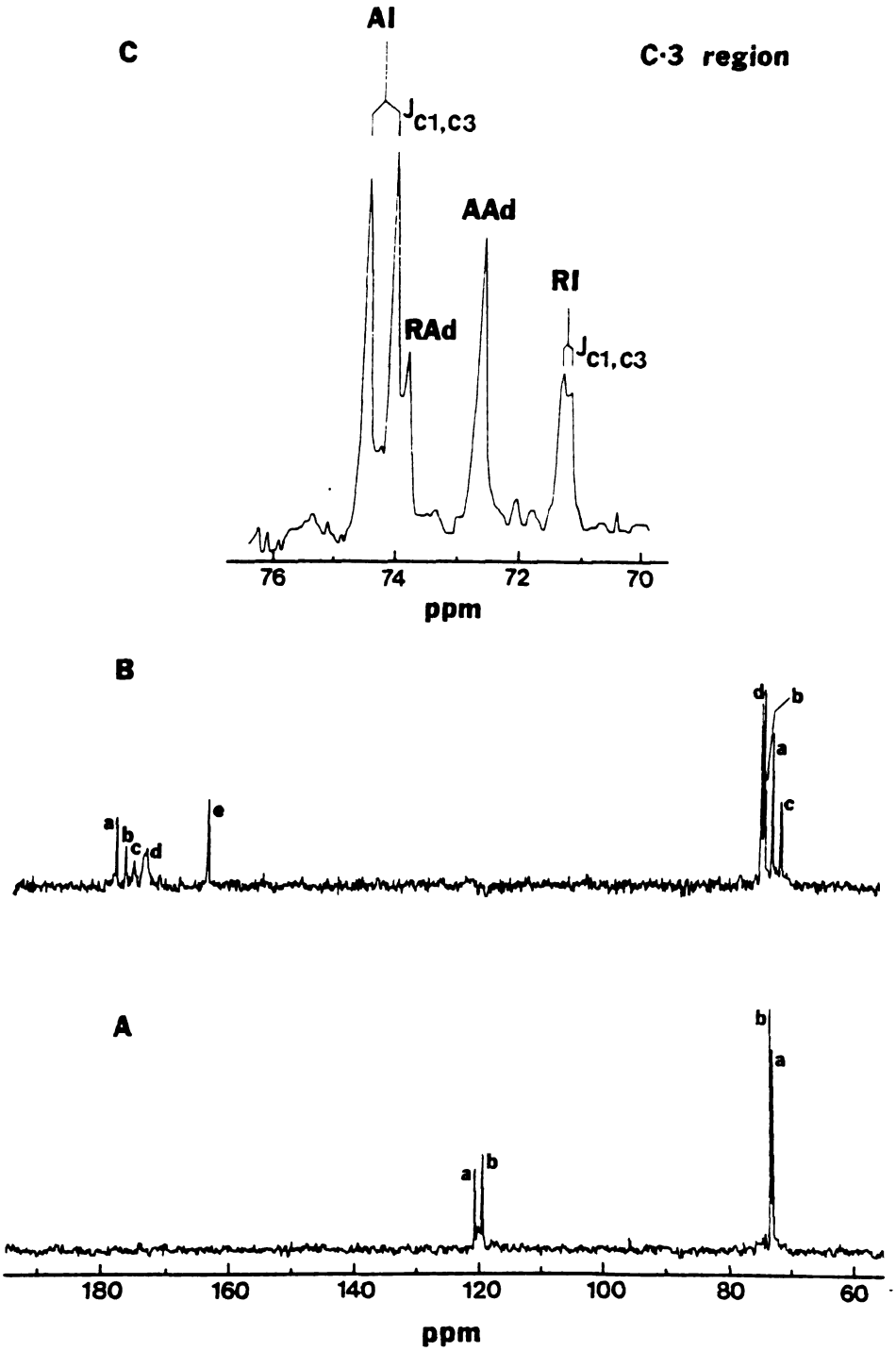
C
C-3 region
AI
$J_{C1,C3}$
AAd
RI
RAd
$J_{C1,C3}$
76
74
72
70
ppm
B
a
b
c
d
e
d
b
a
c
A
a
b
b
a
180
160
140
120
100
80
60
ppm

Figure 23.

Figure 24. Addition of [^{13}C]cyanide to DL-[3-^{13}C]erythrose.

^{13}C NMR spectra show only the [^{13}C]-enriched carbon at C-4, since the acquisition parameters [16 μsec (90°) pulse with no delay time] do not permit the detection of the unprotonated carbon at C-1. (A) ^{13}C NMR spectrum of the reaction mixture after 21.5 min at pH 8.0, showing the C-4 resonances of DL-[1,4-^{13}C]ribononitrile (a) and DL-[1,4-^{13}C]arabinononitrile (b). Inset shows $^{3}J_{C1,C4}$ for the arabino epimer. (B) ^{13}C NMR spectrum of the reaction mixture from A after 10 min at pH 10.5. a, [^{13}C]cyanide; b, DL-[1,4-^{13}C]ribono-imido-1,4-lactone; c, DL-[1,4-^{13}C]-arabinono-imido-1,4-lactone; d, DL-[1,4-^{13}C]ribonamide; e, DL-[1,4^{13}C]-arabinonamide. Inset shows $^{3}J_{C1,C4}$ for DL-[1,4-^{13}C]arabinonamide, and a broadened C-4 resonance for DL-[1,4-^{13}C]ribono-imido-1,4-lactone.

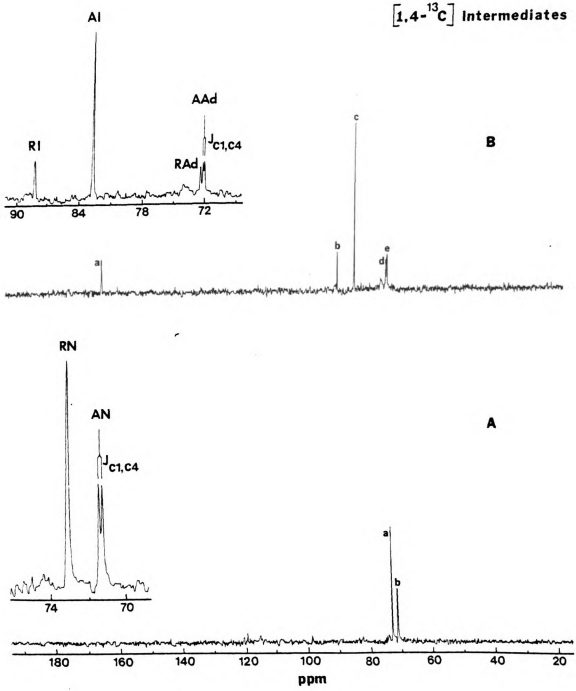
[1,4-13C] Intermediates
AI
AAd
RI
RAd
JC1,C4
90
84
78
72
B
a
b
c
d
e
RN
AN
JC1,C4
74
70
A
a
b
180
160
140
120
100
80
60
40
20
ppm

Figure 24.

obtained by preparing the four diastereomeric [2-^{13}C]aldononitriles from D-[1-^{13}C]erythro, threo-2,3-dihydroxybutanal (Figures 25A, 25B) and KCN having structure *14*. Aldononitriles *14* (Figure 25C) readily convert to imido-1,4-lactones *15* at pH 10.5 (Figure 25D). The C-2 resonances of the 5-deoxyimido-1,4-lactones were assigned based on their close agreement with C-2 of the corresponding 5-oxy analogues (Table 3) and on the ratio of epimeric imidolactones produced from addition of cyanide to D-erythrose and D-threose. The 5-deoxyimido-1,4-lactones hydrolyze readily to the corresponding aldonamides at pH 10.5, as do the corresponding 5-hydroxy compounds.

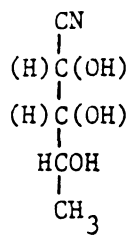

14

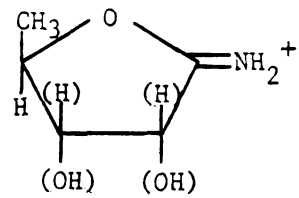

15

Brown, et al. (166) have discussed the behavior of five- and six-membered rings having exo double bonds in a variety of chemical reactions. They concluded that the formation of five-membered rings is more facile due to their greater stability while the reactivity of six-membered rings is greater due to their instability. This difference in ease of formation and in chemical reactivity affects the interpretation of data concerning ring formation in the cyanohydrin reaction. The presence of imido-1,4-lactone in reaction mixtures does not demonstrate that aldononitriles hydrolyze solely through this intermediate. An undetectable amount of imido-1,5-lactone may be present, with hydrolysis proceeding through the 1,5-ring, as shown

Figure 25. Addition of cyanide to D-[1-^{13}C]erythro, threo-2,3-dihydroxybutanal.

^{13}C NMR spectra show only the enriched carbons. (A) ^{13}C NMR spectrum of D-[1-^{13}C]erythro, threo-2,3-dihydroxybutanal. The aldose is hydrated (h) in dilute aqueous solution (<0.1 M). Peaks x are contaminants. (B) ^{13}C NMR spectrum of D-[1-^{13}C]erythro, threo-2,3-dihydroxybutanal at ∿1 M, showing the presence of dimers and/or oligomers and hydrate (h). (C) ^{13}C NMR spectrum of the reaction mixture after 12 min at pH 8.0. The C-2 resonances of the four diastereomeric D-[2-^{13}C] 5-deoxyaldononitriles are observed, with peak b having twice the area of peak a and peak c. (D) ^{13}C NMR spectrum of the reaction mixture from C after 8 min at pH 10.5, showing the formation of imido-1,4-lactones. Inset shows the C-2 resonances of D-[2-^{13}C] 5-deoxy-arabino- (a), xylo-(b), lyxo-(d) and ribo-(f) imido-1,4-lactones, D-[2-^{13}C] 5-deoxyaldonamides (c, e), D-[2-^{13}C] 5-deoxyaldononitriles (g) and contaminants x (h, i). (E) ^{13}C NMR spectrum of the reaction mixture from D after 47 min at pH 10.5, showing increased amounts of D-[2-^{13}C] 5-deoxyaldonamides and the absence of D-[2-^{13}C] 5-deoxyaldononitriles.

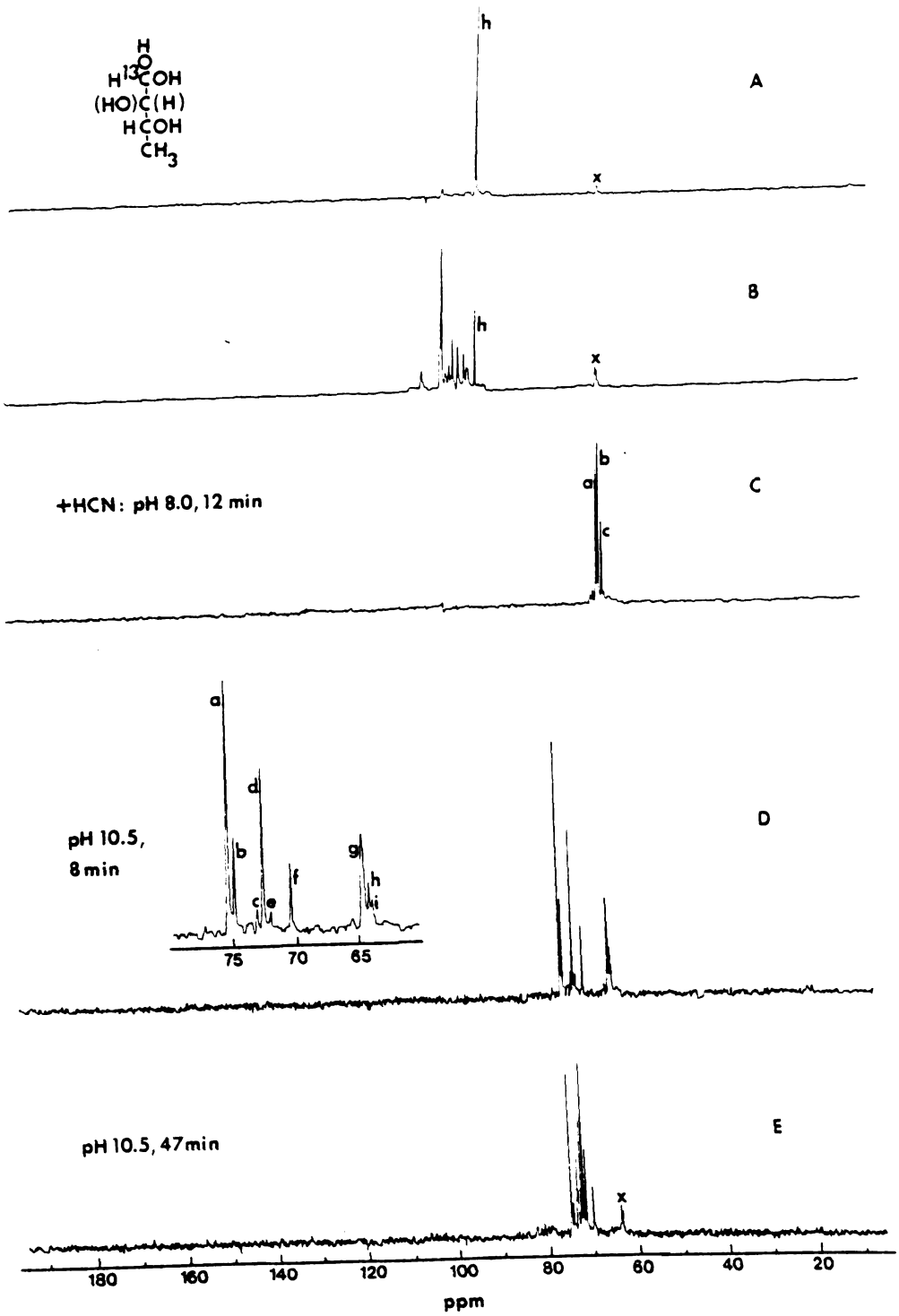
A
B
C
D
E
+HCN: pH 8.0, 12 min
pH 10.5, 8 min
pH 10.5, 47 min
ppm
180
160
140
120
100
80
60
40
20
75
70
65

Figure 25.

in Scheme IX. A significant proportion of aldononitrile will hydrolyze through the 1,5-ring if $k_{10} >> k_9$. Under these conditions, nevertheless, it would appear that hydrolysis proceeded through the 1,4-ring, since $K_6 >> K_7$. The possible involvement of 1,5-rings can be excluded by examining the reaction at pH 7, where aldononitriles cyclize very slowly and imidolactones decompose almost equally to amide and lactone. If the imido-1,5-lactone was hydrolyzing, reaction products would include 1,5-lactone or, more likely, its decomposition product (aldonate) early in the course of reaction. The results show that aldono-1,4-lactone accumulates 2-3 h before

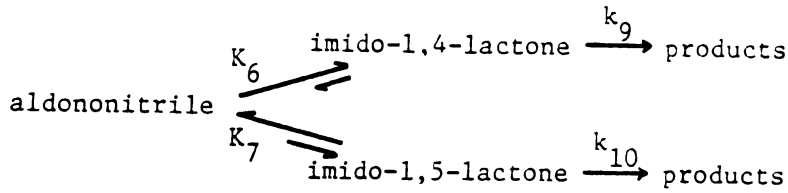

Scheme IX

aldonate is detected and that 1,5-lactone is not observed. Thus, aldonate appears to arise from 1,4-lactone hydrolysis. Imido-1,4-lactone is, therefore, not only formed predominantly from aldononitrile, but appears to be the predominant substrate for hydrolysis at pH 7.

7. Conclusions

The reactions that occur following the addition of cyanide to D-erythrose are summarized in Figure 26. The percentages of products at several pH values are listed in Tables 4 and 5. In the following discussion, the effects of pH and chemical structure on reactions 1-10 of Figure 26 are summarized. The presence of tetrahedral intermediates

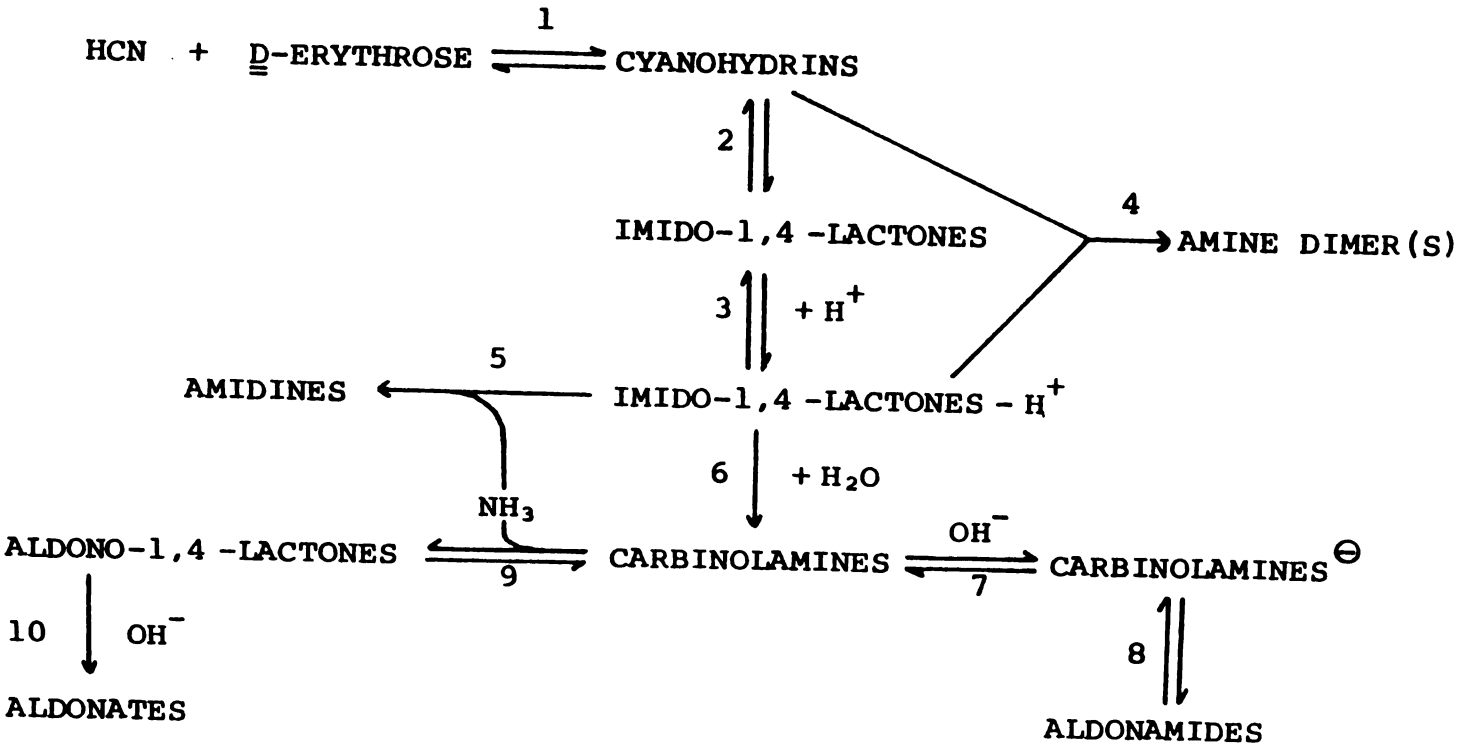

Figure 26. Mechanism of the cyanohydrin reaction applied to D-erythrose.

Table 4. Total percentage of intermediates and products in the cyanohydrin reaction (D-erythrose) at various pH values.

Compound	Percent in reaction mixture[a] (±3%)			
	pH 7.0[b]	pH 8.5[c]	pH 10.5[d]	pH 12.7[e]
nitrile	67	9		
imido-1,4-lactone				
amide	8	36	84	
1,4-lactone	10	2		
aldonate	2	5		100
amidine	10	13		
U1, U2 (dimer *12*)[f]	3	35	16	

[a] Determined by ^{13}C NMR. The absence of an entry indicates that <2% was observed. [b] 6 h of reaction. [c] 4 h of reaction. [d] 55 min of reaction. [e] 3.5 h of reaction. [f] Percentage of dimer *12* was determined by multiplying the fraction of the total spectral area under U1 + U2 x 100.

Table 5. Relative amounts of *arabino* epimers produced during the cyanohydrin reaction (D-erythrose) at various pH values.

Compound	Relative percent of arabino epimer[a] (±3%)			
	pH 7.0[b]	pH 8.5[c]	pH 10.5[d]	pH 12.7[e]
D-arabinononitrile	33	37[g]		∿40
D-arabinono-imido-1,4-lactone		f	84[g]	86
D-arabinono-amidine	90	∿95		
D-arabinono-1,4-lactone	∿90	b		
D-arabinonamide	56	65	73	82

[a] Determined by ^{13}C NMR. Absence of an entry indicates <2% was observed. Relative percent = (*arabino* epimer/*arabino* + *ribo* epimers) x 100. [b] 6 h of reaction. [c] 4 h of reaction. [d] 55 min of reaction. [e] Determined from pH-quench experiments. Amide percent is that observed after 45 min of reaction while the imidolactone percent is that observed after 15 min of reaction and estimated from the 1,4-lactone (acid hydrolysis) products. [f] Only the *arabino* epimer is observable at 40 min. [g] After 10 min of reaction.

(carbinolamines) in the reaction is discussed.

With stoichiometric amounts of reactants, aldononitrile formation (reaction 1) is essentially complete at pH values between 7 and 10.5, while at pH > 11, D-erythrose remains during the first phase of the reaction. The rate of aldononitrile hydrolysis increases with increasing pH. After 6 h at pH 7, 67 percent of the reaction mixture is composed of aldononitriles (Table 4) compared with 9 percent after 4 h at pH 8.5 and none after 1.7 h at pH 12.7 (Figure 16).

Imidolactone formation (reaction 2), while not essential, is the major route of hydrolysis of aldononitriles with hydroxyl groups situated to permit ring-closure. For pentononitriles, imido-1,4-lactone rings are formed in preference to 1,5-rings. At pH values below 9.5, imidolactone formation is slow, whereas, at higher pH (10.5), it is rapid and essentially complete after 10 min (Figure 18A, 18B). At low pH (<4), imidolactones hydrolyze rapidly to lactones via reactions 3, 6 and 9. This reaction was used to establish the presence of imidolactone in reaction mixtures at pH 12.7 (Figure 17). As pH is increased, hydrolysis to aldonamides is favored and occurs via reactions 3, 6, 7 and 8. At pH $\geq$ 10.5, amides are the major products of imidolactone hydrolysis.

Reaction 4 produces the proposed dimer *12*, yielding the greatest amount of product at pH 8.5 and lesser amounts at higher and lower pH values (Table 4). This result is due to the effect of pH on the reactions that affect the availability of nitrile and imidolactone needed for the formation of *12*. At pH 10.5, reaction 2 is essentially complete, leaving a smaller amount of nitrile for reaction 4 than is present at pH 8.5. At pH 7, reaction 2 is slower and reaction 6 is

probably faster, resulting in lower concentrations of imidolactone and faster imidolactone hydrolysis than at pH 8.5. At pH 7, aminolysis (reaction 5) also competes for imidolactone to limit the production of *12*. Increased imidolactone hydrolysis to lactone (reactions 3, 6 and 9) at pH 7 yields more ammonia to stimulate aminolysis, further decreasing the amount of imidolactone available for reaction 4.

The amount of *12* formed during the reaction should be dependent on the concentration of reactants as discussed earlier, since reaction 4 is bimolecular. In support of the proposed reaction, condensation of cyanide with D-erythrose at pH 8.5 and 0.9 M produces 50 percent more *12* than the same reaction at 0.3 M after 4 h.

Reaction 5 was observed only at pH 7 and 8.5 and depends on reaction 9 for ammonia. At pH 8.5, imidolactones hydrolyze predominately to amides (5:1 amide:lactone + aldonate after 4 h) (Table 4). Aldonates produced at pH < 10.5 arise primarily from the sequence imidolactone → lactone → aldonate, and are, therefore, added to the percentage of lactone when partitioning at pH < 10.5 is discussed. Amide hydrolysis proceeds slowly with the release of ammonia. In contrast, imidolactones hydrolyze to amides and lactones in 2:3 proportion at pH 7 after 6 h, liberating ammonia for reaction 5 and leading to increased production of amidines (30 percent of the non-nitrile product after 6 h).

Reaction 6 is implicated by the behavior of imidolactones in acidic and basic solution. Schmir and Cunningham (162) proposed tetrahedral intermediates in the hydrolysis of N-substituted imidolactones, and explained the partitioning between lactone and

N-substituted amide in terms of the presence of different ionic forms of carbinolamine. Neutral carbinolamine (or its zwitterion) was proposed to yield lactone, while anionic carbinolamine yields amide (Figure 26). Although carbinolamine resonances are not observed by ^{13}C NMR, it is reasonable to propose reactions 6 and 7 based on the observed behavior of the imido-1,4-lactones in acidic and basic media and on results reported previously for N-substituted imidolactone hydrolysis (162).

The hydrolysis of amides is facilitated when hydroxyl groups participate to produce cyclic carbinolamine intermediates (167-169). Cunningham and Schmir (169) studied the alkaline hydrolysis of 4-hydroxybutyranilide and concluded that reactions 7, 8, 9 and 10 or 8, 9, and 10 are involved. Aldonamides are stable over several hours at pH < 10, while hydrolysis can be followed at pH > 11. The alkaline hydrolysis of purified D-ribonamide or D-arabinonamide proceeds with retention of configuration at C-2, indicating that the overall reaction does not reverse to reaction 1, where stereochemistry at C-2 can be altered. It is assumed that reaction 1 establishes C-2 configuration, and that the predominant epimer is determined by reactions 1 and 2. Isomerization of imidolactone to eneimine could provide another route for epimerization. This has been ruled out, however, since reactions at pH 8.5 and 12.7 in $^{3}H_2O$ produce products containing only 0.003% and 0.014% tritium, respectively. In addition, only aldonates are observed by ^{13}C NMR during amide hydrolysis, demonstrating that reaction 6 is not appreciably reversible. If present ($\geq$3), imidolactone would be detected under these conditions. The irreversibility of reaction 6 for the hydrolysis of N-substituted

imidolactones has been established by Schmir and Cunningham (162).

The rate of amide hydrolysis appears to depend on amide configuration. Hydrolysis of an equimolar mixture of D-ribonamide and D-arabinonamide at pH 11 shows that D-ribonate is formed about 2.5 times faster than D-arabinonate. This result probably reflects differences in the rates of cyclization of the amides (reaction 8) and/or the rates of carbinolamine breakdown (reactions 7 and 9). This rate difference between C-2 epimers is not anticipated from direct hydroxide ion attack on the carbonyl of linear amides, whereas reactions involving cyclic intermediates would probably show such differences (170).

Reaction 10 occurs rapidly at pH > 10.5 and lactones are not observed in reaction mixtures at these pH values. Lactone hydrolysis is slower at pH 8.5 and lactones are detected in reaction mixtures under these conditions. Lactones in reaction mixtures at these pH values are derived from the hydrolysis of imidolactones, and not from amide hydrolysis.

Differences in the proportions of arabino and ribo epimers are apparent at various stages of the reaction, as shown in Table 5. At all pH values, ribononitrile predominates (63-67%). In comparison, D-erythrose 4-phosphate, which cannot cyclize and exists predominantly as hydrate in aqueous solution, reacts with cyanide at pH 8.0 to yield 58% ribononitrile 5-P. Nitrile cyclization (reaction 2) favors the arabino configuration with arabinono-imido-1,4-lactone accounting for ~85% of the imidolactones under conditions where hydrolysis is slow. The predominance of arabinono-imido-1,4-lactone is reflected in acidic (1,4-lactone) and alkaline (amide) hydrolysis products and in aminolysis products, with 70-90% having the arabino configuration (Table 5).

Reaction 6 may be sensitive to configuration, since the percentage of arabinono-imido-1,4-lactone (~85%) does not equal the epimeric percentage of arabinonate after total hydrolysis, with the latter varying between 68-79 percent (Table 1). As established by the demonstration that aldonamides do not undergo epimerization during hydrolysis, this difference cannot be ascribed to differences in the rates of reactions 7-10.

The slower rate of disappearance of C_4 aldononitrile compared to C_5 aldononitrile (Figure 11) cannot be explained by differences in ring-forms of intermediate imidolactones, since alkaline hydrolysis of C_5 aldononitriles involves the formation of imido-1,4-lactones. The relative ease of cyclization of C_4 and C_5 aldononitriles can be estimated by measuring rates of amidine formation. Ammonia does not react with DL-glyceronitrile at pH 9.5, in agreement with previous studies showing that amidine formation occurs readily from imidates (164), and that the addition of ammonia to acyclic nitriles to form amidines occurs only under more rigorous conditions. Conversion of imido-1,4-lactones to amidines (aminolysis) occurs readily at pH 9.5 and rates of aminolysis of C_4 and C_5 imido-1,4-lactones are not expected to be significantly different. Thus, a difference in the overall rate of conversion of *4* and *6* to amidines will reflect a difference in their rates of cyclization (cyclization is the rate determining step in this process).

Rates of amidine formation are shown in Figure 27. A fivefold faster rate is observed for C_5 aldononitriles than for the C_4-homologue. We conclude that imido-1,4-lactones form less readily when a 1°-OH is participating than when a 2°-OH is involved.

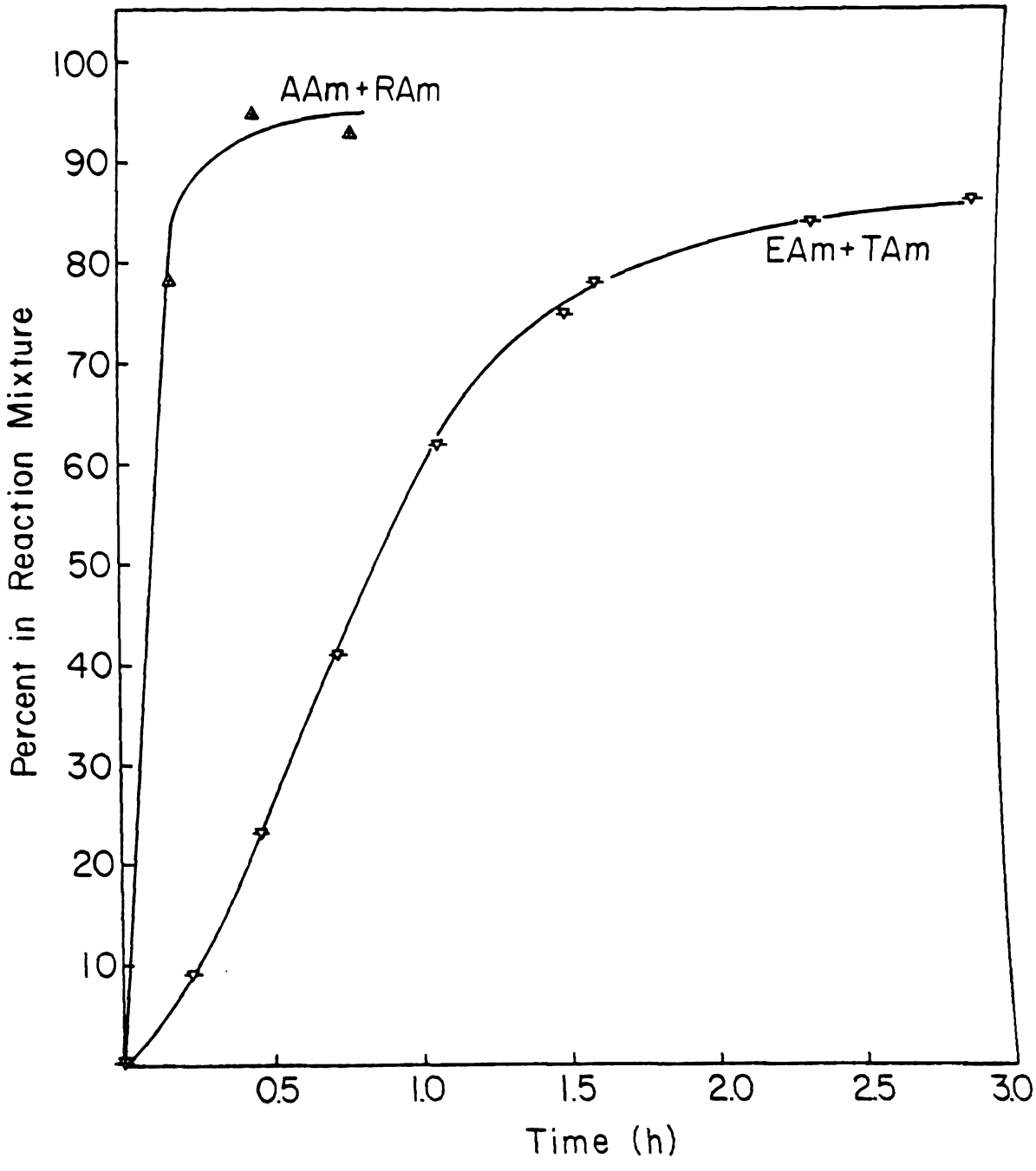

Figure 27. Rates of amidine formation from C_4 and C_5 aldononitriles. Data were obtained from ^{13}C NMR spectra (100-200 scans). Reaction conditions: 0.3 M in aldose (D-glyceraldehyde or D-erythrose), [^{13}C]cyanide and NH_4Cl; 18° ± 1°C; pH 9.5 ± 0.2. AAm, D-[1-^{13}C]arabinono-amidine; RAm, D-[1-^{13}C]ribono-amidine; TAm, D-[1-^{13}C]threono-amidine; EAm, D-[1-^{13}C]erythrono-amidine.

The presence of $-CH_2OH$ or $-CH_3$ substituents on C-4 may orient the 4-OH group for easier attack on the nitrile carbon. The slower rate of C_4 aldononitrile hydrolysis (Figure 11) is primarily due to a slower rate of cyclization to imidolactone.

In summary, we have presented evidence for the following:

a) At pH 7-9, cyanide condenses stoichiometrically with C_1-C_4 aldoses to form aldonitriles quantitatively. Aldoses that form pyranose rings require a threefold excess of cyanide under similar conditions to promote complete condensation.

b) The extent of cyanide addition decreases with increasing pH.

c) The rate of aldononitrile disappearance decreases as pH decreases and is affected by aldononitrile structure. The overall rate of reaction is faster for aldononitriles derived from D-erythrose than for those derived from D-threose. Aldononitriles having the arabino configuration hydrolyze more readily than those having the ribo configuration; aldononitriles having lyxo and xylo configurations hydrolyze at approximately similar rates.

d) Hydroxyl groups in the proper position(s) facilitate aldononitrile hydrolysis through the formation of imidolactones. Cyclization of C_5 aldononitriles occurs at pH 10.5 to form imido-1,4-lactones almost quantitatively. Aldononitriles having the arabino configuration cyclize faster than those having the ribo configuration.

e) C_4 Aldononitriles (erythro, threo) cyclize, and therefore, hydrolyze slower than C_5 aldononitriles (ribo, arabino), although five-membered imido-1,4-lactones are involved in the latter case.

f) Imido-1,4-lactones hydrolyze in basic (pH > 10.5) and acidic (pH < 4) solution to yield aldonamides and aldono-1,4-lactones,

respectively, in agreement with the behavior of N-substituted imido-1,4-lactones (162).

g) D-Arabinonamide and D-ribonamide appear to hydrolyze at different rates at pH 11. with the latter approximately 2.5 times faster than the former.

h) **Amidines** are formed in 85-95 percent yield from the C_4 and C_5 aldononitriles by reaction with one equivalent of ammonia at pH 9.5.

i) Linear compounds having arabino and ribo configurations can be distinguished by $^3J_{C1,C4}$. Furanoids (with an sp^2-hybridized C-1 carbon) having arabino and ribo configuration can be distinguished by $J_{C1,C3}$ and $J_{C1,C4}$ and by ^{13}C chemical shifts; ^{13}C NMR parameters of 1,4-lactones and imido-1,4-lactones are similar.

j) The following epimeric intermediates and products are observed by ^{13}C NMR using $K^{13}CN$ in the reaction with D-erythrose: nitriles, imido-1,4-lactones, amidines, amides, aldono-1,4-lactones and aldonates. A dimer(s) from reaction between imido-1,4-lactones and nitrile is proposed as an intermediate.

B. Preparation of [^{13}C]-Enriched Aldoses, Aldose Phosphates and Their Derivatives

The synthetic route described in this study utilizes the condensation of cyanide with an aldose or aldose derivative, as first described by Kiliani (26). In this classical reaction, a cyanide salt and aldose are mixed in aqueous solution at high pH to produce cyanohydrins which, in the alkaline solution, hydrolyze to aldonic acid salts. We observed, however, that cyanohydrins can be formed rapidly and essentially quantitatively at pH 8.0 ± 0.5 with minimal hydrolysis, and that they are

stable at pH 4.0. As described by Kuhn (64) for the preparation of 2-amino-2-deoxyaldoses from 2-benzylamino-2-deoxyaldononitriles, aldononitriles can be hydrogenolyzed to aldoses in 70-80 percent yield. Furthermore, condensation with $K^{13}CN$ provides a convenient route for the preparation of [^{13}C]-enriched derivatives of all the aldoses and of the C_3 to C_5 aldose phosphates. The mixed aldononitrile epimers produced from cyanide condensation are reduced without purification and the product epimeric aldoses purified by chromatography (88, 89). Aldononitrile phosphate epimers can be separated prior to reduction by chromatography at pH 3.9, illustrating the stability of cyanohydrins and the absence of cyanide exchange at low pH values.

Hydrogen pressure, pH and the structure of the nitrile all affect the ease of hydrogenolysis of cyanohydrins. Hydrogenolysis occurs smoothly in the absence of excess cyanide, which appears to poison the catalyst. In the course of this study it was observed that chloride ion promotes "over-reduction" to aminoalditols. Sulfuric acid rather than HCl is preferred since sulfate ion does not inhibit hydrogenolysis, gives higher yields of aldose, and can be removed more easily than chloride ion. Iodate ion, at low concentrations, inhibits reduction completely.

In addition to the introduction of carbon isotopes, the catalytic hydrogenolysis of cyanohydrins provides a route to carbohydrates enriched with hydrogen and oxygen isotopes. The technique permits the separate or simultaneous incorporation of carbon and hydrogen isotopes at C-1 and H-1, respectively, and oxygen isotopes at O-2 for each cycle of cyanide addition and catalytic reduction. Successive application of condensation and reduction permits the synthesis of derivatives

enriched at sites other than C-1 and C-2. A wide variety of selectively-enriched carbohydrates and their derivatives, which were difficult to prepare previously, are now accessible.

1. Preparation of C_2-C_6 aldononitriles

The addition of cyanide to formaldehyde and the C_2, C_3 and C_4 aldoses proceeds almost quantitatively at low pH with a 1:1 ratio of reactants, as shown in Table 6. Aqueous solutions of the short chain cyanohydrins at pH 4.3 are stable and can be stored at low temperature (-15°C) for extended periods of time.

The formation of aldononitriles is strongly favored by the inability of the starting aldose to exist as a pyranose. The complete conversion of C_5 aldoses to C_6 aldononitriles using stoichiometric amounts of cyanide is hindered by an unfavorable equilibrium. With 1:1 ratios of cyanide to aldose, at least 10% of the starting aldose remains unreacted. Use of a threefold excess of cyanide at pH 7.8-8.0 in these reactions produces aldononitriles in better than 90% yield with little hydrolysis to the aldonates. When cyanide is the limiting reactant during the preparation of [^{13}C]-enriched compounds, an excess of cyanide is used and the unreacted reagent recovered efficiently and almost quantitatively by aerating the acidic mixture (pH 4.2) with nitrogen and trapping the hydrogen cyanide released in 8 M alcoholic potassium hydroxide. The nitriles are stable during removal of cyanide. Excess cyanide, ^{12}C or ^{13}C, should be removed by aeration prior to hydrogenolysis, since cyanide inhibits reduction.

2. Hydrogenolysis of C_5 and C_6 aldononitriles

The catalytic hydrogenolysis of C_6 aldononitriles at pH 4.2 ± 0.1 and 60 lb in^{-2} H_2 proceeds readily to yield hexoses. Figure 28

Table 6. Specific reaction conditions and results for the preparation of aldononitriles[a].

Sugar Reactant	[NaCN]	[Sugar]	pH[b]	Reaction Time (min)	Percent of Nitrile	Percent of Unreacted Sugar	Ratio of Nitriles
Formaldehyde			8.5	20	95	5	
Glycolaldehyde			8.5	30	95	5	
D-Glyceraldehyde			8.5	20	95	5	1:1 (N)
D-Lactaldehyde			8.0	20	95	5	
D-Erythrose	0.1 M	0.10 M	9.0	4	95	5	1.4:1 Rib
D-Threose			9.0	7	95	5	1.6:1 Lyx
2,4-O-Ethylidene-D-erythrose			8.5	30	95	5	1:1 (N)
D-Arabinose			pH_i = 8.5	25	63	15	1.7:1 Man
			6.3	45			
D-Lyxose			pH_i = 8.4	4			
	0.50 M	0.50 M	7.6	11	74	11	1.3:1 Tal
			5.6	45			
D-Ribose			pH_i = 7.0	10	77	16	2.9:1 All[c]
			7.6	20			
D-Xylose			pH_i = 7.0	5	80	20	1.5:1 Gul
			7.5	75			
D-Lyxose			7.6	20	88	3	1:1
D-Xylose	1.50 M	0.50 M	8.0	4	95	5	1.5:1 Gul
D-Ribose			8.0	5	80	5	2:1 All
D-Arabinose			8.0	10	95	5	1.8:1 Man

[a] Percentage and ratios were determined from GLC peak-areas unless the symbol (N) appears with the value. In these cases, determinations were made by ^{13}C NMR spectral analysis. [b] pH_i = initial pH of NaCN solution; pH adjustments were made as indicated. [c] Assignment is tentative.

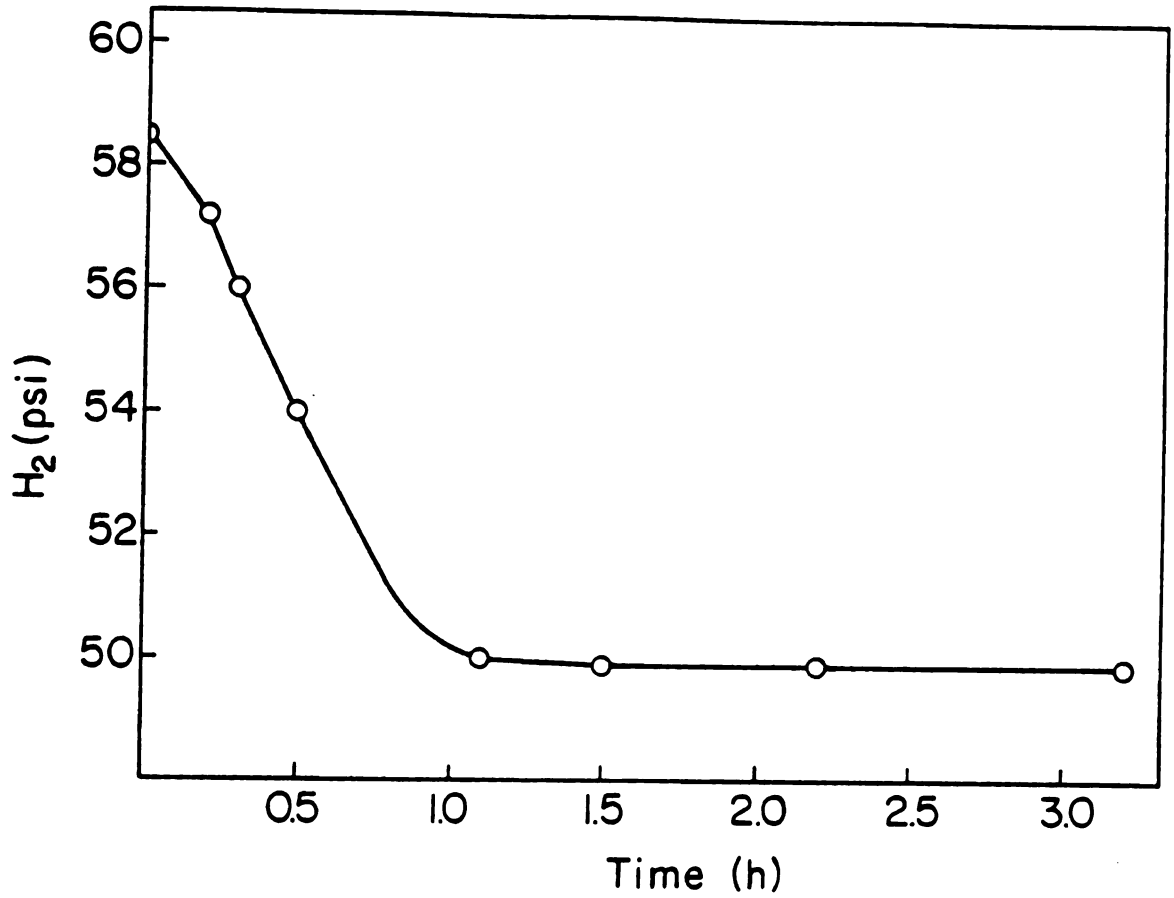

Figure 28. Change in H_2 pressure during hydrogenolysis of hexononitriles at pH 4.2 ± 0.1 and 60 lb in^{-2}. D-[2-^{13}C]Gluconoand mannononitriles (5-6 mmol) were hydrogenolyzed over $Pd/BaSO_4$ in a 250-mL reduction vessel. The drop in H_2 pressure corresponds to an uptake of ∿5-6 mmoles of H_2. The ^{13}C NMR spectrum of the hydrogenolysis products is shown in Figure 29B.

shows the uptake of H_2 during the hydrogenolysis of 6 mmoles of D-[2-^{13}C]glucono- and mannononitriles at 60 lb in^{-2} in a 250-ml reduction vessel. Reduction is complete after 1 h. Typical yields, determined from product weights, GLC analysis and ^{14}C incorporation are presented in Table 7.

In reactions using 1:1 ratios of cyanide and C_5 aldose, the extent of nitrile hydrolysis during their preparation varies from 15 to 20% (Table 7), and 10% of the aldononitriles are reduced to 1-deoxy-1-aminoalditols during catalytic hydrogenolysis. The final mixture of compounds, after treatment with Dowex 1 X8 (OAc^-) contains 70-75% product aldose, with an overall yield based on the starting aldose of about 50%. Total incorporation of cyanide is 80% or better; that is, 50% in product aldoses, 20% in aldonic acids, and 10% in aminoalditols, all of which can be readily separated by ion-exchange chromatography and recovered. The remaining 20% of cyanide remains unreacted due to the cyanohydrin-aldose equilibrium.

The overall yield of hexoses from pentoses is greatly improved when a threefold excess of cyanide is used in the condensation reaction (Table 6). Residual cyanide after aeration is reduced to methylamine or formaldehyde, both of which are separated readily from the products. The ^{13}C NMR spectra obtained at various stages during the synthesis of D-[2-^{13}C]glucose and D-[2-^{13}C]mannose from D-[1-^{13}C]arabinose and a threefold excess of KCN are shown in Figure 29. Spectra were obtained of the reaction mixture after cyanide condensation (Figure 29A), of the products after hydrogenolysis (Figure 29B) and of the purified hexoses (Figures 29C and 29D). The intermediate [2-^{13}C]aldononitriles, byproduct [2-^{13}C] 1-amino-1-deoxyalditols, and

Table 7. Aldose yields based on weights, borohydride reduction products, and radioactivity.

Starting Aldose (10 mmol)	Ratio of CN^- to Sugar	Weight after Dowex 50 (g) (theory 1.8 g)	Weight after Dowex 1 (g) (theory 1.8 g)	Ratio of Product Aldoses	Product Sugars in Dowex 1[a] Residue (Percent)	Overall Yield Based on Total CN^- (Percent)	Overall Yield Based on Reacted CN^- (Percent)
D-Arabinose	1:1	1.6 (73)[b]	1.2	2.3:1 Man	70	47	56
D-Lyxose	1:1	1.5	0.97	1.3:1 Tal	75	40	50
D-Ribose	1:1	1.7 (75)[b]	1.4 (68)[b]	2.3:1 All[c]	70	54	65
D-Xylose	1:1	1.5	1.4	1.5:1 Gul	75	58	70
D-Lyxose	3:1	1.7	1.5	1:1	97		85

[a] Values were obtained by reaction of the residue [after Dowex 1 X8 (OAc^-) treatment] with sodium borohydride. The resulting alditols were determined by GLC. [b] Yield of material based on incorporation of [^{14}C]cyanide. [c] Assignment is tentative.

Figure 29. Preparation of D-[2-^{13}C]glucose and D-[2-^{13}C]mannose from D-[1-^{13}C]arabinose and KCN.

^{1}H-Decoupled 15.08 MHz ^{13}C NMR spectra were taken of the intermediate aldononitriles (A), crude hydrogenolysis products (B), and purified hexoses (C and D). (A) ^{13}C NMR spectrum of the reaction mixture containing D-[2-^{13}C]gluconononitrile (GN) (62.8 ppm) and D-[2-^{13}C]mannononitrile (MN) (62.4 ppm) at pH ∿4. Ac = natural abundance resonances of acetic acid. (B) ^{13}C NMR spectrum of the products from hydrogenolysis of the epimeric [2-^{13}C]hexononitriles: A, D-[2-^{13}C] 1-amino-1-deoxyalditols (68.6 ppm and 70.6 ppm); resonances between 72-76 ppm are due to C-2 of the product [2-^{13}C]hexoses. (C) ^{13}C NMR spectrum of purified D-[2-^{13}C]glucose, showing C-2 of the α- and β-pyranoses at 73.0 ppm and 75.7 ppm, respectively. (D) ^{13}C NMR spectrum of purified D-[2-^{13}C]-mannose, showing C-2 of the α- and β-pyranoses at 72.2 ppm and 72.8 ppm, respectively.

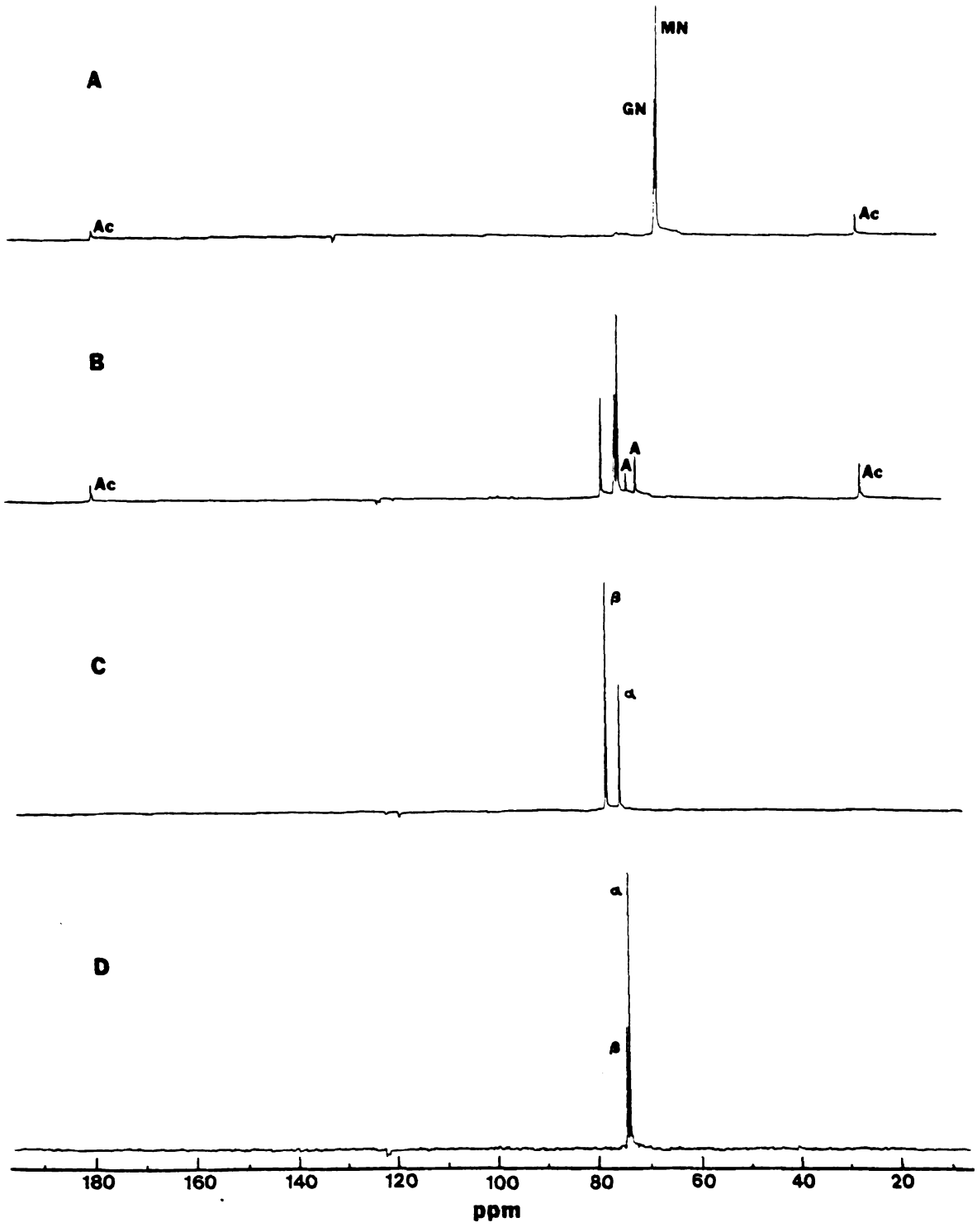

Figure 29.

the product [2-^{13}C]aldoses are readily identified by their characteristic chemical shifts. Quantitation of unreacted starting [1-^{13}C]aldose and [2-^{13}C] products is not hindered by the effect of different ^{13}C relaxation times, since the enriched carbons in the starting aldose (C-1) and in the products (C-2) are methine carbons. The absence of starting [1-^{13}C]aldose after reaction with a threefold excess of KCN is shown in Figure 29A. C-1 Resonances for α- and β- D-arabinopyranose would be observed at 98.2 ppm and 94.0 ppm, respectively. The mixture of crude products of hydrogenolysis (Figure 29B) is predominantly the desired aldoses. D-[2-^{13}C] 1-Amino-1-deoxyalditols are quantitatively removed by treatment of the crude products with Dowex 50 X8 (H^+), and the epimeric [2-^{13}C]aldoses are purified on Dowex 50 X8 (200-400 mesh) in the barium form (88) (Figures 29C and 29D).

The preparation of C_5 aldononitriles is conducted with stoichiometric amounts of tetrose and cyanide (Table 6). Hydrogenolysis of the C_5 aldononitriles derived from D-erythrose at pH 4.2 ± 0.1 and 60 lb in^{-2} H_2 produces about 15% 1-amino-1-deoxyalditols. The overall yield of D-ribose and D-arabinose after purification on Dowex 50 X8 (200-400 mesh) (Ba^{2+}) (88) is about 75%. Hydrogenolysis of the C_5 aldononitriles derived from D-threose under the same conditions typically yields ∿40% 1-amino-1-deoxyalditols. At lower H_2 pressure and pH (1 atm - 20 lb in^{-2} H_2, pH 2-3), less amine (10-15%) is produced.

3. Hydrogenolysis of C_2, C_3 and C_4 aldononitriles

Hydrogenolysis of C_2, C_3 and C_4 aldononitriles proceeds differently than that of the C_5 and C_6 cyanohydrins. Apparently, in the synthesis of the pentoses and hexoses, the intermediate five- and six-carbon imines can cyclize, facilitating formation of the aldose,

presumably through an intermediate glycosylamine (171). In the synthesis of shorter-chain homologues, cyclized intermediates can form only from the four-carbon nitriles. It appears that this process does not occur readily, however, as the reduction of erythrono- and threono-nitriles at pH 4.2 ± 0.1 and 60 lb in^{-2} over palladium-barium sulfate at 25°C affords 1-amino-1-deoxyalditols as the principal products. In this regard, blocking groups that restrict the formation of cyclic intermediates effect the extent of reduction to 1-amino-1-deoxyalditols. Hydrogenolysis of 3,5-O-ethylidene-D-ribono- and arabinononitriles at pH 4.2 ± 0.1 and 60 lb in^{-2} H_2 yields, in addition to the corresponding aldoses, larger percentages (>40%) of amines than the unblocked homologues. Low yields of aldose are also obtained from hydrogenolysis of C_2 and C_3 aldononitriles under these conditions.

The ease with which aldononitriles can be hydrogenolyzed to aldoses at high pressure parallels exactly their susceptibility to alkaline hydrolysis. In both processes, cyclization has been implicated. Slower rates of hydrolysis of D-xylononitrile and D-lyxononitrile compared with D-ribononitrile and D-arabinononitrile, and slower rates of cyclization of the tetrononitriles relative to the C_5 aldononitriles would be predicted based on the quantities of 1-amino-1-deoxyalditols produced during hydrogenolysis. These differences have been observed (Figures 11 and 12).

Aldononitriles that yield imines which cannot cyclize, however, are hydrogenolyzed smoothly and almost quantitatively at 25°C to the corresponding aldehydes at pH 1.7 ± 0.1 and atmospheric pressure over palladium-barium sulfate (Table 8). Presumably, these conditions

permit the intermediate imine to dissociate from the catalyst and to hydrolyze without the intramolecular participation that appears to occur during the preparation of the hexoses and pentoses.

Table 8. Yields of aldoses from hydrogenolysis of two-, three-, and four-carbon aldononitriles[a].

Compound	Conditions			
	$Pd-BaSO_4$, atm. press. pH 1.7	PtO_2, 60 lb in^{-2} pH 0.8	PtO_2, 30 lb in^{-2} pH 0.8	$Pd-BaSO_4$, 60 lb in^{-2} pH 4.2
Glycolaldehyde	90(80)[b]			
DL-Glyceraldehyde	85(75)[b]		trace[c]	<15
D-Threose and D-erythrose	85(70)[d]	trace[c]		<10

[a] Based on ^{13}C NMR peak areas. Spectra were obtained by using a 55° pulse and 10 sec delay time to minimize relaxation effects. Spectra were obtained of reduction mixtures. Integration was performed by computer. [b] Percent yield based on weight of products as gums. [c] Determined by gas chromatography. [d] Percent yield based on weight of products as gums after separation by chromatography on Dowex 50 X8 (200-400 mesh) (Ba^{2+}).

The ^{13}C NMR spectra obtained at various stages during the synthesis of D-[1-^{13}C]erythrose and D-[1-^{13}C]threose from D-glyceraldehyde and $K^{13}CN$ are shown in Figure 30. Spectra were obtained of the reaction mixture after cyanide condensation, of the products after hydrogenolysis, and of the purified tetroses. The C-1 resonances of the intermediate epimeric [1-^{13}C]tetrononitriles are found at 120.9 ppm (Figure 30A). Hydrogenolysis at atmospheric pressure and pH 1.7 ± 1 produces a mixture of the tetroses and small (<10%) amounts of 1-amino-1-deoxyalditols (Figure 30B). The byproduct amines are quantitatively removed with Dowex 50 X8 (H^+), the solution is deionized,

Figure 30. Preparation of D-[1-^{13}C]erythrose and D-[1-^{13}C]threose from D-glyceraldehyde and K^{13}CN.

^{1}H-Decoupled 15.08 Hz ^{13}C NMR spectra were taken of the intermediate aldononitriles (A), crude hydrogenolysis products (B), and the purified tetroses (C and D). (A) ^{13}C NMR spectrum of the reaction mixture containing D-[1-^{13}C]erythrono- and threononitriles (120.9 ppm). (B) ^{13}C NMR spectrum of the products from hydrogenolysis of the epimeric [1-^{13}C]-tetrononitriles: Ac = natural abundance resonances of acetic acid; A, D-[1-^{13}C] 1-amino-1-deoxyalditols (~43 ppm); resonances between 90 and 104 ppm are due to C-1 of the product D-[1-^{13}C]tetroses. (C) ^{13}C NMR spectrum of purified D-[1-^{13}C]erythrose, showing the α- and β-furanose and hydrated (h) forms in solution (96.8 ppm, 102.4 ppm and 90.8 ppm, respectively). The C-1 resonances of dimers and/or oligomers of D-erythrose are observed slightly downfield from the α-furanose and hydrate C-1 resonances. (D) ^{13}C NMR spectrum of purified D-[1-^{13}C]threose, showing the α- and β-furanose and hydrated (h) forms in solution (103.4 ppm, 97.9 ppm and 91.1 ppm, respectively).

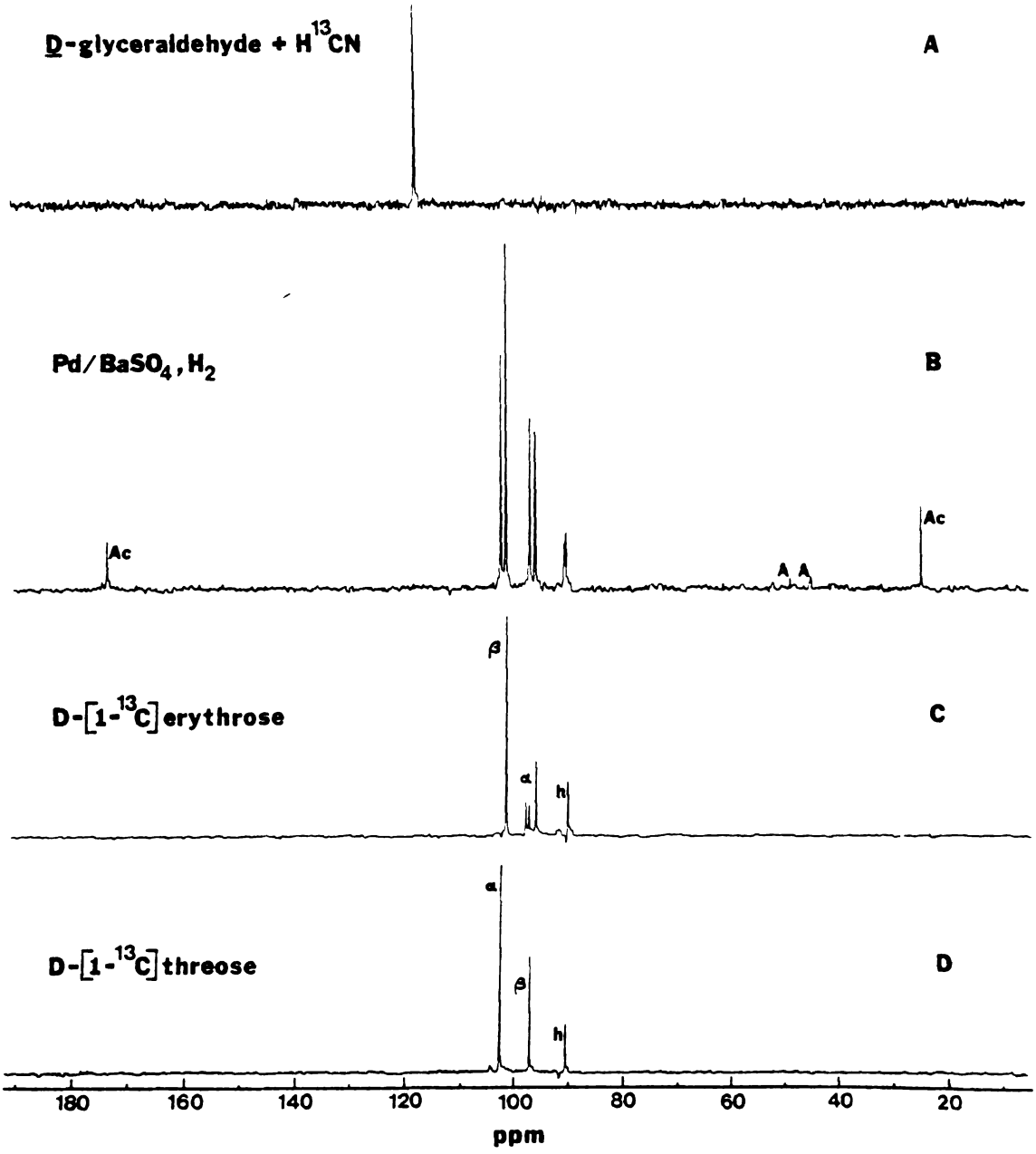
D-glyceraldehyde + H13CN
A
Pd/BaSO4, H2
B
Ac
Ac
A A
D-[1-13C]erythrose
C
β
α
h
D-[1-13C]threose
D
α
β
h
180
160
140
120
100
80
60
40
20
ppm

Figure 30.

and the epimeric tetroses purified on a column of Dowex 50 X8 (200-400 mesh) in the barium form (88). ^{13}C NMR spectra of purified D-[1-^{13}C]erythrose and D-[1-^{13}C]threose are shown in Figure 30C and Figure 30D. The absence of unreacted D-glyceraldehyde at each stage during synthesis was demonstrated by GLC.

Glycolaldehyde, DL-glyceraldehyde and purified erythrose prepared by this method are better than 95% pure by ^{13}C NMR and GLC and compare favorably with compounds prepared by standard methods. Preparation of DL-glyceraldehyde and unpurified erythrose and threose occasionally contain small quantities (<3%) of the keto isomers. Unreacted C_4 aldononitrile and erythrulose will elute with threose during purification on Dowex 50 X8 (200-400 mesh) (Ba^{2+}).

A demonstration of the serial application of this method is illustrated by the preparation of D-[1-^{13}C]erythrose, DL-[2-^{13}C]erythrose and DL-[3-^{13}C]erythrose, whose ^{13}C NMR spectra are shown in Figure 31 A-C. The ^{13}C NMR spectrum in Figure 31D is the natural abundance spectrum of D-erythrose. The [2-^{13}C]- and [3-^{13}C]-enriched tetroses were produced in about a 50% overall yield from glycolaldehyde by two cycles of the reaction, and in about a 40% overall yield from formaldehyde by three cycles of the reaction, respectively. The [1-^{13}C]-, [2-^{13}C]- and [3-^{13}C]-enriched tetroses were used to study the cyanohydrin reaction (Figures 15, 23 and 24), to unequivocally establish ^{13}C chemical shifts of the various forms present in aqueous solution, and to measure several homo- and heteronuclear coupling constants.

4. Preparation of C_3, C_4 and C_5 aldononitrile and aldose phosphates

Cyanide is condensed with C_2, C_3 and C_4 aldose phosphates in essentially the same fashion as described for the simple aldoses.

Figure 31. Demonstration of the serial application of the synthesis.

The proton-decoupled, ^{13}C NMR spectra of the enriched region of (A) D-[1-^{13}C]erythrose, (B) DL-[2-^{13}C]erythrose, and (C) DL-[3-^{13}C]erythrose. Spectrum (D) is the natural-abundance carbon-13 NMR spectrum of D-erythrose, which was prepared according to Perlin (141). Minor resonances are due to dimers and/or oligomers. The symbol (h) denotes the linear hydrate form of D-erythrose.

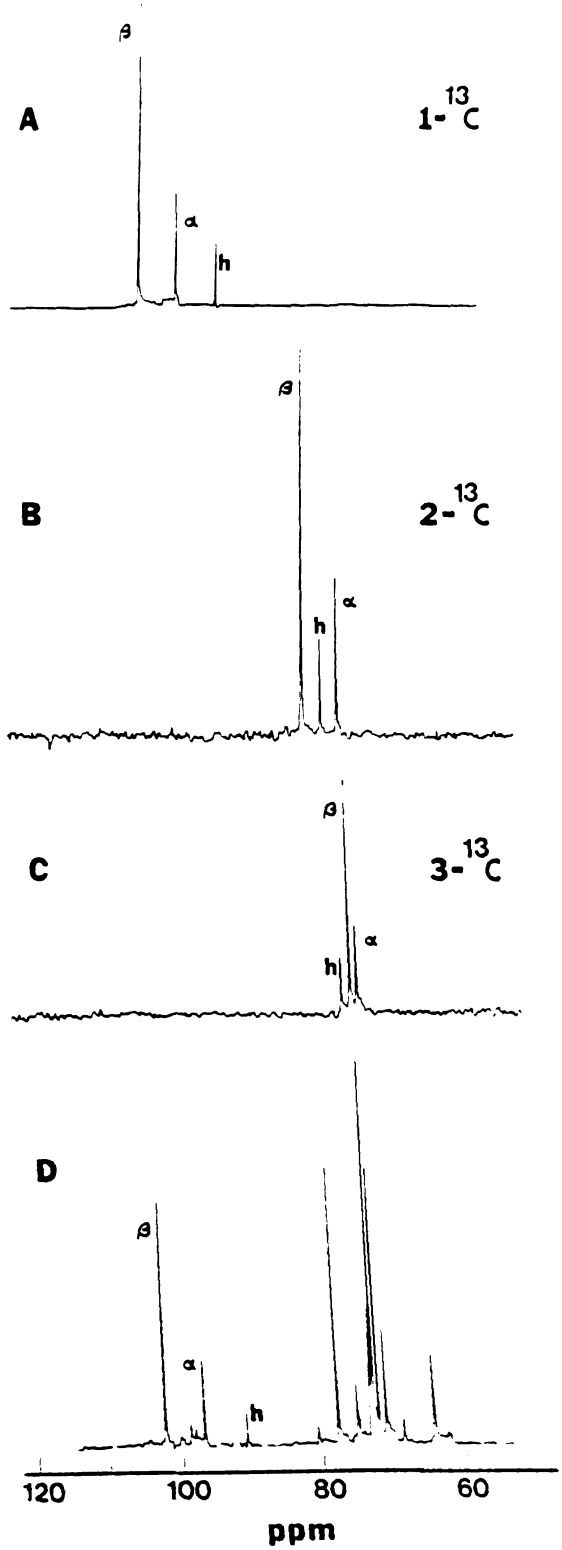

Figure 31.

Condensations are performed with stoichiometric quantities of cyanide and aldose-P at 5°C and pH 7.5-8.0 for 15 min. Reaction mixtures are then incubated at pH 7.5-8.0 and 25°C for 30 min.

Hydrogenolysis of the C_3, C_4 and C_5 aldononitrile phosphates is conducted at pH 1.7 ± 0.1 and atmospheric pressure. After cyanide condensation, DL-glyceronitrile 3-P is reduced directly to DL-glyceraldehyde 3-P without purification. However, in contrast to the preparation of the C_4 and C_5 aldoses, mixtures of epimeric C_4 and C_5 aldononitrile phosphates are not directly hydrogenolyzed. These mixtures are purified by ion-exchange chromatography and the purified aldononitrile phosphates are reduced, since epimeric aldononitrile phosphates are more easily separated than epimeric aldose phosphates. Purification is accomplished by chromatography on Dowex 1 X8 (200-400 mesh) in the formate form at 4°C using linear gradients of sodium formate at pH 3.9, as shown in Figure 32. The yields of aldononitrile phosphates after cyanide condensation and chromatography are 85%. The configuration and epimeric distribution of the purified aldononitrile phosphates after chromatography are found in Table 9.

Epimeric mixtures of aldononitrile phosphates can also be separated on Dowex 1 X8 (chloride) using linear chloride gradients, but hydrogenolysis in the presence of chloride ion consistently yielded larger amounts of 1-amino-1-deoxyalditol phosphates (≈45%). It is important to maintain acidic conditions during the separation and handling of aldononitrile phosphates since the reaction between parent aldose and cyanide is reversible, and, at pH >8, purified aldononitrile phosphates revert to epimeric mixtures.

Analysis of the hydrogenolysis products from DL-[1-^{13}C]

Figure 32. Separation of DL-[1-^{13}C]xylononitrile 5-P and DL-[1-^{13}C]-lyxononitrile 5-P and ^{13}C NMR analyses of the products after hydrogenolysis over palladium.

(A) Chromatography of the 2-epimeric pentononitrile phosphates on a 2.2 x 51 cm Dowex 1 X8 (200-400 mesh) column in the formate form at 4°C developed with a linear gradient of sodium formate (3000 mL, 0.05-0.8 M, pH 3.9). Column effluent was assayed for radioactivity and total phosphate. The xylo epimer was eluted before the lyxo epimer. (B and C) ^{13}C NMR analyses showing resonances due to the enriched carbons of the reduction products from DL-[1-^{13}C]xylononitrile 5-P (B) and DL-[1-^{13}C]-lyxononitrile 5-P (C); C-1 resonances of the [1-^{13}C]-enriched α- and β-furanose and hydrated forms of DL-aldose 5-P appear at approximately 100 ppm, [1-^{13}C]-1-amino-1-deoxyalditol 5-P (a) appears at approximately 43 ppm, and resonances due to natural abundance ^{13}C of acetic acid (Ac), used to adjust pH prior to hydrogenolysis, appear at approximately 23 and 180 ppm. Spectra were obtained at 13 ± 1°C with a sweep width of 3000 Hz and a filter width of 2400 Hz.

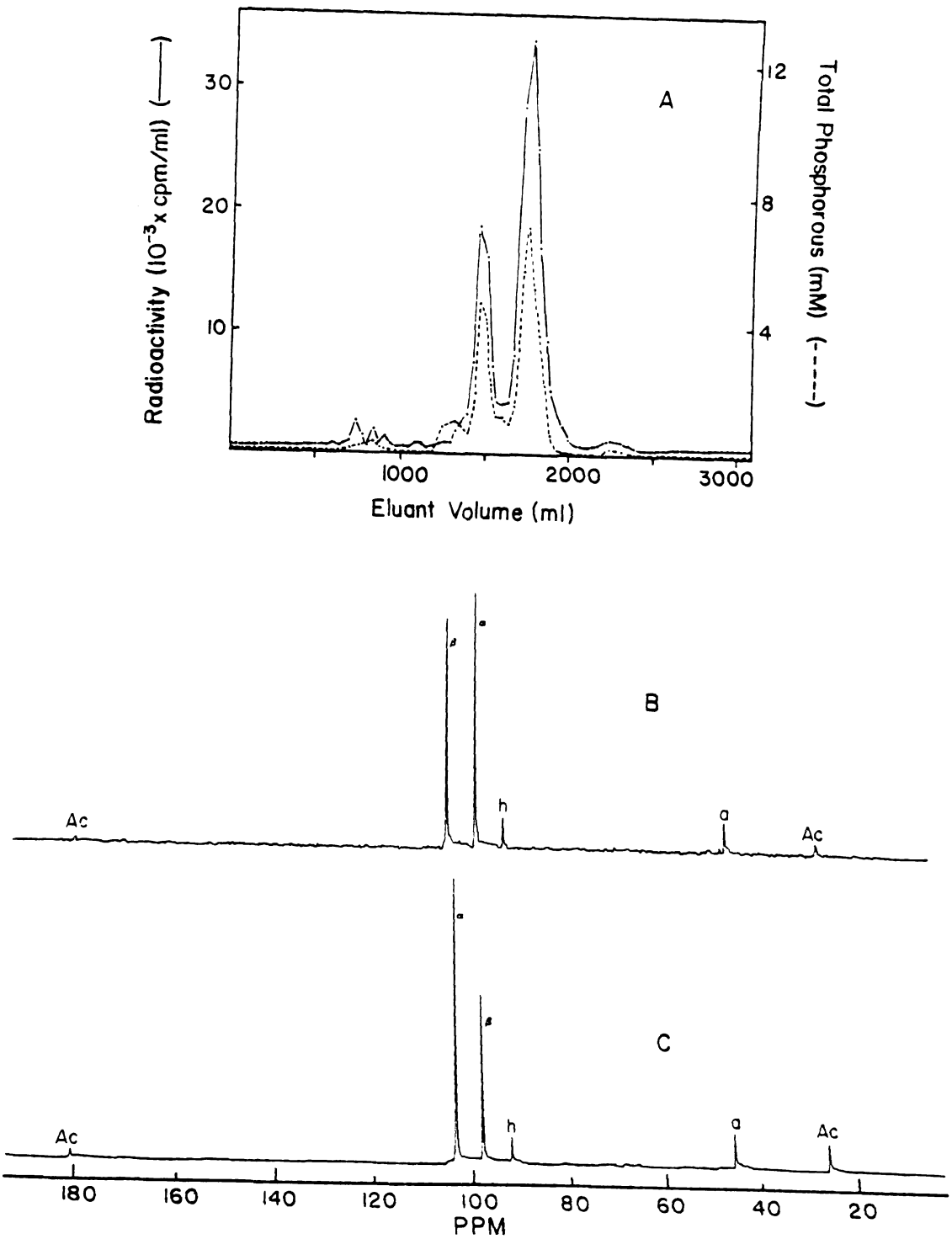
Radioactivity (10^{-3} x cpm/ml) (——)
Total Phosphorous (mM) (- - - -)
A
30
20
10
12
8
4
1000
2000
3000
Eluant Volume (ml)
B
C
Ac
h
a
Ac
180
160
140
120
100
80
60
40
20
PPM

Figure 32.

Table 9. Purification and epimeric distribution of aldononitrile phosphates.

Parent Aldose Phosphates	Chromatography on Dowex 1 X8 (formate)[a]		Ratio of Epimers[c]
	Peak 1[b]	Peak 2[b]	
Glyceraldehyde 3-P	threo	erythro	1.3:1 erythro
Erythrose 4-P	arabino	ribo	1.4:1 ribo
Threose 4-P	xylo	lyxo	1.5:1 lyxo

[a] A 2.2 x 51 cm Dowex 1 X8 (200-400 mesh) column in the formate form was employed. Solutions of aldononitrile phosphates were adjusted to pH 6.5-7.0 prior to application to the column bed. Gradients: for 4-carbon aldononitrile phosphates, 3000 mL, 0.2-0.9 M sodium formate, pH 3.9; for 5-carbon aldononitrile phosphates, 3000 mL, 0.05-0.8 M sodium formate, pH 3.9. Temperature = 4°C; flow rate = 0.5 mL/min; 7 mL per fraction. [b] Aldononitrile-P configurations were determined by reduction to aldose phosphates and incubation with alkaline phosphatase. The ^{13}C NMR spectra of the resulting aldoses were compared with those of standard pentoses. [c] Determined by computerized integration of ^{13}C NMR spectra of epimeric mixtures and by quantitation of organic P in purified preparations.

xylononitrile 5-P and DL-[1-^{13}C]lyxononitrile 5-P by ^{13}C NMR is shown in Figure 32B and 32C, respectively. DL-[1-^{13}C] 1-Amino-1-deoxyalditol 5-phosphates are usually formed in 5-10% yield during reduction. They are removed from the product aldose phosphates by chromatography on DEAE-Sephadex A-25 (OAc^-) at 4°C using linear gradients of sodium acetate at pH 4.5. Recovery from DEAE-Sephadex chromatography is about 90% based on P-assay.

For the preparation of millimolar quantities of aldose phosphates, glycolaldehyde-P and D-glyceraldehyde 3-P were prepared from DL-glycerol 1-P and D-fructose 6-P, respectively, by lead tetraacetate oxidation. Sodium metaperiodate oxidation was also examined, but traces of iodate interfere with hydrogenolysis of the aldononitrile phosphates, and careful chromatographic purification was required. On the other hand, aldononitrile phosphates prepared from lead tetra-acetate oxidation products hydrogenolyze smoothly.

Aldose phosphates, particularly the triose and tetrose phosphates, should be handled at low pH to avoid base-catalyzed isomerizations and β-elimination. The acyclic triose and tetrose phosphates isomerize to give mixtures which include keto compounds when chromatographed on Dowex 1 X8 (formate). Purification of the alkali-sensitive aldose phosphates and the pentose phosphates can be achieved by anion-exchange chromatography on DEAE-Sephadex A-25 at 4°C using linear gradients of acetic acid at pH 4.5 ± 0.1. The tetrose 4-phosphates consistently yielded skewed peaks with notable tailing, whereas triose and pentose phosphates yielded symmetric peaks. Isomerization to keto compounds on DEAE-Sephadex was not observed under the conditions used.

It is usual to prepare aldose phosphates having four or fewer carbons as acetals to protect the base sensitive aldehydic function (73, 74). We find, however, that the free aldose phosphates are stable during long-term storage at pH 1.0-2.0. When stored at -15°C as 50 mM solutions, no detectable changes occur over a two month period as determined by ^{13}C NMR analysis of the [1-^{13}C]-enriched compounds and by inorganic phosphate analysis. Storage at higher temperatures, however, results in degradation of these compounds even in acidic solution.

5. ^{13}C NMR parameters

a. Short-chain aldoses and derivatives

The various forms of the aldoses in solution can be determined with ease from ^{13}C NMR spectra of the [1-^{13}C]-enriched compounds, as shown in Figures 29-32. Formaldehyde (172), glycolaldehyde (173) and glyceraldehyde (174) appear to exist predominantly as gem-diols in dilute, aqueous solution. The observation of carbon-13 resonances of the [1-^{13}C]-enriched derivatives at approximately 90 ppm is not typical of aldehydes or hemiacetals, and has been shown to be characteristic of gem-diols of aldohexose derivatives (175). A significant proportion of gem-diol (hydrate) exists in aqueous solutions of erythrose (∿12%) and threose (∿12%). The remainder of the tetroses is present in aqueous solution as β-furanose (37% threose, 63% erythrose) and α-furanose (51% threose, 25% erythrose) forms. Assignments of the carbon-13 resonances to α- and β-furanoses were made by analogy with those of the methyl α- and β-glycosides (114).

The presence of dimers and/or oligomers of glycolaldehyde, DL-glyceraldehyde (Figure 33), D-erythrose (Figures 30C and 31D) and D-erythro, threo-2,3-dihydroxybutanal (Figure 25) has been observed in

Figure 33. Various forms of glyceraldehyde in aqueous solution.

The natural-abundance ^{13}C NMR spectrum of polymeric D-glyceraldehyde (A) prepared according to Perlin (139), and the ^{13}C NMR spectrum of DL-[1-^{13}C]glyceraldehyde (B) showing only C-1 resonances. Peak (h) is the linear, gem-diol carbon at C-1; the remaining downfield peaks arise from the C-1 resonances of dimers and higher polymers.

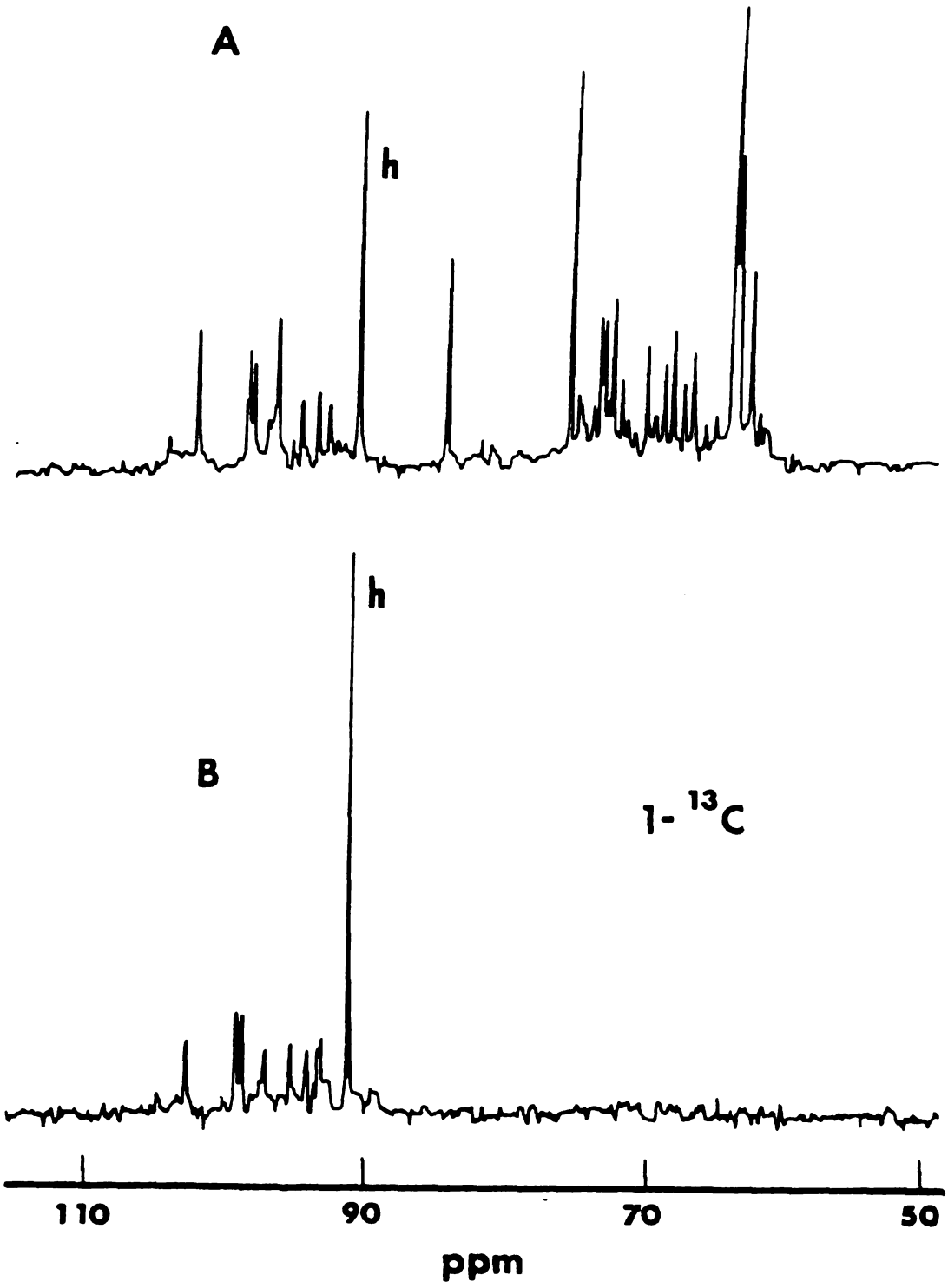

Figure 33.

concentrated solutions or in solutions freshly prepared from syrups. These structures hydrolyze rapidly to the gem-diol monomer in the case of glycolaldehyde (173). The depolymerization of glyceraldehyde is slower but eventually yields monomer (176). Concentrated, neutral solutions of D-[1-^{13}C]erythrose contain dimers and/or oligomers having C-1 chemical shifts at 98.5, 97.9, 92.5 and 92.1 ppm.

Carbon-13 chemical shifts obtained from specific [^{13}C]-enrichment of the short-chain aldoses are presented in Table 10. As demonstrated for erythrose in Figure 31, [^{13}C]-enrichment permits unequivocal assignment of chemical shifts of all carbon atoms.

Several observations regarding these ^{13}C chemical shifts are noted. The nitrile carbon of the aldononitriles is found at approximately 120 ppm, and C-2 of aldononitriles is more shielded than C-2 of the corresponding aldoses and aldonates. For example, C-2 for DL-glyceraldehyde hydrate resonates at 75.5 ppm while C-2 for DL-glyceronitrile is found at 63.2 ppm. The same effect is observed when C-2 is a 1°-hydroxylic carbon. Similar shielding is observed for the protons of acetylene (177).

Cyclization causes a downfield shift in the resonance of the carbon involved in ring-formation. The C-4 resonance of D-erythrose hydrate is found at 64.0 ppm while the C-4 resonances for α- and β- D-erythrofuranoses are observed at 72.9 and 72.4 ppm, respectively. This effect was exploited in determining the ring size of the intermediate imidolactones formed during the cyanohydrin reaction (Figure 24).

Direct ^{13}C-^{13}C coupling constants ($^{1}J_{C,C}$) were measured for several short-chain aldoses and their derivatives and are found in

Table 10. ^{13}C Chemical shifts of short-chain carbohydrates and derivatives.

Compound	Carbon Position, ppm[a]			
	C-1	C-2	C-3	C-4
Formaldehyde, hydrate	83.3			
Glycolaldehyde, hydrate	91.2	66.0		
DL-Glyceraldehyde, hydrate	91.2	75.5	63.4	
DL-Erythrose				
α-furanose	96.8	72.4	70.6	72.9
β-furanose	102.4	77.7	71.7	72.4
hydrate	90.8	74.9	73.0	64.0
DL-Threose				
α-furanose	103.4	82.0	76.4	74.3
β-furanose	97.9	77.5	76.2	71.8
hydrate	91.1	74.6	72.2	64.4
Glycolonitrile	120.6	49.2		
DL-Glyceronitrile	121.0	63.2	64.4	
DL-Erythrono- and	120.9[b]	63.2[b]	73.2[b]	62.9[b]
-threono-nitriles	120.9[b]	63.6[b]	73.4[b]	63.0[b]
DL-Glyceric acid	177.2	72.8	64.8	
D-Erythronate, sodium	179.7	75.1	74.9	63.5
D-Threonate, sodium	180.2	73.7	74.2	64.5

[a] All chemical shifts are relative to Me_4Si as external standard.
[b] Tentative assignment.

Table 11. As expected (178), the magnitude of direct coupling between C-1 and C-2 generally increases as the s-character of the C-1—C-2 bond increases. $^{1}J_{C1,C2}$ is greater for the aldononitriles (∿60 Hz) and aldonates (∿53 Hz) than for the furanoses (∿44 Hz) and hydrates (∿48 Hz). As noted for other aldonates and aldonic acids (Table 3), the values of $^{1}J_{C1,C2}$ for the aldonic acids (∿59 Hz) is about 5 Hz larger than $^{1}J_{C1,C2}$ for the aldonates (∿54 Hz).

Vicinal ^{13}C-^{13}C coupling is observed only in the case of threo derivatives; the nitrile and aldonic acid salts have $^{3}J_{C1,C4}$ values of 4.0 ± 1.5 Hz and 3.7 ± 0.7 Hz, respectively. This result is surprising as, in the acyclic forms of both erythro and threo derivatives, a trans relationship should exist between C-1 and C-4, and be somewhat more stable in the erythro isomers. The observation of coupling only in the threo forms indicates that the arrangement of the hydroxyl substituents along the coupling pathway is important. This dependence on the arrangement of the hydroxyl substituents was observed for several linear compounds having the ribo and arabino configurations, where $^{3}J_{C1,C4}$ was only observed for those compounds having the latter configuration (Table 3, Figure 24). The magnitude of $^{3}J_{C1,C4}$ was explained in terms of preferred solution conformations.

Direct ^{13}C-^{1}H coupling constants were determined from [^{13}C]-enriched compounds and are found in Table 11. Heteronuclear ^{13}C-^{1}H coupling constants can be determined from ^{1}H-coupled ^{13}C NMR spectra, as shown for D-[1-^{13}C]threose in Figure 34. $^{1}J_{C1,H1}$ for the [1-^{13}C]tetroses varies with configuration at C-1 and with sugar conformation, with values ranging from 172-174 Hz for cyclic forms and from 162-164 Hz for acyclic hydrates. Direct C-2—H-2 coupling in the [2-^{13}C]-

Table 11. ^{13}C Coupling constants of enriched carbohydrates and derivatives.

Compound	Coupling Constant, Hz[a]					
	C-1—C-2	C-1—H-1	C-2—H-2	C-3—H-3	C-1—H-2	C-1—C-4
Glycolaldehyde, hydrate	A	163.9	A		b	
Glyceraldehyde, hydrate	A	162.1	143.3	A	b	
Erythrose, hydrate	48.4	164.2	141.5	145.9	b	A
Threose, hydrate	49.0	162.8	141.5	145.0	4.4	A
α-Erythrofuranose	43.3	172.3	150.3	154.0	b	A
α-Threofuranose	45.9	172.3	152.5	152.8	∿1.9	A
β-Erythrofuranose	46.9	172.3	150.3	152.1	∿3.4	A
β Threofuranose	42.3	173.8	151.8	152.8	4.4	A
Glyceronitrile	59.4		A	A	d	
Erythrononitrile	60.8		153.0	A	d	c
Threononitrile	60.8		153.1	A	d	∿4.0
Glyceric acid	59.4		A	A	A	
Erythronate, sodium	52.8		A	A	2.9	c
Threonate, sodium	54.2		A	A	3.7	3.7

[a] Coupling constants are accurate to within ±0.7 Hz. The letter (A) indicates that no experiments were performed to evaluate coupling between the designated atoms. [b] Broadened peaks. [c] No coupling observed. [d] Coupling observed, but could not be reliably measured.

Figure 34. Determination of heteronuclear ^{13}C-^{1}H coupling by ^{13}C NMR.

The proton-decoupled (A) and coupled (B) ^{13}C NMR spectra of the C-1 region of α- and β-D-[1-^{13}C]threose and D-[1-^{13}C]threose hydrate, showing C1—H1 couplings for the three forms in aqueous solution.

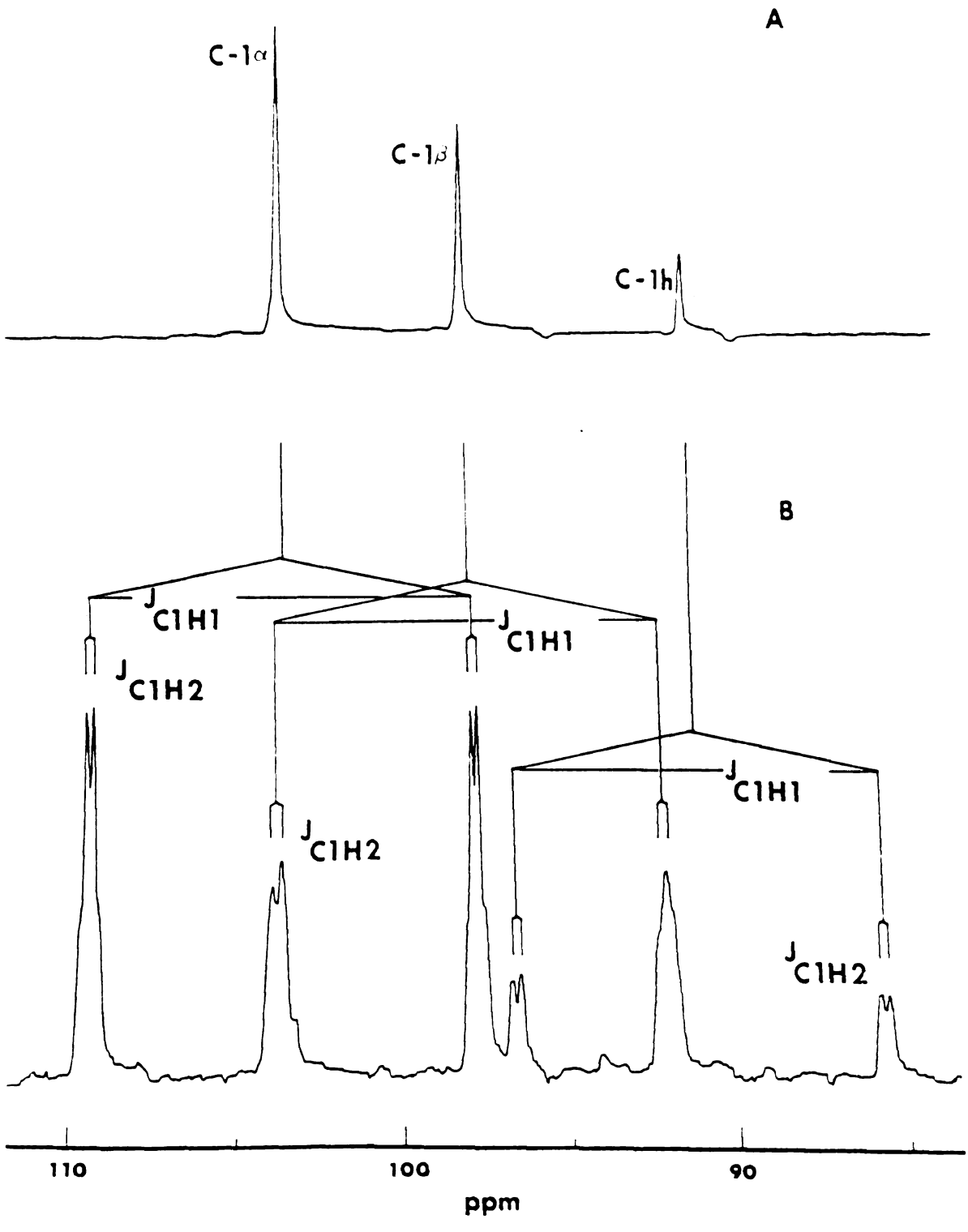
A
C-1α
C-1β
C-1h
B
J C1H1
J C1H1
J C1H2
J C1H1
J C1H2
J C1H2
110
100
90
ppm

Figure 34.

enriched tetroses ranges from 150-153 Hz for cyclic forms and 141-143 Hz for the hydrates. Direct C-3–H-3 coupling in the [3-^{13}C]-enriched tetroses ranges from 152-154 Hz for cyclic forms and 145-146 Hz for acyclic hydrates.

Two-bond C-1 to H-2 coupling appears to be present in the coupled ^{13}C NMR spectra of [1-^{13}C]-enriched compounds (Figure 34), and differences appear to exist between erythro and threo furanoses (Table 11). Although these differences probably reflect the conformational preferences of the various forms, analysis of the ^{1}H NMR spectra will be required to establish the magnitude of $^{2}J_{C1,H2}$ more precisely before conformational inferences are made.

It is noted that $^{2}J_{C,H}$ and $^{3}J_{C,H}$ cannot, in contrast to $^{1}J_{C,H}$, be distinguished solely on the basis of ^{1}H-coupled ^{13}C NMR spectra of the enriched ^{13}C nucleus. Interpretation of the ^{1}H NMR spectra of the [^{13}C]-enriched compounds is required to establish ^{13}C-^{1}H coupling pathways with certainty.

Differences in $^{2}J_{C1,H2}$ are observed between D-erythrose hydrate and D-threose hydrate. The threo isomer has $^{2}J_{C1,H2}$ = 4.4 Hz, whereas the erythro isomer gives broadened resonances. Complex carbon-hydrogen geminal and vicinal couplings were also observed in the [1-^{13}C]-enriched three- and four-carbon aldononitriles. Again, these differences probably reflect the conformational preferences of the acyclic forms, but additional data will be required to confirm and interpret them.

b. Aldose phosphates

i. Solution structure

The structures of the aldose and ketose phosphates in aqueous solution are of considerable interest because of their involvement in enzyme-substrate reactions. Swenson and Barker (179) examined several sugar phosphates by infrared, ultraviolet and circular dichroic spectroscopy to determine the percentage of carbonyl forms present in aqueous solution. Fructose 1-P and glucose 6-P have no, or only trace amounts of, free keto or aldehydo forms in solution. D-Fructose 6-P, D-fructose 1,6-P_2 and DL-glyceraldehyde 3-P have approximately 1%-10% free carbonyl in solution, depending on the compound. 1,3-Dihydroxy-2-propanone-P is 55% keto form in solution.

Using ^{31}P NMR spectroscopy to examine stereochemical analogs of D-fructose 1,6-P_2 (FDP), the methylglycosides of FDP, and specifically deuterated FDP, Gray (180) concluded that four forms of FDP are present in aqueous solution in the following percentages: β-furanose (∿90), α-furanose (∿10), keto (<1.7), and hydrated keto (<0.1). Koerner et al. (181) investigated the tautomeric composition of natural abundance FDP and D-fructose 6-P (F6P) in solution by ^{13}C NMR spectroscopy. In addition to the assignment of ^{13}C chemical shifts, integration of signal intensities yielded the following equilibrium compositions: F6P, α-furanose (19 ± 2%), β-furanose (81 ± 2%); FDP, α-furanose (23 ± 4%) and β-furanose (77 ± 4%). Less than 1.5% keto or hydrated forms was reported in solutions of either fructose phosphate.

Midelfort, Gupta and Rose (182) prepared [UL-^{13}C] F6P and FDP enzymatically and examined them in H_2O and H_2O-DMSO mixtures by ^{13}C NMR.

Despite complications arising from ^{13}C-^{13}C coupling, keto forms were observed at ~215 ppm downfield from Me_4Si. They concluded that F6P and FDP contain 4.1% and 2.0% keto isomer at room temperature, respectively. From ^{13}C line-broadening studies, ring-opening rates for the α-furanose (8 s^{-1}) and β-furanose (35 s^{-1}) forms of FDP were measured and related to the kinetic properties of the aldolases.

In this study, the solution structures of the aldose phosphates are compared with those of the simple aldoses from which they are derived and with those having one less carbon atom. The terminal phosphate eliminates the possibility of hemiacetal formation at the primary hydroxyl group, leaving opportunities for intra- or intermolecular reactions of the carbonyl group similar to those of the smaller non-phosphorylated aldoses.

In dilute solution, glycolaldehyde-P and glyceraldehyde 3-P appear to exist predominantly as monomeric hydrates (linear gem-diol) with C-1 resonances at approximately 91 ppm (Table 12). Resonances in this region of the ^{13}C spectrum are characteristic of linear gem-diol carbons, as discussed previously (Table 10). When the acid form of DL-[1-^{13}C]-glyceraldehyde 3-P is concentrated to dryness, a mixture of dimers and oligomers with C-1 chemical shifts at 105.2, 103.8, 102.9, 97.3, 93.1, 92.8, 89.7 and 89.0 ppm is formed. These revert rapidly to the hydrate in dilute aqueous solution (0.1 M) at pH 1-2. Dilute aqueous solutions of DL-glyceraldehyde 3-P contain about 5-10% of these higher structures at pH 5.5. Dimers and oligomers of [1-^{13}C]glycolaldehyde and DL-[1-^{13}C]glyceraldehyde have also been observed (Figure 33) in dilute aqueous solution at pH 6.

The tetrose 4-phosphates exist principally as monomeric hydrates

Table 12. ^{13}C Chemical shifts of aldose phosphates and related compounds.

Compound	pH[b]	Carbon Position (ppm)[a]				
		C-1	C-2	C-3	C-4	C-5
glycolaldehyde-P, hydrate[c]	7.5	90.7[d]	68.2[d]			
D-glyceraldehyde 3-P, hydrate[c]	7.5	91.3	74.9[d]	66.0[d]		
DL-erythrose 4-P, hydrate	1.5	90.3	73.8	71.4[d]	68.0[d]	
DL-threose 4-P, hydrate	4.5	90.8	74.1	70.6[d]	67.0[d]	
D-arabinose 5-P						
α-furanose	5.5	102.2	82.2	76.7	83.1[d]	65.1[d]
β-furanose	5.5	96.3	77.0	75.1	81.1[d]	66.2[d]
hydrate	5.5	91.2				
D-ribose 5-P						
α-furanose	5.5	97.5	71.9	71.3	83.6[d]	65.8[d]
β-furanose	5.5	102.4	76.4	71.7	82.5[d]	66.6[d]
hydrate	5.5	90.7				
DL-xylose 5-P						
α-furanose	5.5	96.9	76.8			
β-furanose	5.5	103.0	81.3			
hydrate	5.5	90.9				
DL-lyxose 5-P						
α-furanose	5.5	101.9	78.2			
β-furanose	5.5	96.5	72.5			
hydrate	5.5	90.4				
DL-glyceronitrile 3-P[c]	2.5	120.3	62.0[d]	67.1[d]		
DL-erythrononitrile 4-P	1.7	120.3	63.1	71.8[d]	65.9[d]	
DL-threononitrile 4-P	1.7	120.2	62.6	71.6[d]	65.4[d]	
D-arabinononitrile 5-P	4.6	122.6	62.7[e] (3.2)			
D-ribononitrile 5-P	4.6	121.2	64.2[e] (0.8)			
DL-xylononitrile 5-P	4.3	120.5	63.3[e] (3.2)			
DL-lyxononitrile 5-P	4.3	121.4	63.1[e] (3.8)			

Table 12 (cont'd.).

[a] Chemical shifts were determined at 13 ± 1°C with a sweep width of 1500 Hz and a filter width of 2400 Hz. Chemical shifts which are not entered were not measured. [b] Solutions were adjusted to the given pH (±0.1 unit) at 25°C prior to NMR analysis. [c] These determinations were made at 34 ± 1°C. [d] Resonance appears as a doublet arising from ^{31}P-^{13}C coupling. [e] Chemical shifts were measured at the pH value shown in parentheses.

in dilute aqueous solution at pH 2-5, but chemical shifts at 97.9 and 98.4 ppm, typical of hemiacetals, indicate the presence of up to 15% of dimers and/or oligomers in solutions of [1-^{13}C]erythrose 4-P. Blackmore et al. (183) examined the spontaneous dimerization of erythrose 4-P in aqueous solution and proposed a structure for the dimer based on data from mass spectrometry. In concentrated solutions of D-[1-^{13}C]erythrose, C-1 resonances at 98.5, 97.9, 92.5 and 92.1 ppm have been attributed to dimeric or higher order structures (Figures 30C and 31D).

Aqueous solutions of the [1-^{13}C]pentose 5-phosphates at pH 5.5 contain predominantly α- and β-furanose forms, with a small proportion (1-5%) of linear gem-diol (Table 13). In comparison, solutions of

Table 13. Structural forms of the pentose 5-phosphates in aqueous solution[a].

Pentose 5-P	% Composition, ±3%[b]		
	β	α	Hydrate
Arabinose 5-P	40	58	2
Ribose 5-P	64	34	≈1
Xylose 5-P	45	51	4
Lyxose 5-P	25	70	5

[a] Determined at 13 ± 1°C and pH 5.5 ± 0.1. [b] Determined by computer integration of ^{13}C NMR spectra of [1-^{13}C]-enriched pentose 5-phosphates. Aldehydo forms were not observed.

[1-^{13}C]tetroses contain approximately 12% hydrate. Assignment of the chemical shifts to the α- and β-furanose forms of the pentofuranose phosphates was made by analogy to those assigned to the α- and β-methyl furanosides (114).

Furanose rings having OH-1 trans to OH-2 (Figure 35) are generally more stable than those having the corresponding cis arrangement (99), and the α-lyxo, α-arabino-, and β-ribofuranose phosphates which have this arrangement are the predominant anomers in aqueous solution at pH 5.5 (Table 13). D-xylo-Pentofuranose phosphate is an exception to this rule, indicating that destabilization arising from two cis-1,3 interactions in the β-anomer (Figure 35) is equivalent to that arising from a single cis-1,2 interaction in the α-anomer.

As observed by Ritchie et al. (114), a useful relationship exists between the chemical shift of C-1 and the anomeric configuration in the furanose ring. As in the methyl furanosides, the resonances for C-1 of anomers of the aldofuranose phosphates having OH-1 trans to OH-2 are typically downfield (≈105 ppm) from those with the cis arrangement (≈97 ppm) (Table 12, Figure 35).

It is well established that the relative positions of hydroxyl groups in pyranoses and furanoses determine the relative stabilities of anomers and various ring forms (99). Although the conformations of the furanose rings in the aldose phosphates are not established, certain relative configurations of hydroxyl groups appear to be preferred leading to the observed anomeric preferences listed in Table 13. Specifically, the pentose phosphates with OH-2 trans to OH-3 generally have a greater proportion of the anomer with OH-1 cis to OH-2 than do those pentose phosphates with OH-2 cis to OH-3 (Figure 35).

ii. Assignment of chemical shifts (Table 12)

Chemical shifts for C-1 have been discussed above in terms of the various forms present in aqueous solution. Assignments of carbons bearing the phosphate group and adjacent carbons have been made on the

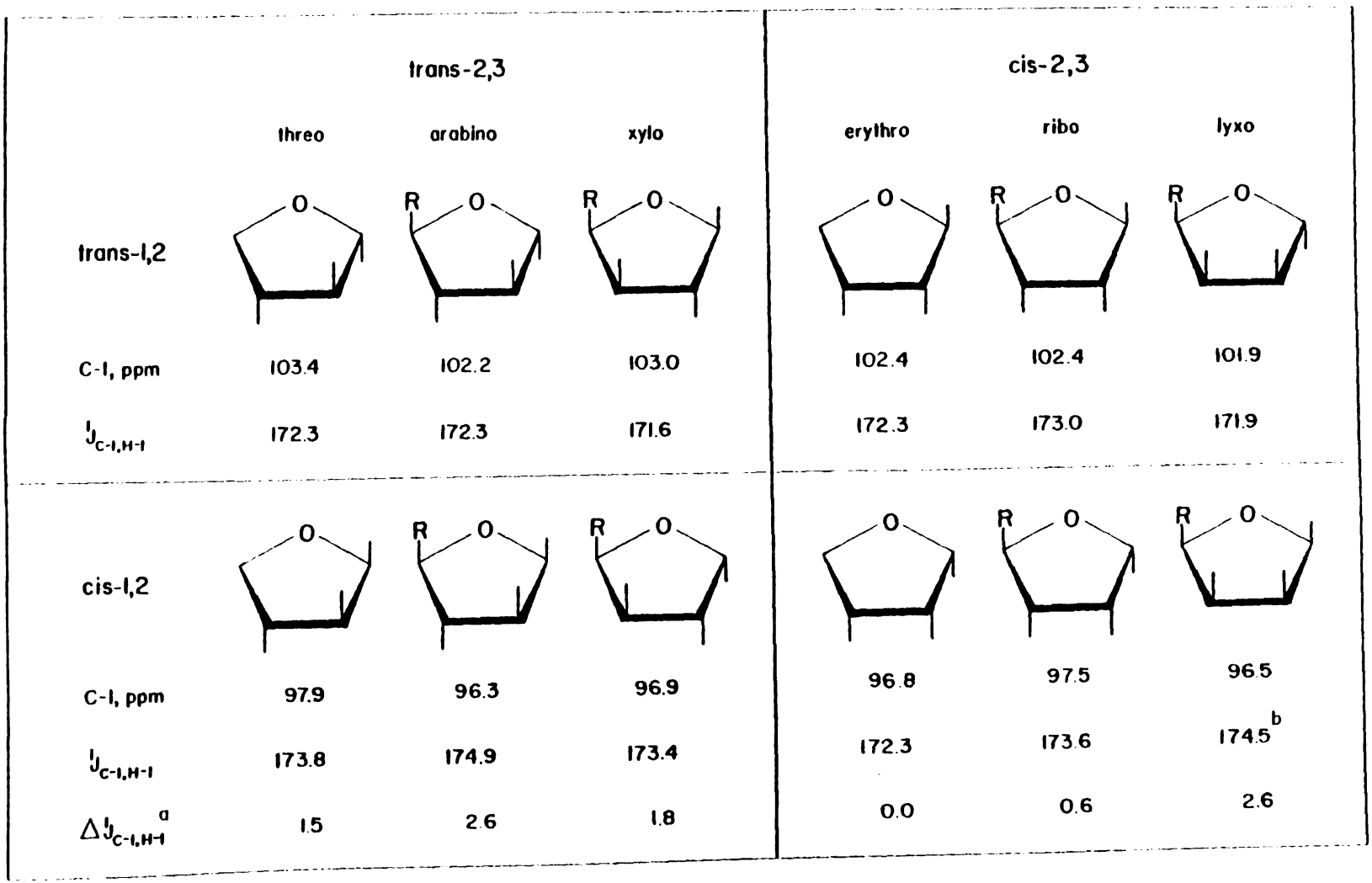

Figure 35. Structural and ^{13}C NMR spectral relationships between the furanose forms of the pentose 5-phosphates and the tetroses. a, $^1J_{C1,H1}$ (cis-1,2) − $^1J_{C1,H1}$ (trans-1,2) = ΔJ. b, The error in this coupling constant is 1.5 Hz due to the complexity of the coupled signals. All other C-H couplings are accurate to ±0.7 Hz. Chemical shifts are accurate to ±0.1 ppm. R = CH_2OP.

basis of comparison with standards and on the predictable coupling pattern of phosphorus to carbon (184, 185). C-2 Resonances were assigned on the basis of ^{13}C-^{13}C coupling to C-1 in [1-^{13}C]-enriched compounds. The [2-^{13}C]-enriched compounds prepared also permit unequivocal assignment of C-2 and of C-3 chemical shifts by difference (the close proximity of C-2 and C-3 resonances causes the C-3 resonance to be obscured in several of the [2-^{13}C]-enriched compounds). As observed by Ritchie et al. (114) for glycosides, and for the tetrofuranoses (Table 10), the C-2 and C-3 chemical shifts for the pentofuranose 5-phosphates in which OH-2 and OH-3 are <u>trans</u> (arabino, xylo) are downfield from those of the <u>cis</u> compounds (ribo, lyxo) (Table 12 and Figure 35). The relative configuration at C-2 and C-3 does not apparently affect the chemical shifts of C-1, C-4 and C-5. Ritchie et al. (114) have observed that substitution of CH_2OH for H at C-4 of a tetrofuranoside to produce a pentofuranoside causes a downfield shift of the C-4 resonance of approximately 10 ppm. The C-4 resonance in the tetrofuranoses (Table 10) also shifts downfield approximately 10 ppm when a 4-H is replaced by CH_2OP to produce the pentose 5-P, suggesting that phosphorylation at the primary alcohol may not significantly alter electron density at C-4. Alternately, the CH_2OP group may alter the through-bond effect on a neighboring group and, at the same time, propagate a through-space effect that cancels the through-bond effect.

The nitrile group shields the α-carbon in the aldononitrile phosphates, producing an upfield shift of approximately 10 ppm from the α-carbon of the aldose phosphates. This effect is expected and is analogous to proton shielding observed in the acetylene system by Pople (177).

iii. Carbon-phosphorus coupling constants

Two-bond coupling between carbon and phosphorus is not very sensitive to changes in structure of the phosphate ester. Two-bond ($^2J_{POC}$) coupling constants observed in this study (Table 14) are typical of those observed in other phosphate esters, ranging from 4.4 Hz for threose 4-P (pH 4.5) to 5.5 Hz for α-ribose and α-arabinose 5-phosphates (pH 5.5). The measured $^2J_{POC}$ of 4.8 Hz for β-D-ribose 5-P is similar to the reported $^2J_{POC}$ value of 4.7 Hz for the β-D-ribose 5-P moieties in UMP and AMP (186) at pH 6.3.

Three-bond ($^3J_{POCC}$) coupling (Table 14) is dihedral-angle dependent and can be used to determine molecular orientations in solution. For β-D-ribose 5-P and the β-D-ribose 5-P moieties in 5'-UMP and 5'-AMP, $^3J_{POCC}$ = 8.4 Hz (pH 5.5), 8.5 Hz (pH 6.3), and 8.7 Hz (pH 6.3), respectively. The magnitude of these couplings indicates that the preferred position of the phosphate group is <u>trans</u> to C-4 and <u>gauche</u> to H-5' and H-5" (186). The values of $^3J_{POCC}$ for both cyclic and acyclic aldose phosphates (Table 14) indicate that in these compounds a <u>trans</u> arrangement is preferred. It should be noted that $^3J_{POCC}$ couplings for several α-glycosyl 1-phosphates indicate that the preferred position of the phosphate is <u>trans</u> to C-2 and <u>gauche</u> to C-1 and to O-5, but substantial amounts of other rotamers may be present since the maximum values for $^3J_{POCC}$ may be 12 Hz or more when the <u>trans</u> arrangement is fixed (187).

iv. Carbon-hydrogen coupling constants

Carbon-hydrogen coupling constants can provide useful information about carbohydrate structures, as shown by Bock et al. (115), Walker et al. (59), and Schwarcz and Perlin (120). These couplings are

Table 14. ^{13}C-P and ^{13}C-H Coupling constants of aldose phosphates and related compounds.

Compound	pH	^{13}C-P Coupling Constant (Hz)[a]		^{13}C-H Coupling Constant (Hz)[a]		
		$^{2}J_{POC}$	$^{3}J_{POCC}$	$^{1}J_{C1,H1}$	$^{1}J_{C2,H2}$	$^{2}J_{C1,H2}$
glycolaldehyde-P, hydrate[d]	7.5	5.1	7.7			
DL-glyceraldehyde 3-P, hydrate[d]	7.5	5.1	6.2	159.8		b
DL-erythrose 4-P, hydrate	1.5	5.1	8.1	163.9		c
DL-threose 4-P, hydrate	4.5	4.4	8.1	162.6[e] (2.1)		3.5[e] (2.1)
DL-arabinose 5-P						
α-furanose	5.5	5.5	8.1	172.3	149.6	c
β-furanose	5.5	4.8	8.4	174.9	147.4	c
DL-ribose 5-P						
α-furanose	5.5	5.5	8.4	173.6	152.9	1.6
β-furanose	5.5	4.8	8.4	173.0	153.6	b
DL-xylose 5-P						
α-furanose	5.5			173.4	150.7	b
β-furanose	5.5			171.6	153.6	b
DL-lyxose 5-P						
α-furanose	5.5			171.9	145.2	b
β-furanose	5.5			174.5	147.4	4.8
DL-glyceronitrile 3-P[d]	2.5	4.7	8.8			
DL-erythrononitrile 4-P	1.7	5.1	8.4			
DL-threononitrile 4-P	1.7	5.5	8.4			
DL-arabinononitrile 5-P	3.2				152.9	
DL-ribononitrile 5-P	0.8				153.6	
DL-xylononitrile 5-P	3.2				153.2	c
DL-lyxononitrile 5-P	3.8				154.5	4.6

Table 14 (cont't.).

[a] Coupling constants were measured with a sweep width of 1500 Hz and a filter width of 2400 Hz at 13 ± 1°C at the pH values (±0.1 unit) indicated and are accurate to within ±0.7 Hz. [d] Couplings which are not entered were not measured. [b] Broadening observed. [c] No coupling observed. [d] These determinations were made at 34 ± 1°C. [e] Couplings were measured at the pH shown in parentheses.

particularly easy to observe in [^{13}C]-enriched compounds, and some useful correlations of magnitude of coupling constants to structure emerge from this study. The ^{13}C-^{1}H couplings observed in the [^{13}C]-enriched aldose phosphates and their derivatives are listed in Table 14.

$^{1}J_{C1,H1}$ coupling for the gem-diol triose and tetrose phosphates range from 160 to 164 Hz. Formation of the furanose phosphate ring increases the value of $^{1}J_{C1,H1}$ by about 10 Hz. This increase upon cyclization has been observed for erythro- and threofuranoses (Table 11) and provides another parameter, in addition to chemical shift, for the identification of linear hydrates in solution by ^{13}C NMR and ^{1}H NMR.

Bock et al. (115), Bock and Pedersen (116, 117), and Walker et al. (59) have shown that $^{1}J_{C1,H1}$ in the pyranoses is dependent on the configuration at C-1 and is useful in assigning anomeric configuration of carbohydrates. In these rings, $^{1}J_{C,H}$ for an axial H-1 is approximately 10 Hz smaller than $^{1}J_{C,H}$ for an equatorial H-1. One-bond C-1 to H-1 coupling in the pentose 5-phosphates and tetroses is also sensitive to the configuration at C-1. The cis-1,2 anomers of threofuranose and arabino-, xylo-, and lyxofuranose phosphates have larger C-1 to H-1 coupling constants than the respective trans-1,2 anomers (Table 14 and Figure 35), although differences between anomers are smaller ($\Delta^{1}J_{C1,H1}$ = 1.5 - 2.6 Hz) than those observed for the pyranoses. $^{1}J_{C1,H1}$ for erythrofuranose and ribofuranose phosphate is not as sensitive to configuration at C-1. Differences in $^{1}J_{C1,H1}$ for the furanose ring probably reflect conformational preferences (188) which must be determined before a full interpretation of ^{13}C-^{1}H coupling with respect to furanose configuration can be made.

$^{1}J_{C2,H2}$ couplings are typically 20-25 Hz less than $J_{C1,H1}$

couplings for both the linear and furanose forms of phosphorylated (Table 14) and simple aldoses (Table 11). Examinations of $^{1}J_{CH}$ in the pyranoses have shown similar differences between $^{1}J_{C1,H1}$ and $^{1}J_{C2,H2}$ (116, 117).

Several geminal $^{2}J_{C1,H2}$ coupling constants for the [1-^{13}C]aldose phosphates were observable (Table 14). Threose 4-P and threose hydrate (Table 11) show $^{2}J_{CCH}$ couplings of 3.5 and 4.4 Hz, respectively, whereas erythrose 4-P and erythrose hydrate do not exhibit coupling. Proton-coupled ^{13}C NMR spectra of [1-^{13}C]- and [2-^{13}C]pentofuranose 5-phosphates vary in complexity with furanose configuration. For example, geminal and longer range ^{13}C-^{1}H coupling is not apparent in α- and β-[1-^{13}C]-arabinofuranose 5-P, whereas α- and β-[1-^{13}C]lyxofuranose 5-P show complex coupling patterns. Analysis by ^{1}H NMR will be required to identify specific ^{13}C-^{1}H and ^{1}H-^{1}H couplings and relate the value of these couplings to furanose conformation and configuration.

C. Preparation of [^{2}H]-Enriched Aldoses and Their Derivatives

1. Hydrogenolysis with $^{2}H_2$

For the incorporation of ^{2}H into the aldoses, cyanide condensation and hydrogenolysis are carried out in $^{2}H_2O$ instead of H_2O to avoid exchange of ^{1}H for ^{2}H on the catalytic surface. This exchange decreases the incorporation of ^{2}H at H-1. Under the conditions used for hydrogenolysis, ^{1}H-^{2}H exchange does not occur at other positions, as determined by ^{1}H NMR. In several cases, nitrile (~15%) remained in the reduction mixtures after 10 h of hydrogenolysis. Complete conversion to products was achieved by adding new catalyst and continuing the reduction.

The methods for the preparation of aldononitriles in $^{2}H_{2}O$ and their hydrogenolysis with $^{2}H_{2}$ are the same as those for the preparation of the undeuterated compounds. Yields are also comparable.

The use of [^{13}C, ^{2}H]-enriched compounds facilitates the observation of the deuterated carbon (Figure 36). The ^{13}C NMR spectrum of D-[1-^{13}C]threose in aqueous solution shows the presence of three major tautomeric forms, namely, the α- and β-furanoses, and a linear gem-diol (hydrate) (Figure 36A). The proton-decoupled ^{13}C NMR spectrum of D-[1-^{13}C,^{2}H]threose (Figure 36B) shows four lines for each tautomeric form, three arising from ^{13}C-^{2}H coupling, and one from the residual protonated carbon. The percent isotopic incorporation is not reflected in peak areas, since nuclear Overhauser enhancement is smaller for deuterated than for protonated methine carbons (189). For example, the ^{1}H NMR spectrum of the same preparation of D-[1-^{13}C,^{2}H]threose shows no resonance for H-1, indicating deuterium enrichment of at least 97 percent, whereas the proton-decoupled ^{13}C NMR spectrum (Figure 36B) gives the appearance of a significant proportion of ^{1}H at H-1.

2. NMR parameters

a. ^{13}C NMR parameters

Substitution of ^{2}H for ^{1}H permits the assignment of ^{13}C resonances of the directly-bound and nearby carbons due to decreased nuclear Overhauser effects and characteristic isotope shifts. In addition, ^{13}C-^{2}H coupling can be measured. The effect of ^{2}H substitution for ^{1}H on the ^{13}C chemical shift of the derivatized carbon is shown in Table 15 for several carbohydrates. The values observed are similar to those observed by Gorin (79) and Gorin and Mazurek (118). The use of [^{13}C,^{2}H]-enriched compounds permits an easier evaluation of the

Figure 36. Incorporation of ^{2}H into a [^{13}C]-enriched carbohydrate.

(A) The 15.08 MHz proton-decoupled ^{13}C NMR spectrum of the enriched region for D-[1-^{13}C]threose. The three predominant tautomeric forms in aqueous solution are α- and β-furanose (103.4 and 97.9 ppm, respectively) and acyclic hydrate (91.1 ppm). (B) The 15.08 MHz proton-decoupled ^{13}C NMR spectrum of the enriched region of D-[1-^{13}C,^{2}H]-threose, showing the splitting of C-1 of each form by the directly-bound deuteron. Isotope shift is shown for each species as the difference in the positions between the protonated C-1 and the center of gravity of the triplet arising from the deuterated C-1.

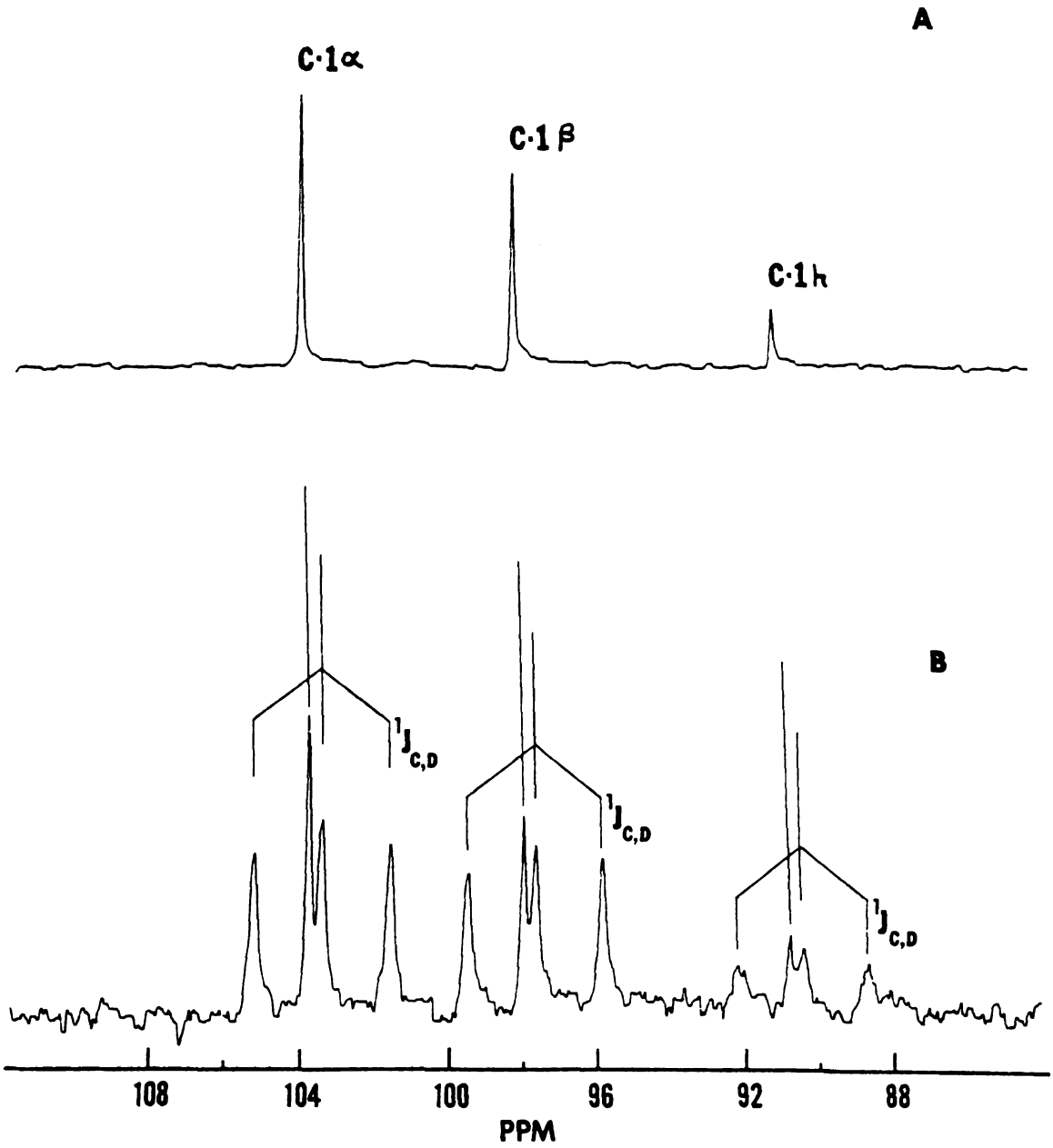

Figure 36.

magnitudes of $^{1}J_{^{13}C,^{2}H}$ and the isotope shift, as shown in Figure 36. A directly-bound deuterium nucleus, with a spin of 1, will split a carbon resonance into a triplet with $^{1}J_{^{13}C,^{2}H} \simeq 24$ Hz. The ^{13}C-^{2}H isotope shift can be estimated from the difference in resonance position between the protonated carbon and the center of gravity of the deuterated carbon triplet. The deuterated carbon is upfield ($\sim$5 Hz) from the protonated carbon.

In Table 15, $^{1}J_{^{13}C,^{2}H}$ coupling constants are listed for several carbohydrates and derivatives. The data indicate that $^{1}J_{^{13}C1,^{2}H1}$ is larger when OH-1 and OH-2 are cis in the furanose ring, and that this coupling is larger in the ring forms than in the acyclic hydrates. The same relationships were observed for $^{1}J_{^{13}C,^{1}H}$ (Tables 11 and 14, Figure 35). Colli et al. (190) have shown for several non-carbohydrate compounds that the ratio $^{1}J_{^{13}C,^{1}H}$:$^{1}J_{^{13}C,^{2}H}$ is very close to the value predicted from the magnetogyric ratios for ^{1}H and ^{2}H. The value of ΔJ indicates the extent of variation between observed and predicted values of $^{1}J_{^{13}C,^{2}H}$, and is zero for perfect agreement. As shown in Table 15, values for ΔJ are within the error of the determinations.

b. ^{1}H NMR parameters

Replacement of ^{1}H with ^{2}H often simplifies ^{1}H NMR spectra, facilitating the assignment of chemical shifts and coupling constants. For example, whereas the 180 MHz ^{1}H NMR spectrum of D-erythrose is essentially first-order, that of D-threose is complex (Figure 37A). The complexity was eliminated in the spectrum of DL-[3-^{2}H]threose and it was shown that, in D-threose, the ^{1}H NMR spectrum is complicated by the near magnetic equivalence of H-3α and H-4α which perturbs the resonances of these nuclei and produces a complex multiplet for H-4'α.

Table 15. ^{13}C Chemical shifts, ^{13}C-^{1}H and ^{13}C-^{2}H coupling constants for several [^{13}C,^{2}H]-enriched carbohydrates and derivatives.

Compound	$^{1}J_{C,^{1}H}$ (Hz)	$^{1}J_{C,^{2}H}$ (Hz)	Carbon Chemical Shift, ppm[a] ^{13}C-^{1}H	^{13}C-^{2}H	$\Delta\nu$[c] (Hz)	ΔJ[d] (±5.3)
α-D-[1-^{13}C,^{2}H]-Threose	172.3	26.0	103.5	103.2	5.9	2.9
β-D-[1-^{13}C,^{2}H]-Threose	173.8	26.4	98.0	97.7	5.1	1.8
D-[1-^{13}C,^{2}H]-Threose, hydrate	162.8	24.9	91.0	90.8	4.8	0.6
α-D-[1-^{13}C,^{2}H]-Erythrose	172.3	26.8	96.9	96.5	5.1	-2.3
β-D-[1-^{13}C,^{2}H]-Erythrose	172.3	26.0	102.5	102.1	5.9	2.9
D-[1-^{13}C,^{2}H]-Erythrose, hydrate	164.2	25.3	90.8	90.5	5.1	-0.6
Methyl α-D-[2-^{13}C,^{2}H]-Ribofuranoside		22.5	72.5	72.1	5.1	
Methyl β-D-[2-^{13}C,^{2}H]-Ribofuranoside		23.8	75.7	75.3	5.1	
α-D-[2-^{13}C,^{2}H]-Arabinopyranose		22.4	73.4	72.9	6.6	
β-D-[2-^{13}C,^{2}H]-Arabinopyranose		22.0	70.0	69.6	5.9	
α-D-[1-^{13}C,^{2}H]-Ribose 5-Phosphate	173.6	26.8	97.6	97.3	4.4	-1.0
β-D-[1-^{13}C,^{2}H]-Ribose 5-Phosphate	173.0	26.0	102.3	102.0	4.4	3.6
DL-[1-^{13}C,^{2}H]-Glyceraldehyde 3-Phosphate	159.8	24.9	90.8	90.5	5.1	-2.4

[a] Chemical shifts are given relative to external Me_4Si and are accurate at ±0.1 ppm. Carbon spectra were obtained with broad-band proton decoupling at 30°C. [b] Coupling constants are accurate to ±0.7 Hz. [c] $\Delta\nu = \nu_{(^{1}H)} - \nu_{(^{2}H)}$, where $\nu_{(^{1}H)}$ and $\nu_{(^{2}H)}$ are equal to the resonance frequencies of the protonated and deuterated carbons, respectively. $\Delta\nu$ is positive since the observed isotope shifts upon deuteration are upfield from the protonated homologue. [d] $\Delta J = {}^{1}J_{^{13}C,^{1}H} - \gamma_{^{1}H}\,{}^{1}J_{^{13}C,^{2}H}/\gamma_{^{2}H}$, where $\gamma_{^{1}H}$ and $\gamma_{^{2}H}$ are the magnetogyric ratios for ^{1}H and ^{2}H, respectively.

Figure 37. 180.04 MHz ^{1}H NMR spectra of the H-2 to H-4 regions of D-threose and DL-[3-^{2}H]threose.

(A) The 180.04 MHz ^{1}H NMR spectrum of the H2-H4 region of D-threose. (B) The 180.04 MHz ^{1}H NMR spectrum of the same region of DL-[3-^{2}H]-threose. Deuteration at C-3 simplifies the spectrum so that assignment of resonances can be made as shown. The upfield half of the doublet from H-2β (due to coupling to H-1) is observed, with the other half hidden by the H-2α doublet. The magnitude of the coupling is confirmed by observation of H-1β (not shown). The chemical shifts of H-3α and H-3β, determined by computer simulation, are 4.20 ppm and 4.30 ppm, respectively. Lines between the resonances due to H-4'β appear to arise from H-4 and H-4' of the acyclic hydrate. H-4' was arbitrarily designated as the more shielded H-4 of each form.

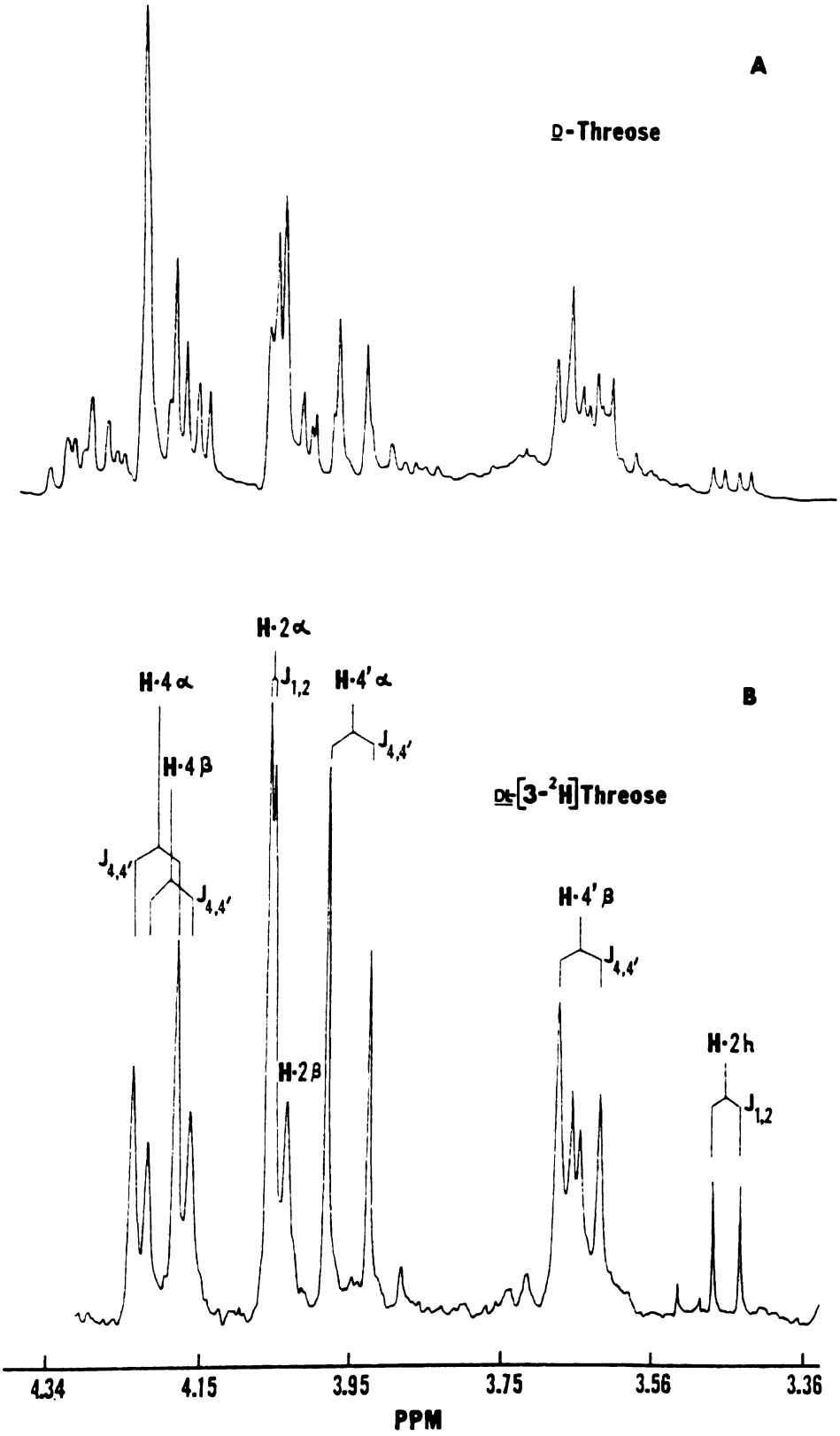
A
D-Threose
H·2α
H·4α
H·4'α
H·4β
H·4'β
H·2β
H·2h
B
DL-[3-²H]Threose
4.34
4.15
3.95
3.75
3.56
3.36
PPM

Figure 37.

Substituting ^{2}H for ^{1}H at H-3 in threose removes three vicinal ^{1}H-^{1}H couplings and the resonances due to H-3 from the spectrum, greatly simplifying assignment and analysis. D-Threose exists primarily as three tautomeric forms in aqueous solution in the ratio α-furanose: β-furanose:hydrate of 4.2:3.1:1 (Figure 36A). Although H-2 can be identified by selective homonuclear decoupling of H-1 or by [^{13}C]-enrichment at C-2, neither technique permits the unequivocal assignment of H-3, H-4 and H-4' for each tautomer. Figure 37B shows the H2-H4 region of the 180 MHz ^{1}H NMR spectrum of DL-[3-^{2}H]threose. The H-2, H-4 and H-4' resonances are easily identified for the furanose forms on the basis of their proportions in solution. In addition, the spectrum is essentially first-order, permitting direct determination of several geminal and vicinal ^{1}H-^{1}H coupling constants. The H-2 resonance of the hydrate is at 3.46 ppm, but resonances due to H-3, H-4 and H-4' for this form are not readily assigned. However, from the ^{1}H NMR spectrum of the 3-^{2}H derivative (Figure 37B), it is clear that H-4 and H-4' for the linear hydrate lie in the same region as H-4' for the β-furanose, permitting the position of these resonances to be estimated by computer simulation. Chemical shifts for H-3 for the cyclic forms of D-threose were estimated by comparison of the normal and deuterated compounds and refined by computer simulation. Apparent and intrinsic proton chemical shifts and ^{1}H-^{1}H coupling constants for the tetroses are given in Tables 16 and 17.

In both tetroses, H-1 of the hydrate is more shielded than H-1 for the furanoses, while H-2 of the hydrate is the most shielded nucleus.

Heteronuclear ^{2}H-^{1}H coupling has been observed in both high resolution ^{1}H and ^{2}H spectra (190, 191). However, the ^{1}H NMR spectra of DL-[3-^{2}H] threose (Figure 37B) and DL-[3-^{2}H]erythrose at 180 MHz

do not exhibit ^{2}H-^{1}H couplings. Only vicinal or long-range ^{1}H-^{2}H coupling pathways would be expected in these compounds. Since ^{1}H-^{2}H coupling constants are about 15% (1/6.5144) of their ^{1}H-^{1}H analogs, triplets with $^{3}J_{^{1}H,^{2}H}$ values of 0.15-0.77 Hz would be difficult to resolve. As discussed by Mantsch et al. (192), ^{1}H spectra often exhibit an average ^{1}H-^{2}H coupling because the remaining ^{1}H-^{1}H couplings are considerably larger than the ^{1}H-^{2}H couplings or the ^{2}H-induced isotope shifts in the ^{1}H spectrum, and the ^{1}H spectrum is consequently deceptively simple (193). Line broadening (~0.7 Hz) due to pseudorotation of the furanose ring also hinders observation of the smaller ^{1}H-^{2}H couplings.

Specific deuteration has been useful in establishing long-range ^{1}H-^{1}H coupling in the furanose ring. For example, deuteration of D-erythrose at either H-1 or H-3 simplifies the H-3 or H-1 multiplets, respectively, for the β-anomer, indicating that a small (~0.6 Hz) coupling exists between these nuclei. The α-anomer shows no such coupling. Interestingly, methyl α-D-arabinofuranoside has $^{4}J_{H1,H3}$ = 0.5 Hz, whereas the β-anomer shows no coupling (102).

Heteronuclear spin-spin coupling between ^{13}C and ^{1}H is valuable in examining conformations of carbohydrates in solution. Generally, two- and three-bond ^{13}C-H coupling constants are difficult to obtain from ^{1}H-coupled ^{13}C NMR spectra, even when [^{13}C]-enriched compounds are used. These studies are greatly facilitated at high fields (67.89 MHz for carbon) as demonstrated recently (124), but, even in this case, deuterated analogues and heteronuclear selective ^{1}H decoupling were used to confirm assignments. An alternative approach has been to analyze [^{13}C]-enriched compounds by ^{1}H NMR (120, 121, 194-198). In cases

where ^{1}H NMR spectra are complex, the synthesis of compounds with [^{2}H]- and/or [^{13}C]-enrichment may aid interpretation. For example, Figure 38A shows the 180 MHz ^{1}H NMR spectrum of the H2 to H5 region of methyl β-D-ribofuranoside. The spectrum of the [2-^{13}C,^{2}H]-enriched derivative (Figure 38B) is simplified by the loss of a quartet at 4.02 ppm due to H-2. The multiplet centered at 4.14 ppm is altered. In Figure 38A, $^{3}J_{H3,H4}$ and $^{3}J_{H2,H3}$ can be assigned. Inspection of the coupling patterns for H-1 (not shown) and H-2 confirms the assignment of the multiplet at 4.14 ppm to H-3. In Figure 38B, the H-3 multiplet contains $^{3}J_{H3,H4}$ and a new coupling, $^{2}J_{C2,H3}$ = 1.6 Hz. Loss of the H-2 multiplet in this spectrum permits H-4 to be assigned and $^{3}H_{H4,H5}$ and $^{3}J_{H4,H5'}$ to be evaluated from the H-4 multiplet. Note that H-4 is slightly broadened in the [^{13}C]-enriched compound, suggesting a small three-bond coupling of this nucleus to C-2. This broadening probably does not arise from ^{1}H-^{2}H coupling (see above). Resonances due to H-5 and H-5' are quartets centered at 3.79 and 3.59 ppm, respectively. In [2-^{13}C,^{2}H]methyl α-D-ribofuranoside, $^{2}J_{C2,H3}$ is small, producing a broadening of the H-3 doublet.

The apparent and intrinsic ^{1}H chemical shifts and ^{1}H-^{1}H coupling constants for methyl ribo and arabino furanosides determined from the experimental and computer-simulated data, respectively, are listed in Tables 16 and 17. Although in several instances the use of [^{2}H]-enriched compounds was not required to make these assignments, there is no doubt of the value of multiply-enriched derivatives for use in more complex instances.

Figure 38. 180.04 MHz ^{1}H NMR spectra of the H-2 to H-5 regions of methyl β-D-ribofuranoside and methyl β-D-[2-^{13}C,^{2}H]ribofuranoside.

(A) The 180.04 MHz ^{1}H NMR spectrum of the H-2—H-5 region of methyl β-D-ribofuranoside, showing the assignment of multiplets. H-5' was arbitrarily designated as the more shielded H-5. (B) The 180.04 MHz ^{1}H NMR spectrum of the same region of methyl β-D-[2-^{13}C,^{2}H]ribofuranoside, showing the loss of the H-2 multiplet and coupling of H-3 to ^{13}C-2. The H-4 multiplet is broadened while H-5 and H-5' are unchanged. Residual [2-^{13}C,^{2}H] compound would produce two H-2 multiplets split by $^{1}J_{C2,H2} \approx 152$ Hz (Tables 11 and 14). One of these multiplets would appear at approximately 3.59 ppm in this spectrum. It is not observed.

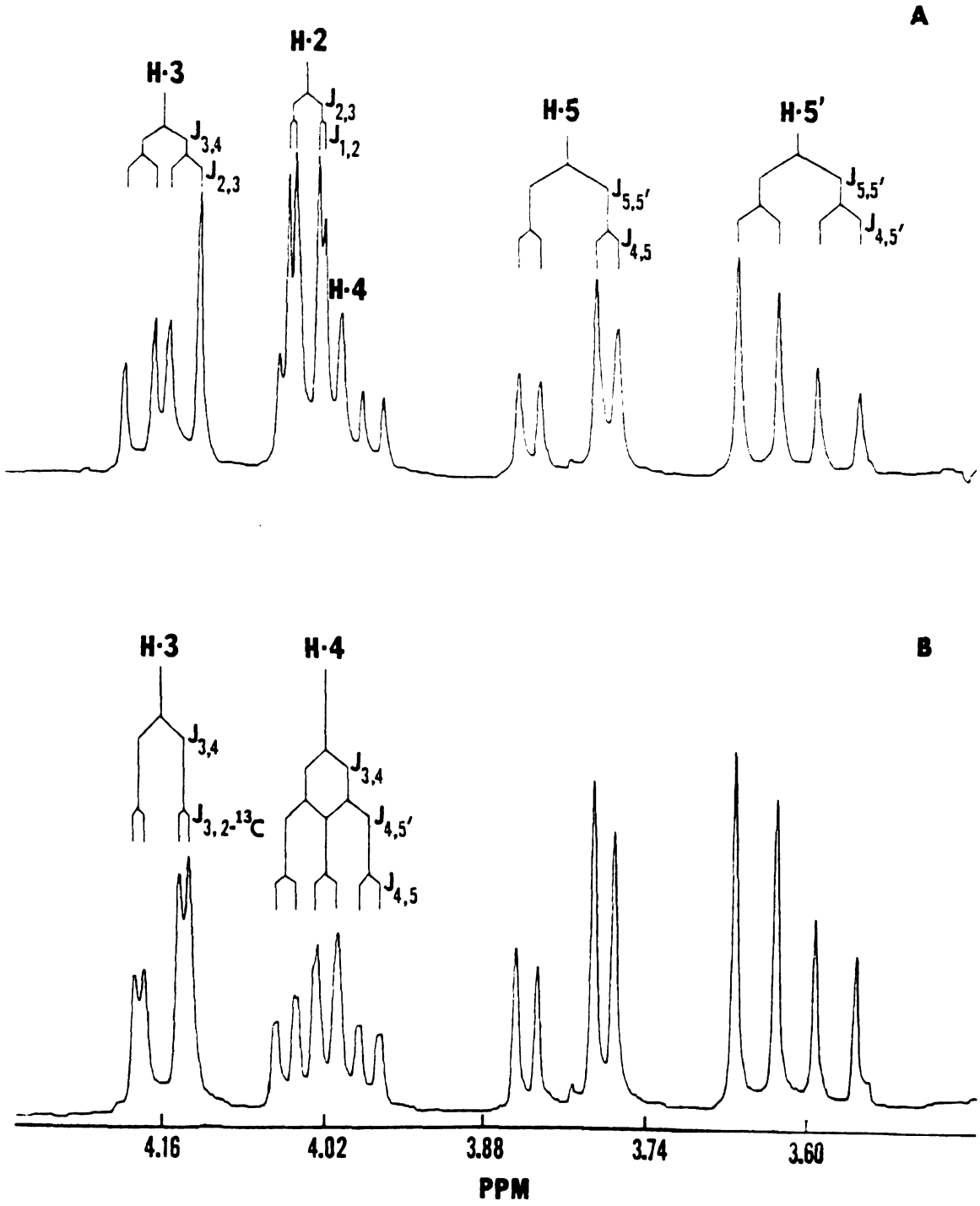
A
H·2
H·3
J2,3
J1,2
J3,4
J2,3
H·5
H·5′
J5,5′
J4,5
J5,5′
J4,5′
H·4
B
H·3
H·4
J3,4
J3,2-13C
J3,4
J4,5′
J4,5
4.16
4.02
3.88
3.74
3.60
PPM

Figure 38.

Table 16. Apparent and intrinsic ^1H chemical shifts for the tetroses and some methyl pentofuranosides in ^2H_2O.

Compound	Chemical Shifts, ppm[a]							
	H1	H2	H3	H4	H4'	H5	H5'	CH_3
α-D-Erythrose	5.27[b]	4.10	4.28	4.03 (4.02)	3.92			
β-D-Erythrose	5.25	4.02	4.39	4.20	3.79			
D-Erythrose, hydrate	5.09	3.54		3.79	3.64			
α-DL-Threose	5.24	4.05	(4.20)	4.20	3.95			
β-DL-Threose	5.40	4.04	(4.30)	4.18	3.65			
DL-Threose hydrate	5.02	3.46		3.67[c]	3.63[c]			
Methyl α-D-Ribofuranoside	4.99	4.11	4.02 (4.03)	4.09		3.74 (3.73)	3.64 (3.66)	3.43
Methyl β-D-Ribofuranoside	4.88	4.02	4.14	3.99 (4.00)		3.79 (3.78)	3.59	3.38
Methyl α-D-Arabinofuranoside	4.91	4.04	3.92 (3.93)	4.02		3.81 (3.80)	3.68 (3.69)	3.40
Methyl β-D-Arabinofuranoside	4.89	4.13	4.00	3.88		3.76	3.60 (3.61)	3.41

[a] Chemical shifts are given relative to internal sodium 3-(trimethylsilyl)-1 propanesulfonate and are accurate to ±0.01 ppm. Spectra of reducing sugars and glycosides were taken at pH 6.5 and 8.0, respectively. Intrinsic chemical shifts determined by computer simulation are given in parentheses when they are significantly different from experimental values. Assignments of H4, H4' and H5, H5' are arbitrary. [b] Assignment aided by 360 MHz ^1H NMR spectrum obtained at the Purdue Biochemical Magnetic Resonance Laboratory, Department of Chemistry, Purdue University. [c] Values accurate to ±0.02 ppm.

Table 17. Apparent and intrinsic geminal and vicinal ^{1}H-^{1}H coupling constants for the tetroses and some methyl pentofuranosides in $^{2}H_2O$.

Compound	Coupling Constant, Hz[a]							
	1,2	2,3	3,4	3,4'	4,4'	4,5	4,5'	5,5'
α-D-Erythrose	4.7 (4.7)	5.0[b] (5.2)	5.0[b] (5.1)	3.1 (3.0)	-10.0 (-10.1)			
β-D-Erythrose	3.4 (3.4)	4.8 (4.8)	5.0 (4.9)	3.4 (3.5)	- 9.7 (- 9.7)			
D-Erythrose, hydrate	4.0	6.6		7.6	-12.1[b]			
α-DL-Threose	1.2 (1.2)	1.8 (1.8)	(5.6)[b]	(2.6)[b]	-10.1 (-10.1)			
β-DL-Threose	4.2 (4.0)	4.1 (4.0)	(5.3)	(3.6)	- 9.6 (- 9.6)			
DL-Threose, hydrate	6.2	2.7						
Methyl α-D-Ribofuranoside	4.2 (4.3)	6.2 (6.2)	3.1 (3.3)			3.4 (3.1)	4.4 (4.8)	-12.3 (-12.4)
Methyl β-D-Ribofuranoside	1.2 (1.2)	4.7 (4.6)	6.8 (6.9)			3.7 (3.1)	6.4 (6.6)	-12.3 (-12.2)
Methyl α-D-Arabinofuranoside	1.7 (1.7)	3.3 (3.3)	5.8 (5.9)			3.4 (3.1)	5.6 (6.1)	-12.2 (-12.2)
Methyl β-D-Arabinofuranoside	4.5 (4.6)	7.9 (8.0)	6.7 (7.1)			3.4 (3.2)	6.7 (7.4)	-12.1 (-12.0)

[a] Coupling constants are accurate to ±0.15 Hz. Values found in parentheses are intrinsic coupling constants (±0.2 Hz) determined by computer simulation. Assignments of H4, H4' and H5, H5' are arbitrary.
[b] Values are accurate to within ±0.3 Hz.

D. Enzymatic Conversions Using [^{13}C]-Enriched Aldoses and Aldose Phosphates

The principal interests in [^{13}C]-enriched compounds lie in their value as useful derivatives to study carbohydrate structure and behavior in solution, as ^{13}C NMR probes to examine enzyme-substrate interactions (199), and as tracers to follow enzymatic conversions by ^{13}C NMR spectroscopy (200). In this regard, we have prepared several [^{13}C]-enriched carbohydrates enzymatically from [^{13}C]-enriched substrates synthesized according to methods described in this report primarily to demonstrate the biological activity of these substrates and to emphasize the versatility of combining chemical and biochemical synthetic routes for the preparation of [^{13}C]-labeled carbohydrates.

1. D-[2-^{13}C]Ribose 5-P to D-[2-^{13}C]ribulose 1,5-P_2

The ^{13}C NMR spectrum of D-[2-^{13}C]ribose 5-P has strong resonances at 71.9 and 76.5 ppm due to C-2 of the α- and β-furanose forms, respectively (Figure 39A). Addition of D-ribose 5-P isomerase causes the appearance of a resonance downfield (213.7 ppm) (Figure 39B) which is characteristic of the free keto form of D-[2-^{13}C]ribulose 5-P. The equilibrium favors the aldose phosphate (72%) at 36°C as previously observed by Axelrod and Jang (201). Addition of D-ribulose-5-P kinase and Mg^{2+}-ATP converts the downfield singlet into a doublet arising from carbon-phosphorus coupling and shifts the equilibrium toward the product, D-[2-^{13}C]ribulose 1,5-P_2. The ^{13}C NMR spectrum of purified D-[2-^{13}C]ribulose 1,5-P_2 (Figure 39C) at pH 7.6 shows doublets centered at 211.7 ppm (88%, $^{3}J_{POCC}$ = 7.3 Hz) and 97.6 ppm (12%, $^{3}J_{POCC}$ = 6.6 Hz), indicating that aqueous solutions of D-ribulose 1,5-P_2 at pH 7.6 contain 88% keto and 12% hydrated forms. This result compares favorably

Figure 39. The enzymatic conversion of D-[2-^{13}C]ribose 5-P to D-[2-^{13}C]ribulose 1,5-P_2 as followed by ^{13}C NMR.

Peaks identified by "X" are unidentified components. Only resonances of the enriched nuclei are shown. (A) The ^{13}C NMR spectrum of D-[2-^{13}C]ribose 5-P at 36°C, showing α- and β-furanose forms. (B) The addition of phosphoriboisomerase to A produces a downfield resonance (k) originating from the keto form of D-[2-^{13}C]ribulose 5-P. (C) The addition of phosphoribulokinase and Mg^{2+}-ATP to B produces D-[2-^{13}C]-ribulose 1,5-P_2, whose ^{13}C NMR spectrum is shown after purification. The doublet at approximately 210 ppm originates from the keto form, whereas the doublet at approximately 95 ppm originates from the keto-hydrate form. Splitting of these resonances is caused by ^{31}P-^{13}C coupling. Spectra were obtained at 36 ± 1°C with a sweep width of 3000 Hz and a filter width of 6000 Hz.

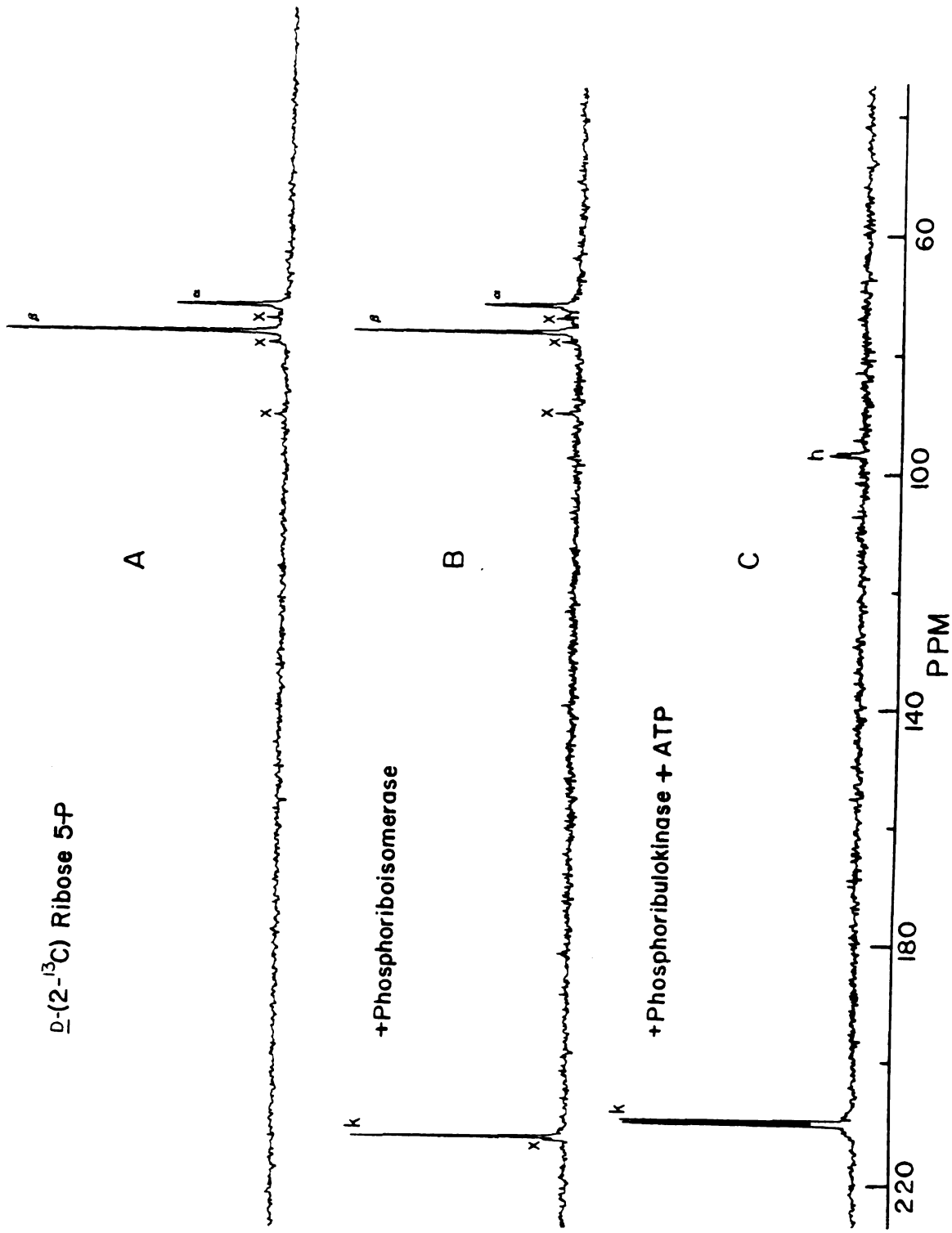
D-(2-13C) Ribose 5-P
A
+Phosphoriboisomerase
B
+Phosphoribulokinase + ATP
C
PPM
220
180
140
100
60

Figure 39.

with a determination made by infrared spectroscopy (202). D-[2-^{13}C]-Ribulose 1,5-P_2 provides a standard for the chemical shift of a keto hydrate and may serve as a useful probe of the active site of D-ribulose-1,5-P_2 carboxylase/oxygenase.

2. DL-[1-^{13}C]Glyceraldehyde 3-P to L-[3,4-^{13}C]sorbose 1,6-P_2

Incubating DL-[1-^{13}C]glyceraldehyde 3-P with triose phosphate isomerase produces a mixture of L-[1-^{13}C]glyceraldehyde 3-P (91.3 ppm) and [3-^{13}C]dihydroxyacetone-P (66.7 and 65.6 ppm) (Figure 40A). The two chemical shifts for [3-^{13}C]dihydroxyacetone-P arise from the keto (65%) and hydrated keto (35%) forms, in agreement with earlier estimations based on ^{1}H NMR spectroscopy by Gray and Barker (202). The addition of D-fructose 1,6-P_2 aldolase to this mixture causes the rapid formation of both L-[3,4^{13}C]sorbose 1,6-P_2 (77.9 and 77.5 ppm) and D-[3,4-^{13}C]fructose 1,6-P_2 (76.7 and 76.2 ppm) (Figure 40B). After incubation for an additional 4 h and removal of protein, four resonances are observed at 77.8, 77.2, 77.0, and 76.5 ppm (Figure 40C) due to the major equilibrium product, L-[3,4-^{13}C]sorbose 1,6-P_2. The chemical shifts for C-3 and C-4 of sorbose 1,6-P_2 are expected to be similar to those of fructose 1,6-P_2 reported by Koerner et al. (181). At 15.08 MHz, the difference in frequency between C-3 and C-4 is smaller (approximately 30 Hz) than the expected ^{13}C-^{13}C coupling constant (40-50 Hz) and a complex spectrum is observed from which the coupling constant cannot be estimated readily (Figure 40C). Using computer simulation, we estimated $^{1}J_{C3,C4}$ to be 47.7 ± 1.0 Hz. It should be noted that this parameter can only be measured in doubly-enriched compounds. In singly-enriched compounds, the resonance due to the enriched carbon will obscure the resonance due to the unenriched adjacent

Figure 40. The enzymatic conversion of DL-[1-^{13}C]glyceraldehyde 3-P to L-[3,4^{13}C]sorbose 1,6-P_2 as followed by ^{13}C NMR.

Peaks designated by "X" are unidentified components. Only the resonances of enriched nuclei are shown. (A) The ^{13}C NMR spectrum of DL-[1-^{13}C]glyceraldehyde 3-P hydrate (a) after the addition of triosephosphate isomerase, producing resonances due to C-3 of the keto (b) and keto-hydrate (c) forms of [3-^{13}C]dihydroxyacetone-P. (B) The addition of D-fructose-1,6-P_2 aldolase to A causes the appearance after 10 min of resonances due to C-3 and C-4 of D-[3,4-^{13}C]fructose 1,6-P_2 (3), with a smaller amount of L-[3,4-^{13}C]sorbose 1,6-P_2 (d). (C) The same reaction mixture as analyzed by ^{13}C NMR after 4 h shows little unreacted [1-^{13}C]glyceraldehyde 3-P and [3-^{13}C]dihydroxyacetone-P and the major product, L-[3,4-^{13}C]sorbose 1,6-P_2. Spectra were obtained at 34 ± 1°C with a sweep width of 3000 Hz and a filter width of 2400 Hz.

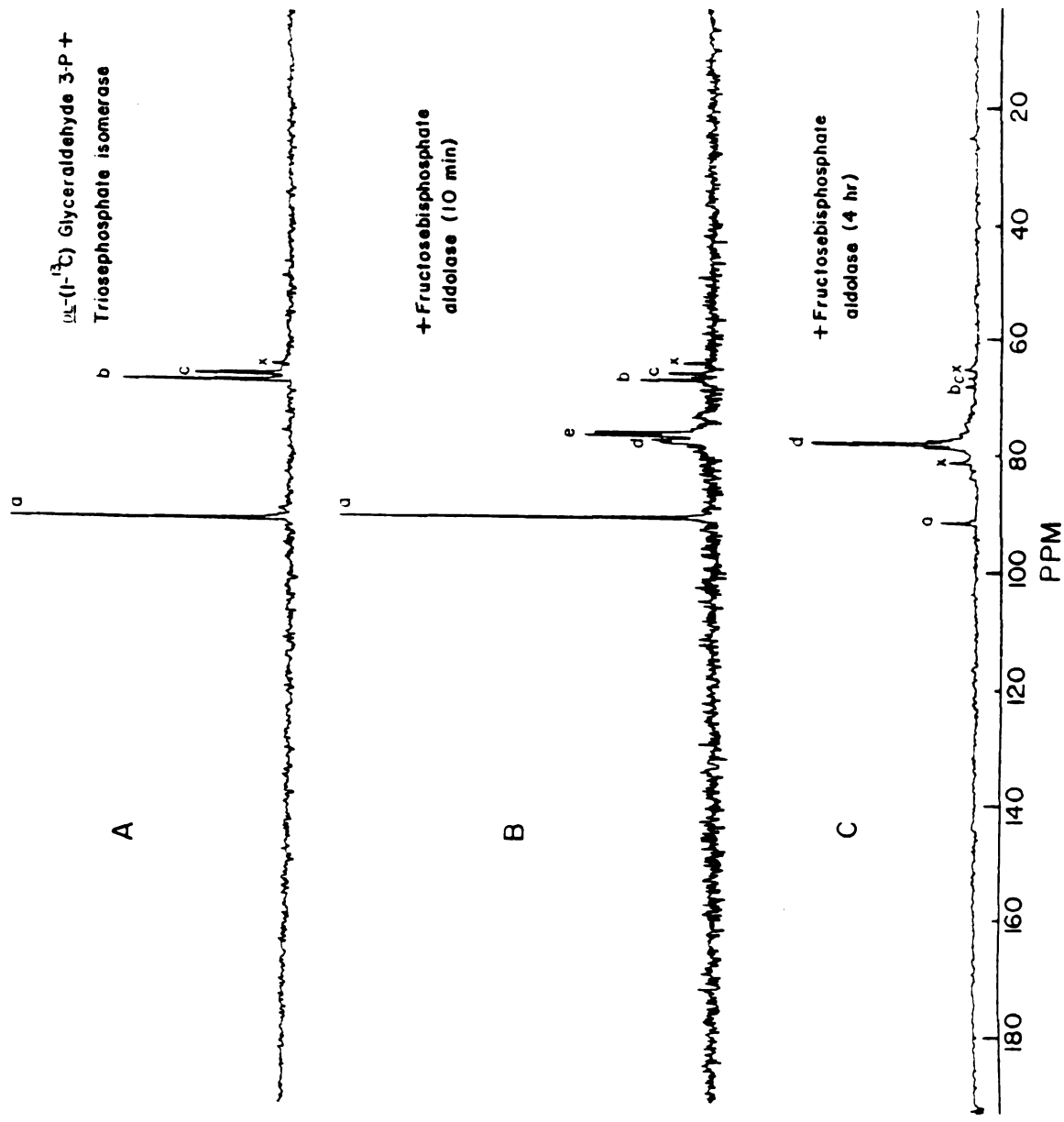
A
B
C
a
b
c
d
e
x
DL-(1-13C) Glyceraldehyde 3-P +
Triosephosphate isomerase
+Fructosebisphosphate
aldolase (10 min)
+Fructosebisphosphate
aldolase (4 hr)
180
160
140
120
100
80
60
40
20
PPM

Figure 40.

carbon. The fundamental resonances of coupled carbons must be at least 100 Hz apart to permit easy estimation of coupling in singly enriched compounds.

3. D-[2-^{13}C]Glucose to D-[2-^{13}C]fructose 1,6-P_2

The ^{13}C NMR spectrum of D-[2-^{13}C]glucose, prepared as shown in Figure 29, has two strong resonances at 73.0 and 75.7 ppm due to C-2 of the α- and β-pyranose forms, respectively (Figure 41A). Addition of hexokinase, myokinase, phosphoglucoisomerase and Mg^{2+}-ATP causes the appearance of two new resonances at 106.0 and 103.1 ppm (Figure 41B) due to C-2 of α- (13%) and β-furanose (87%) forms of D-[2-^{13}C]fructose 6-P, respectively. Resonances at 73.1 and 75.8 ppm are the C-2 resonances of α- and β-D-[2-^{13}C]glucose 6-P, respectively. Addition of phosphofructokinase and Mg^{2+}-ATP converts the 6-phosphates to D-[2-^{13}C]-fructose 1,6-P_2 (Figure 41C). Doublets centered at 105.8 and 102.1 ppm are the C-2 resonances of α- (15%) and β-furanose (85%) forms of FDP, respectively. Splittings of 8.8 and 8.1 Hz for the α- and β-anomers, respectively, are caused by three-bond ^{13}C-^{31}P coupling ($^3J_{C2,P1}$). Addition of aldolase and triosephosphate isomerase causes the formation of D-[2,5-^{13}C]fructose 1,6-P_2 (Figure 41D) which has essentially 45 atom % ^{13}C at C-2 and C-5 based on the summation of the atom percent ^{13}C isotope in four distinct [^{13}C]-enriched species. Doublets centered at 82.9 and 80.8 ppm are the C-5 resonances of the α- and β-furanose forms of FDP. Splittings of 8.8 and 8.1 Hz for the α- and β-anomers, respectively, are caused by three-bond ^{13}C-^{31}P coupling ($^3J_{C5,P6}$).

^{13}C NMR spectra in Figure 41 A and B were obtained at 34°C, whereas spectra in Figure 41 C and D were obtained at 18°C to minimize line-broadening caused by anomerization of the diphosphate (182). It is

Figure 41. The enzymatic conversion of D-[2-^{13}C]glucose to D-[2-^{13}C]-fructose 1,6-P_2 (FDP) as followed by ^{13}C NMR.

^{13}C NMR spectra show only the enriched nuclei. (A) The ^{13}C NMR spectrum of D-[2-^{13}C]glucose, showing α- and β-pyranose forms. (B) Addition of hexokinase, myokinase, phosphoglucoisomerase and Mg^{2+}-ATP to A produces a mixture of D-[2-^{13}C]glucose 6-P (G6P) and D-[2-^{13}C]fructose 6-P (F6P). Resonances between 73-76 ppm and between 106-103 ppm are the α- and β-forms of G6P and F6P, respectively. (C) Addition of phosphofructo-kinase to B produces a set of doublets originating from the α- (105.8 ppm) and β-furanose (102.1 ppm) forms of D-[2-^{13}C]FDP. Splitting of these resonances is caused by ^{13}C-^{31}P coupling. (D) Addition of aldo-lase and triosephosphate isomerase to C produces D-[2,5-^{13}C]FDP. Re-sonances between 80-83 ppm are C-5 of the α- and β-furanose forms, with splitting due to ^{13}C-^{31}P coupling.

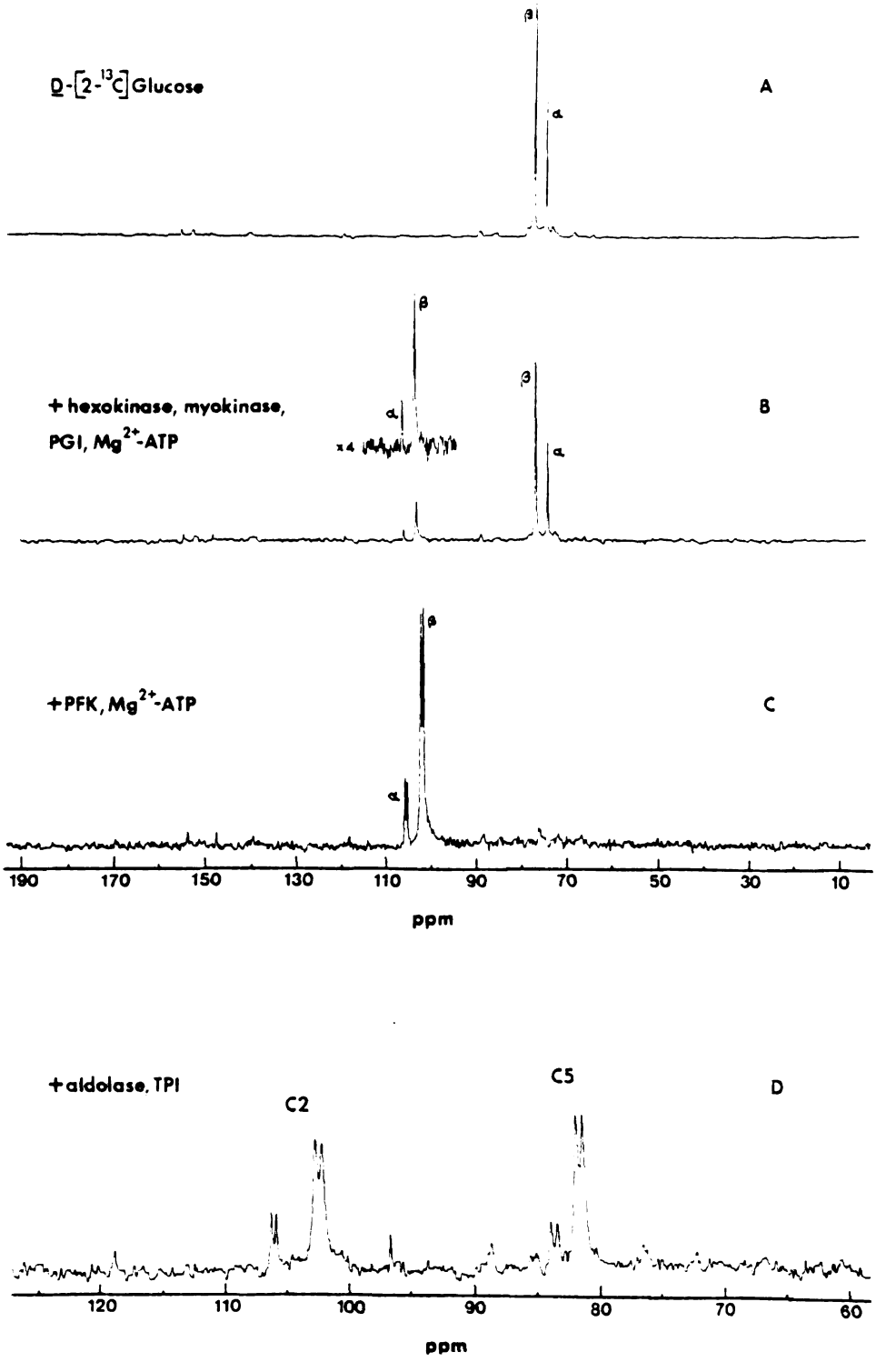
D-[2-13C]Glucose
A
β
α
+ hexokinase, myokinase,
PGI, Mg2+-ATP
B
x4
+PFK, Mg2+-ATP
C
190
170
150
130
110
90
70
50
30
10
ppm
+aldolase, TPI
C2
C5
D
120
110
100
90
80
70
60
ppm

Figure 41.

interesting that line-widths of the anomeric carbons of D-[2-^{13}C]fructose 6-P and the D-[1-^{13}C]pentose 5-phosphates are also temperature-dependent, with high temperatures (40°-50°C) producing line-widths greater than 5 Hz. Rates of anomerization as well as activation energies for ring-opening can be determined from line-width analysis of these [^{13}C]-enriched derivatives since line-widths can be related to rates of chemical exchange (2, 182).

4. Action of glycerol kinase on DL-[2-^{13}C]glyceraldehyde

DL-[2-^{13}C]Glyceraldehyde (Figure 42A) was incubated with glycerol kinase and Mg^{2+}-ATP at pH 7.5 for 2.5 h. The ^{13}C NMR spectrum of the products is shown in Figure 42B. Approximately 45 percent of the glyceraldehyde (δ_{C2} = 75.5 ppm) is converted to the 3-phosphate whose C-2 resonance at 74.9 ppm is split by phosphorus ($^{3}J_{C2,P3}$ = 6.6 Hz). The product 3-phosphate has been shown to have the L-configuration (203, 204). In proof, the unreacted glyceraldehyde was separated from the 3-phosphate by chromatography on DEAE-Sephadex A-25 in the acetate form and incubated with aldolase and 1,3-dihydroxy-2-propanone phosphate. D-[5-^{13}C]Fructose 1-P (91%) and L-[5-^{13}C]sorbose 1-P (9%) were produced, indicating that 91% of the unreacted glyceraldehyde is the D-isomer. Rabbit muscle aldolase acts on DL-[2-^{13}C]glyceraldehyde to produce an equimolar mixture of D-[5-^{13}C]fructose 1-P and L-[5-^{13}C]-sorbose 1-P.

By the use of glycerol kinase and Mg^{2+}-ATP, [^{13}C]-enriched L-glyceraldehyde 3-P can be prepared from [^{13}C]-enriched DL-glyceraldehyde. A convenient preparation of [^{13}C]-enriched D-glyceraldehyde 3-P, however, is not yet available, but the enzyme, triokinase (205), has been reported to convert D-glyceraldehyde to D-glyceraldehyde 3-P in

Figure 42. The ^{13}C NMR spectra of DL-[2-^{13}C]glyceraldehyde (A), 35 mM in water, and the mixture (B) produced by treatment with 1.5 molar equivalents of Mg^{2+}-ATP and glycerol kinase at pH 7.5 for 3 h at 36°C.

Approximately 45% of the starting glyceraldehyde is converted to the L-3 phosphate, and generates a doublet at 74.9 ppm having $^{3}J_{^{13}C,^{31}P}$ = 6.6 Hz. The [2-^{13}C]glyceraldehyde remaining after phosphorylation was found to be 91% D-enantiomer. Peak (C) is an unidentified contaminant. The resonance at 91 ppm is [1-^{13}C]glyceraldehyde remaining from the preparation of DL-[2-^{13}C]glyceraldehyde.

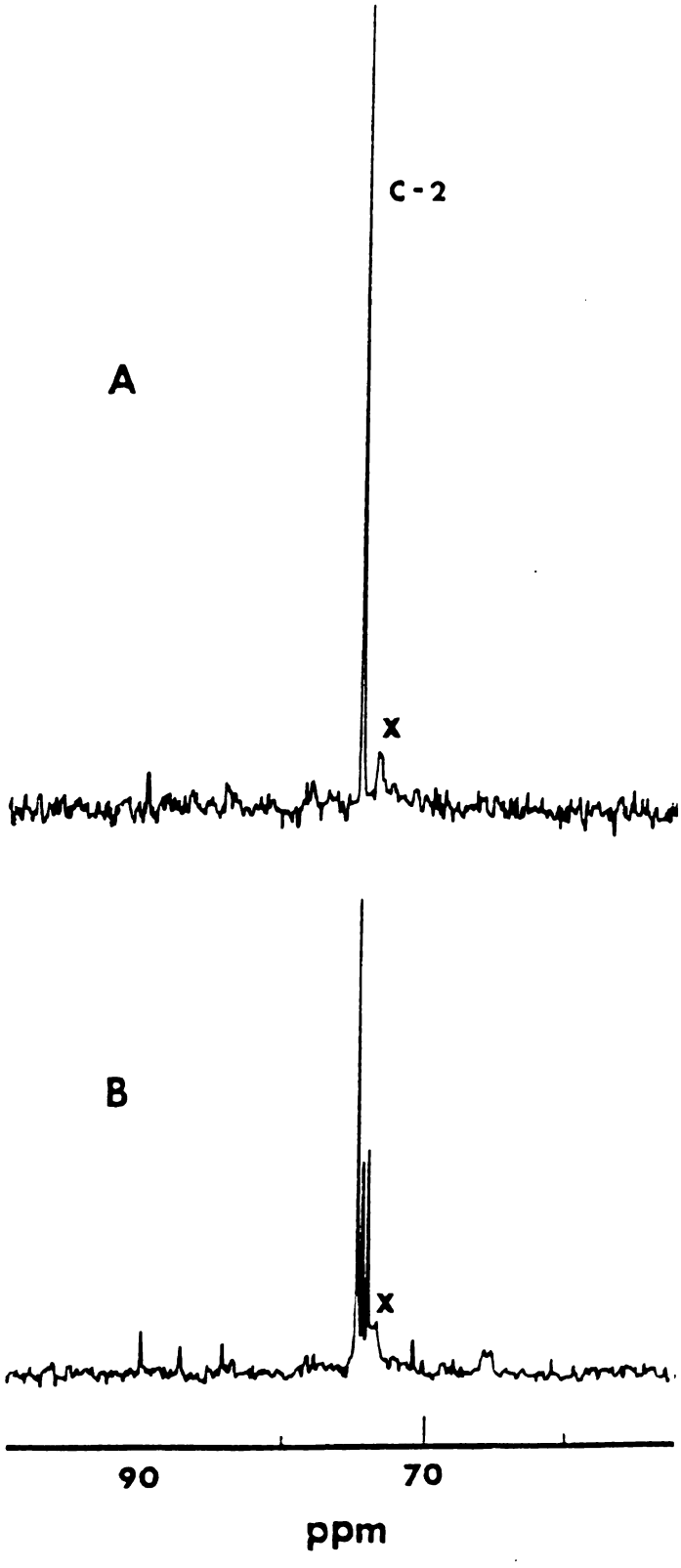

Figure 42.

the presence of Mg^{2+}-ATP.

E. Miscellaneous Applications of [^{13}C]-Enriched Carbohydrates

1. Detection of aldehydo forms in solutions of aldoses

The equilibrium solution of D-glucose contains only 0.0026% aldehydo form, as determined by polarography (206). Aldehydo forms have also been detected by ^{1}H NMR where the aldehydo proton appears as a weak signal at very low fields (207-209). ^{13}C NMR of [1-^{13}C]-enriched aldoses provides another tool for the detection of aldehydo forms in solution.

In this regard, D-[1-^{13}C]erythrose (0.25 M) was dissolved in 80% v/v dioxane-water and analyzed by ^{13}C NMR at 20°C. The spectrum of the anomeric region is shown in Figure 43A. Several forms of D-erythrose are observed: β-furanose (75 ± 3%), α-furanose (25 ± 3%), hydrate (0.7% ± 3%) and dimers and/or oligomers (1.5% ± 3%). A significant decrease in the proportion of hydrated form is observed in 80% dioxane-H_2O in comparison to the proportion found in aqueous solution. In aqueous solution, the hydrate comprises 12 ± 3% of the solution, with the remaining forms contributed by β-(63 ± 3%) and α-furanoses (25 ± 3%) (Figure 31A). Decreasing the concentration of water from 55.5 M to 14 M causes an increase in the proportion of dimers and/or oligomers and a decrease in the amount of hydrate. Changes in the proportions of the tautomeric forms in solution may be important when considering the forms of carbohydrates in the living cell, where the concentration of water is not 55.5 M.

The same solution was examined by ^{1}H-gated-decoupled ^{13}C NMR (Figure 43B). In this spectrum, aldehydo form was observed at 203.7

Figure 43. The ^{13}C NMR spectrum of D-[1-^{13}C]erythrose in 80% dioxane-water.

^{13}C NMR spectra show only the enriched nuclei. (A) ^{1}H-Decoupled ^{13}C NMR spectrum of the anomeric region of D-[1-^{13}C]erythrose in 80% dioxane-water at 20°C and 0.25 M. The α- and β-furanose forms are present with small proportions of hydrate (h) and dimers and/or oligomers (a, b, c, d). (B) ^{1}H-Gated decoupled ^{13}C NMR spectrum of A showing the aldehydo and anomeric regions. C-1 chemical shift of the aldehydo form is found at 203.7 ppm with $^{1}J_{C1,H1}$ = 179.1 ± 0.8 Hz. $^{1}J_{C1,H1}$ (β-furanose) = 170.7 ± 0.8 Hz and $^{1}J_{C1,H1}$ (α-furanose) = 174.0 ± 0.8 Hz.

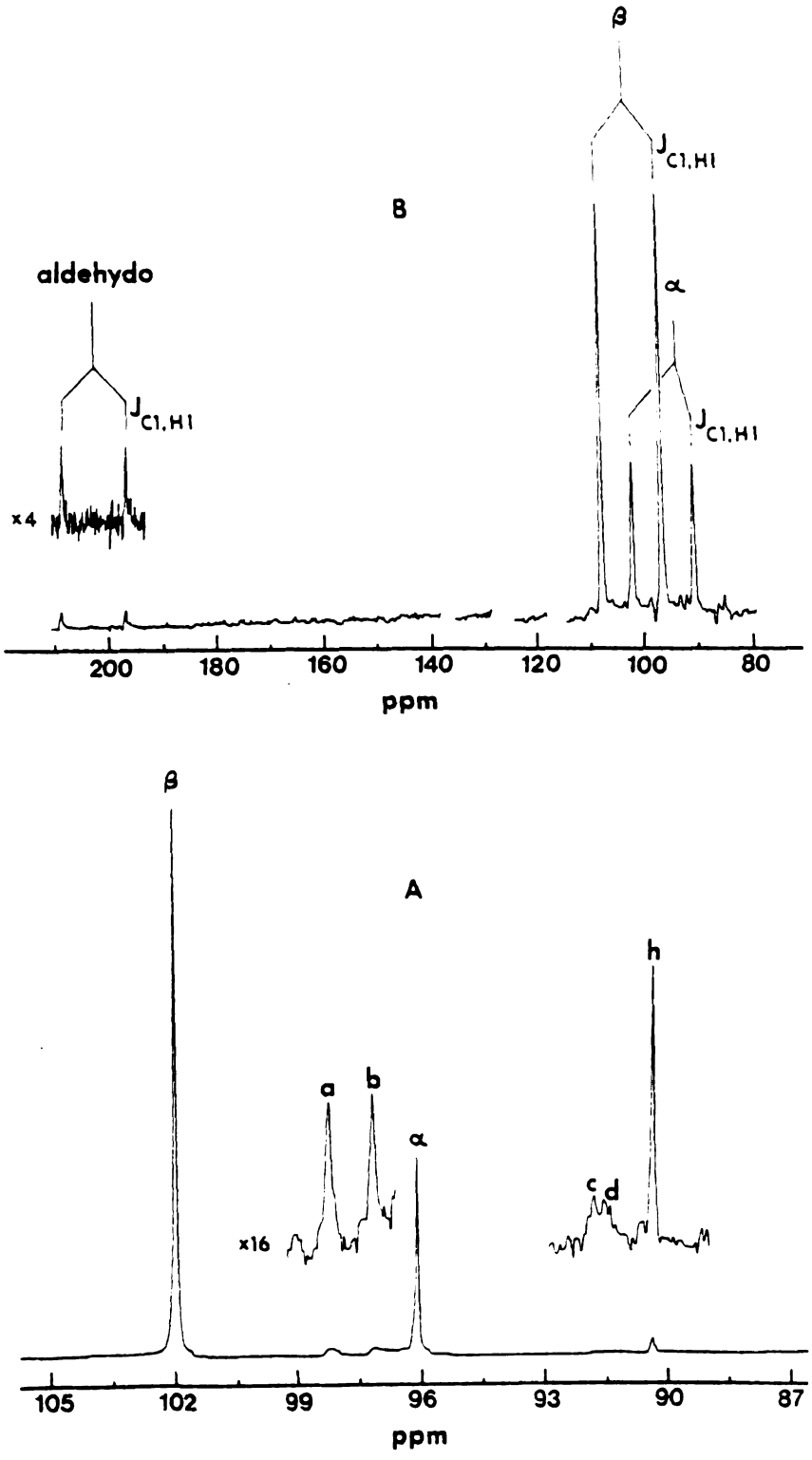
β
$J_{C1,H1}$
B
aldehydo
α
$J_{C1,H1}$
$J_{C1,H1}$
x4
200
180
160
140
120
100
80
ppm
β
A
h
a
b
α
c
d
x16
105
102
99
96
93
90
87
ppm

Figure 43.

ppm with $^{1}J_{C1,H1}$ = 179.1 ± 0.8 Hz. $^{1}J_{C1,H1}$ for the α- and β-furanose forms are 174.0 ± 0.8 Hz and 170.7 ± 0.8 Hz, respectively. $^{1}J_{C1,H1}$ for the aldehydo form is larger than that for the furanose forms, in agreement with predictions based on the s-character of C-1 (178). $^{1}J_{C1,H1}$ for the furanoses in 80% dioxane-H_2O is different from $^{1}J_{C1,H1}$ in water (Table 11) and probably reflects conformational differences caused by solvent effects and/or differences in rates of anomerization.

2. Use of $^{2}J_{C2,H1}$ to determine aldose configuration and conformation

Bock and Pedersen (124) have recently related $^{2}J_{C1,H2}$ and $^{2}J_{C2,H1}$ in several carbohydrate derivatives to the orientation of oxygen atoms along the coupling pathway through a projection-sum. We have examined $^{2}J_{C2,H1}$ for several furanoses, furanosides and pyranoses (Table 18) and have found that the predicted couplings, based on projection-sums, and observed couplings are in good agreement. Furanose rings in which OH-1 and OH-2 are <u>trans</u> show small $^{2}J_{C2,H1}$ couplings (0 Hz - 1 Hz). Calculation of the projection-sums from models for all conformational forms that affect the relative orientation of substituents on C-1 and C-2 (E_2, E_o, $^{3}T_2$, E^2, E^o, $^{2}T_3$) for <u>trans</u>-1,2 furanose rings predicts a range of values for $^{2}J_{C2,H1}$ of approximately 0 Hz - 2 Hz. A similar calculation for <u>cis</u>-1,2 furanose rings predicts a range of values for $^{2}J_{C2,H1}$ of approximately 2 Hz to 5 Hz. As shown in Table 18, the experimental results are in close agreement. These results suggest that $^{2}J_{C2,H1}$ may be a more sensitive probe than $^{1}J_{C1,H1}$ (Figure 35) in the determination of relative configuration about the C-1—C-2 bond in furanose rings.

$^{2}J_{C2,H1}$ for α-D- and β-D-arabinopyranoses and α-D- and β-D-ribopyranoses were also determined (Table 18). Projection-sums for

Table 18. $^{2}J_{C2,H1}$ Values for several carbohydrates and their derivatives.

Compound	$^{2}J_{C2,H1}$ (Hz)[a]			
	Furanoses		Hydrates	Pyranoses
	cis 1,2	trans 1,2		
α-D-Erythrose	3.1			
β-D-Threose	4.0			
α-D-Ribofuranose	3.0			
β-D-Arabinofuranose	2.5			
Methyl α-D-Ribofuranoside	2.3			
3-O-Acetyl-1,2:5,6-di-O-isopropylidene-α-D-allofuranose	5.1[b]			
3-O-Acetyl-1,2:5,6-di-O-isopropylidene-α-D-glucofuranose	5.5[b]			
β-D-Erythrose		0		
α-D-Threose		<1		
β-D-Ribofuranose		br		
Methyl β-D-Ribofuranoside		br		
D-Erythrose, hydrate			2.0	
D-Threose, hydrate			0	
β-D-Ribopyranose				br
α-D-Arabinopyranose				br
α-D-Ribopyranose				4.1
β-D-Arabinopyranose				br

[a] Coupling constants were determined by analysis of the H-1 region of the ^{1}H NMR spectra obtained at 180.04 MHz, and are accurate to within ±0.2 Hz. [b] These values were taken from reference 124.

β-D-ribopyranose predict a small $^{2}J_{C2,H1}$ (∿0.5 Hz) for both $^{1}C_{4}$ and $^{4}C_{1}$ conformations. For α-D-ribopyranose, projection sums predict a small value for $^{2}J_{C2,H1}$ (∿0.5 Hz) for the $^{4}C_{1}$ conformation and a large value (∿7 Hz) for the $^{1}C_{4}$ conformation. As shown in Table 18, $^{2}J_{C2,H1}$ for α-D- and β-D-ribopyranose are 4.1 Hz and <0.5 Hz, respectively, in agreement with previous determinations of conformation (94).

For α-D-arabinopyranose, which exists predominately in the $^{1}C_{4}$ conformation (77), the predicted (∿0.5 Hz) and measured (<0.5 Hz) values for coupling between C-2 and H-1 are in close agreement. Lemieux and Stevens (77) were unable to establish the conformation of β-D-arabinopyranose by ^{1}H NMR at 100 MHz, although Rudrum and Shaw (210) have assigned the $^{1}C_{4}$ conformation to this compound. Recent ^{1}H NMR measurements at 300 MHz on L-arabinopyranose (106) have shown that $^{3}J_{H2,H3}$ are 9.8 Hz and 9.6 Hz for α-L- and β-L-arabinopyranose, respectively, suggesting that H-2 and H-3 are axial-axial in both anomers. The $^{4}C_{1}$ conformation for both L-anomers is consistent with this data. The predicted values of $^{2}J_{C2,H1}$ for β-D-arabinopyranose are ∿0.5 Hz and ∿7 Hz for the $^{1}C_{4}$ and $^{4}C_{1}$ conformations, respectively. The observed coupling, <0.5 Hz, is consistent with a preferred $^{1}C_{4}$ conformation for the D-series (Table 18).

LIST OF REFERENCES

LIST OF REFERENCES

1. Jenkins, F.A. and Ornstein, L.S. *Proc. Acad. Sci. Amsterdam 35* (1932):1212.

2. Mann, B.E. *Progress in NMR Spectroscopy 11* (1977):95.

3. Stothers, J.B. In *Topics in Carbon-13 NMR Spectroscopy* (Levy, G.C., ed.), Vol. I (1974), pp. 230-286, John Wiley & Sons, New York.

4. Rappoport, Zvi, ed. *The Chemistry of the Cyano Group.* Interscience Publishers, New York, N.Y., 1970.

5. Nagata, W. and Yoshioka, M. *Org. Reactions 25* (1977):255.

6. Boullanger, P., Marmet, D.& Descotes, G. *Tetrahedron 35* (1979): 163.

7. Prelog, V. and Wilhelm, M. *Helv. Chim. Acta 37* (1954):1634.

8. Evans, D.A., Carroll, G.L. and Truesdale, L.K. *J. Org. Chem. 39* (1974):914.

9. Corey, E.J., Crouse, D.N. and Anderson, J.E. *J. Org. Chem. 40* (1975):2140.

10. Strecker, A. *Ann. Chem. 75* (1850):27.

11. Lotfield, R.B. and Eigner, E.A. *Biochem. Biophys. Acta 130* (1966): 449.

12. Harada, K. and Okawara, T. *J. Org. Chem. 38* (1973):707.

13. Bayly, R.J. and Turner, J.C. *J. Chem. Soc. C* (1966):704.

14. Lapworth, A. *J. Chem. Soc. 83* (1903):995.

15. Lapworth, A. *J. Chem. Soc. 85* (1904):1206.

16. Franzen, V. and Fikentscher, L. *Ann. 613* (1958):1.

17. Breslow, R. *J. Amer. Chem. Soc. 79* (1957):1762.

18. Breslow, R. *J. Amer. Chem. Soc. 80* (1958):3719.

19. Holzer, H. and Beaucamp, K. *Angew. Chem. 71* (1959):776.

20. Haisman, D.R. and Knight, D.J. *Biochem. J. 103* (1967):528.

21. Bove, C. and Conn, E.E. *J. Biol. Chem. 236* (1961):207.

22. Ferris, J.P. In *The Chemistry of the Cyano Group* (Rappoport, Zvi, ed.). Interscience Publishers, New York, N.Y., pp. 717-742, 1970.

23. Calvin, M. *Chemical Evolution*. Oxford University Press, New York, 1969.

24. Simpson, M. and Gautier, A. *Compt. rend. 65* (1867):414.

25. Staedeler, G. *Ann. 111* (1859):320.

26. Kiliani, H. *Ber. 18* (1885):3066.

27. Kiliani, H. *Ber. 19* (1886):221.

28. Kiliani, H. *Ber. 19* (1886):772.

29. Kiliani, H. *Ber. 19* (1886):767.

30. Kiliani, H. *Ber. 19* (1886):1128.

31. Kiliani, H. *Ber. 19* (1886):3029.

32. Kiliani, H. *Ber. 20* (1887):282.

33. Kiliani, H. *Ber. 20* (1887):339.

34. Kiliani, H. *Ber. 21* (1888):915.

35. Kiliani, H. *Ber. 22* (1889):521.

36. Rupp, E. and Holzle, A. *Arch. Pharm. 253* (1915):404.

37. Hudson, C.S., Hartley, O. and Purves, C.B. *J. Amer. Chem. Soc. 56* (1934):1248.

38. Militzer, W.E. *Arch. Biochem. 9* (1946):91.

39. Robert, L., Mednieks, M. and Winzler, R.J. *Biochim. Biophys. Acta 63* (1962):327.

40. Militzer, W. *Arch. Biochem. 21* (1949):143.

41. Isbell, H.S., Karabinos, J.V., Frush, H.L., Holt, N.B., Schwebel, A. and Galkowski, T.T. *J. Res. Nat. Bur. Stds. 48* (1952):163.

42. Frush, H.L. and Isbell, H.S. *J. Res. Nat. Bur. Stds. 51* (1953): 307.

43. Isbell, H.S., Frush, H.L. and Holt, N.B. *J. Res. Nat. Bur. Stds. 53* (1954):325.

44. Isbell, H.S., Frush, H.L. and Holt, N.B. *J. Res. Nat. Bur. Stds. 53* (1954):217.

45. Schaffer, R. and Isbell, H.S. *J. Res. Nat. Bur. Stds. 56* (1956): 191.

46. Varma, R. and French, D. *Carbohydr. Res. 25* (1972):71.

47. Wohl, A. *Ber. 24* (1891):994.

48. Ruff, O. *Ber. 31* (1898):1573.

49. Fischer, E. *Ber. 22* (1889):2204.

50. Hudson, C.S. *Adv. Carb. Chem. 1* (1945):1.

51. Pictet, A. and Barbier, A. *Helv. Chim. Acta 4* (1921):924.

52. Sowden, J.C. *Adv. Carb. Chem. 6* (1951):291.

53. Wolfrom, M.L. and Wood, H.B. *J. Am. Chem. Soc. 73* (1951):730.

54. Pichat, L. In *The Chemistry of the Cyano Group* (Rappoport, Zvi, ed.). Interscience Publishers, New York, N.Y., pp. 743-790, 1970.

55. Philippe, L.H. *Ann. Chim. Phys. 26* (1912):289.

56. Bhattacharjee, S.S., Schwarcz, J.A. and Perlin, A.S. *Carbohydr. Res. 42* (1975):259.

57. Kohn, P., Samaritano, R. and Lerner, L. *J. Amer. Chem. Soc. 87* (1965):5475.

58. Guidici, T. and Fluharty, A.L. *J. Org. Chem. 32* (1967):2043.

59. Walker, T.E., London, R.E., Whaley, T.W., Barker, R. and Matwiyoff, N.A. *J. Amer. Chem. Soc. 98* (1976):5807.

60. Fischer, E. and Leuchs, H. *Ber. 36* (1903):24.

61. Kuhn, R. and Kirschenlohr, W. *Angew.Chem. 67* (1955):786.

62. Kuhn, R. and Kirschenlohr, W. *Ann. 600* (1956):115.

63. Kuhn, R. and Bister, W. *Ann. 602* (1957):217.

64. Kuhn, R. and Fischer, H. *Ann. 641* (1961):152.

65. Kuhn, R. and Klesse, P. *Chem. Ber. 91* (1958):1989.

66. Harvey, W.E., Michalski, J.J. and Todd, A.R. *J. Chem. Soc.* (1951):2271.

67. Lampson, G.P. and Lardy, H.A. *J. Biol. Chem. 181* (1949):693.

68. Moffat, J.G. and Khorana, H.G. *J. Amer. Chem. Soc. 79* (1957): 1194.

69. Stverteczky, J., Szabo, P. and Szabo, L. *J. Chem. Soc. Perkin Trans. 1* (1973):872.

70. Michelson, A.M. and Todd, A.R. *J. Chem. Soc.* (1949):2476.

71. Anderson, J.M. and Percival, E. *J. Chem. Soc.* (1956):814.

72. Maehr, H. and Smallheer, J. *Carbohydr. Res. 62* (1978):178.

73. Ballou, C.E. and Fischer, H.O.L. *J. Amer. Chem. Soc. 77* (1955): 3329.

74. Ballou, C.E., Fischer, H.O.L. and MacDonald, D.L. *J. Amer. Chem. Soc. 77* (1955):5967.

75. Klybas, V., Schramm, M. and Racker, E. *Arch. Biochem. Biophys. 80* (1959):229.

76. Leloir, L.F. and Cardini, C.E. In *Comprehensive Biochemistry* (Florkin, M. and Stotz, E.H., eds.), Vol. V (1963), pp. 113-145.

77. Lemieux, R.U. and Stevens, J.D. *Can. J. Chem. 44* (1966):249.

78. Gray, G.R. and Barker, R. *Carbohydr. Res. 20* (1971):31.

79. Gorin, P.A.J. *Can. J. Chem. 52* (1974):458.

80. Topper, Y.J. and Stetten, D. *J. Biol. Chem. 189* (1951):191.

81. Rutter, W.J. and Lung, K.H. *Biochim. Biophys. Acta 30* (1958):71.

82. Rose, I.A. and O'Connell, E.L. *J. Biol. Chem. 236* (1961):3086.

83. Rose, I.A. and O'Connell, E.L. *Biochim. Biophys. Acta 42* (1960): 159.

84. McDonough, M.W. and Wood, W.A. *J. Biol. Chem. 236* (1961):1220.

85. Barnett, J.E.G. and Corina, D.L. In *Advances in Carbohydrate Chemistry and Biochemistry* (Stuart, R.S. and Horton, D., eds.), Vol. XXVII (1972), pp. 127-190.

86. Koch, H.J. and Stuart, R.S. *Carbohydr. Res. 59* (1977):C1-C6.

87. Balza, F., Cyr, N., Hamer, G.K., Perlin, A.S., Koch, H.J. and Stuart, R.S. *Carbohydr. Res. 59* (1977):C7-C11.

88. Jones, J.K.N. and Wall, R.A. *Can. J. Chem. 38* (1960):2290.

89. Samuelson, O. *Methods Carbohydr. Chem. 6* (1972):65.

90. Gorin, P.A.J. and Mazurek, M. *Carbohydr. Res. 67* (1978):479.

91. Clark, E. and Barker, R., unpublished results.

92. Karplus, M. *J. Chem. Phys. 30* (1959):11.

93. Karplus, M. *J. Amer. Chem. Soc. 85* (1963):2870.

94. Bundle, D.R. and Lemieux, R.U. *Methods Carbohydr. Chem. 7* (1976): 79.

95. Coxon, B. *Methods Carbohydr. Chem. 6* (1972):513.

96. Hough, L. and Richardson, A.C. *Rodd's Chemistry of Carbon Compounds.* 2nd ed., Vol. I (1967):67.

97. Booth, H. *Prog. NMR Spectros. 5* (1969):149.

98. Bentley, R. *Ann. Rev. Biochem. 41* (1972):953.

99. Angyal, S.J. *Angew. Chem. 8* (1969):157.

100. Davies, D.B. *Prog. NMR Spectros. 12* (1978):135.

101. Hall, L.D. *Chem. and Ind.* (1963):950.

102. Stevens, J.D. and Fletcher, H.G. *J. Org. Chem. 33* (1968):1799.

103. Alfoldi, A., Peciar, C., Palovcik, R. and Kovac, P. *Carbohydr. Res. 25* (1972):249.

104. Angyal, S.J. and Pickles, V.A. *Aust. J. Chem. 25* (1972):1695.

105. Angyal, S.J. and Pickles, V.A. *Aust. J. Chem. 25* (1972):1711.

106. DeBruyn, A. and Anteunis, M. *Bull. Soc. Chim. Belg. 84* (1975): 831.

107. Horton, D. and Wander, J.D. *Carbohydr. Res. 15* (1970):271.

108. Paul, E.G. and Grant, D.M. *J. Amer. Chem. Soc. 86* (1964):2977.

109. Que, L. and Gray, G.R. *Biochem. 13* (1974):146.

110. Angyal, S.J., Bethell, G.S., Cowley, D.E. and Pickles, V.A. *Aust. J. Chem. 29* (1976):1239.

111. Angyal, S.J. and Bethell, G.S. *Aust. J. Chem. 29* (1976):1249.

112. Dorman, D.E. and Roberts, J.D. *J. Amer. Chem. Soc. 92* (1970): 1355.

113. Perlin, A.S., Casu, B. and Koch, H.J. *Can. J. Chem. 48* (1970): 2596.

114. Ritchie, R.G.S., Cyr, N., Korsch, B., Koch, H.J. and Perlin, A.S. *Can. J. Chem. 53* (1975):1424.

115. Bock, K., Lundt, I. and Pedersen, C. *Tetrahedron Letters 13* (1973):1037.

116. Bock, K. and Pedersen, C. *J. Chem. Soc. Perkin Trans. 2* (1974): 293.

117. Bock, K. and Pedersen, C. *Acta Chem. Scand., Ser. B 29* (1975): 258.

118. Gorin, P.A.J. and Mazurek, M. *Can. J. Chem. 53* (1975):1212.

119. Gorin, P.A.J. and Mazurek, M. *Carbohydr. Res. 48* (1976):171.

120. Schwarcz, J.A. and Perlin, A.S. *Can. J. Chem. 50* (1972):3667.

121. Schwarcz, J.A., Cyr, N. and Perlin, A.S. *Can. J. Chem. 53* (1975):1872.

122. Cyr, N., Hamer, G.K. and Perlin, A.S. *Can. J. Chem. 56* (1978): 297.

123. Walker, T.E., London, R.E., Barker, R. and Matwiyoff, N.A. *Carbohydr. Res. 60* (1978):9.

124. Bock, K. and Pedersen, C. *Acta Chem. Scand., Ser. B 31* (1977): 354.

125. Marshall, J.L. and Müller, D.E. *J. Amer. Chem. Soc. 95* (1973): 8305.

126. Barfield, M., Burfitt, I. and Doddrell, D. *J. Amer. Chem. Soc. 97* (1975):2631.

127. Pearson, H., Gust, G., Armatage, I.M., Huber, H., Roberts, J.D., Stark, R.E., Vold, R.R. and Vold, R.L. *Proc. Nat. Acad. Sci. 72* (1975):1599.

128. Leloir, L.F. and Cardini, C.E. *Methods Enzymol. 3* (1957):840.

129. Lumry, R., Smith, E.L. and Grant, R.R. *J. Amer. Chem. Soc. 73* (1951):4330.

130. Liebig, J. *Ann. 77* (1851):102.

131. Deniges, G. *Compt. rend. 117* (1893):1078.

132. Clark, J., Jr. and Switzer, R.L. *Experimental Biochemistry.* W.H. Freeman and Company, San Francisco, 2nd ed., (1977):166.

133. Park, J.T. and Johnson, M.J. *J. Biol. Chem. 181* (1949):149.

134. Walker, J.F. *Formaldehyde.* Reinhold, New York, 3rd ed., (1964): 486.

135. Frisell, W.R. and MacKensie, C.G. *Methods Biochem. Anal. 6,* Interscience Publishers, Inc., New York, (1958):63.

136. Lewis, K.F. and Weinhouse, S. *Methods Enzymol. 3* (1957):269.

137. Hodge, J.E. and Hofreiter, B.T. *Methods Carbohydr. Chem. 1* (1962):380.

138. Vogel, A.I. *Elementary Practical Organic Chemistry.* John Wiley and Sons, Inc., New York, (1958):758.

139. Perlin, A.S. *Methods Carbohydr. Chem. 1* (1962):61.

140. Zagalak, B., Frey, P.A., Karabatsos, G.L. and Abeles, R.H. *J. Biol. Chem. 241* (1966):3028.

141. Perlin, A.S. *Methods Carbohydr. Chem. 1* (1962):64.

142. Ball, D.H. *J. Org. Chem. 31* (1966):220.

143. Schaffer, R. and Isbell, H.S. *Methods Carbohydr. Chem. 2* (1963): 11.

144. Hudson, C.S. and Komatsu, S. *J. Amer. Chem. Soc. 41* (1919):1141.

145. Conchie, J., Hay, A.J., Strachan, I. and Levvy, G.A. *Biochem. J. 102* (1967):929.

146. Ballou, C.E. and MacDonald, D.L. *Methods Carbohydr. Chem. 2* (1963):289.

147. Ballou, C.E. *Methods Carbohydr. Chem. 2* (1963):282.

148. McCloskey, C.M. and Coleman, G.H. *Org. Synth. 34* (1955):434.

149. Ballou, C.E. *Methods Enzymol. 6* (1963):479.

150. Gaudry, R. *Org. Synth. 34* (1955):436.

151. Duuren, Van. *J. Natl. Cancer Inst. 48* (1972):1431.

152. Horecker, B.L., Hurwitz, J. and Weissbach, A. *J. Biol. Chem. 213* (1956):785.

153. Byrne, W.L. and Lardy, H.A. *Biochim. Biophys. Acta 14* (1954): 495.

154. Barker, R. and Fletcher, H.G., Jr. *J. Org. Chem. 26* (1961): 4605.

155. Austin, P.W., Hardy, F.E., Buchanan, J.G. and Baddiley, J. *J. Chem. Soc.* (1963):5350.

156. Augestad, I. and Berner, E. *Acta Chem. Scand. 8* (1954):251.

157. Maltby, J.G. *J. Chem. Soc.* (1929):2769.

158. Rosenfeld, D.A., Richtmyer, N.K. and Hudson, C.S. *J. Amer. Chem. Soc. 73* (1951):4907.

159. Stanek, J., Cerný, M., Kocourek, J. and Pacak, J. *The Monosaccharides.* Academic Press, Inc., New York, N.Y., (1963): 171.

160. Berl, W.G. and Feazel, C.E. *J. Amer. Chem. Soc. 73* (1951): 2054.

161. Gutsche, C.D., Redmore, D., Buriks, R.S., Nowotny, K., Grassner, H. and Armbruster, C.W. *J. Amer. Chem. Soc. 89* (1967):1235.

162. Schmir, G.L. and Cunningham, B.A. *J. Amer. Chem. Soc. 87* (1965): 5692.

163. Cunningham, B.A. and Schmir, G.L. *J. Amer. Chem. Soc. 88* (1966): 551.

164. Hand, E.S. and Jencks, W.P. *J. Amer. Chem. Soc. 84* (1962):3505.

165. Kuhn, R. and Weiser, D. *Angew. Chem. 69* (1957):371.

166. Brown, H.C., Brewster, J.H. and Shechter, H. *J. Amer. Chem. Soc. 76* (1954):467.

167. Wolfrom, M.L., Bennett, R.B. and Crum, J.D. *J. Amer. Chem. Soc. 80* (1958):944.

168. Bruice, T.C. and Marquardt, F. *J. Amer. Chem. Soc. 84* (1962): 365.

169. Cunningham, B.A. and Schmir, G.L. *J. Amer. Chem. Soc. 89* (1967): 917.

170. Hudson, B.G. and Barker, R. *J. Org. Chem. 32* (1967):3650.

171. Kuhn, R. and Grassner, H. *Ann. 612* (1958):55.

172. Bieber, R. and Trumpler, G. *Helv. Chim. Acta 30* (1947):1860.

173. Collins, G. and George, W.O. *J. Chem. Soc. B* (1971):1352.

174. Bell, R.P. and McDougal, A.O. *Trans. Faraday Soc. 56* (1960): 1281.

175. Grindley, T.B., Gulasekharam, V. and Tulshian, D.B. Abstr. Pap., 2nd Joint Conf., Chem. Inst. Canada, Am. Chem. Soc., Division of Carbohydrate Chemistry, (1977), No. 12.

176. Beck, W.S. *Methods Enzymol. 3* (1957):205.

177. Pople, J.A. *Proc. R. Soc. London, Ser. A, 239* (1957):541.

178. Frei, K. and Bernstein, H.J. *J. Chem. Phys. 38* (1963):1216.

179. Swenson, C.A. and Barker, R. *Biochem. 10* (1971):3151.

180. Gray, G.R. *Biochem. 10* (1971):4705.

181. Koerner, T.A.W., Cary, L.W., Bhacca, N.S. and Younathan, E.S. *Biochem. Biophys. Res. Commun. 51* (1973):543.

182. Midelfort, C.F., Gupta, R.K. and Rose, I.A. *Biochem. 15* (1976): 2178.

183. Blackmore, P.F., Williams, J.F. and MacLeod, J.K. *FEBS Letters 64* (1976):222.

184. Lapper, R.D. and Smith, I.C.P. *J. Amer. Chem. Soc. 95* (1973): 2880.

185. Lapper, R.D., Mantsch, H.H. and Smith, I.C.P. *J. Amer. Chem. Soc. 95* (1973):2878.

186. Alderfer, J.L. and Ts'o, P.O.P. *Biochem. 16* (1977):2410.

187. O'Connor, J.V., Nunez, H.A. and Barker, R. *Biochem. 13* (1979): 500.

188. Bishop, C.T. and Cooper, F.P. *Can. J. Chem. 41* (1963):2743.

189. Stothers, J.B. In *Topics in Carbon-13 NMR Spectroscopy* (Levy, G.C., ed.), Vol. I (1974), p. 229, John Wiley & Sons, New York.

190. Colli, H.N., Gold, V. and Pearson, J.E. *J. Chem. Soc. Chem. Commun. 408* (1973).

191. Bernstein, H.J. and Sheppard, N. *J. Chem. Phys. 37* (1962):3012.

192. Mantsch, H.H., Saito, H. and Smith, I.C.P. *Prog. NMR Spectros. 11* (1977):211.

193. Abraham, R.J. *Analysis of High Resolution NMR Spectra.* Elsevier, London, (1971), 268.

194. Perlin, A.S. and Casu, B. *Tetrahedron Letters* (1969):2921.

195. Lemieux, R.U., Nagabhushan, T.L. and Paul, B. *Can. J. Chem. 50* (1972):773.

196. Lemieux, R.U. *Ann. N.Y. Acad. Sci. 222* (1973):915.

197. Perlin, A.S., Cyr, N., Ritchie, R.G.S. and Parfondy, A. *Carbohydr. Res. 37* (1974):C1.

198. Ritchie, R.G.S., Cyr, N. and Perlin, A.S. *Can. J. Chem. 54* (1976):2301.

199. Mildvan, A.S. and Cohn, M. *Adv. Enzymol. 33* (1970):1.

200. Ugurbil, K., Brown, T.R., Den Hollander, J.A., Glynn, P. and Shulman, R.G. *Proc. Nat. Acad. Sci. 75* (1978):3742.

201. Axelrod, B. and Jang, R. *J. Biol. Chem. 209* (1954):847.

202. Gray, G.R. and Barker, R. *Biochem. 9* (1970):2454.

203. Hayashi, S. and Lin, E.C.C. *J. Biol. Chem. 242* (1967):1030.

204. Janson, C.A. and Cleland, W.W. *J. Biol. Chem. 249* (1974):2562.

205. Hers, H.G. *Methods Enzymol. 5* (1962):362.

206. Los, J.M., Simpson, L.B. and Wiesner, K. *J. Amer. Chem. Soc. 78* (1956):1564.

207. Anet, E.F.L.J. *Carbohydr. Res. 3* (1966):251.

208. Anet, E.F.L.J. *Carbohydr. Res. 8* (1968):164.

209. Perlin, A.S. *Can. J. Chem. 44* (1966):1757.

210. Rudrum, M. and Shaw, D.F. *J. Chem. Soc.* (1965):52.

APPENDIX

APPENDIX

List of Publications, Abstracts and Acknowledgements

A. Publications

1. A.S. Serianni, H.A. Nunez and R. Barker, Carbon-13 Enriched Carbohydrates. Preparation of Aldononitriles and Their Reduction with a Palladium Catalyst, *Carbohydr. Res. 72* (1979):71.

2. A.S. Serianni, E. Clark and R. Barker, Carbon-13 Enriched Carbohydrates. Preparation of Erythrose, Threose, Glyceraldehyde, and Glycolaldehyde with ^{13}C-Enrichment in Various Carbon Atoms, *Carbohydr. Res. 72* (1979):79.

3. H.A. Nunez, T.E. Walker, R. Fuentes, J. O'Connor, A. Serianni and R. Barker, Carbon-13 as a Tool for the Study of Carbohydrate Structures, Conformations and Interactions, *J. Supramol. Struct. 6* (1977): 535.

4. A.S. Serianni and R. Barker, Isotopically-Enriched Carbohydrates: The Preparation of [^{2}H]-Enriched Aldoses by Catalytic Hydrogenolysis of Cyanohydrins with $^{2}H_2$, *Can. J. Chem. 57* (1979): 3160.

5. A.S. Serianni, J. Pierce and R. Barker, Carbon-13 Enriched Carbohydrates: Preparation of Triose, Tetrose and Pentose Phosphates, *Biochem. 18* (1979):1192.

6. A.S. Serianni, H.A. Nunez and R. Barker, The Cyanohydrin Synthesis: Studies with [^{13}C]Cyanide, *J. Org. Chem.* submitted for publication.

B. Abstracts

1. A.S. Serianni, H.A. Nunez and R. Barker, The Cyanohydrin Synthesis: Studies by Carbon-13 NMR Spectroscopy, 178th ACS National Meeting, Div. of Carbohydr. Chem., Sept. 1979, Abstr. No. 63.

2. A.S. Serianni, H.A. Nunez, J. Pierce, E. Clark and R. Barker, Synthesis of Isotopically-Enriched Carbohydrates, 178th ACS National Meeting, Div. of Biological Chem., Sept. 1979.

C. Acknowledgements

1. Stable Isotope Labeling of Sugars Simplified, Chemical and Engineering News, May 7, 1979.